A BIOINORGANIC STUDY OF SOME COBALT(II) SCHIFF BASE COMPLEXES OF VARIOUSLY SUBSTITUTED HYDROXYBENZALDIMINES

SUBMITTED IN FULFILMENT OF THE REQUIREMENTS FOR THE DEGREE OF

DOCTOR OF PHILOSOPHY

IN THE
DEPARTMENT OF CHEMISTRY,
FACULTY OF SCIENCE,
RHODES UNIVERSITY

BY

Rafiu Olarewaju Shaibu

MARCH 2007

Abstract

Syntheses of Schiff bases were carried out by reacting salicylaldyhde, *ortho*-vanillin, *para*-vanillin or vanillin with aniline, 1-aminonaphthalene, 4- and 3-aminopyridine, and also with 2- and 3-aminomethylpyridine.

The various Schiff bases obtained from the condensation reaction were reacted with $CoCl_2.6H_2O$, triethylamine stripped $CoCl_2.6H_2O$ or $Co(CH_3COO)_2$ to form cobalt(II) complexes of ratio 2:1. The complexes obtained from cobalt chloride designated as the "A series" are of the general formulae $ML_2X_2.nH_2O$, (L = Schiff base, X = chlorine) while those obtained from cobalt acetate or triethylamine stripped cobalt chloride denoted as "B" and C" are of the general formulae $ML_2.nH_2O$. The few complexes that do not follow the general formulae highlighted above are: 1A $[M(HL)_3.Cl_2]$, (L = *N*-phenylsalicylaldimine), 4A = $(MLCl_2)$, (L = *N*-phenylvanaldiminato), 7A and 21A (ML_2), (L = *N*-naphthyl-o-vanaldiminato, and *N*-methy-2-pyridylsalicylaldiminato respectively), 8A = MLCl, (L = *N*-naphthylvanaldiminato), 12A = $M_2L_3Cl_2$, (L = *N*-4-pyridylvanaldiminato), 15A (MLCl), (L = *N*-3-pyridyl-o-vanaldiminato).

The ligands and their complexes were characterized using elemental analyses and cobalt analysis using ICP, FT-IR spectroscopy (mid and far-IR), NIR-UV/vis (diffuse reflectance), UV/vis in an aprotic and a protic solvents, while mass spectrometry, ^{1}HNMR and ^{13}CNMR, was used to further characterized the ligands.

The tautomeric nature of the Schiff bases were determined by examining the behaviour of Schiff bases and their complexes in a protic (e.g. MeOH) and non-protic (e.g. DMF) polar solvents. The effects of solvents on the electronic behaviour of the compounds were also examined. Using $CDCl_3$, the NMR technique was further used to confirm the structures of the Schiff bases.

The tentative geometry of the complexes was determined using the spectra information obtained from the far infrared and the diffuse reflectance spectroscopy. With few exceptions, most of the "A" series are tetrahedral or distorted tetrahedral, while the "B + C" are octahedral or pseudo-octahedral. A small number of complexes are assigned square-planar geometry owing to the characteristic spectral behaviour shown.

In order to determine their biological activity, two biological assay methods (antimicrobial testing and brine shrimp lethality assay) were used. Using disc method, the bacteriostatic and fungicidal activities of the various Schiff bases and their respective complexes to *Escherichia coli*, *Staphylococcus aureus*, *Pseudomonas aeruginosa* as well as *Aspergillus niger,* were measured and the average inhibition zones are tabulated and analysed.

Both the Schiff bases and their complexes showed varying bacteriostatic and fungicidal activity against the bacteria and fungus tested. The inhibition activity is concentration dependent and potential antibiotic and fungicides are identified.

To determine the toxicity of the ligands and their corresponding cobalt(II) complexes, brine shrimp lethality assay was used. The LD_{50} of the tested compounds were calculated and the results obtained were tabulated for comparison.

Acknowledgements

All praise is due to All'ah for sparing my life till this day and making the stopover at Rhodes University a success.

I like to thank Dr. G. M. Watkins for his support since the first day of my arrival in Grahamstown till the last day and for accepting to embark on a rollercoaster ride with me which is almost at an end. His support as a supervisor as well as the financial supports is highly commendable and appreciated. Your method creates independent growth and development needed by students for the incessant challenges in the real world.

Special thanks to all the staff of the department of Chemistry, most especially Prof. P. Kaye (HOD Chemistry), Mr. A. W. Sonemann for helping to run most of the mass spectroscopy of the Schiff bases, Mr A. Adrian for his help in making the glass spreaders used for the antimicrobial studies, Mr Andy Soper for running automated NMR runs of the ligands.

I also say a big thank you to Dr. J. Dames for making her laboratory and facility in room 318, microbiology department of the University, available for use during the period used in studying the antimicrobial assay. The biconcave lens in her laboratory was used in counting the number of dead shrimps as well as the number of survivors. I like to thank Anna Clarke of the same department for providing the cultures of the strains of bacteria used.

A special thanks to Dr. D. Beukes for providing the eggs of the brine shrimps and other materials used in carrying out the brine shrimp lethality test. His analysis of some of the NMR spectra proved priceless in the elaboration of this work.

Special thanks to the Dr Eric Hosten at Nelson Mandela metropolitan University for running the cobalt analysis, Mr Piero Benincasa, at University of Cape Town and Mr Bathabile Soko, University KwaZulu-Natal, South Africa for running the microanalysis of the Schiff bases and the complexes.

I also like to appreciate the support and help of Mr Emmanuel Lamprecht. He was there for me from my first day in South Africa till the last day of this PhD program. You are one in a million. The appreciation would not be completed without acknowledging Ross van Vuuren, my friend from Zimbabwe, Komenin from Namibia, Nomapomdo and Estelle from South Africa for the good time we had together in LAB F5, during the period of their respective programs at Rhodes University. Special gratitude to all other friends and staff of Rhodes University for the cordial relationship shared and enjoyed.

I like to give big salutations to the Nigerian community at Rhodes University, (past and present) in Grahamstown and in Port-Elizabeth for the good brotherhood we enjoyed having found ourselves outside the shores of Nigeria. Special thanks to Dr Bola Ogunsipe (Lapasco, Usmith), Dr Elijah Oyeyemi, Prince Olumide Alebiosu and my special friend Mr Saheed Adekilekun (Sidor, Kaya) for the nice time we had together. I also like to give special gratitude to the Muslim community of Grahamstown for contributing to my spiritual growth.

Thanks to all the friends outside the University, with special thanks to Denise Booysen and her family in Grahamstown and in Cape Town for their support. Special thanks to all other friends I met while at Rhodes University.

I use this medium to say thank you to all my friends and uncles who contributed financially during the period of this program. Special thanks to Barrister Mamud Isa, Rasaq Aboyeji, Demeji Sikiru, Abu-Bakr Muhammad, Mustapha Akinola, Isiaka Ibrahim, Teslim Oladejo to mention but a few for their financial support during the PhD period. I pray to All'ah to reward you abundantly. I also like to acknowledge the support of Emmanuel Uwhukhor, a chemist turned a chartered accountant and his wife, Tessy for the regular visit and supports for my wife and kids since I left the shore of Nigeria. I pray to God to reward you abundantly and answer your prayers in earnest.

I also like to recognize the support of my superior officers, all my colleagues in Queens' College, and the Federal Ministry of Education for granting me study leave. No doubt, the study period has seen new development and growth that would be beneficial to our beloved Nigeria and the entire humanity.

The completion of this PhD program was achieved by my beloved wife, Omobola and sister Haditha, my daughter and brother Muktar, my son. I thank them for their supports, understanding, prayers, throughout the PhD period. I hope to be able to makeup for the separated years. I pray to All'ah to continue to bless my wife. This thesis is dedicated to Omobola (my lovely wife), Ayomide (my daughter) and Ayodeji (my son).

Lastly, I pray to All'ah to grant my parents eternal rest for the support given me while they were alive.

TABLE OF CONTENTS

LIST OF TABLES

LIST OF SCHEME

LIST OF FIGURES

1 INTRODUCTION TO DRUG DISCOVERY

This study is concerned with the syntheses, characterization and biological studies of Schiff bases and their cobalt(II) complexes, for potential use as antimicrobial or anticancer drugs. Accordingly, this chapter covers a brief overview of drug development, antimicrobial and cancer chemotherapies, anticancer agents' developments, as well as other relevant literature reviews.

1.1 Drug discovery and development

The developments of new drugs over the past century have revolutionized the practice of medicine; converting many once fatal diseases into almost routine therapeutic exercises.[1] It has irrevocably changed the fabric of the society, improving both the individual quality of life and life expectancy. No longer is surgery a desperate gamble with human life. The perils of childbirth are greatly lessened with the control of puerperal fever. The death of children and young adults from meningitis, tuberculosis, polio, smallpox and septicemia, once commonplace, is now uncommon. The development of power to control infections due to microorganism has also had a profound effect upon human life and society as a result of recent developments in the field of medicine.

Nearly all diseases affecting millions of people, such as tuberculosis, malaria, leprosy and schistosomiasis could be abolished or reduced to minor proportions. However, cost is the only great obstacle to achieving this.

In light of the current global situation of health and diseases, the need for ongoing development of new drugs requires no emphasis. Prior to the twentieth century, portions and herbs were the only sources of medicines.[2] Active ingredients of the remedies were only isolated and purified in the mid-nineteenth century. Since then, naturally occurring drugs such as morphine from opium, cocaine from coca leaves, quinine from the bark of the cinchona tree, etc. have been obtained and their structures determined.

Traditionally, the process of drug development has revolved around a screening approach, as nobody knows whether the compound can serve as a drug or therapy. The shortcoming of traditional drug discovery, as well as the fascination of a more deterministic approach to combating disease has lead to the concept of "rational drug design".[3] However, many other

approaches have been introduced to enhance drug discovery and development. Some of the methods that are currently being used are mentioned briefly in the next paragraph.

The first step in the development of a new drug is the discovery or synthesis of a potential new drug molecule. Most potential drugs are identified through one or more of four approaches: (a) chemical modification of a known molecule; (b) random screening for biological activity of large numbers of natural products, banks of previously discovered chemical entities, or large libraries of peptides, nucleic acids, or other organic molecules; (c) rational drug design based on an understanding of biological mechanisms and chemical structure; and, increasingly, (d) biotechnology and cloning using genes to produce larger peptides and proteins.[4]

In the past, the mechanism by which a drug worked at the molecular level was rarely understood, hence drug research focused on isolating the principle compound, known as the "lead compound",[2] from natural source or a synthetic compound produced in the laboratory. In this day and age, rapid advances in the biological sciences have resulted in a much understanding of how the body functions at the cellular as well as the molecular level, consequently, leading to the revolutionary changes in the medicinal chemistry.[2]

In designing a new drug, it is significant to know about the disease or infectious process. Then, a suitable target in the body is identified; and a drug to interact with that target is thereafter designed. To prevent interaction with different targets and thus have undesirable side effects, modern medicinal chemistry research target specificity and selectivity between species,[2] (for example, sulfonamides inhibit a bacterial enzyme not present in human cells), and selectivity within the body (for example, enzyme inhibitors should only inhibit the target enzyme and not some other enzyme).

The sequence of experimentation and characterization called drug screening is carried out on candidate molecules regardless of the source. Such screening approach is very time – consuming and laborious. For instance, anti-infective drugs will generally be tested first against a variety of infectious organisms, and hypoglycemic drugs tested for their ability to lower blood sugar. To demonstrate selectivity of the drug, the molecule is also studied for broad array of actions.[4]

1.2 An outline of historical development of antimicrobial agents

The fight against bacterial infections over the years has been one of the greatest achievements of medicinal chemistry. While deaths from bacterial infections have dropped in the developed world, it is still a major cause of death in the developing world. The use of antimicrobial herbs or potions for the treatment of microbial infections for many centuries is well documented. For instance, the healing properties of plants and animals have been recorded for thousands of years in such documents as Dioscorides' "de Materia Medica" from 75 AD and the 3500-yr-old papyrus "Ebers".[5] In the last four millennia, natural products entrenched in more sophisticated drug-delivery systems, continue to help humankind.[5] Lovastatin, digitoxin, morphine, reserpine and cyclosporine A are examples of modern natural products that have helped in the healings of humans.

Biologically active compounds are usually produced by plants, marine organisms, and microbes in defense against predators and competition with neighbors.[5] These account for the logical reason why most of drugs derived from natural sources have anticancer or anti-infective properties.[6] Natural products are just one source of antimicrobial agents among today's world of chemical libraries. They also offer an almost unlimited reservoir of unique structures.[5] Few examples of drugs derived from natural sources include vincristine, taxol, and camptothecin (anticancer), quinine and artemisinin (antimalarial), tetracycline, cephalosporin (antibacterial) and polyenes, sordarins (antifungal).[7] Drug discovery such as penicillin was serendipitous and as contributed to the success stories of medicinal chemistry.[5]

Although, antimicrobial drug discovery is more systematic and elaborate in the 21st century, so also are the pathogenic microbes. Nevertheless, many antimicrobial agents are now available and the vast majority of infectious diseases have been brought under control.

1.2.1 Early remedies

Of the numerous early tradition and folk remedies, two sources of antimicrobial compounds have survived to the present day. These are cinchona bark for the treatment of malaria and ipecacuanha root for amoebic dysentery.[1] Cinchona barks' active principle, quinine, was isolated in 1820. Quinine remained the only treatment for malaria until well into the twentieth century and still has a place in chemotherapy. Emetine, the active constituent of ipecacuanha root was isolated in 1817 and was shown in 1891 to have a specific action against amoebic dysentery. It is

still used for the treating this disease. These early remedies were used along with many ineffectual nostrums without any understanding of the nature of the diseases.

1.2.2 Antiseptic and disinfection

Like the early remedies – cinchona bark and ipecacuanha root- the use of disinfectants and antiseptics also preceded understanding of their action. It was believed to have arisen from the observation, that certain substances stopped purification of meat or rotting of wood.[1]

In the middle ages, Arabian physicians treated sepsis in open wounds with mercuric chloride. Labaraque, in 1825, introduced chlorinated soda for the treatment of infected wounds. The tincture of iodine was first used in 1839. The publication of Pasteur in 1863 led to the acceptance of these pioneer attempts at antisepsis. Lister later introduced the use of phenol in surgery. His measure was revolutionary, and the antiseptic technique opened the way to great surgical advances. Koch, from 1881 gave insight into the functions of antiseptics, which enables the introduction of techniques on which modern bacteriology was built.[1]

Koch perfected the methods of obtaining pure cultures of bacteria, demonstrated how to grow them on solid media and demonstrated practical methods of sterile working. With the giant stride taken by Koch, it became possible to handle bacteria in a controlled environment, hence making it possible to study the action of disinfectants and antiseptics. Kronig and Paul published work of 1897 serves as the pioneer work on the scientific approach to antiseptics and disinfectant.[1]

The publications of Pasteur and Koch, firmly established that micro-organisms are the causes of infectious disease, though for some diseases the causative agents still remained to be discovered.[1]

1.3 The beginning of Chemotherapy

Chemotherapy really began with Paul Ehrlich. His work from 1902 foreshadowed almost all concepts which have governed subsequent work on synthetic antimicrobial agents. He expressed belief that infectious disease could be combated by treatment with synthetic chemicals.[1]

1.3.1 Chemotherapy theories

Ehrlich postulated that cells possess chemical receptors, which are concerned with the uptake of nutrients. Drugs that affect the cell must bind to one or other of these receptors. He believed that antimicrobial agents must be essentially toxic compounds, and that they must bind to the micro-organism in order to extent their action.[1] The toxicity of a drug is determined firstly by its distribution in the body. However, in the treatment of an infection, the ability of a drug, binding to the parasite, relative to the host cell, determines the effectiveness of the drug.[1] Such measurements are still of prime importance in chemotherapy today.

Thus Ehrlich recognized the importance of quantitative measurement, of the relationship between the doses of a compound required producing a therapeutic effect, and the dose that will cause toxic reactions. The problem was to discover compounds having selective action against the microbial cell, compared with the cells of the host animal.

1.3.2 'Screening' approaches

The main stay of search for new drugs is based on Ehrlich pioneering methods. One aspect of his approach was the use of 'screening'.[1] This is the application of a relatively simple test to large numbers of compounds, in order to obtain evidence of biological activity in types of chemical structure not previously examined. The second of Ehrlich's methods was the deliberate synthesis of chemical variants of compounds, known to have the required activity. The new compounds were examined for increased activity or for improvements in some other property such as reduced toxicity. Ehrlich believes that a useful drug possesses an ideal combination of structural features which cannot be predicted at the outset.[1]

According to Ehrlich, a chemotherapeutic substance has two functional features, the 'haptophore' or binding group which enables the compound to attach to the cell receptors and the 'toxophore' or toxic group that brings about an adverse effect on the cell.[1]

This idea has frequently been used in cancer chemotherapy in an attempt to bring about specific concentration of toxic agents or antimetabolities in tumor cells.[1] In antimicrobial compound research, it has also helped to explain some features of the biochemical action of antimicrobial compounds.

Another feature of Ehrlich's work was his recognition of the possibility that drugs may be activated by metabolism in the body.[1] This suggestion was prompted by the observation that the compound atoxyl was active against trypanosomal infections but was inactive against isolated trypanosomas.

It is to be noted that when chemotherapy of bacterial diseases is compared with chemotherapy of cancer, the latter presents a problem. It has been possible to find agents with selective toxicity for many microorganisms, because in addition to being quantitatively different in biochemical terms from human cells, microorganisms are also qualitatively different; but it has proved difficult to find general, exploitable, biochemical differences between cancer cells and normal cells.[8] Some of the characteristics of cancer cells are mentioned briefly in section 1.4.1.

1.4 Cancer chemotherapy

Cancer still remains as the most feared diseases in the modern world. According to the World Health Organization, cancer is the largest cause of death after heart disease. Cancer is not a single disease but a general term for more than hundred diseases in which abnormal cells grow out of control.[9] It affects different organ systems of the body.

Cancer is associated with the uncontrolled, accelerated growth of cells and the sometimes spread of abnormal cells from their site of origin. Most cancers are initiated by specific genetic mutations.[10] Genetic mutations affect the factors controlling cell division. This is done either by stimulating cell division or by deactivating the processes that control cell division in the cell cycle.[11,12] The sequence of interacting proteins that induces and coordinates the duplication of cell contents and division, controls the cell cycle. Consequently, a mutation of the gene coding structural or regulatory proteins for cell division causes the change of a normal cell into a tumor cell.[10,13,14] In normal cells, two types of genes are responsible for growth and division regulations. Proto-oncogene,[15] a normal gene that can become an oncogene, either after mutation or through increased expression, and an oncogene,[15] a modified gene, or a set of nucleotides that codes for a protein, which increases the malignancy of a tumor cell. Some oncogenes, usually involved in early stages of cancer development, increase the chance that a normal cell develops into a tumor cell, possibly resulting in cancer. Two events can cause the initiation of tumor formation. The first is when proto-oncogene is transformed into an oncogene. The second possible event is the inactivation of a tumor suppressor gene.[16] Chemical carcinogens have been

implicated as one of the causes of cancers. They cause local changes in nucleotide sequences. Exposure to ionizing radiation, such as X-rays, γ-rays, and β-particles are also, other major causes of cancer. Exposure to this ionizing radiation causes chromosome alteration and translocations. Viruses are also known to cause cancer by introducing foreign DNA into a cell.[17]

In general, tumors are classified as either *benign* or *malignant.*[18] Benign tumors cannot spread; they only grow locally, hence are not necessarily life- threatening, unlike malignant or cancerous tumors that invades nearby tissue and transforms normal cells into cancerous cell. Malignant tumors can spread by invasion or metastases. It is a complex series of steps in which cancer cells leave the original tumor site and migrate to other parts of the body via the bloodstream or lymphatic system. By definition, the term "cancer" applies only to malignant tumors. Nevertheless, some tumors with benign histology can behave as malignant tumors, for example in brain tumors, where treatment has to be as aggressive as with malignant disease.

In contrast, neoplasma[19] is a term used for any abnormal growth of new tissue; a proliferation of cells no longer under normal physiologic control. These may be benign (non-cancerous) or malignant (cancerous).

Surgery, radiotherapy and chemotherapy are the major treatments modalities for dealing with established cancer. Each of these approaches has its limitations. The role of each of these depends on the type of tumor and the stage of its development. Surgery, which is a major curative and invasive modality for localized disease, cannot alone heal neoplasms which are widely distributed or which have invaded critical structures.

Radiotherapy, although useful in curing localized neoplasm and eradicating microscopic metastases, cannot be use to control widely disseminated cancer. In addition, there are certain clinical circumstances in which the success of radiotherapy is restricted either by extremely radio resistant neoplasms or by a tumor invading a very radio sensitive normal tissue. In either of these situations, it may be impossible to deliver a curative dose of radiation to the tumor without causing unacceptable damage to the critical normal tissues.

Alternative methods of cancer treatment include the use of radioisotopes, and photodynamic therapy. Radiopharmaceuticals (combined with radioisotopes) have a high specificity and

sensitivity for tumor cells and deliver radiation (γ, β,-rays and α-particles) *in situ* to cancer cells; with minimal damage to the surrounding tissue.[20]

Photodynamic therapies make use of hematoporphyrin derivatives (HPD) and dyes. HPD and dyes clear from tumor cells at a slower rate than from normal cell due to the lower activity of lymphatic drainage from tumors, resulting in the selective accumulation of the drug in the tumor cells. To destroy the tumor cell, red light from tunable laser is directed at the tumor, generating singlet oxygen radicals, which selectively destroy the tumor cells. The singlet oxygen radicals chemically destroy membrane proteins, sterols, and unsaturated lipids, and this leads to a change in cell permeability and cytolysis. Red light is chosen due to its penetrating power in human tissue and to the fact that it is not absorbed by chromophores present in normal tissue.[21, 22]

By directing cytotoxic agents towards proliferating cells, significant advances en route to the curing of human cancer by chemotherapy have been achieved. Childhood tumors and Hodgkin's lymphoma are rapidly growing cancers, they respond dramatically to existing chemotherapy, and both disseminated malignancies and localized are frequently cured. However, the major causes of mortality from cancer are the slow-growing solid tumors and they are responsible for many of the socioeconomic problems associated with human malignancies.[23] Carcinomas of the lung, colon, and breast are examples of relatively slow-growing solid tumors, and constitute the majority of human cancers. These neoplasms, in general, respond poorly to existing chemotherapeutic agents, and curative treatment by any therapeutic modality or combination of modalities is uncommon in patients presenting with extensive disease.

Adjuvant therapy i.e. chemotherapy combined with surgery or radiotherapy or both, has increased survival rates for a number of solid tumors that were formerly treated by only one therapeutic modality.[24] Modern combination chemotherapy has three important theoretical advantages over single-agent therapy. First, it can maximize cell kill while minimizing host toxicities by using agents with non-overlapping dose-limiting toxicities. Second, it may increase the range of drug activity against tumor cells with endogenous resistance to specific types of therapy. Finally, it may also prevent or slow the development of newly resistant tumor cells.

In the past decade, there has been a remarkable advance in the understanding of cell proliferation, which has led to better understanding of the biology of the cancer cell,[13] this in turn is beginning to lead to new approaches to the development of anticancer agents.[25]

The value of approaches such as immunotherapy and biological response modifiers (e.g. interferons, haemoietic growth factors, etc) in cancer treatment are being investigated.[24]

1.4.1 Some of the characteristics of cancer cells

Cancer cells manifest four characteristics that distinguish them from normal cells:[8]

a) Uncontrolled proliferation: The propagation of cancer cells is not controlled by the process that normally regulates cell division and tissue growth. It is this, rather than their rate of production, that distinguishes them from normal cells.

b) Loss of function: the loss - to a varying degree - of capacity to differentiate. Poorly differentiated cancers multiply fast, and have a poorer prognosis than the well-differentiated cancer cells.

c) Invasiveness: normal cells develop certain special relationships with respect to each other during differentiation and growth of tissues and organs. This characteristic is lacking in cancer cells.

d) Metastases: these are secondary tumors formed by cells that have been released from the initial or primary tumor and have reached other sites through blood vessels or lymphatic or as a result of being shed into the body cavities.

1.4.2 Summary of some milestones in the development of cancer chemotherapy

The concept of treating cancer with drugs has a long history, dating back centuries. It started when preparations of silver, zinc, and mercury were used.[24] However, 1865 was the first year when cancer treatment was documented. Lissauer was reported to have given potassium arsenite to a patient with leukemia and noted positive effect.[24] Successful systemic cancer chemotherapy was not really developed until almost 80 years later. The first effective anticancer drug – nitrogen mustard – appeared in the context of war, not medicine.[24] It is of interest to note, that clinical sources of the patient treated with nitrogen mustard is still reflected in the use of anticancer drugs today.

Antimetabolities are the second successful anticancer drugs used clinically.[26-7]Antimetabolities structurally resemble a natural metabolite necessary for cellular function and interfere with its normal utilization. They are of three types: antifolates, antipurines, and antipyrimidines.

In 1954, Sidney and Farber introduced another class of drugs called actinomycin D into the clinic.[24] The effectiveness of these drugs led to the development of a large number of antitumor antibiotics.

Serendipity played a role in the introduction of the vinca alkaloids, antimitotic agents that are extracted from periwinkle plants. Although, periwinkle has been used in folk medicine for centuries, a claim that an extract of these plants could produce hypoglycemia led to testing for this effect.[28] Four alkaloids showed activity in periwinkle plant, but only vincristine and vinblastine have been used to treat cancer in humans.

New drugs are still appearing, but most of them descend from parent compounds developed years ago. Antitumor drugs came into clinical use at a relatively fast rate between 1955 and 1970.

1.4.3 Drugs used in cancer chemotherapy

Anticancer drugs can be divided into the following categories: [8]

1.4.3.1 Cytotoxic drugs

The term 'cytotoxic drug' is used for any drug that can damage or kill cells. It is used more restrictively to mean drugs that hinder cell division and potentially useful in cancer chemotherapy. Examples of cytotoxic drugs are

a. Alkylating agents and related compounds which act by forming covalent bonds with DNA and thus impeding DNA replication. Mechlorethamine, chlorambucil, melphalan, cisplatin, carboplatin, oxaliplatin, etc are drugs with mechanisms of action that involves alkylation.
b. Antimetabolities, which block or subvert one or more of the metabolic pathways involved in DNA synthesis. Examples include methotrexate, capecitabine, fluorouracil, thioguanine, etc.
c. Cytotoxic antibiotics, i.e substances of microbial origin which prevent mammalian cell division. Mercaptopurine and thioguanine are examples of cytotoxic antibiotics.

d. Vinca alkaloids and related compounds-substances of plant origin that specifically affect microtubule function and hence the formation of the mitotic spindle. Examples include vinblastine, vincristine, vinorelbine, epipodophyllotoxins, etc.

1.4.3.2 Hormones

The most important are steroids, namely glucocorticoids, oestrogens and androgens. These drugs suppress hormone secretion or antagonize hormone action. Hormonally active agents include tamoxifen, megestrol acetate, anastrozole etc.

1.4.4 Bioinorganic chemistry and metal-based chemotherapy agents

Medicinal inorganic chemistry is a relatively new branch of bioinorganic chemistry and serves as interface between medicine and inorganic chemistry. It includes metal-based drugs, metal sequestering or mobilizing agents, metal-containing diagnostic aids, and the medicinal recruitment of endogenous metal ions. The number of moderately comprehensive reviews of the topic are very few,[29-32] although, the field is said to be growing exponentially.[33] Rapid growth can be attributed to some spectacular successes, most notably Cisplatin for treatment of testicular cancer, gadolinium complexes in magnetic resonance imaging (MRI), and the rise of nuclear medicine, for both therapy and diagnosis.[34]

Most chemotherapeutic agents are organic, with very few containing metal. However, the use of inorganic complexes as chemotherapeutic agents dated back centuries. The ancient Chinese, Egyptian, Greek and Indian were attracted by the lure of precious metals, such as gold and silver, and use them in cures of various sorts. Copper and iron have also been used since antiquity in metal-based therapies. There has always been a questioning link between the discovery of a new valuable element and its quick movement into the medicinal repository.[29] For instance, the use of gold complexes in the treatment of arthritis has a long history, so also is the salts of silver as antibacterial and gallium for the treatment of hypercalcemia of malignancy.[31]

Nowadays, healing applications of inorganic chemistry in medicine varied; encompassing many aspects of the introduction of metal ions into the body (or their intentional removal) for therapeutic or diagnostic effect. Cisplatin can be considered the archetypal inorganic drug, as it

contains not one atom of carbon.[35] These days, metal-based pharmaceuticals are constructed with carbon-based ligands.

The first systematic studies in the field of tumor inhibiting metal complexes were described by Collier and Krauss, in 1931. They proposed that the "type and structure of the compounds and not the metal alone, determines the effect of heavy metal on experimental murine cancer".[36] The use of metal complexes as chemotherapeutic agents was limited until the discovery of anticancer activity of cis-diamminedicholoroplatinum(II) (Cisplatin). Its potential as an antitumor agent was recognized through the observation made by Rosenberg et al.[37] that certain group VIIIb transition metal compounds inhibit bacterial division. They observed that neutral platinum complexes inhibited division and induced filamentous growth of *Escherichia coli*. Cisplatin, originally discovered by Michele Peyrone in 1844,[38] was shown to cause filamentous growth, whereas the trans-isomer had no effect.[39] Cisplatin found its first clinical application in the early 1970s and following approval in 1978, is currently one of the most successful cancer chemotherapeutics.

As a result of extensive basic research, a great deal is now known about the modes of binding of platinum(II) complexes to biological molecules and the likely mechanisms of Cisplatin antitumor activity. The probable mechanism is analogous to that of the alkylating agents.[40] When it enters the cell, the chloride ions dissociate leaving a reactive diamine platinum complex which reacts with water and then interact with DNA. It is thought that it causes intrastrand cross-linking which results in the breaking of the hydrogen bonds between the guanine and cytosine bases and thus local denaturation of the DNA chain.[41]

The success of cisplatin stimulated further research in the search for other metal-based anticancer drugs. Available literatures confirmed that complexes of rhodium, cobalt, copper, tin, ruthenium, germanium, gallium, gold, molybdenum and titanium have shown significant anticancer activity.[42-50] A combination of the ruthenium drugs with cisplatin, has given the most successful treatment yet for a secondary tumor.[51]

Although, complexes of other metals have been shown to have antitumor activity, much less is still known about the antitumor and, in some cases, antiviral properties of these metal complexes.

In addition, many metal complexes are used as DNA markers, only compounds of the platinum family are widely used medically as chemotherapeutic agents. Cisplatin is widely used alone in a broad range of solid tumors, including non-small cell and small cell lung cancer, esophageal and gastric cancer, head and neck cancer, and genitourinary cancers, particularly testicular, ovarian, and bladder cancer or in combination with other chemotherapeutic drugs in the treatment of aggressive cancer such as nonseminomatous testicular and bladder carcinomas.[52]

Although Cisplatin has proved to be a valuable drug for the treatment of a number of cancers, it is known to have side effects. It has low myelotoxicity but causes severe nausea and vomiting. Tinnitus and hearing loss in the high frequency range may occur, as may peripheral neuropathies, hyperuricaemia and anaphylactic reactions. [52]

A major problem in cancer chemotherapy is drug resistance. Some tumor types, e.g. non-small cell lung cancer and colon cancer, exhibit primary resistance, i.e. absence of response on the first exposure, to currently available standard agents.

Resistance to Cisplatin can develop and the drug itself is toxic to the patient, with the kidneys, gastrointestinal tract, bone marrow and the nervous system all experiencing distress resulting from treatment.[53] As a result of the several drawbacks, new sets of platinum complexes with low toxicity have been prepared and screened, hoping to get drugs that can be used to treat Cisplatin-resistance cancers.[36]

Carboplatin and oxaliplatin are second and third-generation platinum analogs respectively. Their mechanisms of actions are identical to that of Cisplatin. Second generation complexes differ from cisplatin by having different leaving groups, while oxaliplatin have different amines.

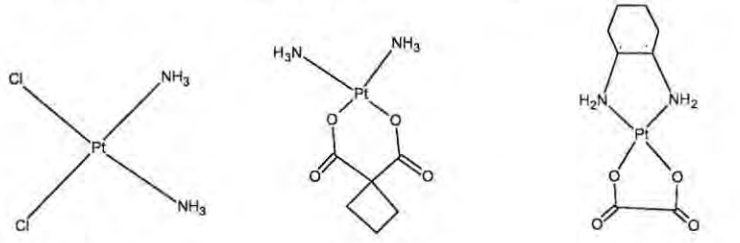

Cisplatin Carboplatin Oxaliplatin

Figure 1:1 Structures of first, second and third-generation platinum anticancer drugs. [31,53]

1.4.5 Anticancer drug development

As in the other areas of drug development, development of new, effective anticancer drugs that are safe to use in humans is slow, tedious, and expensive. Novel anticancer agents are obtained from a number of sources: synthetic analogs of known effective drugs; natural products isolated from marine organisms, microorganisms or plants; 'rational' drug design, based on their potential for inhibition of enzymes or other components essential for tumor cell growth.[52]

However, for over three decades now, there have been concerted efforts to develop anticancer drugs through both empirical screening and rational design of new compounds. The synthesis of peptides and proteins with recombinant DNA technique and monoclonal antibodies[52] (process by which large quantities of antibodies targeted against a particular antigen X can be produced) are some of the advances in this field. Few well-characterized transplantable animal tumor systems have been employed for the drug development program testing.

The following are the new classes of anticancer drugs that have entered clinical development. Signal transduction inhibitors,[52] focused on critical signaling pathways essential for cell growth and proliferation; microtubule inhibitors, directed against the mitotic spindle apparatus; inducers of differentiation, intended to force neoplasm cells past a maturation block to form end-stage cells with little or no proliferation potential; antimetastatic drugs, designed to perturb surface properties of malignant cells and thus alter their invasive and metastatic potential; anti-antigenic agents designed to inhibit the formation of tumor vasculative; hypoxic tumor stem cell-specific agents,[52] designed to exploit the greater capacity for reductive reactions in these therapeutically resistant cells created by oxygen deficiency within solid tumors; tumor radio-sensitizing and normal tissue radio-protecting drugs aimed at increased therapeutic effectiveness of radiation therapy; cytoprotective agents, focused on protecting certain normal tissues against the toxic effects of chemotherapy; and biologic response modifiers,[52] which alter tumor-host metabolic and immunologic relationships.

1.4.6 Non-classical Cisplatin

In recent times, complexes that are not structurally related to Cisplatin have be synthesized and shown to have significant antitumor activities.[54,55] Structural–activity relationship was formulated for the classical Cisplatin and characteristics believed to be responsible for the biological activity shown. While designing new class of cobalt complexes as antitumor agents,

Gust and co-worker[56 -60] studied the effects of having hydroxyphenyl and methoxyphenyl as substituents in a series of complexes, consequently demonstrating the significance of structural–activity relationship of these groups in designing agents with high tumor activity and selectivity.

1.4.7 Design of ligands for metal-based pharmaceuticals

As mentioned above, ligands are very significant in modifying the biological effects of metal-based drugs. Ligands can be use to modify the oral or general bioavailability of metal ions, and can assist in targeting specific tissues or enzymes.[34] They can also deliver, protect or sequester a particular metal ion or act to enhance uptake of pharmacologically beneficial metal ions. Ligands can serve as modifying reactivity and or substitutional inertness.

In addition to the choice of ligand, oxidation state of the metal is also important in designing of a metallopharmaceuticals. The oxidation state of the metal ion can be decisive in regulating the immediate *in vitro* and *in vivo* responses to metal-based pharmaceutical agents. The oxidation state of the metal ion also dictates particular coordination geometries, hence limiting appropriate binding for different ligand sets.[34]

Consequently, kinetic and thermodynamic properties of metallopharmaceuticals can be controlled by optimizing the choice of ligand(s) and the oxidation state of the metal. The detailed knowledge of the factors that controls ligand substitution and redox reactions, have help in the successful designing of second- and third-generation platinum anticancer drugs, now widely used in the clinic. The chemical reactivity of the complexes can be chosen so as to balance the inertness required for the drug to reach its target site (e.g., DNA) and minimize attack on other sites (side effects) yet allow activation necessary for binding to the target.

1.5 References

1. T. J. Franklin, G. A. Snow, *Biochemistry of antimicrobial action*, 2nd ed., Chapman and Hall, London, 1975.
2. P. L. Graham, *An introduction to medicinal chemistry*, 3rd ed. Oxford University Press, New York, 2005.
3. I. D. Kuntz., Science; 1992, **257**, 1078-82
4. B. A. Berkowitz., *Basic and clinical pharmacology*, 9th ed. B. G. Katzung, (Ed.), McGraw-Hill Companies, U.S.A. 2004.
5. M. R. Jacob, L. A. Walker, *Methods in molecular medicine, antifungal agents: methods and protocols,*., E.J. Ernst, P.D. Rogers, (Eds.), Humana Press Inc., Totowa, NJ.; 2005.
6. D. Newman, G. Cragg, K. Snader, J. Nat. Prod.; 2002, **66**, 1022-1037.
7. D. Barret, Biochim. Biophyis. Acta; 2002, **1587**, 224-233.
8. H. P. Range, M. M. Dale, J.M. Ritter; *Pharmacology*, 3rd ed., Churchill Livingstone, Edinburgh, 1995.
9. S. P. Gupta, Chem. Rev.; 1994, **94**, 1507-1551.
10. K. B. Burck, E. T. Liu, J. W. Larrick, *Oncogenes: an introduction to the concept of cancer genes*, Springer-Verlag, New York, 1988.
11. J. B. Weitzman, M. Yaniv, Nature; 1999, **400**, 401-402.
12. W. C. Hahn, C. M. Counters, A. S. Lundberg, R. L. Beijersbergen, M. W. Brooks. R. A. Weinberg, Nature; 1999, **400**, 464-468.
13. A. W. Murray, Nature; 1992, **359**, 599-604.
14. L. H. Hartwell, M. B. Kastan, Science; 1994, **266**, 1821-8, (CAN 122:52808).
15. Oncogene, http://en.wikipedia.org/wiki/Oncogene, accessed 12/09/2006
16. K. Kinzler, B.Vogelstein, Nature. 1997, **386**, 761–763.
17. B. Alberts, D. Bray, J. Lewis, M. Raff, K. Roberts, J. D. Watson, *Molecular Biology of the Cell*, 3rd ed. Garland Publishers, inc., New York, 1994.
18. The history of cancer, http://www.cancer.org/, accessed 22/04/2004.
19. http://en.wikipedia.org/wiki/Cancer, accessed 8/03/2007.
20. J. R. Dilworth, S. J. Parrott, Chem. Soc. Rev.; 1998, **27**, 43-55.
21. F. Dall'Acqua, G. Jori, Ch. 41, *Principles of medicinal chemistry*, 4th ed. W.O. Foye, T.L. Lemke, D.A. Williams (Eds.), Williams and Wilkins, London, 1995.
22. T. J. Dougherty, C. J. Gomer, B.W. Henderson, G. Jori, D. Kessel, M. Korbelik, J. Moan, Q. Peng, J. Natl. Cancer Inst., 1998, **90**, 889-96.
23. *Anonymous*, 1979 Cancer Facts and Figures, American Cancer Society, New York,1978.

24. W. B. Pratt, R.W. Ruddon, *The anticancer cancer drugs*, New York Oxford University Press, 1979.
25. G. Powis, Pharmacol. Sci.; 1991, **12**, 188-194.
26. D. R. Seeger, D. B. Cosulich, J. M. Smith, M. E. Hultquist, J. Am. Chem. Soc.; 1949, **71**, 1753-1758.
27. S. Farber, L. K. Diamond, R. D. Mercer, R. F. Sylevester, J. A Wolff, New Eng J. Med.; 1948, **234**, 787-793.
28. I. S. Johnson, J.G. Armstrong, M. Gorman, J. P. Burnett, Jr.; Cancer. Res.; 1963, **23**, 1390-1427, CAN 60:12233.
29. H. E. Howard-Lock and C. J. L. Lock, *Comprehensive coordination chemistry*. G. Wilkinson, R. D. Gillard, J. A. McCleverty (Eds.), Pergamon, New York, 1987.
30. P. J. Sadler, Adv. Inorg. Chem.; 1991, **36**, 1-48, (CAN 115: 149556)
31. N. Farrell, Coord. Chem. Rev.; 2002, **232**, 1-4.
32. K. H. Thompson, C. Orvig, Science; 2003, **300**, 936-939.
33. C. Orvig, M. J. Abrams, Chem. Rev.; 1999, **99**, 2201-2203.
34. K. H. Thompson, C. Orvig, Dalton Trans.; 2006, 761–764.
35. M. J. Abrams, B. A. Murrer, Science; 1993, **261**, 725-730.
36. B. K. Keppler, *Metal complexes in cancer chemotherapy*, VCH, New York, 1993.
37. B. Rosenberg, L. Van Camp, T. Krigas, Nature; 1965, **205**, 698-9.
38. M. Peyrone, Liebigs Ann. Chem, 1844, **51**, 1.
39. B. Rosenberg, L. Van Camp, E. B. Grimley, A. J. Tomson, J. Biol. Chem. 1967, **242**, 1347-52.
40. B. Drewinko, J. A. Gottlieb, Cancer Chemother. Rep.; 1975, **59**, 665-673.
41. Z. Guo, P. J. Sadler, Angew, Chem. Int. Ed.; 1999, **38**, 1521-1531.
42. R. Gust, I. Ott, D. Posselt, K. Sommer, J. Med. Chem.; 2004, **47**, 5837-5846.
43. O. M. N. Dhubhghaill, W. R. Hagen, B. K. Kepplar, K.G. Lipponer, P. J. Sadler, J. Chem. Soc. Dalton Trans.; 1994, 3305-10.
44. L. Y. Kuo, M. G. Kanatzidis, M. Sabat, A. L. Tipton, T. J. Marks, J. Am. Chem. Soc.; 1991, **113**, 9027-45.
45. H. T. Chifotides, K. R. Dunbar, J. H. Matonic, N. Katsaros, Inorg. Chem.; 1992, **31**, 4628-34.
46. D. T. Hill, G. R. Girard, F. L. McCabe, R. K. Johnson, P. D. Stupik, J. H. Zhang, W. M. Reiff, D. S. Eggleston, Inorg. Chem.; 1989, **28**, 3529-33.

47. B. Moubaraki, K. S. Murray, J. D. Ranford, J. J. Vittal, X. Wang, Y. Xu., J. Chem. Soc., Dalton Trans.; 1999, 3573-78.
48. D. L. Banville, W. D. Wilson, L. G. Marzill, Inorg. Chem.; 1985, **24**, 2479-83.
49. H. Tamura, H. Imai, J. Kuwahara, Y. Sugiura, J. Am. Chem. Soc.; 1987, **109**, 6870-1.
50. S. J. Berners-price, R. K. Johnson, C. K. Mirabelli, L. F. Faucette, F. L. McCabe, P. J. Sadler, Inorg. Chem.; 1987, **26**, 3383-7.
51. P. J. Dyson, G. Sava, Dalton Trans., 2006, 1929-33.
52. E. Chu, A. C. Sartorelli, Basic *and clinical pharmacology*, 9th ed. B. G. Katzung (Ed.), McGraw-Hill Companies, U.S.A. 2004.
53. J. Reedijk, Chem. Commun.; 1996, 801-6.
54. K. Schmidt, M. Jung, R. Keilitz, B. Schnurr, R. Gust, Inorg. Chim. Acta; 2000, **306**, 6-16.
55. I. Ott, B. Kirchner, R. Gust, J. Inorg. Biochem.; 2004, **98**, 485-489.
56. M. Jennerwein, B. Wappes, R. Gust, H. Schonenberger, J. Engel, S. Seeber, R. Osieka, J. Cancer Res. Clin. Oncol.; 1998, **114**, 347-358.
57. R. Muller, R. Gust, G. Bernhardt, C. Keller, H. Schonenberger, S. Seeber, R. Osieka, A. Eastman, M. Jennerwein, J. Cancer Res. Clin. Oncol.; 1990, **116**, 237-244.
58. S. Schertl, R. Gust, R. Muller, T. Spruss, H. Schonenberger, Arch. Pharm.; 1992, **325**, 113-118.
59. T. Spruss, R. Gust, R. Muller, J. Engel, H. Schonenberger, Arch. Pharm.; 1990, **323**, 99-102.
60. J. Reedijk, Proc. Natl. Acad. Sci.; USA, 2003, **100**, 3611-6.

2 REVIEW OF THE PHYSICAL AND CHEMICAL CHARACTERIZATION

As mentioned in chapter one, the focus of this work is to syntheses, characterized and study the biological activities of Schiff bases and their corresponding cobalt(II) complexes. This chapter is concerned with the review of information on cobalt(II) complexes with respect to this work, literature appraisal of Schiff bases that are relevant to this thesis, as well as brief information on the steps used in characterizing the ligands and their corresponding complexes. Emphases will be centered on the relationship between electronic spectra and geometry of the complexes. Brief information is also given about the use of substituents parameters in relation to spectroscopic properties as well as biological activities.

2.1 Cobalt(II) ion

The importance of cyanocobalamin (Vitamin B) to the body is well known. It is the only vitamin having tightly bound cobalt ion.[1] It is also relevant to note that cobalt compounds have been under an increasing interest as potential antitumor agent,[2] hence, the reason why cobalt-containing complexes are been investigated.

Cobalt(II) ion, has seven d electrons, and is best known in four-coordinate tetrahedral and six-coordinate octahedral stereochemistries.[3] Cobalt(II) forms more tetrahedral complexes than any other transition metal ion. This is attributable to the relatively low difference in crystal field stabilization energies between octahedral and tetrahedral cobalt(II) (d^7) complexes.[4] No case of geometrical isomerism has yet been reported for this ion. Equilibrium distribution of ligands is rapidly reached in solution since the coordination sphere is labile.[3]

$$CoPy_2X_{2(Tetrahedral)} + 2Py \rightarrow CoPy_4X_{2\ (Octahedral)}$$

The four – coordinate tetrahedral and the six – coordinate octahedral are the idealized geometries for few, if any complexes have been shown to attain symmetry high enough to be called tetrahedral or octahedral in the group theoretical sense.[3]

When more than one type of ligand enters the coordination sphere, true cubic symmetry is lost. These are typified by tetrahedral $[CoPy_2Cl_2]$ and the octahedral $CoCl_2.2H_2O$, which attains an octahedral geometry by bridging chloride ions.[3]

2.1.1 Electronic spectra of cobalt(II)

As a result of availability of information on the electronic spectra of cobalt(II) in its various stereochemistries, several generalizations can readily be made. It is known that the spectrum of tetrahedral cobalt is more intense than that of octahedral cobalt (factor of 10^2 in extinction coefficient), strongly structured peak are the characteristics in the visible region.[3] The differences in band positions[5] can be regarded as diagnostic of stereochemistry of the cobalt(II) complexes. Unfortunately, both are known to give rise to bands near 20 000 cm^{-1} (500 nm) although tetrahedral compounds more frequently exhibit maxima near 15 000 cm^{-1} (667 nm). If the spectrum is not complicated by overlap with a strong UV (charge transfer) tail, intensity is the best spectral indicator of stereochemistry.[3]

Cotton and Holm[6,7] also proved that electronic spectra as well as magnetic moments of cobalt(II) complexes depend upon the geometry of the complexes. Colour is not a useful criterion of stereochemistry. While many tetrahedral complexes are "blue", octahedral compounds are "pink" or "brick red".[3] Several contradictory examples are well documented. For example, Co_2SiO_4 is purple and octahedral[8] while cobalt dipivaloylmethanide is pink and tetrahedral.[9]

No empirical correlation of spectral with square planar Co(II) is available because few compounds have been shown definitely to contain this geometry.[3]

Liehr[10] did theoretical exploration of the spectra of cobalt(II) ion. His paper presents the results of complete calculations of the energy with respect to the ligand field columbic (Dq), spin-orbit (λ), and electron correlation parameters (Racah B and C) for tetrahedral and octahedral cobalt(II). Liehr presented his results in graphical form, and also pointed out the weakness of the method. The conclusion drawn from his paper is that simple ligand field theory cannot be used to answer all questions of transition chemistry.[11]

According to the simplified energy level diagram, high spin octahedral Co(II) complexes have three electronic transitions. The spectra have a band in the near infrared which is assigned to the lowest energy transition $^4T_{1g} \rightarrow {}^4T_{2g}$. A band in the visible region near 20 000 cm^{-1} assigned to the $^4T_{1g} \rightarrow {}^4T_{1g}(P)$ transition. The $^4T_{1g} \rightarrow {}^4A_{2g}$ transition is frequently not observed. The first two transitions have normal intensities of octahedral spin-allowed Laporte forbidden bands, while the $^4T_{1g} \rightarrow {}^4T_{2g}$ transition involves a two-electron process for strong fields; consequently, it is expected to be very much weaker.[4] The fine structure or shoulder in the visible region has been

attributable to the $^4T_{1g} \rightarrow {}^4A_{2g}$ transition but it may also have originated from spin-orbit coupling, vibrational broadening, low symmetry components to the ligand field or transitions to doublet states.[4]

The simplified energy level diagram of tetrahedral Co(II) also has three electronic transitions.[4] The first transition, ν_1 [$^4T_2 \rightarrow {}^4A_2$], occurs at energy of 10Dq. This band has been rarely observed, it is expected to occur in the 3,000- 5000 cm^{-1} (3,333 – 2000 nm) region. Goodgame[12] reported the near infrared spectra of tetrahedral cobalt(II).

The second transition, ν_2 [$^4A_2 \rightarrow {}^4T_1(F)$], has broad band and appears in the near infrared; ν_3 [$^4A_2 \rightarrow {}^4T_1(P)$] is intense, broad and is known to exhibits a great deal of structure.[4] The ν_3 usually occurs in the 15,000 – 20,000 cm^{-1} region and is known to give the characteristic blue color common in tetrahedral cobalt complexes. The intensities of the spectral bands of tetrahedral complexes have been shown to be due in large part to molecular orbital mixing (covalency).[4] Both ν_2 and ν_3 show fine structure and have considerable breadth. The fine structure is attributable to spin-orbit coupling.[13] While this might be true for fine structure, it cannot account for the breadth of the bands. Low symmetry components of the crystal filed and transitions to the doublet[14] states are perhaps the main causes of the multiple absorption bands.

Ferguson[14] did careful measurements of tetrahedral cobalt, while Cotton, Goodgame, and Goodgame[15] did extensive survey of the electronic structure of tetrahedral cobalt complexes. Ferguson[14] and coworkers[16] concluded that the procedures outlined above are only useful quantitatively since spin-orbit coupling, vibrational interactions, and distortions from cubic symmetry have important effects on the spectra.

2.1.2 Magnetic susceptibility

It would be futile attempting to list the magnetic properties of every cobalt complexes that has been reported. The few lines below outlined the basic information needed to go about using magnetic susceptibility to characterized cobalt complexes. Schlapp and Penneg[17] gave the theory of the paramagnetic susceptibility of Co^{2+} in order to account for the susceptibility of Tutton salt, $(NH_4)_2Co(SO_4)_2.6H_2O$. The magnetic moment would not be diagnostic of stereochemistry of Co^{2+} if it exhibited a spin-only moment; fortunately, however, this situation does not occur.

Thus, for tetrahedral Co^{2+} the $^4T_1$ and $^4T_2$ states are mixed into the ground state $^4A_2$ state under the action of spin-orbit coupling.

Figgis and Nylolm,[18] gave very good summary of magnetic behavior of cobalt while an extensive survey was done by Figgis and Lewis;[19] Cotton, Goodgame, and Goodgame[12] review tetrahedral cobalt.

The ground state ($^4T_1$) in an octahedral field is orbitally degenerate and causes an orbital angular momentum contribution to the magnetic moment. The moment then lies between the limit of spin only, $\mu = [4S(S+1)]^{1/2} = 3.88$ B.M., and $\mu = [4S(S+1) + L(L+1)]^{1/2} = 5.2$ B.M., where S is the total spin angular momentum of (3/2)h and L is total orbital angular momentum of 3h. The actual value depends upon the amount of L remaining associated with the ground state orbital triplet.[3] Experimental moments for octahedral cobalt are usually in the range 4.7 – 5.2 B.M while that of tetrahedral mostly lie in the range of 4.4 – 4.7 B.M.

2.2 Schiff bases

2.2.1 Properties and applications

A Schiff base is a product of the condensation of a primary amine with aldehydes or ketones. They have relatively simple preparation procedure. It is possible to introduce different substituents into the existing skeleton of the molecule, hence enabling the designing of compounds with suitable structural, electronic and biological properties.

Schiff bases are importance in diverse field of chemistry and biochemistry owing to their biological activities.[20] For instance, Schiff bases of amino- and aminoalkylpyridines are known to be structurally related to compounds participating in vitamin B_6 chemistry.[21] Schiff bases play biological roles,[22] for example, in vision; in determining the flexibility of the wall of veins, etc. 2-salicylideneaminopyridine has also been shown to have anti-inflammatory activity.[23]

Schiff bases are known to have slight antitumor activities,[24] consequently more Schiff bases have been synthesized in order to find compounds with greater antitumor activities. For example, Cancer Chemotherapy National Center screened some of Schiff bases, $R'C_6H_4CH=NC_6H_4R$ against lymphoid leukemia L1210 in the mouse and intramuscular Walker sarcoma 256 in the

rat. They were found to slow the growth of several animal tumors.[25] The antitumor activities were reported with attempts to correlate activities with the chemical structures of the compounds. They studied the structure-activity relationship (SAR), and concluded that the aldehyde group is more important to the antitumor activity than the amine group.[25] It was also observed that the biological activities of the Schiff bases were difficult to determined because of their rapid hydrolysis in aqueous solution.[26] Consequently, solutions for injection were prepared shortly before use.

Owing to their characteristic intramolecular charge transfer, salicylaldiminato Schiff bases have been used as DNA cleavage.[27] Schiff base products obtained from aminopyridines and o-hydroxyaromatic aldehydes have been demonstrated to serve as analytical reagent[28-30] for metal analyses, hence encouraging investigations of the corresponding metal complexes.

Schiff bases are also known to have wide range of applications in organic syntheses: reduction to amines,[31] addition to –C=N- bond,[32] they undergo radical dimerization[33] and it is possible to add to the carbonyl atoms of ketoses. Schiff bases have been used for the synthesis of β-lactams.[34]

In addition to biological activities, application in organic syntheses , salicylidine types of Schiff bases are known to exhibit photochromism[35-37] and thermochromism, [38,39] hence their application in various areas such as the control and measurement of radiation, intensity, display system and optical computers.[40]

They have played a significant role in the development of coordination chemistry because they readily form stable complexes with most transition metals. Schiff base compounds are often used as ligands in coordination chemistry owing to their metal binding ability, and in particular salicylaldimines are useful for the synthesis of transition metal complexes. For instance, ortho hydroxylated Schiff bases have received an overwhelming attention as a result of their ability to form stable complexes.[41,42.]

2.2.2 Metal complexes derived from Schiff bases

There are a huge number of publications confirming structures and stereochemistry of metal complexes of Schiff bases. The information resulting from spectral and magnetic measurements

have been used to determine the structures of these complexes. Schiff bases complexes have interesting catalytic and biological activities.

Tetradentate Schiff bases with a N_2O_2 donor atom set are well known to form complexes with various metal ions;[43-45] consequently, many researchers have been attracted to studying their physicochemistry to biochemistry. Symmetric tetradentate Schiff base complexes of cobalt(II) have been used extensively as macrocyclic models.[46] They have provided a foundation for the building of contemporary macrocyclic chemistry.

Considerable attention has been paid to the chemistry of metal complexes of Schiff bases containing nitrogen and other donors. This is attributable to their importance in oxidative catalysis, electrochemistry and potential application in many other fields.[47] Schiff bases complexes have been used as blue emitter and showed good stability in electroluminescent devises with good efficiency.[48] Schiff base complexes have been used in organic reactions as redox catalysts. Worthy of mentioning is oxidation of alcohols by many ruthenium Schiff base complexes.[49-51.]

Many Schiff base complexes have been found to have interesting biological properties such as antitumor activity.[25,52-54]

Earlier work has shown that some drugs show increased activity when administered as metal chelates rather than as organic compounds.[55,56] For instance, the screening of cobalt complexes of Schiff bases of salicylaldehyde prepared earlier[24,25] against the im Walker sarcoma 256 of rat and animal tumors illustrate this facts.[25,57] Results of screening on the tested compounds show that most of the compounds have significant activity on the tumor system. However, it was difficult measuring their antitumor activities because of their low solubilities in both aqueous and organic media. Consequently, they were administered as suspensions, and it was believed that the particle size may have affected their antitumor activity. Inflammatory activity of cobalt(II) complex of 2-salicylideneaminopyridine has been reported.[23] Some Schiff base complexes are known to have antimicrobial activities.[58,59] Co(II) complexes have been used to model biological processes.

2.2.3 Synthesis of Schiff bases

Owing to the relative simple preparation procedures, it is possible to obtain Schiff bases having different characteristics by selecting appropriate reactants. The condensation of primary amines with aldehydes or ketones gives products known as imines which contain a C=N double bond. These compounds rapidly decompose or polymerize unless there is at least an aryl group bonded to the nitrogen or to the carbon atom. The latter imines are called Schiff bases, since their synthesis was first reported by Schiff. [60]

The most common method of obtaining a Schiff base is indicated below. An aldehyde or a ketone (A) combines with primary amine (B) to give Schiff base (D) and water. Hemiaminal (C) is formed as an intermediate product. The nature of amine as well as that of carbonyl determines the position of equilibrium.[31] When diphenyl or phenylalkyl ketones are used, it is advisable to remove water as it is formed by distillation or by using an azetrope-forming solvent to enhanced quick formation of the required product.[61,62]

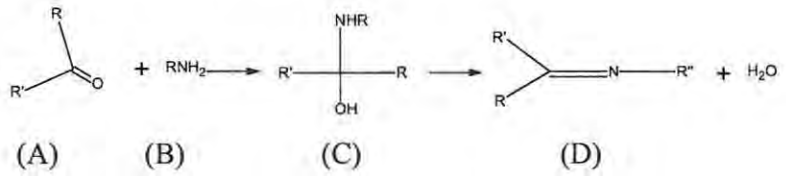

(A) (B) (C) (D)

Scheme 2:1 Synthesis of a Schiff base from an aldehyde or a ketone with a primary amine

Aromatic aldehydes react smoothly under mild conditions and at low temperature in a suitable solvent or without it. In the formation of Schiff base by condensation of an aromatic amine with an aromatic aldehyde, electron-attracting substituents in the para position of the amine reduces the rate of reaction, while increasing it when on the aldehyde.[63]

Dayagi and Degani reviewed other methods of preparing Schiff base, reactions of carbonyl groups with amino groups and other related reactions.[64] However, it must be noted that few Schiff bases commonly used as ligands have been prepared and characterized in the uncomplexed state, since the corresponding metal complexes have been directly obtained using other methods.[31] For example, many Schiff base metal complexes may be obtained directly by reaction between metal ions, aldehydes and amines.[31] In the formation of azomethines, both syn

and anti isomers may be formed.[64] As a rule, the isolation of a pure isomer is impossible, because the energy barrier between them is low.[64]

Schiff bases derived from o-hydroxybenzaldehyde and related aldehydes are stabilized by chelate formation, and can be isolated. Although an azomethine is usually formed by the condensation of an amine and an aldehyde or ketone, it must be noted that in a few cases the tautomeric enamine is more stable and is the one which is preferably obtained.[65]

2.2.4 Spectroscopic properties

All the C=N stretching frequencies of the ligands occur in the region between 1680-1603 cm^{-1} when H, alkyl or phenyl groups are bonded to carbon and nitrogen atoms.[66] The position of the stretching frequency in the range mentioned above is affected by the following factors:[66] the physical state of the compound, the nature of the substituent groups, conjugation with either carbon or nitrogen, or both, and hydrogen bonding.

Fabian et al.[67] was reported to found a frequency range of 1650 – 1638 cm^{-1} for Schiff base of the type Ar-CH=N-R when Ar is an unsubstituted phenyl group, while Suydam[68] reported a smaller range of 1650 – 1645 cm^{-1}. The range[67] widens to 1656 – 1631 cm^{-1} if nitro or halogen is present in the phenyl ring. Frequency region of 1631 – 1613 cm^{-1} were found for the compounds of the type Ar-CH=N-Ar.[69] The presence of an OH groups at the 2-position of the phenyl ring effects a red shift (bathochromic) with a frequency shift of about -8 cm^{-1} using N-benzylideneaniline as a reference.[70,71]

A lot has been published on the association between the OH and C=N groups and the effect of intramolecular hydrogen bond on the C=N stretching frequencies.[72-78] The bathochromic shift observed is expected for a chelated hydrogen bonded system but the corresponding shift in the C=O stretch for salicylaldehyde is well known to be much larger. This has been attributed to intramolecular hydrogen bond formation, with the benzenoid form (E) preferred over the quinoid one (F).[31]

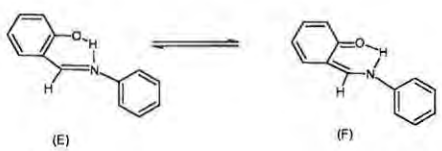

(E) (F)

Scheme 2:2 Enol and keto tautomers

In these compounds, the phenolic C-O stretching vibration occurs between 1288 and 1265 cm^{-1}. A decrease of the C=N frequency is generally observed upon coordination to metal ions through both O and N.[31] Curran and Sigga,[66] Sandorfy[79] reported IR spectra and properties of Schiff bases, covering the literature until 1970. Recent work on the characterization of Schiff bases agreed with this earlier review.

Notable among the recent characterization of Schiff bases are the work of Yeap et al.;[40] Gust et al.;[80] Ramesh and Maheswaran;[81] Zhoa et al.;[82] Zolezzi et al.;[83] Yildiz et al.;[84] Nazir et al.;[85] Berkesi et al.;[86] Al-Allaf and Sheet;[87] Guofa et al.;[88] etc. They all directed their efforts looking at changes in the stretching frequencies of C=N, OH and C-O of Schiff bases and complexes. The information obtained has been used to predict tautomeric nature of the Schiff bases.

NMR studies have been mainly used to elucidate the structural features[66] of the Schiff bases in solution. For instance, proton n.m.r. was used by Staab et al.[89] to elucidate the syn- and anti-isomerism of Schiff bases. Dudek and his coworkers[65, 90-92] studied the keto-enol equilibria in a variety of Schiff bases obtained from ketones. Recently, Cimerman et al.;[37] Nazir et al.;[85] Yeap et al.;[40] Yildiz et al.[84] etc. used the signals of the methine and hydroxyl protons to determined whether a Schiff base is enol-imino or keto-amine tautomer . However, the existence of phenol-imine or ketone-amine tautomer in solution depends on the intra molecular hydrogen bonding. Salman and coworker [93] claimed that keto-amine tautomerism is dominant in naphthaldimine, while phenol-imine is dominant in salicyladimine Schiff bases, depending on the solvent polarities.

The Schiff bases have been previously studied using electronic spectroscopy. [35, 94-96] Electronic spectra of salicyladimine ligand in methanol solution have been previously presented[95,97] Bonnett[98] reviewed the electronic spectra of many azomethines including Schiff bases. The UV/vis spectra of several 2-hydroxy Schiff bases have also been studied in both polar and non-polar solvents.[84, 99-101] They agreed that the appearance of any bands greater than 400 nm is an indication of the presence of keto form of Schiff base. In the Schiff base obtained from condensation of salicylaldehyde and aniline, no new band at > 400 nm was observed in polar and non-polar solvents, but it was observed in acidic media.[102]

The Schiff bases synthesized by Abd-Elzaher[103] exhibited three peaks at about 270, 333 and 372 nm and were characterized as follows: The first two peaks were attributed to benzene $\pi \rightarrow \pi^*$ and imino $\pi \rightarrow \pi^*$ transitions while 372 nm was assigned to $n \rightarrow \pi^*$ transitions. Ramesh and Maheswaran[81] also assigned 295-249 nm and 330-346 nm to $\pi \rightarrow \pi^*$ and $n \rightarrow \pi^*$ transitions to the C=N of the Schiff bases. However,[82] Zhoa et al. assigned the band at 334 nm to the azomethine chromophore $\pi \rightarrow \pi^*$ transition while the bands at higher energies (212 and 281 nm) were regarded as associated with the benzene $\pi \rightarrow \pi^*$ transition.

In the complexes, the azomethine chromophore $\pi \rightarrow \pi^*$/ $n \rightarrow \pi^*$ transition always shifted to lower or higher wavelength depending on the Schiff base or/and the metal, and it is constantly used as an indication that the imino nitrogen is involved in coordination to the metal ion. The bands assigned to benzene $\pi \rightarrow \pi^*$ transitions are always slightly affected.

Elias and Gillis[104] studied a series of substituted N-benzylideanilines using mass spectrometry. They found that the molecular ion was the base peak in all except for *ortho* substituted compounds. *Meta* and *para* substituted compounds all went through loss of the azomethine proton to yield $(M-1)^+$, with peak of variable intensity. Peaks typical of aromatic structures were observed. It was observed that fission was more easily accomplished at the ring-nitrogen bond rather than at the ring-carbon bond.

Spectra obtained from *ortho* substituted compounds are decidedly different[66] from *meta* and *para* compounds. Peaks were interpreted in terms of four-membered ring formation.

2.2.5 Photochromism and thermochromism

As earlier highlighted, salicylidine types Schiff bases may exhibit thermochromic or photochromic properties. These attention grabbing properties are connected to structural features[85] i.e., the exhibition of the property is linked to the possibility of proton transfer complex formation.

Photochromism is the ability to color markedly under UV irradiation. This phenomenon has been explained by authors[31,36] to be due to a reversible tautomerism with the quinoid structure of the salicylidine as depicted in scheme 2:2. According to Ledbetter, an intermolecular hydrogen bond bridge between the o-hydroxy and the imine groups is a requirement for the process. The

tautomerism occurs through an intramolecular hydrogen transfer. The salicylaldehyde Schiff base was observed to change color from yellow to red.[97]

Thermochromism is a thermally induced change in color which increases with an increase of the temperature. This phenomenon has also been attributed to intermolecular hydrogen transfer,[60] such as that depicted in scheme 2 above. The presence of ortho hydroxyl group favors the existence of intramolecular hydrogen bonding (O–H· · ·N and O· · ·H–N), hence the tautomerism which accounts for the formation of either enol-imino or keto-amino tautomer.

Both processes are reversible and mutually exclusive[60] for the same compounds in a given crystalline form. However, since the same compound may exhibit polymorphism, it may be thermochromic in one crystalline form and photochromic in the other.

2.2.6 Ligands and metals chelates of aniline, 1-aminonaphthalene, aminopyridine and aminoalkylpyridine with derivatives of substituted hydroxybenzaldimines

This section of work reviews the available information specific to the ligands and complexes synthesized and employed in the present study. However, most of the compounds synthesized are novel.

Ettling[105] in 1840 was reported to be the first to isolate the first metal complexes while in 1869, Schiff[60] characterized them. Ligands which bear a functional group, usually OH, near the site of condensation are effective in coordinating with the metals to form stable complex. Of all the Schiff base complexes, salicylaldimines have been the most thoroughly studied. Salicylaldimines have considerable flexible synthetic procedure, consequently making it possible to prepare a wide variety of them. Zhao et al.,[106] studied the photochromism of salicylaldehyde-derived Schiff bases from a view-point of structure-property relationship. They found that the π-conjugated system and the flexibility of the molecule skeleton play an important role in the determination of the photochromic behavior. Kodera studied the mechanism of photochromism processes of salicylidineaniline and its derivatives.[107]

Several reviews[108-112] have been published in relation to the chemistry of salicyladimine complexes. Syntheses, magnetic moments, paramagnetism, stereochemistry, crystal structures, dipole moments, polarography, stability constants, reactions of coordinated ligands, as well as

the proton and carbon NMR, electronic and IR spectra are variously addressed in these publications.

The νC=N and νC–O of several copper chelates of N-aryl salicylaldimines were assigned[113] 1616-1602 cm^{-1} and 1330-1310 cm^{-1} respectively. Similar assignments were made by other workers for complexes of various imines and diimines of o-hydroxylcarbonyl.[114,115]

Bamfield[116] reacted cobalt chloride with N-phenylsalicylideneimine in ethanol to form a green complex which is shown to be tris-[2-(N-phenylaminomethylene)cyclohexa-3,5-dien-1-one]cobalt(II) chloride. On treatment with a base, the green complex is deprotonated and loses one molecule of the ligand to give bis-(N-phenylsalicylideneiminato)cobalt(II). The complexes were characterized by elemental analyses, IR, magnetic susceptibility, molar conductivity and mass spectral data. Pseudo-tetrahedral arrangement of ligands around the cobalt(II) ion was suggested. West[117] studied the magnetic moments and structures of some N-substituted salicyladimine complexes of cobalt(II). The results of the magnetic moments indicated that the complexes had tetrahedral configuration in the solid state and in benzene solution but took up pyridine to assume an octahedral configuration in pyridine. Kurzak et al.,[5,118] studied UV-VIS-NIR spectroscopy and color of bis(N-phenylsalicyladiminato)cobalt(II) in a variety of solvents. They used electronic spectra to postulate tetrahedral geometry for the species in solution.

Balog,[119] prepared a series of iron(III) complexes from aromatic Schiff bases derived from o-vanillin and a series of amines. He studied the absorption spectra of the compounds in ethanol, pyridine, and dimethylsulphoxide.

Zelentsov et al.,[120] synthesized the chelate compounds of Co(II) with substituted N-phenyl-o-vanylalimines. They measure the magnetic susceptibility at 80-300 K and used the results to determine the stereochemistry and also to evaluate the parameters of electronic structure of chelates.

Csaszar and Balog[121] studied UV, visible, and IR spectra of Schiff bases formed from salicylaldehyde and o-vanillin with aniline and substituted anilines. At 400- 450 nm, an intense band indicative of benzoid-quinoid tautomer equilibrium was observed. They found correlations between the intensities of these bands, the tautomer equilibrium constants, and the dielectric constants of the solvents. Yeap et al.,[41] also synthesized eight Schiff bases derived from 2-

hydroxy-3-methoxybenzaldehyde and different para-substituted anilines. The structures of the Schiff bases were elucidated by physical measurements and FT-IR, NMR assignments were made using 1D and 2D NMR. Vladimirtsev et al.[122] evaluated the biological activity of benzylideneaniline and salicyladimine derivatives on oats, lettuce, and cucumber seedlings. The phytotoxic properties of the compounds were also determined. Salicylalaniline derivatives were found to be the most toxic.

Chatterjee and Douglas[123] studied the near ultraviolet spectra of some o-hydroxy aromatic Schiff bases, while Abramenko[124] synthesized a series of azomethines by reacting derivatives of benzaldehyde or salicylaldehyde with aromatic amines having different substituents in the aromatic ring, and then explain the influence of electronic and steric factors on the composition and properties of the compounds. They also investigated the syntheses of molecular complexes of $MoOCl_4$ with azomethines.

Brown and Nonhebel[125] used NMR to studied intramolecular hydrogen bonding in Schiff bases of o-hydroxy carbonyl and β-diketones. They concluded that equilibrium mixtures of the keto-enamine and enol-imine forms exist. The influence of electronic effects in the aromatic amines in the hydrogen-bond strength was also investigated. Yoshida and Yamada[126] synthesized cobalt(II) complexes of Schiff bases derived from 3-methoxysalicylaldehyde and amines. Terent've et al.[127] synthesized and studied some properties of ortho-substituted azomethines and their copper and cobalt chelates. Ohmori et al.[128] studied the electronic chemical oxidation of Schiff bases derived from o-vanillin and various primary amines. Csaszar et al.[129] studied the electronic spectral data for the Schiff bases formed from the condensation of 2-, 3-, or 4- HOC_6H_4CHO with anilines, aminopyridines, hydrazine, or alkylenediamines. The data they obtained indicated that in certain cases quinoid tautomers were formed. However, they were not able to observe these tautomers by IR and NMR, possibly because of solvents used. They discussed the linear free energy relationship for the substituents. Katayama et al.,[130] studied the effect on N-(2-hydoxy-3-methoxybenzylidene)aniline by a method of two dimensional correlation analysis using NMR. Csaszar[131] also studied the spectra and molecular conformations of aromatic Schiff bases. He calculated torsional angles of the aniline ring in numerous benzylideneanilines and hydroxy-benzylideneanilines from spectral data. Viswanathamurthi et al.,[132] synthesized several ruthenium(II) complexes by reacting ruthenium with Schiff base derived from o-vanillin with aniline, o-toluidine in benzene in the presence of NEt_3. The new complexes were characterized from elemental analyses, IR, electronic, EPR and cylic voltammetry. They tentatively proposed

an octahedral structure for all the complexes. The Schiff bases and their complexes were tested in vitro against pathogenic fungi, *Aspergillus* and *Fusarium* species.

A number of workers have reported the preparation of Schiff base derived from o-vanillin and aniline. It has been used as lubricating composition as a result of its antifriction; anti-wear properties.[133-135] Cui and Song[136] studied the indium complex of Schiff base derived from o-vanillin with aniline. The complexes and the ligands were characterized by elemental analysis, IR, UV, and NMR. Possible structure and antifungal activities of the compounds were studied.

Suzuki and Arai[137] studied the photochromism and thermochromism of hydrogen bonded Schiff bases. They examined equilibrium between the enol and keto form in the triplet state of salicylidineanilines and salicylidenebenzylamines in non-polar solvent, based on the observation of phosphorescence and triplet-triplet absorption spectra.

Lin et al.,[138] studied the effect of intermolecular O-H.....N-H bond and intramolecular O-H.....O-H bond in 2-methoxy-4-(phenyliminomethyl)phenol. They also reported the crystallography data of the compound. Nguyen et al.,[139] also prepared azomethines from vanillin derivatives and aromatic amines. They observed that azomethines of nitrovanillin have potent antibacterial and antifungal activities. Singh et al.[140] also synthesized a series of Schiff bases derived from vanillin and substituted aniline. They reduced the Schiff bases to secondary amines using $NaBH_4$.

Skorokhod et al.,[141] synthesized Co(II) and Ni(II) complexes Schiff bases prepared by the condensation of 1-aminonaphthalene with salicylaldehyde. The compounds were characterized using X-ray powder diffraction, TG, measurements of magnetic susceptibility, and spectroscopy (IR and diffuse reflectance). A coordination number four were realized for most of the complexes.

Zhang et al.,[142] prepared and characterized the coordination compounds of rare earth chlorides with Schiff base derived from o-vanillin and vanillin with 1-aminonaphthalene. The general formulae were determined by elemental analyses.

Lui et al.,[143] also prepared and characterized the coordination compounds of rare earth nitrate with Schiff base derived from o-vanillin and 1-aminonaphthalene. They used elemental analysis,

IR spectra, Raman spectra, UV/vis spectra, molar conductance and thermal analysis to determine the formulae of the compounds. The infrared and Raman spectra of complexes derived from rare earth nitrates with Schiff base obtained from the condensation of o-vanillin and 1-aminonaphthalene were studied by Liu et al.[144]

Beringhelli et al.[145] studied the spectroscopic and spectromagnetic properties of cobalt(II) bis derivatives with Schiff bases obtained by condensation of 2-(aminomethyl)pyridine with salicylaldehyde and with 3-methoxysalicylaldehyde. The Schiff bases acted as a tridentate ligand, forming high-spin CoL_2, while magnetic measurements and electronic behavior indicate field distortion from octahedral symmetry.

Coppola et al.,[146] studied the mass spectrometric behavior of polydentate Schiff bases derived from 2-(aminomethyl)pyridine with 3-methoxysalicylaldehyde and six other aldehydes. Beringhelli et al.,[147] synthesized and characterized polydentate Schiff base cobalt(II) complexes and characterized by magnetic measurement, electronic diffused reflectance and ESR spectra methods. Their behavior in solid state and solution were also studied.

Oehmke and Bailar[148] isolated and characterized some coordination compounds of 2-(salicylideneaminomethyl)pyridine. They observed that the Co(II) complexes irreversibly absorbed one mole of elemental oxygen per mole of complex when exposed to air. Cimerman et al;[149] used Schiff bases derived from aminopyridines as spectrofluorimetric analytical reagents. Cimerman et al.[21,30,150,151] also conducted a series of work on tautomeric and protonation equilibria of Schiff bases of salicylaldehyde with aminopyridines, studies their structure and tautomeric properties as well as the use as highly sensitive analytical reagents.

Al-Allaf and Sheet[152,153] synthesized a series of Schiff bases from benzaldehyde, salicylaldehyde and 2- or 3-aminopyridine. The Schiff base complexes with platinum, palladium and nickel compounds were reported.

Shinlchiro et. al.,[154] synthesized and studied the crystal structure of copper with N-salicylidene-3-aminopyridine while Al-Allaf et al.,[155] reported the diorganotin(IV) complexes of Schiff bases derived from 2- or 3- aminopyridine with 2-hydroxy, 2-methoxy- or 2-hydroxy-3-methoxy-benzaldehyde. The complexes were screen against seven species of bacteria. Ayad et al.,[156] synthesized complexes of Cu(II) with Schiff bases derived from 3-amino- and 2-aminopyridine

and its derivatives with salicylaldehyde, then using elemental analysis, infrared, electronic spectra and DTA to characterized them. Hadjoudis and Moustakali-Mavridis,[157,158] studied the photochromic and thermochromic properties of N-salicylidene-2-, -3-, and -4-aminopyridines. Csaszar and Balog[159] prepared Ni complexes of Schiff bases of salicylaldehyde with the 3-, 4-, 5-, and 6 methyl derivatives of 2-aminopyridine. Chemical analysis, IR, electronic spectra and NMR were used to characterize them.

2.3 Linear Free Energy Relationship

2.3.1 Hammett and other substituents parameters

There exist a quantitative correlation between structure of compounds and their reactivity. These quantitative relationships have been widely studied. The Hammett equation[160,161] is one of the earliest and most familiar theories developed to account for this relationship. The Hammett equation (and its extended forms) has been widely used to study and interpret organic reactions and their mechanisms.[162] It has been used to treat almost every kind of organic reaction. It relates equilibrium and rate constants for the reactions of *meta*- and *para*- substituted benzene derivatives. The existence of correlation between the acid strengths of benzoic acids and the effects of substituents in benzene derivatives reactions, led Hammett to proposed a general quantitative relationship between the nature of substituents (R) in such a system and the reactivity of a side chain *meta* or *para* to R. Hammett equation can be written as

$$\log(k / k_o) = \sigma\rho \quad \ldots\ldots\ldots\ldots (1)$$

Here k and k_o are rate or equilibrium constants for the reactions of the substituted and unsubstituted compounds respectively; σ denotes the substituents constant, and its depend on the rate of the reaction and the nature of the side chain. The reaction constant is denoted as ρ. While σ measures the electron releasing or electron withdrawing ability of the substituents relative to the hydrogen atom, ρ measures the sensitivity of the reaction to the ring substitution.

The ionization of benzoic acid has been arbitrarily chosen as a standard reaction for type in which ρ is fixed as unity while σ has its value set to zero. A positive value for σ indicates that the

substituent withdraws electrons relative to the hydrogen atom, while a negative value indicates that electrons are released.

The Hammett relationships have been used successfully for the determination of substituent parameters in *meta-,* and *para*-substitution. Due to steric interference which makes quantitative relationship unrealistic, Hammett relationship has not been used for *ortho*-substituents.

Jaffe[163] recalculated Hammett's substituent constants values using more recent values of ionization and rate or equilibrium constants obtained for a wide series of reactions. McDaniel and Brown[164] re-determined σ_m and σ_p values for the ionization of substituted benzoic acids and recommended that these values be used for the substituent constants rather than the mean values obtained from all available reactions. The attempt to extent Hammett equation to a linear combination of fundamental components of the substituent constants was the more exacting and far more useful solution. Taft and Lewis[165] suggested the extended Hammett equation. Their suggestion led to the introduction of both inductive and resonance effects. Swain and Lupton[166] made a fresh appraisal of the field and, invoking fewer assumptions than earlier studies, introduced pure Field (F) and resonance (R) constants and were shown to have the qualitative characteristics of σ_I and σ_R respectively.

Infrared spectroscopy has been extensively used in substituted aromatic, heterocyclic and aliphatic compounds to confirm that correlation exist between the substituent constants and the frequencies of various ligand vibrations. It has been reported that linear correlations exist between σ and σ^* and the symmetric and asymmetric νN-H of anilines,[167] and amines, νC=O of aliphatic ketones.[168] and νO-H of phenols[169]

In the field of coordination chemistry, correlations have been established between substituent constants σ or σ^* and νM-L in metal (II) salicylaldimines complexes, [170-172] νCo-N for aniline and pyridine adducts of the dinitrobis(acetylacetonate)Co(III) ion[176] etc.

There are numerous reports on how nuclear magnetic resonance have been used to show correlations between substituent constants and the chemical shifts of various protons in organic molecules.[173] The single substituent parameter approach which represent is represent by the equation has been used to correlate the chemical shift of *m*- and *p*-substituted compounds using

the Hammett σ_m and σ_p values. Slater et al.,[174] reported values of $^{13}\sigma$ for system of *m*- and *p*-substituted cinnamic acids in order to have a better correlation of ^{13}C chemical shift. Another approach which divides the effect of substituent effect into Swain and Lupton's inductive and resonance parameters have also been used to show correlation between substituent constant and the chemical shift. The approach is called dual substituent parameter.[175]

$$\delta = \rho\sigma + \delta_o \quad \ldots\ldots (2)$$

$$\delta = \rho_I\sigma_I + \rho_R\sigma_R + \delta_o \quad \ldots\ldots (3)$$

2.3.2 Quantitative Structure-Activity Relationship (QSAR)

While Hammett was successful in treating the electronic effect of substituents on the rates and equilibrium of organic reactions, Taft and other workers complements Hammett efforts by extending Hammett equations to accommodate virtually all compounds. From late 1970s, octanol / water partition coefficients (P) were introduced to explain the hydrophobic effects of organic compounds interacting with biological systems.[176] The combination of electronic and steric parameters with log P (for whole molecule) or π (for substituent), has opened up whole new regions of biochemical and pharmacological reactions to study.[165.]

Crowin Hansch extended the concept of linear-free energy relationships (LFER) to describe the effectiveness of a biologically-active molecule. He quantitatively relates the structure of a compound to its activity.[177] The combination of electronic, steric, hydrophobic, hydrophilic, and hydrogen-bonding parameters[178] has been used to derive quantitative structure-activity relationship (QSAR) for a host of interactions of organic compounds with living systems or parts thereof. Today, these equations are also called quantitative structure-property relationships (QSPR). From these equations, electronic and lipophilicity (also called hydrophobicity) have been the commonest properties that have been used to correlate biological activity. σ, Hammett value is used to measure electronic parameter while π, a lipophilicity constant developed specifically for QSAR by Hansch, is used to measure lipophilicity. Many other parameters have been investigated using QSAR equations, but none have found the wide acceptance of π and σ.[179]

The binding of organic compounds to proteins,[180] their interactions with enzymes, tissues[181] and cells,[182] their uses as anti–malarial[183] and antitumor agents, [182, 184] their inhibition of organelles, as well as their use in pesticide design, in toxicology, in mutagenicity, etc have all been treated

via QSAR.[165] QSAR applications to biological systems, drugs, pesticides, toxicology, etc has led to the explosive growth of correlation analysis of biological processes via substituent constants, hence has change the focus in the development of substituent constant. It must be noted that the parameters can only be useful if a series of compounds are prepared.[179] These sets of compounds should have different substituents with a range of properties (electron-donating/withdrawing and lipo/hydrophilic) and measurable biological activity. Linear regression analysis can then be used to determine a best-fit line for the data that would be generated.

2.4 References

1. S. K. Eajpai, P. R. Shukla, Ind. J. Pharmac.; 1975, **7**, 21-25.
2. M. D. Sergej, I. Levitin, L. Bubnovskaya, A. Sigan, I. Ganusevich, V. Michailenko, T. Kovelskaya, 6th Internet World Congress for Biomedical Science.
3. R. L. Carlin, *Stereochemistry of cobalt(ii) in transition metal chemistry*, A series of advances vol. 1, Edward Arnold (Publisher) Ltd., London, Marcel Dekker, Inc., New York, 1965.
4. D. Nicholls, *Comprehensive inorganic chemistry*, J.C. Bailar, H.J. Emeleus, R. Nyholm, A.F. Trotman-Dickenson (Eds.), Pergamon Press, Oxford, 1973.
5. I. Kuzniarska-Biernacka, A. Bartecki, K. Kurzak, Polyhedron, 2003, **22**, 997-1007.
6. F. A. Cotton, R. H. Holm, J. Am. Chem. Soc.; 1960, **82**, 2979-83.
7. F. A. Cotton, R. H. Holm, J. Am. Chem. Soc.; 1960, **82**, 2983-86.
8. M. Goodgame, F. A. Cotton, J. Phys. Chem.; 1961, **65**, 791-2.
9. F. A. Cotton, R. H. Soderberg, J. Am. Chem. Soc.; 1962, **84**, 872-9.
10. A. D. Liehr, J. Phys. Chem.; 1963, **67**, 1314-1328.
11. R. L. Carlin, Transt. Met. Chem.; 1965, **1**, 1-32
12. D. M. L. Goodgame, M. Goodgame, Inorg. Chem.; 1965, **4**, 139-143.
13. H. A. Weakliem, J. Chem. Phys.; 1962, **36**, 2117-40
14. J. Ferguson, J. Chem. Phys.; 1963, **39**, 116-28.
15. F. A. Cotton, D. M. L. Goodgame, M. Goodgame, J. Am. Chem. Soc.; 1961, **83**, 4690-9.
16. J. Ferguson, D. L. Wood, C. K. Knox, J. Chem. Phys.; 1963, **39**, 881-9.
17. R. Schlapp, Wm. G. Penney, Phys. Rev.; 1932, **42**, 666-86.
18. B. N. Figgis, R. S. Nyholm, J. Chem. Soc.; 1959, 338-46
19. B. N. Figgis, J. Lewis, Prog. Inorg. Chem.; 1964, **6**, 37-39.
20. A. D. Garnovskii, A. L. Nivorozhkin, V. I. Minkin, Coord. Chem. Rev.; 1993, **126**, 1-69.
21. Z. Cimerman, R. Kiralj, N. Galic, J. Mol. Struct.; 1994, **323**, 7-14.
22. D. Voet, J. G. Voet, *Biochemistry*, Wiley, New York, 1995.
23. R. K. Parashar, R. C. Sharma, A. Kumar, G. Mohan, Inorg. Chim. Acta, 1988, **151**, 201-8.
24. E. M. Hodnett, W. Willie, Proc. Okla. Acad. Sci., 1966, **46**, 107.
25. E. M. Hodnett, W. J. Dunn, III, Journal of Chemistry, 1970, **13**, 768-70.
26. R. L. Revees, J.Org. Chem., 1965, **30**, 3129-35.
27. H. Y. Shrivastava, M. Kanthimathi, B.U. Nair, Biochem. Biophys. Res. Commum., 1999, **265**, 311-19.

28. S. Yamada, K. Yamanouchi, Bull Chem. Soc. Jpn., 1969, **42**, 2562-6.
29. G. A. Kolawole, J. Coord. Chem., 1987, **16**, 67-73.
30. Z. Cimerman, N. Galic, B. Bosner, Anal. Chim. Acta; 1997, **343**, 145-153.
31. S. Patai, *The chemistry of carbon-nitrogen double bond*, Wiley, New York, 1970, 276.
32. K. Harada, *The chemistry of carbon-nitrogen double bond*, S. Patai (Ed.), Wiley, NY, 1970, 266.
33. H. Tanaka, H. Dhimane, H. Fujita, Y. Ikemoto, S. Torii, Tetrahedron Lett.; 1988, **29**, 3811-14.
34. M. J. Brown, Heterocycles; 1989, **29**, 2225-44.
35. M. D. Cohen, G. M. J. Scmidt, S. Flavian, J. Chem. Soc.; 1964, 2041-51.
36. M. D. Cohen, G. M. J. Scmidt, J. Phys. Chem; 1962, **66**, 2442-5.
37. E. Hadjoudis, J. Photochem.; 1981, **17**, 355-63.
38. N. Hoshino, T. Inabe, T. Mitani, Y. Maruyama, Bull. Chem. Soc. Jpn.; 1988, **61**, 4207-14.
39. R. Nakagaki, T. Kobajyashi, J. Nakamura, S. Nagakura, Bull. Chem. Soc. Jpn., 1977, **50**, 1909-12.
40. G. Y. Yeap, S.T. Ha, N. Ishizawa, K. Suda, P. L. Boey, W. A. K. Mahmood, J. Mol. Struct.; 2003, **658**, 87-89.
41. G. Y. Yeap, S.G. Teoh, S.B. Teo, S.C.. Loh, H.K. Fun, Polyhedron; 1996, **15**, 3941-3946.
42. Z. Popovic, V. Roje, G. Pavlovic, D.M. Calogovic, G. Giester, M. Rajic. Inorg. Chim. Acta.; 2001, **322**, 65-73.
43. R. Atkins, G. Breweg, E. Kakot, G. M. Mockler, E. Sinn, Inorg. Chem.; 1985, **24**, 127-34.
44. L. J. Boucher, C. G. Coe, Inorg. Chem.; 1976, **15**, 1334-40.
45. R. Yuan, Y. Chai, D. Liu, D. Gao, J. Li, R. Yu, R. Anal. Chem.; 1993, **65**, 2572-5.
46. D. Chen, A.E. Martel, Inorg. Chem.; 1987, **26**, 1026-30.
47. R. Ramesh, P. K. Suganthy, K. Natarajan, Synth. React. Inorg. Met.-Org. Chem.; 1996, **26**, 47-60.
48. T. Sano, N. Nisho, Y. Hamada, H. Takahashi, T. Usuki, K. Shibata, J. Mater. Chem., 2000 , **10**, 157-161.
49. M. G. Bhowon, H. L. K. Wah, R. Narain, Polyhedron; 1998, **18**, 341-345.
50. A. M. El-Hendawy, A. El.Ghany, A. E. El-Kourashy, M. M. Shanab, Polyhedron; 1992, **11**, 523-30.

51. A. M. El-Hendawy, A. H. Alkubaisi, A. El.Ghany, A. E. El-Kourashy, M. M. Shanab, Polyhedron; 1993, **12**, 2343-50.
52. S. K. Chattopadhyay, S. Ghosh, Inorg. Chim. Acta.; 1987, **131**, 15-20.
53. F. Bregant, S. Pacor, S. Ghosh, S. K. Chattopadhyay, G. Sava, Anticancer Res.; 1993, **13**, 10111-17.
54. P. J. Blower, Transition Met. Chem.; 1998, **23**, 109-112.
55. P. Singh, R. L. Goel, B. P. Singh, J. Indian Chem. Soc., 1975, **52**, 958-9.
56. A. Mohindru, J. M. Fisher, M. Rabinovitz, Nature; 1983, **303**, 64-5.
57. Anonymous, *Cancer Chemotherapy National Service Center* (CCNSC), Cancer Rep. 1962, **25**, 1- 18.
58. P. Sengupta, S. Ghosh, T. C. W. Mak, Polyhedron; 2001, **20**, 975-980.
59. C. Jayabalakrishnan, R. Karvembu, K. Natarajan, Trans. Met. Chem.; 2002, **27**, 790-794.
60. M. Calligaris, L. Randaccio, *comprehensive coordination chemistry, the synthesis, reactions, properties and applications of coordination compounds*, volume 2, G. Wilkinson, R.D. Gillard, J.A. McCleverty (Eds.), Pergamon Press, Oxford, 1987.
61. M. Freifelder, J. Org. Chem.; 1966, **31**, 3875-7.
62. R. B. Moffett, W. H. Hoehn, J. Am. Chem. Soc.; 1947, **69**, 1792-4.
63. E. F. Pratt, M. J. Kamlet, J. Org. Chem.; 1961, **26**, 4029-31.
64. S. Dayagi, Y. Degani, The *chemistry of the carbon-nitrogen double bond*, S. Patai,(ED.) Wiley-Interscience, New York, 1970, 67-129.
65. G. O. Dudek, G. P. Volpp, J. Am. Chem. Soc.; 1963, **85**, 2697-702.
66. D. J. Curran, S. Siggia, *The chemistry of the carbon-nitrogen double bond*, S. Patai (Ed.), Wiley-Interscience, New York, 1970, 162-180.
67. J. Fabian, M. Legrand, Bull. Soc. Chim, France; 1956, 1461-3.
68. F. H. Suydam, Anal. Chem.; 1963, **35**, 193-5.
69. L. E. Clougherty, J.A. Sousa, G. M. Wyman, J. Org. Chem.; 1957, **22**, 462-9.
70. H. H. Freedman, J. Am. Chem. Soc.; 1961, **83**, 2900-5.
71. Z. Meic, G. Baranovic, Pure Appl. Chem.; 1989, **61**, 2129-38.
72. A. W. Baker, A. T. Shulgin, J. Am. Chem. Soc.; 1959, **81**, 1523-9.
73. J. W. Ledbetter, J. Phys. Chem.; 1977, **81**, 54-9.
74. J. W. Ledbetter, J. Phys. Chem.; 1982, **86**, 2449-51.
75. K. Worzniak, H. He, J. Klinowski, W. Jones, T. Dziembowska, E. Grech, J. Chem. Soc. Faraday Trans.; 1995, **91**, 77-85.

76. A. G. J. Ligtenbarg, R. Hage, A. Meetsma, B. L. Feringa, J. Chem. Soc. Perkin Trans. 2; 1999, 807-12.
77. Z. Rozwadowski, E. Majewski, T. Dziembowska, H. P. Erik, J. Chem. Soc. Perkin Trans. 2; 1999, 2809-2812.
78. A. Filarowski, A. Koll, T. Glowia, J. Chem. Soc., Perkin Trans. 2; 2002, 835-42.
79. C. Sandorfy, *The chemistry of the carbon-nitrogen double bond*, S. Patai, (Ed.) Wiley-Interscience, New York, 1970, 37-60.
80. R. Gust, I. Ott, D. Posselt, K. Sommer, J. Med. Chem.; 2004, **47**, 5837-5846.
81. R. Ramesh, S. Maheswaran., J. inorg. Biochem.; 2003, **96**, 457-462.
82. Y, Zhou, X. Ye, F. Xin, X. Xin, Trans. Met. Chem.; 1999, **24**, 118-120.
83. S. Zolezzi, A. Decinti, E. Spodine, Polyhedron, 1999, **18**, 897-904.
84. M. Yildiz, Z. Kilic, T. Hokelec, J. Mol. Struct.; 1998, **441**, 1-10.
85. H. Nazir, M. Yildiz, H. Yilmaz, M. N. Tahir, D. Ulku, J. Mol. Struct.; 2000, **524**, 241-250.
86. O. Berkesi, T. Kortvelyesi, C. Hetenyi, T. Nemeth, I. Palinko, Phys. Chem. Chem. Phys.; 2003, **5**, 2009-2014.
87. T. A. K. Al-Allaf, A. Z. M. Sheet, Polyhedron; 1995, **14**, 239-248.
88. L. Guofa, S. Tongshun, Z. Yongnian, J. Mol. Struct.; 1997, **412**, 75-81.
89. H. A. Staab, F. Vogtle, A. Mannschreek, Tetrahedron Letters, 1965, 697-702.
90. G. O. Dudek, E. P. Dudek, J. Am. Chem. Soc.; 1964, **86**, 4283-7.
91. G. O. Dudek, R. H. Holm, J. Am. Chem. Soc.; 1962, **84**, 2691-6.
92. G. O. Dudek, J. Am. Chem. Soc.; 1963, **85**, 694-7.
93. S. R. Salman, S. H. Shawkat, G. M. Al-Obaidi, Can. J. Spect.; 1990, **35**, 25-30.
94. E. Hadjoudis, M. Vitttorakis, I. Moustakali-Mavridis, Tetrahedron; 1987, **43**, 1345-60.
95. M. D. Cohen, Y. Hirshberg, G. M. J. Schmidt, J. Chem. Soc.; 1964, 2051-9.
96. M. D. Cohen, Y. Hirshberg, G. M. J. Schmidt, J. Chem. Soc.; 1964, 2060-7.
97. J. W. Ledbetter, Jr., J. Phys. Chem. 1966, **70**, 2245-9.
98. R. Bonnett, *The chemistry of the carbon-nitrogen double bond*, S. Patai (Ed.), Wiley-Interscience, New York, 1970, 181.
99. Z. Popovic, G. Pavlovic, V. Roje, N. Doslic, D. Matkovic-Calogovic, I. Leban, Struct. Chem.; 2004, **15**, 587-598.
100. M. Yildiz, H. Unver, D. Erdener, N. Ocak, A. Erdonmez, T. Nur, Durlu, Cryst. Res. Technol.; 2006, **41**, 600-06.
101. H. Unver, D. M. Zengin, K. Guven, J. Chem. Crystallogr; 2000, **30**, 359-64.

102. H. Unver, E. Kendi, K. Guven, T. Nur, Durlu, Z. Natur. Forsch.; 2002, **576**, 685-90.
103. M. M. Abd- Elzaher, J. Chin. Chem. Soc.; 2001, **48**, 153-58.
104. D. J. Elias, R. G. Gills, Aust. J. Chem., 1966, **19**, 251-5.
105. C. Ettling, Ann., 1840, **150**, 241.
106. J. Z. Zhao, B. Zhao, W. Q. Xu, J.Z. Liu, Goadeng Xuexiao Huaxue Xuebao; 2003, **24**, 324-328, (CAN 139:108534).
107. Y. Kodera, Natl. Inst. Resour. Environ. Jpn.; 1994, **39(11)**, 279-89, (CAN 122:80765).
108. R. H. Holm, G. W. Everett, A. Chakravorty, Progr. Inorg. Chem.; 1966, **7**, 83-214.
109. L. Sacconi, Coord. Chem. Rev.; 1966, **1**, 126-132.
110. S. Yamada, Coord. Chem. Rev.; 1966, **1**, 415-437.
111. E. K. Barefield, D.H. Busch, S. M. Nelson, Quart. Rev. Chem. Soc.; 1968, **22**, 457-98.
112. R. H. Holm, M. J. O'Connor, Progr. Inorg. Chem.; 1971, **14**, 241-401.
113. J. E. Kovaic, Spectrochim. Acta, 1967, **23A**, 183-6.
114. E. L. Olszewski, D. F. Martin, J. Inorg. Nucl. Chem.; 1964, **26**, 1577.
115. P. Teyssie, J. J. Charette, Spectrochim. Acta, 1963, **19**, 1407-23.
116. P. Bamfield, J. Chem. Soc. (A); 1967, 804-808.
117. B. O. West, J. Chem. Sac.; 1962, 1374-8.
118. K. Kurzak, I. Kuzniarska-Biernacka, Pol. J. Chem.; 2001, **55**, 913-931.
119. J. Balog, Hung. Acta Phys. Chem. 1962, **8**, 111-122, (CAN 59:7051).
120. V. V. Zelentsov, A. P. Bogdanov, E. G. Rukhadze, G.P. Talyzenkova, Zh. Struk. Khimi, 1973, **14**, 564-6; CAN 79:119819.
121. J. Csaszar, J. Balog, Hung. Acta Chim.; 1975, **86**, 100-116.
122. I. F. Vladimirtsev, Yu.V. Karabanov, S. S. Khripko, I. V. Boldyrev, Fiziologicheski Aktivnye Veshchestva, 1966-1992, 1972, **4**, 136-8, (CAN 79:39226)
123. K. K. Chatterjee, B. E. Douglas, Spectrochim. Acta; 1965, **21**, 1625-31.
124. V. L. Abramenko, Russ. J. Coord. Chem.; 2001, **27**, 819-822.
125. N. M. D. Brown, D.C. Nonhebel, Tetrahedron; 1968, **24**, 5655-64.
126. E. Yoshida, S. Yamada, Bull. Chem. Soc. Jpn.; 1967, **40**, 1395-8.
127. A. P. Terent'ev, E. G. Rukhadze, G. P. Povolotskaya, E. M. Mosk, Zhurnal Obshchei Khimii, 1968, **38**, 93-99, (CAN 69:43572).
128. H. Ohmori, A. Matsumoto, M. Masui, H. Sayo, J. Electrochem. Soc.; 1977, **124**, 1849-54.
129. J. Csaszar, J. Balog, A. Makary, Hung. Acta Phys. Chem.; 1978, **24**, 471-84.

130. S. Katayama, S, Tani, Y. Akahori, S. Yamada, Yakugaku Zasshi, 1979, **99**, 1201-06, (CAN 92:214680).

131. J. Csaszar, Hung. Acta Phys. Chem., 1983, **29**, 133-138, (CAN 101:54140).

132. P. Viswanathamurthi, N. Dharmaraj, K. Natarajan, Syn. React. Inorg. Met-Org. Chem.; 2000, **30**, 1273-1285.

133. G. G. Chigarenko, A.G. Ponomarenko, G. P. Barchan, USSR Vestnik Mashinostroeniya, 1984, **2**, 47-49; CAN 100: 194673.

134. G. P. Barchan, G.G. Chigarenko, A.G. Ponomarenko, E. G. Rukhadze, G. P. Talyzenkova, 1980, (CAN 94:159548).

135. G. G. Chigarenko, A.G. Ponomarenko, V. S. Bolotnikov, V. A. Alekseev, A. S. Burlov, A. D. Garnovskii, G. P. Barchan, Trenie i Iznos, 1989, **10**, 1050-61, (CAN 113:26536).

136. G. H. Cui, Y. L. Song, Hebei Ligong Xueyuan Xuebao, 1998, **20**, 65-68, (CAN 129:239047).

137. T. Suzuki, T. Arai, Chemistry Letters, 2001, **2**, 124-125, (CAN 134:346352).

138. Z. D. Lin, Z.D. Lin, X. Li, Y, Huang, Acta Cryst. Sect. E; 2005, **E61**, 3032-3033, (CAN 144:160662).

139. K. T. Nguyen, T. S. Giang, M. B. Tran, Tap Chi Duoc Hoc, 1998, **3**, 9-10, (CAN 129:189079).

140. A. Singh, M. Rai, K. K. Singal, Ind. J. Chem.; 1975, **13**, 991-2, (CAN 84:73798).

141. L. S. Skorokhod, I. I. Seifullina, S. A Dzhambek, Russ. J. Coord. Chem.; 2002, **28**, 643-646.

142. L. Zhang, X, Xu, G. Liu, T. Shi, Synth. React. Inorg. Metal-Org. Chem.; 1999, **29**, 233-244.

143. G. Liu, Y. Zhao, X. Liu, Huaxue Xuebao, 1992, **50**, 473-8, (CAN 117:82354).

144. G. Liu, T. Shi, Y, Zhao, J. Mol. Struct.; 1997, **412**, 75-81.

145. T. Beringhelli, A. Gervasini, G. A. Franca; Dip. Chim. Inorg. Metallorg.; 1985, **115**, 181-6, (CAN 102:21414148).

146. M. Coppola, S. Catinella, P. Traldi, P. Guerriero, S. Tamburini, P.A. Vigato, Org. Mass Spec.; 1994, **29**, 566-70, (CAN 122:30858).

147. T. Beringhelli, F. Morazzoni, A. Giacomelli, M. Pasquali, Congr. Naz. Chim. Inorg., [Atti], 15th , 1982, 233-6, (CAN 100:150034).

148. R. W. Oehmke, J. C. Bailer, Jr., J. Inorg. Nucl. Chem.; 1965, **27**, 2209-15, (CAN 63:78179).

149. Z, Cimerman, S. Miljanic, N. Galic, Croatica Chem. Acta, 2000, **73**, 81-95.

150. Z. Cimerman, N. Galic, B. Bosner, Anal. Chim. Acta, 1997, **343**, 145-153.
151. Z. Cimerman, R. Kiralj, N. Galic, J. Mol. Struct.; 1994, **323**, 7-14.
152. Z. Cimerman, Z. Stefanac, Polyhedron, 1985, **4**, 259-268.
153. N. Galic, Z. Cimerman, V. Tomisie, Anal. Chim. Acta.; 1997, **343**, 135-143.
154. T. A. K. Al-Allaf, A. Z. M. Sheet, Polyhedron, 1995, **14**, 239-248.
155. T. A. K. Al-Allaf, A. Z. M. Sheet, Asian J. Chem. 1996, **8**, 305-14, (CAN 125:24842).
156. N. Shinlchiro, K. Mitsuru, K. Susumu, I. Tomohiko, M. Hiroyuki, Y. Masahiro, Mol. Cryst. Liq Cryst.; 2000, **342**, 231-236.
157. T. A. K. Al-Allaf, M. A. As-Shama'a, L. J. Rashan, Appl. Orgmet. Chem.; 1996, **10**, 545-548, (CAN 125:301120).
158. M. I. Ayad, S. A. Sallam, H. E. Mabrouk, Thermochim. Acta; 1991, **189**, 65-73.
159. E. Hadjoudis; I. Moustakali-Mavridis, Mol. Cryst. Liq. Cryst.; 1983, **93**, 61-67.
160. E. Hadjoudis, M. Vittorrakis, I. Moustakali-Mavridis, Tetrahedron; 1987, **43**, 1345-60.
161. J. Csaszar, J. Balog, Acta Chim. Acad.; 1975, **80**, 321-30, (CAN 84:173169).
162. L. P. Hammett, Chem. Rev.; 1935, **17**, 125-36.
163. L. P. Hammett, *Physical Organic Chemistry*, McGraw-Hill, New York, 1940, p. 148.
164. C. Hansch, A. Leo, R. W. Taft, Chem. Rev.; 1991, **91**, 165-195.
165. H. H. Jaffe, Chem. Rev.; 1953, **53**, 191-261.
166. D. H. McDaniel, H.C. Brown, J. Org. Chem.; 1958, **23**, 420-7.
167. R. W. Taft, Jr., I. W. Lewis, J. Am. Chem. Soc.; 1958, **80**, 2436-43.
168. C. G. Swain, E. C. Lupton, J. Am. Chem. Soc.; 1968, **90**, 4328-37.
169. P. J. Krueger, H. W. Thompson, Proc. Roy. Soc.; 1957, **234A**, 143-54.
170. H. W. Thompson, D. A. Jameson, Spectrochim. Acta.; 1958, **13**, 236-47.
171. P. J. Stone, H. W. Thompson, Spectrochim. Acta.; 1957, **10**, 17-20.
172. G. C. Percy, D. A. Thornton, J. Inorg. Nucl. Chem.; 1972, **34**, 3357-3367
173. G. C. Percy, D. A. Thornton, J. Inorg. Nucl. Chem.; 1972, **34**, 3369-76.
174. G. C. Percy, D.A. Thornton, J. Inorg. Nucl. Chem.; 1973, **34**, 3369.
175. C. A. Fleming, D. A. Thornton, Spectros. Lett.; 1973, **6**, 245-51.
176. D. J. Craik, R. T. C. Brownlee, Prog. Phys. Org. Chem.; 1983, **14**, 1-73, (CAN 99:138983).
177. C. D. Slater, C. N Robinson, R. Bies, D. W. Bryan, K. Chang, A.W. Hill, W.H. Moore, Jr., T. G. Otey, M. L. Popperlreiter, J. R. Reisser, G.E. Stablein, V.P. III. Waddy, W.O. Wilkinson, W.A. Wray, J. Org. Chem., 1985, **50**, 4125-30.
178. O.J, Kyu, S.U. Ji, K.L. Chang, Bull. Korean Chem. Soc., 2002, **23**, 1241-1246.

179. C, Hansch, A. Leo, *Substituents Concepts for Correlation Analysis in Chemistry and Biology*, Wiley-Interscience: New York, 1979.

180. C. Hansch, A. Leo, R. W. Taft, Chem. Rev.; 1991, **91**, 165-195.

181. C. Hansch, T. Fujita, J. Am. Chem. Soc.; 1964, **86,** 1616-1626.

182. M. H. Abraham, P. L. Grellier, D.V. Prior, R. W. Taft, J. J. Morris, P. J. Taylor, C. Laurence, M. Berthelot, R. M. Doherty, M. J. Kamlet, J. L. M. Abboud, K. Sraidi, G. Guiheneuf, J. Am. Chem.Soc.; 1988, **110**, 8534-6.

183. http://www.chm.davidson.edu/erstevens/QSAR/QSAR.thml, accessed 23/08/2006

184. F. Helmer, K. Kiehs, C. Hansch, Biochemistry; 1968, **7**, 2858-63.

185. M. H. Abraham, M. J. Kamlet, R. W. Taft, P. K. Weathersby, J. Am. Chem. Soc.; 1983, **105**, 6797-801.

186. C. D. Selassie, C. D. Strong, C. Hansch, T. J. Delcamp, J. H. Freisheim, T. A. Khwaja, Cancer Res., 1986, **46**, 744-56, (CAN 106:162).

187. K. H. Kim, C. Hansch, J. Y. Fukunaga, E. E. Steller, P. Y. C. Jow, P. N. Craig, J. Page, J. Med. Chem., 1979, **22**, 366-91, (CAN 90:161939)

188. W. A. Denny, B. F. Cain, G. J. Atwll, C. Hansch, A. Panthananickal, A, Leo, J. Med. Chem., 1982, **25**, 276-315, (CAN 96:79437).

3 Experimental (Physical and Chemical methods)

3.1 Physical methods

3.1.1 Mid infrared spectroscopy (MIR)

Mid infrared spectra were recorded on a Perkin-Elmer spectrum 2000 FT-IR spectrometer. The spectra were determined using a KBr beam splitter and a DTG detector, in the region 4000 - 400 cm^{-1} with typically 16 scans at an average resolution of 4 cm^{-1}. Samples were run in a KBr matrix as a pressed disc or as mulls in Nujol or hexachlorobutadiene on KBr windows. Due to the possibility of rearrangement or halide substitution brought about by the effect of pressure, the mull technique was adopted in preference to pellet die technique.

3.1.2 Far infrared spectroscopy (FIR)

Far infrared spectra were recorded on a Perkin-Elmer spectrum 2000 FT-IR spectrometer. The spectra were recorded in the region 650 – 100cm^{-1} with typically 64 scans and at an average resolution of 12 cm^{-1}. Samples were run as mulls in Nujol on polyethylene windows.

3.1.3 Nuclear magnetic resonance spectroscopy (NMR)

All ^{1}H and ^{13}C NMR spectra were recorded on an Avance Bruker AMX 400 MHz spectrometer. Base on the varying solubility properties of the ligands, deuterated chloroform, was used as solvent, while tetramethylsilane (TMS) was used as the internal reference. All spectra were recorded at ambient temperature. Chemical shifts were measured in parts per million (ppm) downfield of the reference signal.

3.1.4 Microanalyses

Carbon, hydrogen and nitrogen combustion microanalyses were carried out using a Fisons Elemental Analyzer 1108 CHNS-O, (University of Cape Town, South Africa and University KwaZulu-Natal, South Africa).

3.1.5 Cobalt analyses (ICP/MS)

The quantity of cobalt in all the isolated complexes were determined using inductively coupled plasma/ mass spectrometry, on a Perkin-Elmer Sciex ELAN 6100 ICPMS, (University of Port Elizabeth, South Africa).

3.1.6 Melting point

Melting points were determined using a Gallenkamp melting point apparatus. The results were uncorrected.

3.1.7 Mass spectrometry

Low resolution mass spectra were obtained using a Finnigam Mat LCQ ion trap mass spectrometer equipped with an electrospray ionization source. 2 mg of the Schiff bases were dissolved in chloroform.

3.1.8 Diffuse reflectance spectroscopy

The diffuse reflectance spectra of the ligands and the complexes were measured by using a Cary 500 UV/vis/NIS spectrometer fitted with a Cary diffuse reflectance accessory. The spectra were collected in % reflectance at a spectra bandwidth of 2 nm and at a rate of 200 nm / min between 200 – 800 nm for UV/vis measurement and 700 – 2000 nm for VIS – NIR measurement. PTFE powered was used as background. The spectra have been smoothened and derivatized by using the Savitsky-Golay method employing 45 and 55 convolution points for UV-VIS and VIS – NIR respectively. The spectra were then converted to absorbance for comparison with solution spectra.

3.1.9 Electronic spectra (UV/vis solution)

The ultraviolet –visible (UV/vis) spectra were recorded on a Varian Cary 500 spectrophotometer. The ligands and complexes were dissolved in DMF and methanol. The concentration after dissolving was approximately $C \sim 5.0 \times 10^{-4}$ M.

3.2 Synthetic methods

All chemicals were obtained from Sigma-Aldrich and used without further purification. All the chemicals used were of AnalaR grade. Aniline was distilled prior to use. The solvents were dried and distilled before use according to standard procedures.

3.2.1 Synthesis of Schiff bases

3.2.1.1 Aniline-based Schiff bases

The aniline based ligands were synthesized by the condensation of salicylaldehyde or its derivatives- (*ortho*-vanillin, *para*-vanillin and vanillin) and aniline dissolved in 95% ethanol, using published methods.[1-3] Thereafter, the methods were modified slightly when it was observed that the reported methods were not giving appreciable results, particularly with the salicylaldehyde derivatives. For all the syntheses, a 1:1 ratio of amine to aldehyde was used resulting in the targeted bidentate ligands.

3.2.1.1.1 Method 1

The Schiff bases (Scheme 3.1) were prepared by using the following standard methods with modifications where necessary. The aniline and the salicylaldehyde were purified under reduced pressure while the derivatives of salicylaldehyde were used as supplied. A 10 ml ethanolic solution of (0.456 ml, 5 mmol) aniline was refluxed with 10 ml ethanolic solution of salicylaldehyde (0.365 ml, 5 mmol) in 100 cm^3 round bottom flask, for 2, 3, 6 and 12 hours alternatively. After cooling, the precipitated product was filtered and recrystallized from ethanol, and then dried under reduced pressure over silica gel. The optimization study revealed that there was not much difference in the yields when the syntheses were done in 2, 3, 6, or 12 hours, hence, subsequent syntheses were carried out under reflux for 2hours. The general structure is shown in scheme 3:1.

3.2.1.1.2 Method 2

The aniline-based Schiff bases were also prepared by a modification of the reported method.[4] A 15ml of ethanolic solution of (0.912 ml, 10 mmol) aniline was slowly added to ethanolic solution of (0.730 ml, 10 mmol) salicylaldehyde or its derivates. The reaction mixture was stirred for two

hours at 40 – 50°C. The precipitate was cooled and collected by filtration. The precipitate was washed several times using distilled water, then cold ethanol, followed by recrystallization from ethanol and drying at 50°C. The ligands obtained using the methods highlighted above are listed in Table 3:1.

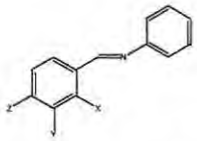

No.	X	Y	Z
1	OH	H	H
2	OH	3-OCH_3	H
3	OH	H	4-OCH_3
4	H	3-OCH_3	4-OH

Scheme 3:1 Aniline-based Schiff bases

Table 3:1 Aniline-based ligands

No.	Ligand	IUPAC name	Structure
1	saani	(E)-2-((phenylimino)methyl)phenol	
2	pvaani	(E)-5-methoxy-2-((phenylimino)methyl)phenol	
3	ovaani	(E)-2-methoxy-6-((phenylimino)methyl)phenol	
4	vaani	(E)-2-methoxy-4-((phenylimino)methyl)phenol	

3.2.1.2 1-Aminonaphthalene-based Schiff bases

The procedure for the preparation of 1-aminonaphthalene-based Schiff bases is typified by the following highlighted steps.

3.2.1.2.1 Method used for the syntheses of the 1-aminonaphthalene-based Schiff bases

An ethanolic (15 ml) solution of (0.761 g, 5 mmol) *o*-vanillin was added to ethanolic (15 ml) of (0.715 g, 5 mmol) aminonaphthalene. The equimolar mixture was refluxed for about 3 hours. The reaction mixture was then allowed to cool to room temperature. The formed crystals were collected, recrystallized from ethanol, and then dried under reduced pressure over silica gel or in

an oven at 50°C. The rate of the formation of the precipitated substances is substituents dependent. Scheme 3-2 represents the proposed general structures for the aminonaphthalene-based ligands. The substituents X, Y and Z are the same as depicted for Group 1 in Scheme 3:1

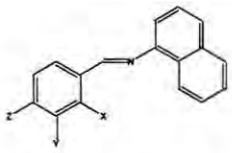

No.	X	Y	Z
5	OH	H	H
6	OH	3-OCH_3	H
7	OH	H	4-OCH_3
8	H	3-OCH_3	4-OH

Scheme 3:2 1-Aminonaphthalene-based Schiff bases

While it was possible isolating the Schiff bases 6, 7 and 8, it was almost impossible isolating the free Schiff base 5 as a solid.

Although it was difficult isolating Schiff base 5, Skorokhod et al.,[5] reported the synthesis of the ammonium salt. However, the reported product is different from the product synthesized in our laboratory because it is not the free Schiff base but rather the ammonium salts of the ligand, hence the difference in properties. Nevertheless, NMR, microanalysis and mass spectrometer were used to confirm the synthesis of this free ligand. The properties of this ligand when compared with the other three in the same series followed the expected pattern. The ligands isolated using the method highlighted above are listed in Table 3:2.

Table 3:2 Aminonaphthalene-based ligands

No.	Ligand	IUPAC name	Structure
5	sallamnap	(E)-2-((naphthalen-1-ylimino)methyl)phenol	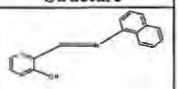
6	pvanlamnap	(E)-5-methoxy-2-((naphthalen-1-ylimino)methyl)phenol	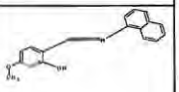
7	ovanlamnap	(E)-2-methoxy-6-((naphthalen-1-ylimino)methyl)phenol	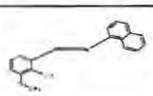
8	vanlamnap	(E)-2-methoxy-4-((naphthalene-1-ylimino)methyl)phenol	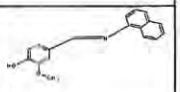

3.2.1.3 Aminopyridines and aminoalkylpyridines ligands

THF (tetrahydrofuran) was used as solvent for the syntheses of the 4-aminopyridine while ethanol was used for the syntheses of the 3-aminopyrdine-, 2- and 3-methylaminopyridine-based ligands. The procedure used in synthesizing the aminopyridines and the aminomethylpyridines is typified by the steps highlighted below:

3.2.1.3.1 Method used for the syntheses of the aminopyridine-based Schiff bases

A 10 ml hot ethanolic or THF solution of (0.730 ml, 10 mmol) salicylaldehyde or its derivatives was refluxed with 10 ml hot ethanolic solution of the aminopyridine (1.522 g, 10 mmol) in 100 cm^3 round bottom flask, for 2 to 3 hours. After cooling, the precipitated product was filtered and recrystallized from ethanol, and then dried under reduced pressure over silica gel. The proposed structures for the isolated Schiff bases belonging to groups 3 and 4 are shown in Scheme 3:3. While it was possible isolating the 3-aminopyridine-based Schiff bases, it was slightly difficult isolating the 4-aminopyridine-based analogues, particularly van4amp (ligand 12).

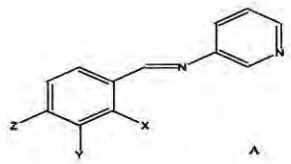

A

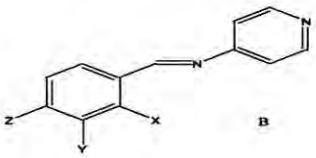

B

No.	X	Y	Z	No
9	OH	H	H	13
10	OH	3-OCH_3	H	14
11	OH	H	4-OCH_3	15
12	H	3-OCH_3	4-OH	16

Scheme 3:3 3-aminopyridine (A) and 4-aminopydine-based (B) Schiff bases

Table 3:3 4- and 3-aminopyridine-based ligands

No.	Ligand	IUPAC name	Structure
9	sal4amp	(E)-2-((pyridin-4-ylimino)methyl)phenol	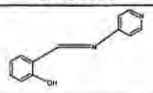
10	pvan4amp	(E)-5-methoxy-2-((pyridin-4-ylimino)methyl)phenol	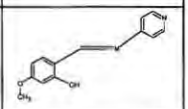
11	ovan4amp	(E)-2-methoxy-6-((pyridin-4-ylimino)methyl)phenol	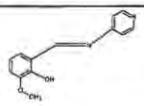
12	van4amp	(E)-2-methoxy-4-((pyridin-4-ylimino)methyl)phenol	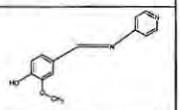
13	sal3amp	(E)-2-((pyridin-3-ylimino)methyl)phenol	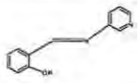
14	pvan3amp	(E)-5-methoxy-2-((pyridin-3-ylimino)methyl)phenol	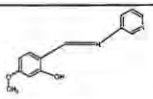
15	ovan3amp	(E)-2-methoxy-6-((pyridin-3-ylimino)methyl)phenol	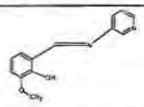
16	van3amp	(E)-2-methoxy-4-((pyridin-3-ylimino)methyl)phenol	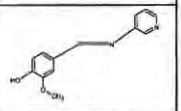

3.2.1.3.2 Method used for the syntheses of the aminomethylpyridine-based Schiff bases

The procedure for the syntheses of the 2- and the 3-aminomethylpyridine-based ligands is typified by the steps highlighted below: A 10 ml hot ethanolic solution of (1.522 g, 10 mmol) vanillin was refluxed with 10 ml hot ethanolic solution of the aminomethylpyridine (1.018 ml, 10 mmol) in 100 cm^3 round bottom flask, for 3 hours. The solvent was evaporated using Rotavapour till the volume of the mixture was approximately 5 ml, and it was cooled. 10 ml petroleum ether (60-80°C range fraction) was added to the mixture with constant stirring. Some of the ligands in these groups remained oil. The proposed general structures for the isolated Schiff bases belonging to these groups are shown in Scheme 3:4. The list of all the ligands obtained using the highlighted procedure for the syntheses are presented in Table 3:4.

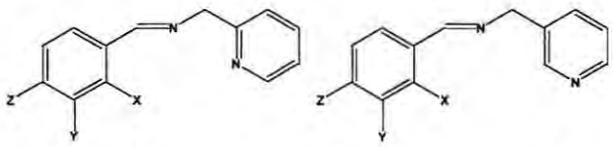

No.	X	Y	Z	No.
17	OH	H	H	21
18	OH	3-OCH_3	H	22
19	OH	H	4-OCH_3	23
20	H	3-OCH_3	4-OH	24

Scheme 3:4 2-aminomethylpyridine (A) and 3-aminomethylpyridine-based (B) Schiff bases

Table 3:4 3- and 2-aminomethylpyridine-based ligands

No.	Ligand	IUPAC name	Structure
17	sal3pico	E)-2-((pyridin-3-ylmethylimino)methyl)phenol	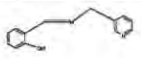
18	pvan3pico	E)-5-methoxy-2-((pyridin-3-ylmethylimino)methyl)phenol	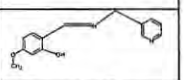
19	ovan3pico	E)-2-methoxy-6-((pyridin-3-ylmethylimino)methyl)phenol	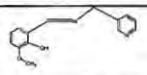
20	van3pico	(E)-2-methoxy-4-((pyridin-3-ylmethylimino)methyl)phenol	
21	sal2pico	E)-2-((pyridin-2-ylmethylimino)methyl)phenol	
22	pvan2pico	E)-5-methoxy-2-((pyridin-2-ylmethylimino)methyl)phenol	
23	ovan2pico	E)-2-methoxy-6-((pyridin-2-ylmethylimino)methyl)phenol	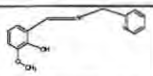
24	van2pico	(E)-2-methoxy-4-((pyridin-2-ylmethylimino)methyl)phenol	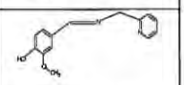

3.2.2 Syntheses of cobalt(II) complexes

For the syntheses of the complexes, cobalt acetate ($Co(CH_3COO)_2.4H_2O$) and cobalt chloride ($CoCl_2.6H_2O$) were used. The general methods outlined below were used for all the syntheses. However, when it was observed that the complexes obtained from the reaction of cobalt acetate with Schiff bases were not the same as those obtained from cobalt chloride, triethylamine was introduced using the idea of Hariharan and Urbach,[6] Balasubramaniam et al;[7] with some modifications to their methods. The complexes obtained were the same as the products formed from cobalt acetate. 2:1 ratios of the ligands to metal were used for all the syntheses of the complexes.

3.2.2.1 Cobalt chloride-based or cobalt acetate-based complexes

Dayagi and Degani[8] observed that few Schiff bases commonly used as ligands have been prepared and characterized in the uncomplexed state. Only the complexes of group 1 ligands (the aniline-based ligands) and 7A were synthesised from the Schiff bases, all others were synthesised in situ by the reaction between metal ions, salicylaldehyde or its derivatives, and the amines. The various methods used are typified by the three methods highlighted below.

3.2.2.1.1 Method 1

To an ethanolic solution (15 ml) of 1-aminonaphthalene (0.7160 g, 5 mmol) was added ethanolic solution (15 ml) of vanillin (0.7608 g, 5 mmol). The mixture was refluxed in a round bottom flask. After refluxing for 2 hour, the solution was allowed to cool at room temperature.

A methanolic solution (15 ml) of cobalt chloride ($CoCl_2.6H_2O$), (0.5948 g, 2.5 mmol) or cobalt acetate (0.6226 g, 2.5 mmol) was added to the ligand solution. The mixture refluxed for another 1 hour. The complex was allowed to crystallize. The crystals were filtered, washed with diethyl ether, and cold methanol. The crystals were dried in the oven at 50°C. The list of complexes isolated using the method highlighted above is presented in Table 3:5 below.

3.2.2.1.2 Method 2

To methanolic solution (10 ml) of ovan3amp {(E)-2-methoxy-6-((pyridin-3-ylimino)methyl)phenol} (0.5707 g, 2.5 mmol) was added methanolic solution (5 ml) of cobalt chloride ($CoCl_2.6H_2O$) (0.2974 g, 1.25 mmol). The mixture was refluxed in a 100 ml round bottom flask. After refluxing for 2 hour, the solution was allowed to cool at room temperature. The precipitate formed was filtered, washed with diethyl ether and kept dry for analyses. The list of all the complexes isolated using this method is presented in Table 3:5 below.

3.2.2.1.3 Method 3

To a solution of 3-aminomethylpyridine (0.5091 ml 5 mmol) in tetrahydrofuran (20 ml) was added salicylaldehyde (0.3648 ml, 5 mmol) and refluxed for 30 minutes. The mixture cooled, and filtered. The mixture of trimethylamine (0.6969 ml 5 mmol) and cobalt chloride

($CoCl_2.6H_2O$, 0. 5948 g, 2.5 mmol) was added to the filtered Schiff base solution. The mixture was refluxed for another 1 hour. The solution was allowed to cool to room temperature. The precipitate obtained was filtered, washed with diethyl ether, cold methanol and dried over silica gel under reduced pressure. The list of all the complexes obtained from this method is presented in Table 3:5

Table 3:5 List of complexes isolated from the three synthetic methods

Method 1		Method 2		Method 3	
Complex		Complex		Complex	
6A	$Co(p\text{-}van\ 1\ amnap)_2Cl_2 \cdot \frac{1}{2}H_2O$	1A	$Co(saani)_3 \cdot 3H_2O$	1C	$Co(saani)_2$
8A	$Co(van\ 1\ amnap)Cl \cdot 2H_2O$	1B	$Co(saani)_2 \cdot \frac{1}{2}H_2O$	2C	$Co(pvaani)_2 \cdot \frac{1}{2}H_2O$
9A	$Co(sal4amp)_2Cl_2$	2A	$Co(pvaani)_2Cl_2$	3C	$Co(ovaani)_2 \cdot \frac{1}{2}H_2O$
9B	$Co(sal4amp)_2$	2B	$Co(pvaani)_2$	5C	$Co(sal\ 1\ amnap)_2 \cdot 2H_2O$
10A	$Co(pvan4amp)_2Cl_2.2H_2O$	3A	$Co(ovaani)_2Cl_2 \cdot \frac{1}{2}H_2O$	6C	$Co(p\text{-}van\ 1\ amnap)_2 \cdot 2H_2O$
10B	$Co(pvan4amp)_2.6H_2O$	3B	$Co(ovaani)_2 \cdot 2H_2O$	8C	$Co(van\ 1\ amnap)_2 \cdot 5H_2O$
11A	$Co(ovan4amp)_2Cl_2 \cdot 3H_2O$	4A	$Co(vaani)Cl_2$	9C	$Co(sal4amp)_2 \cdot 2H_2O$
11B	$Co(ovan4amp)_2 \cdot 5H_2O$	7A	$Co(o\text{-}van\ 1\ amnap)_2 \cdot 3H_2O$	10C	$Co(pvan4amp)_2.7H_2O$
12A	$Co_2(van4amp)_3Cl_2 \cdot 5H_2O$	13A	$Co(sal3amp)_2Cl_2$	11C	$Co(ovan4amp)_2 \cdot 3H_2O$
12B	$Co(van4amp)_2 \cdot \frac{1}{2}H_2O$	13B	$Co(sal3amp)_2 \cdot \frac{1}{2}H_2O$	12C	$Co(van4amp)_2 \cdot \frac{1}{2}H_2O$
17A	$Co(sal3pico)_2Cl_2 \cdot \frac{1}{2}H_2O$	14A	$Co(pvan3amp)_2Cl \cdot H_2O$	13C	$Co(sal3amp)_2 \cdot \frac{1}{2}H_2O$
17B	$Co(sal3pico)_2 \cdot H_2O$	14B	$Co(pvan3amp)_2 \cdot \frac{1}{2}H_2O$	14C	$Co(pvan3amp)_2 \cdot 3H_2O$
18A	$Co(pvan3pico)_2Cl_2$	15A	$Co(ovan3amp)_2Cl_2 \cdot 3H_2O$	15C	$Co(ovan3amp)_2 \cdot \frac{1}{2}H_2O$
18B	$Co(pvan3pico)_2 \cdot H_2O$	15B	$Co(ovan3amp)_2 \cdot \frac{1}{2}H_2O$	16C	$Co(van3amp)_2 \cdot \frac{1}{2}H_2O$
19A	$Co(ovan3pico)_2Cl_2 \cdot 1\frac{1}{2}H_2O$	16A	$Co\ (van3amp)_2Cl_2 \cdot 5H_2O$	17C	$Co(sal3pico)_2 \cdot 1\frac{1}{2}H_2O$
19B	$Co(ovan3pico)_2 \cdot H_2O$			18C	$Co(pvan3pico)_2 \cdot H_2O$
20A	$Co\ (van3pico)_2Cl_2 \cdot 3H_2O$			19C	$Co(ovan3pico)_2 \cdot H_2O$
20B	$Co(van3pico)_2 \cdot 5H_2O$			21C	$Co(sal2pico)_2 \cdot 4H_2O$
21A	$Co(sal2pico)_2$			22C	$Co(pvan2pico)_2 \cdot 4\frac{1}{2}H_2O$
21B	$Co(sal2pico)_2 \cdot 4H_2O$			23C	$Co(ovan2pico)_2 \cdot 2H_2O$
22A	$Co(pvan2pico)_2Cl_2 \cdot 2H_2O$				
22B	$Co(pvan2pico)_2 \cdot 4H_2O$				
23A	$Co(ovan2pico)_2Cl_2 \cdot 3H_2O$				
23B	$Co(ovan2pico)_2 \cdot 1\frac{1}{2}H_2O$				
24A	$Co_2(van2pico)_3Cl_2 \cdot H_2O$				
24B	$Co(van2pico)_2 \cdot 4H_2O$				

3.3 References

1. O. West, J. Chem. Soc.; 1954, 395-400.
2. N. Raman, Y. Pitchaikani, A. Kulandaisamy, Proc. Indian Acad. Sci. (Chem. Sci.); 2001, **113**, 183-89
3. G. Y. Yeap, S.T. Ha, N. Ishizawa, K. Suda, P. L. Boey, W.A.K. Mahmood, J. Mol. Struct.; 2003, **658**, 87-89.
4. M. M. Abd-Elzaher, J. Chin. Chem. Soc.; 2001, **48**, 153-8.
5. L. S. Skorokhod, I. I. Seifullina, S. A. Dzhambek, Russ. J. Coord. Chem.; 2002, **28**, 643-646.
6. M. Hariharan, F. L. Urbach, Inorg. Chem.; 1969, **8**, 556-9.
7. R. Viswanathan, M. Palaniandavar, T. Balasubramaniam, P. T. Muthiah, J. Chem. Soc.; Dalton Trans.; 1996, 2519-25
8. S. Dayagi, Y. Degani, *The Chemistry of the carbon-nitrogen double bond*, ed. S. Patai, Wiley-Interscience, New York, 1970, 67-129.

4 RESULTS (PHYSICAL AND CHEMICAL STUDY)

All the results obtained from all the techniques used in characterizing the ligands and their corresponding cobalt(II) complexes are listed in this chapter.

4.1 Physicochemical data for the ligands

Table 4:1 Microanalysis and analytical data for the aniline-based Schiff bases

No.	Ligand	Structure	Molecular formula	% Found (Calculated)			Color	Yield (%)	M.p. (°C)	Molar mass	M+
				% C	% H	% N					
1	saani	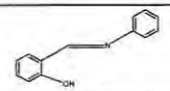	$C_{13}H_{11}NO$	78.68 (79.16)	5.82 (5.62)	6.93 (7.10)	yellow	90	51-2	197	196
2	pvaani	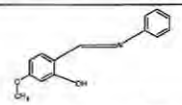	$C_{14}H_{13}NO$	74.15 (73.99)	5.70 (5.77)	5.96 (6.16)	yellow	57	65-6	227	226
3	ovaani	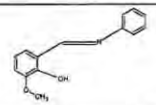	$C_{14}H_{13}NO$	73.97 (73.99)	5.74 (5.77)	6.09 (6.16)	orange	97	82-3	227	227
4	vaani	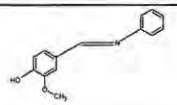	$C_{14}H_{13}NO$	74.01 (73.99)	5.95 (5.77)	6.09 (6.16)	cream	54	148-9	227	226

Table 4:2 Microanalysis and analytical data for the 1-aminonaphthalene-based Schiff bases

No.	Ligand	Structure	Molecular formula	% Found (Calculated) % C	% H	% N	Color	Yield (%)	M.p. (°C)	Molar mass	M+
5	sal1amnap		$C_{17}H_{13}NO$	82.11 (82.57)	5.30 (5.30)	5.77 5.66	dark brown	85	43-44	247	247
6	pvan1amnap	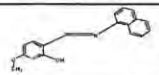	$C_{18}H_{15}NO_2$	77.64 (77.96)	5.39 (5.45)	4.90 (5.05)	light brown	97	69-70	277	277
7	ovan1amnap	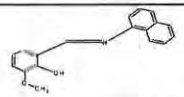	$C_{18}H_{15}NO_2$	77.62 (77.96)	5.45 (5.45)	4.89 (5.05)	orange	90	90-2	277	277
8	van1amnap	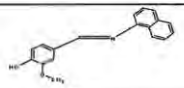	$C_{18}H_{15}NO_2$	76.86 (76.71)	5.52 (5.37)	4.88 (4.97)	dark brown	`90	100-1	277	-

Table 4:3 Microanalysis and analytical data for 4-aminopyridine-based Schiff bases

No.	Ligand	Structure	Molecular formula	% Found (Calculated) % C	% H	% N	Color	Yield (%)	M.p. (°C)	Molar mass	M+
9	sal4amp	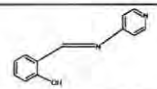	$C_{12}H_{10}N_2O$	72.47 (72. 17)	5.57 (5.08)	13.62 (14.13)	yellow	67	42-3	198	198
10	pvan4amp($2\frac{1}{2}H_20$)	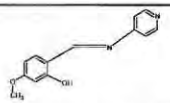	$C_{13}H_{17}N_2O_4$	57.13 (57.13)	5.27 (6.27)	10.83 (10.25)	reddish brown	51	88-90	228	228
11	ovan4amp(H_2O)	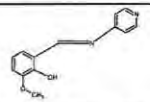	$C_{13}H_{14}N_2O_3$	62.96 (63.40)	5.60 (5.73)	11.07 (11.38)	brown	58	150-2	228	228
12	van4amp	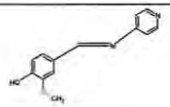	$C_{13}H_{12}N_2O_2$	(68.41)	(5.30)	(12.27)	yellow	62	oily	228	-

(a) microanalysis data not available

Table 4:4 Microanalysis and analytical data for the 3-aminopyridine-based Schiff bases

No.	Ligand	Structure	Molecular formula	% Found (Calculated) % C	% H	% N	Color	Yield (%)	M.p. (°C)	Molar mass	M+
13	sal3amp	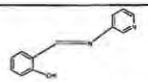	$C_{12}H_{10}N_2O$	71.60 (71.10)	5.03 (4.97)	13.78 (13.82)	orange	94	70-71	198	197
14	pvan3amp	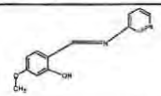	$C_{13}H_{12}N_2O_2$	67.93 (68.41)	5.23 (5.30)	12.05 (12.27)	yellow	67	114-5	228	228
15	ovan3amp	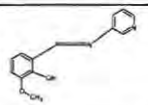	$C_{13}H_{12}N_2O_2$	67.57 (68.41)	5.28 (5.30)	11.94 (12.27)	orange	75	119-20	228	228
16	van3amp	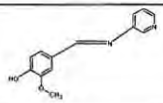	$C_{13}H_{12}N_2O_2$	68.20 (68.41)	5.39 (5.30)	11.83 (12.27)	cream	76	142-3	228	228

Table 4:5 Microanalysis and analytical data for the 3-aminomethylpyridine-based Schiff bases

No.	Ligand	Structure	Molecular formula	% Found (Calculated) % C	% H	% N	Color	Yield (%)	M.p. (°C)	Molar mass	M+
17	sal3pico	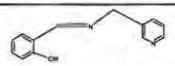	$C_{13}H_{12}N_2O$	(73.56) 73.28	(5.70) 5.53	(13.20) 13.16	yellow	75	53-55	212	211
18	pvan3pico	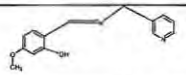	$C_{14}H_{12}N_2O_2$	63.24 (63.66)	5.69 5.34	13..92 14.02	brown	87	oily	242	243
19	ovan3pico	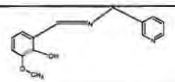	$C_{14}H_{12}N_2O_2$	69.46 (69.41)	5.82 (5.82)	11.65 (11.56)	brown	60	oily	242	243
20	van3pico	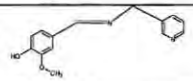	$C_{14}H_{12}N_2O_2$	69.53 (69.41)	5.80 (5.82)	11.25 (11.56)	Cream	85	139-140	242	241

Table 4:6 Microanalysis and analytical data for the 2-aminomethylpyridine-based Schiff bases

No.	Ligand	Structure	Molecular formula	% Found (Calculated) % C	% H	% N	Color	Yield (%)	M.p. (°C)	Molar mass	M+
21	sal2pico	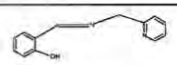	$C_{13}H_{12}N_2O$	72.31 (72.09)	5.73 (5.60)	13.09 (12.90)	yellow	68	oily	211	211
22	pvan2pico	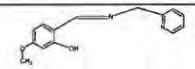	$C_{14}H_{16}N_2O_3$	69.96 (69.41)	6.29 (5.82)	11.52 (11.56)	brown	57	oily	242	243
23	ovan2pico	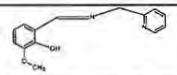	$C_{14}H_{14}N_2O_2$	68.68 (69.41)	5.88 (5.82)	11.22 (11.56)	brown	90	94-5	242	243
24	van2pico	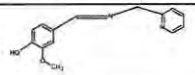	$C_{14}H_{14}N_2O_2$	65.03 (64.60)	6.10 (6.20)	10.26 (10.76)	brown	81	102-4	242	-

4.2 Physicochemical data for the complexes

Table 4:7 Microanalysis and analytical data for the complexes of ligand 1 (saani)

No.	Complex	Molecular formula	Molar mass	% Found (Calculated) % C	% H	% N	% Co	Color	Yield (%)	M.p. (°C)
1A	$Co(saani)_3Cl_2.1½H_2O$	$C_{39}H_{38}Cl_2CoN_3O_5$	750.6	62.18 (62.41)	4.68 (4.54)	5.58 (5.57)	8.20 (7.81)	green	48	190-92[d]
1B	$Co(saani)_2.½H_2O$	$C_{26}H_{21}CoN_2O_2$	460.4	68.21 (67.83)	4.51 (4.60)	6.46 (6.09)	12.44 (12.80)	reddish brown	31	181-2
1C	$Co(saani)_2$	$C_{26}H_{20}CoN_2O_2$	451.4	68.79 (69.18)	4.37 (4.47)	6.15 (6.21)	12.81 (13.06)	reddish brown	82	181-2

(d) Decomposed

Table 4:8 Microanalysis and analytical data for the complexes of ligand 2 (pvaani)

No.	Complex	Molecular formula	Molar mass	% Found (Calculated) % C	% H	% N	% Co	Color	Yield (%)	M.p. (°C)
2A	$Co(pvaani)_2Cl_2$	$C_{28}H_{24}Cl_2CoN_2O_4$	584.4	57.60 (57.55)	4.36 (4.14)	4.71 (4.79)	10.60 (10.09)	green	67	235-6
2B	$Co(pvaani)_2$	$C_{28}H_{24}CoN_2O_4$	511.4	65.47 (65.76)	4.30 (4.73)	5.17 (5.48)	11.32 (11.52)	reddish brown	82	209-10
2C	$Co(pvaani)_2.\ ½H_2O$	$C_{28}H_{25}CoN_2O_4$	520.4	64.10 (64.62)	4.75 (4.84)	5.20 (5.38)	11.70 (11.32)	reddish brown	77	209-10

Table 4:9 Microanalysis and analytical data for the complexes of ligand 3 (ovaani)

No.	Complex	Molecular formula	Molar mass	% Found (Calculated) % C	% H	% N	% Co	Color	Yield (%)	M.p. (°C)
3A	$Co(ovaani)_2Cl_2.½H_2O$	$C_{28}H_{25}Cl_2CoN_2O_4$	591.4	56.57 (56.87)	4.38 (4.26)	4.64 (4.74)	9.50 (9.97)	green	50	235-6
3B	$Co(ovaani)_2.\ ½H_2O$	$C_{28}H_{25}CoN_2O_4$	520.4	64.17 (64.62)	4.42 (4.84)	5.33 (5.38)	11.20 (11.32)	reddish brown	85	251-2
3C	$Co(ovaani)_2.\ ½H_2O$	$C_{28}H_{25}CoN_2O_4$	520.4	64.67 (64.62)	4.27 (4.84)	5.05 (5.38)	11.83 (11.32)	reddish brown	80	251-2

Table 4:10 Microanalysis and analytical data for the complex of ligand 4 (vaani)

No.	Complex	Molecular formula	Molar mass	% Found (Calculated) % C	% H	% N	% Co	Color	Yield (%)	M.p. (°C)
4A	$Co(vaani)Cl_2$	$C_{13}H_{10}Cl_2CoNO$	325	46.93 (47.22)	4.06 (4.55)	3.70 (3.93)	18.56 (18.07)	green	50	>340

Table 4:11 Microanalysis and analytical data for the complex of ligand 5 (sal1amnap)

No.	Complex	Molecular formula	Molar mass	% Found (Calculated) % C	% H	% N	% Co	Color	Yield (%)	M.p. (°C)
5C	$Co(sal1amnap)_2.2H_2O$	$C_{34}H_{28}CoN_2O_4$	587.53	65.61 (65.49)	5.51 (5.17)	4.20 (4.49)	9.65 (9.45)	brown	85	142-3

Table 4:12 Microanalysis and analytical data for the complexes of ligand 6 (pvan1amnap)

No.	Complex	Molecular formula	Molar mass	% Found (Calculated) % C	% H	% N	% Co	Color	Yield (%)	M.p. (°C)
6A	$Co(pvan1amnap)_2Cl_2.½H_2O$	$C_{36}H_{29}Cl_2CoN_2O_4$	693.5	62.87 (62.24)	4.33 (4.21)	4.00 (4.04)	9.00 (8.50)	green	83	238-40
6C	$Co(pvan1amnap)_2.2H_2O$	$C_{36}H_{34}CoN_2O_6$	629.6	68.76 (68.68)	4.33 (4.80)	3.95 (4.45)	9.52 (9.36)	yellowish brown	83	210-11

Table 4:13 Microanalysis and analytical data for the complex of ligand 7 (ovan1amnap)

No.	Complex	Molecular formula	Molar mass	% Found (Calculated) % C	% H	% N	% Co	Color	Yield (%)	M.p. (°C)
7A	$Co(ovan1amnap)_2.3H_2O$	$C_{36}H_{36}CoN_2O_7$	667.6	64.93 (64.77)	5.49 (5.44)	3.70 (4.20)	8.41 (8.83)	brown	24	260-2

Table 4:14 Microanalysis and analytical data for the complexes of ligand 8 (van1amnap)

No.	Complex	Molecular formula	Molar mass	% Found (Calculated) % C	% H	% N	% Co	Color	Yield (%)	M.p. (°C)
8A	$Co(van1amnap)Cl.2H_2O$	$C_{18}H_{20}ClCoNO_4$	408.7	52.80 (52.89)	4.59 (4.93)	3.24 (3.43)	14.95 (14.42)	green	68	>320
8C	$Co(van1amnap)_2.5H_2O$	$C_{36}H_{38}CoN_2O_9$	701.6	61.58 (61.63)	5.30 (5.46)	3.67 (3.99)	9.00 (8.40)	cream	85	> 320

Table 4:15 Microanalysis and analytical data for the complexes of ligand 9 (pvan4amp)

No.	Complex	Molecular formula	Molar mass	% Found (Calculated) % C	% H	% N	% Co	Color	Yield (%)	M.p. (°C)
9A	$Co(sal4amp)_2Cl_2$	$C_{24}H_{18}Cl_2CoN_4O_2$	524.3	54.86 (54.98)	3.14 (3.46)	(a) (10.69)	10.93 (11.24)	green	48	190-92
9B	$Co(sal4amp)_2.4H_2O$	$C_{24}H_{26}CoN_4O_6$	525.1	54.90 (54.86)	4.63 (4.99)	(a) (10.66)	11.53 (11.22)	reddish brown	31	181-2
9C	$Co(sal4amp)_2.2H_2O$	$C_{24}H_{24}CoN_4O_4$	491.4	58.28 (58.66)	4.40 (4.92)	11.06 (11.40)	11.60 (11.99)	reddish brown	82	181-2

(a) Microanalysis of nitrogen unavailable

Table 4:16 Microanalysis and analytical data for the complexes of ligand 10 (ovan4amp)

No.	Complex	Molecular formula	Molar mass	% Found (Calculated) % C	% H	% N	% Co	Color	Yield (%)	M.p. (°C)
10A	$Co(pvan4amp)_2Cl_2.2H_2O$	$C_{26}H_{28}Cl_2CoN_4O_6$	622.4	50.41 (50.18)	4.06 (4.53)	(a) (9.00)	9.85 (9.47)	orange	62	228-30
10B	$Co(pvan4amp)_2.6H_2O$	$C_{26}H_{34}CoN_4O_{10}$	621.5	50.31 (50.25)	4.09 (5.51)	(a) (9.01)	9.65 (9.48)	Light brown	33	284-6
10C	$Co(pvan4amp)_2.7H_2O$	$C_{26}H_{26}CoN_4O_6$	549.4	48.32 (48.83)	4.54 (5.67)	(a) (8.76)	9.78 (9.22)	Light brown	33	284-6

(a) Microanalysis of nitrogen unavailable

Table 4:17 Microanalysis and analytical data for the complexes of ligand 11 (ovan4amp)

No.	Complex	Molecular formula	Molar mass	% Found (Calculated) % C	% H	% N	% Co	Color	Yield (%)	M.p. (°C)
11A	$Co(ovan4amp)_2Cl_2.3H_2O$	$C_{26}H_{30}Cl_2CoN_4O_7$	640.4	48.31 (48.76)	4.46 (4.72)	(a) (8.75)	10.05 (9.20)	yellowish brown	0.7371	170-1
11B	$Co(ovan4amp)_2.5H_2O$	$C_{26}H_{34}CoN_4O_9$	605.5	51.60 (51.57)	5.17 (5.66)	9.24 (9.25)	10.05 (9.73)	orange brown	97	182-3
11C	$Co(ovan4amp)_2.3H_2O$	$C_{26}H_{34}CoN_4O_7$	569	54.87 (54.84)	4.87 (5.31)	9.83 (9.84)	10.05 (10.35)	orange brown	90	183-4

(a) Microanalysis of nitrogen unavailable

Table 4:18 Microanalysis and analytical data for the complexes of ligand 12 (van4amp)

No.	Complex	Molecular formula	Molar mass	% Found (Calculated) % C	% H	% N	% Co	Color	Yield (%)	M.p. (°C)
12A*	$Co_2(van4amp)_3Cl_2.5H_2O$	$C_{39}H_{45}Cl_2CoN_6O_{11}$	962.6	48.17 (48.66)	4.47 (4.71)	(a) (8.73)	12.07 (12.24)	grey	58	>342
12B	$Co(van4amp)_2.2½H_2O$	$C_{26}H_{29}CoN_4O_6$	560.5	55.93 (55.72)	4.78 (5.01)	9.67 (10.00)	10.81 (10.52)	coffee brown	90	183-4
12C	$Co(van4amp)_2.3H_2O$	$C_{26}H_{28}CoN_4O_7$	567.5	54.72 (55.03)	4.47 (4.97)	9.29 (9.87)	10.80 (10.39)	coffee brown	90	183-4

(a) Microanalysis of nitrogen unavailable

Table 4:19 Microanalysis and analytical data for the complexes of ligand 13 (sal3amp)

No.	Complex	Molecular formula	Molar mass	% Found (Calculated) % C	% H	% N	% Co	Color	Yield (%)	M.p. (°C)
13A	$Co(sal3amp)_2Cl_2$	$C_{24}H_{20}Cl_2CoN_4O_2$	526.3	54.62 (54.77)	3.75 (3.83)	10.65 (10.65)	11.00 (11.20)	leaf green	81	217-8
13B	$Co(sal3amp)_2.½H_2O$	$C_{24}H_{21}CoN_4O_2$	464.4	62.11 (62.35)	3.86 (3.96)	12.05 (12.07)	12.44 (12.69)	yellowish brown	83	341-2
13C	$Co(sal3amp)_2.½H_2O$	$C_{24}H_{23}CoN_4O_4$	462.4	62.06 (62.35)	3.96 (3.92)	11.78 (12.12)	12.26 (12.75)	yellowish brown	81	341-2

Table 4:20 Microanalysis and analytical data for the complexes of ligand 14 (pvan3amp)

No.	Complex	Molecular formula	Molar mass	% Found (Calculated) % C	% H	% N	% Co	Color	Yield (%)	M.p. (°C)
14A	$Co(pvan3amp)_2Cl.H_2O$	$C_{26}H_{26}ClCoN_4O_5$	568.9	55.08 (54.89)	4.06 (4.61)	9.95 (9.85)	10.29 (10.36)	Green	66	181-2
14B	$Co(pvan3amp)_2.½H_2O$	$C_{26}H_{22}CoN_4O_4$	522.4	59.26 (59.78)	4.16 (4.25)	10.53 (10.72)	11.36 (11.28)	greenish yellow	84	316-8
14C	$Co(pvan3amp)_2.3H_2O$	$C_{26}H_{30}CoN_4O_7$	569.5	54.54 (55.03)	4.52 (4.97)	10.17 (9.84)	10.47 (10.35)	greenish yellow	87	316-8

Table 4:21 Microanalysis and analytical data for the complexes of ligand 15 (ovan3amp)

No.	Complex	Molecular formula	Molar mass	% Found (Calculated) % C	% H	% N	% Co	Color	Yield (%)	M.p. (°C)
15A	$Co(ovan3amp)Cl_2.2H_2O.$	$C_{13}H_{15}Cl_2CoN_2O_4$	394.1	40.20 (39.72)	3.75 (3.85)	6.95 (7.13)	15.18 (14.99)	leaf green	66	181-2
15B	$Co(ovan3amp)_2.½H_2O$	$C_{26}H_{23}CoN_4O_4$	522.4	59.52 (59.78)	4.11 (4.25)	10.74 (10.72)	11.48 (11.28)	greenish yellow	78	262-3
15C	$Co(ovan3amp)_2.½H_2O$	$C_{26}H_{23}CoN_4O_4$	522.4	59.81 (59.78)	4.76 (4.25)	10.35 (10.72)	11.66 (11.28)	greenish yellow	77	262-3

Table 4:22 Microanalysis and analytical data for the complexes of ligand 16 (van3amp)

No.	Complex	Molecular formula	Molar mass	% Found (Calculated) % C	% H	% N	% Co	Color	Yield (%)	M.p. (°C)
16A	$Co(van3amp)Cl_2.2½H_2O.$	$C_{26}H_{29}Cl_2CoN_4O_6$	631.4	49.17 (49.46)	4.75 (4.47)	8.53 (8.87)	9.30 (9.33)	black	65	115-7
16C	$Co(van3amp)_2.2H_2O$	$C_{26}H_{34}CoN_4O_9$	605.5	51.71 (51.57)	5.52 (5.66)	9.07 (9.25)	9.38 (9.73)	brown	85	196-8

Table 4:23 Microanalysis and analytical data for the complexes of ligand 17 (sal3pico)

No.	Complex	Molecular formula	Molar mass	% Found (Calculated) % C	% H	% N	% Co	Color	Yield (%)	M.p. (°C)
17A	$Co(sal3pico)_2Cl_2.½H_2O$	$C_{26}H_{24}Cl_2CoN_4O_2$	563.3	55.35 (55.44)	3.98 (4.47)	9.96 (9.95)	10.17 (10.46)	leaf green	80	237-8
17B	$Co(sal3pico)_2.H_2O$	$C_{26}H_{24}CoN_4O_3$	499.4	62.34 (62.53)	4.67 (4.84)	11.11 (11.22)	11.43 (11.80)	yellowish green	91	282-4
17C	$Co(sal3pico)_2.1½H_2O$	$C_{26}H_{25}CoN_4O_3$	508.4	61.79 (61.42)	4.46 (4.96)	11.50 (11.01)	11.72 (11.59)	yellowish green	87	280-2

Table 4:24 Microanalysis and analytical data for the complexes of ligand 18 (pvan3pico)

No.	Complex	Molecular formula	Molar mass	% Found (Calculated) % C	% H	% N	% Co	Color	Yield (%)	M.p. (°C)
18A	$Co(pvan3pico)_2Cl_2$	$C_{28}H_{25}Cl_2CoN_4O_4$	614.4	54.30 (54.74)	4.27 (4.59)	9.04 (9.12)	9.82 (9.59)	grey brown	85	287-8
18B	$Co(pvan3pico)_2.H_2O$	$C_{28}H_{28}CoN_4O_5$	560.4	60.37 (60.00)	4.71 (5.21)	10.03 (10.00)	10.36 (10.52)	dirty yellow	94	295-6
18C	$Co(pvan3pico)_2.H_2O$	$C_{28}H_{28}CoN_4O_5$	560.4	60.56 (60.00)	4.77 (5.21)	10.09 (10.00)	10.24 (10.52)	dirty yellow	93	295-6

Table 4:25 Microanalysis and analytical data for the complexes of ligand 19 (ovan3pico)

No.	Complex	Molecular formula	Molar mass	% Found (Calculated) % C	% H	% N	% Co	Color	Yield (%)	M.p. (°C)
19A	$Co(ovan3pico)_2Cl_2.1½H_2O$	$C_{28}H_{31}Cl_2CoN_4O_5$	641.4	52.49 (52.43)	4.50 (4.87)	8.37 (8.74)	9.52 (9.19)	green	80	241-2
19B	$Co(ovan3pico)_2.H_2O$	$C_{28}H_{28}CoN_4O_5$	559.5	60.32 (60.11)	4.55 (5.05)	10.03 (10.01)	10.92 (10.53)	greenish yellow	90	274-6
19C	$Co(ovan3pico)_2.H_2O$	$C_{28}H_{28}CoN_4O_5$	559.5	60.56 (60.11)	4.77 (5.05)	10.03 (10.01)	10.92 (10.53)	greenish yellow	93	274-6

Table 4:26 Microanalysis and analytical data for the complexes of ligand 20 (van3pico)

No.	Complex	Molecular formula	Molar mass	% Found (Calculated) % C	% H	% N	% Co	Color	Yield (%)	M.p. (°C)
20A	$Co(van3pico)_2Cl_2.3H_2O$	$C_{28}H_{34}Cl_2CoN_4O_7$	668.4	50.24 (50.31)	5.59 (5.13)	8.75 (8.38)	8.78 (8.82)	black	59	120-2
20B	$Co(van3pico)_2.5H_2O$	$C_{28}H_{38}CoN_4O_9$	633.6	53.27 (53.08)	6.03 (6.05)	8.33 (8.84)	9.72 (9.30)	black	56	244-5

Table 4:27 Microanalysis and analytical data for the complexes of ligand 21 (sal2pico)

No.	Complex	Molecular formula	Molar mass	% Found (Calculated) % C	% H	% N	% Co	Color	Yield (%)	M.p. (°C)
21A	$Co(sal2pico)_2$	$C_{26}H_{28}Cl_2CoN_5O_3$	588.4	53.53 (53.07)	4.91 (4.80)	11.34 (11.90)	9.93 (10.02)	green	85	237-8
21B	$Co(sal2pico)_2.4H_2O$	$C_{26}H_{32}CoN_4O_6$	555.5	55.85 (56.22)	5.31 (5.81)	10.40 (10.09)	10.88 (10.46)	black	54	200-2
21C	$Co(sal2pico)_2.4H_2O$	$C_{26}H_{31}CoN_4O_6$	555.5	56.68 (56.22)	5.06 (5.81)	10.44 (10.09)	10.91 (10.46)	black	52	200-1

Table 4:28 Microanalysis and analytical data for the complexes of ligand 22 (pvan2pico)

No.	Complex	Molecular formula	Molar mass	% Found (Calculated) % C	% H	% N	% Co	Color	Yield (%)	M.p. (°C)
22A	$Co(pvan2pico)_2Cl_2.2H_2O$	$C_{28}H_{32}Cl_2CoN_5O_6$	675.0	50.21 (49.80)	4.87 (5.22)	9.87 (10.36)	8.97 (8.73)	black	52	145-6
22B	$Co(pvan2pico)_2.4H_2O$	$C_{28}H_{36}CoN_4O_8$	615.5	54.87 (54.63)	5.25 (5.89)	9.24 (9.10)	9.96 (9.57)	black	83	176-8
22C	$Co(pvan2pico)_2.4½H_2O$	$C_{28}H_{37}CoN_4O_8$	624.6	53.69 (53.85)	5.39 (5.97)	9.07 (8.97)	9.29 (9.44)	black	79	177-9

Table 4:29 Microanalysis and analytical data for the complexes of ligand 23 (ovan2pico)

No.	Complex	Molecular formula	Molar mass	% Found (Calculated) % C	% H	% N	% Co	Color	Yield (%)	M.p. (°C)
23A	$Co(ovan2pico)_2Cl_2.3H_2O$	$C_{28}H_{34}Cl_2CoN_4O_7$	668.4	49.91 (50.31)	4.99 (5.13)	8.04 (8.38)	8.22 (8.82)	green	18	192-4
23B	$Co(ovan2pico)_2.2½H_2O$	$C_{28}H_{31}CoN_5O_5$	584.5	57.32 (57.54)	4.87 (5.35)	11.56 (11.98)	9.50 (10.08)	black	91	180-2
23C	$Co(ovan2pico)_2.3½H_2O$	$C_{28}H_{33}CoN_5O_6$	602.5	55.40 (55.82)	5.44 (5.52)	11.60 (11.62)	9.63 (9.78)	black	90	180-2

Table 4:30 Microanalysis and analytical data for the complexes of ligand 24 (van2pico)

No.	Complex	Molecular formula	Molar mass	% Found (Calculated) % C	% H	% N	% Co	Color	Yield (%)	M.p. (°C)
24A	$Co(van2pico)_2Cl_2.H_2O$	$C_{28}H_{28}Cl_2CoN_4O_5$	630.4	53.23 (53.35)	4.51 (4.48)	9.31 (8.89)	9.08 (9.35)	shining black	58	162-4
24B	$Co(van2pico)_2.4H_2O$	$C_{28}H_{34}CoN_4O_8$	622.53	53.74 (54.02)	5.18 (5.67)	9.51 (9.00)	9.10 (9.47)	black	86	104-6

4.3 Mid infrared data for the ligands

Table 4:31 Mid infrared frequencies (cm^{-1}) of the aniline-based Schiff bases

No.	Compound	Structure	νO-H	$\nu C{=}N_{(imine)}$	νC-O	$\Delta\nu C{=}N_{(imine)}$	LFER Σσ
ref	benzylideneaniline		-	1630	-	-	-
1	saani	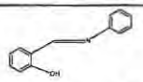	3440	1621	1285	- 9	1.22[1]
2	pvaani	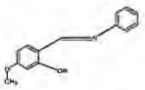	3442	1619	1290	- 11	0.95[1]
3	ovaani	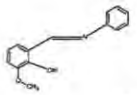	3443	1616	1254	- 14	1.34[1]
4	vaani	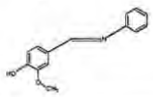	3444	1622	1284	- 8	-0.25[2]

Table 4:32 Mid infrared frequencies (cm^{-1}) of the 1-aminonaphthalene-based Schiff bases

No.	Compound	Structure	νO-H	$\nu C{=}N_{(imine)}$	νC-O	LFER Σσ
5	sal1amnap	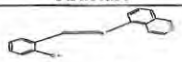	3420	1618	1281	1.22[1]
6	pvan1amnap	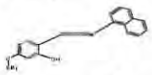	3442	1613	1290	0.95[1]
7	ovan1amnap		3440	1609	1254	1.34[1]
8	van1amnap	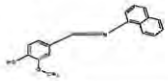	3439	1621	1284	-0.25[2]

Table 4:33 Mid infrared frequencies (cm^{-1}) of the 4-aminopyridine-based Schiff bases

No.	Compound	Structure	νO-H	$\nu C{=}N_{(imine)}$	$\nu C{=}N_{(pyridine)}$	νC-O	LFER Σσ
9	sal4amp	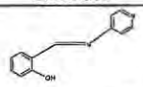	3432	1630	1576	1275	1.22[1]
10	pvan4amp(2½ H_2O)	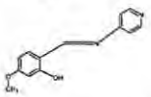	3407	1633	1601	1267	0.95[1]
11	ovan4amp(H_2O)	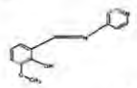	3358	1645	1603	1278	1.34[1]
12	van4amp	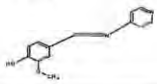	3348	1652	1588	1264	-0.25[2]

Table 4:34 Mid infrared frequencies (cm^{-1}) of the 3-aminopyridine – based Schiff bases

No.	Compound	Structure	νO-H	$\nu C{=}N_{(imine)}$	$\nu C{=}N_{(pyridine)}$	νC-O	LFER Σσ
13	sal3amp	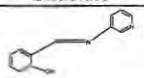	3442	1616	1569	1285	1.22[1]
14	pvan3amp		3442	1610	1586	1297	0.95[1]
15	ovan3amp	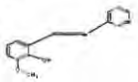	3440	1615	1565	1259	1.34[1]
16	van3amp	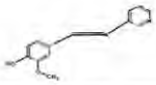	3432	1623	1599	1286	-0.25[2]

Table 4:35 Mid infrared frequencies (cm^{-1}) of the 3-aminomethylpyridine–based Schiff bases

No.	Compound	Structure	νO-H	$\nu C{=}N_{(imine)}$	$\nu C{=}N_{(pyridine)}$	νC-O	LFER Σσ
17	sal3pico	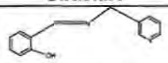	3432	1626	1576	1274	1.22[1]
18	pvan3pico		3209	1627	1580	1290	0.95[1]
19	ovan3pico	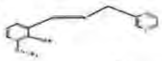	3391	1625	1601	1274	1.34[1]
20	van3pico		3432	1634	1580	1286	-0.25[2]

Table 4:36 Mid infrared frequencies (cm^{-1}) of the 2-aminomethylpyridine–based Schiff bases

No.	Compound	Structure	νO-H	$\nu C{=}N_{(imine)}$	$\nu C{=}N_{(pyridine)}$	νC-O	LFER Σσ
21	sal2pico		3417	1627	1589	1303	1.22[1]
22	pvan2pico		3442	1618	1590	1287	0.95[1]
23	ovan2pico		3440	1617	1589	1259	1.34[1]
24	van2pico		3355	1648	1583	1232	-0.25[2]

4.4 Mid and far infrared data for the complexes

Table 4:37 Infrared frequencies (cm^{-1}) of the saani-based complexes

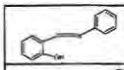

Compound		νO-H	νC=$N_{(imine)}$	νC-O	ν_aM-O	ν_sM-O	ν_aM-N	ν_sM-N	νM-Cl_{tet}	other	
1	saani	3440	1625 [(a)]	1285	-	-	-	-	-	-	-
1A	$Co(saani)_3 \cdot 3H_2O$	3434	1638, 1612	1285	588	504	446	400	-	324	293
1B	$Co(saani)_2 \cdot ½H_2O$	3435	1605	1305	589	540	451	398	-	322	302
1C	$Co(saani)_2$	3442	1605	1306	588	541	464	-	-	-	-

Footnote : (a) = split band

Table 4:38 Infrared frequencies (cm^{-1}) of the pvaani-based complexes

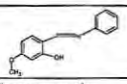

Compound		νO-H	νC=$N_{(imine)}$	νC-O	ν_aM-O	ν_sM-O	ν_aM-N	ν_sM-N	νM-Cl_{tet}	other	
2	pvaani	3445	1622	1290	-	-	-	-	-	-	-
2A	$Co(pvaani)_2Cl_2$	3445	1635, 1611	1300	595, 557	540	464	-		365	289, 277
2B	$Co(pvaani)_2$	3441	1611	1306	567	535	482, 438	390	-	-	267
2C	$Co(pvaani)_2 \cdot ½H_2O$	3442	1612	1305	597, 558	541	488, 434	400	-	363	-

Table 4:39 Infrared frequencies (cm^{-1}) of the ovaani-based complexes

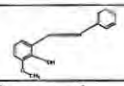

Compound		νO-H	νC=$N_{(imine)}$	νC-O	ν_aM-O	ν_sM-O	ν_aM-N	ν_sM-N	νM-Cl_{tet}	other	
3	ovaani	3447	1616	1254	-	-	-	-	-	-	-
3A	$Co(ovaani)_2Cl_2 \cdot ½H_2O$	3438	1638, 1609	1300	598, 562	514, 493	464	-	-	-	289
3B	$Co(ovaani)_2 \cdot 2H_2O$	3442	1603	1231	540	518	427	394	-	357	-
3C	$Co(ovaani)_2 \cdot ½H_2O$	3441	1603	1230	544	517	427	391	-	357	-

Table 4:40 Infrared frequencies (cm^{-1}) of the vaani-based complex

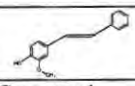

Compound		νO-H	νC=$N_{(imine)}$	νC-O	ν_aM-O	ν_sM-O	ν_aM-N	ν_sM-N	νM-Cl_{tet}	other	
4	vaani	3444	1622[(a)]	1284	-	-	-	-	-	-	-
4A	$Co(vaani)Cl_2$	3446	1646	1307	594	544, 510	-	384	352	-	226

(a) = split band

Table 4:41 Infrared frequencies (cm^{-1}) of the sal1amnap-based complexes

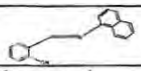

	Compound	νO-H	$\nu C{=}N_{(imine)}$	νC-O	$\nu_a M{-}O$	$\nu_s M{-}O$	$\nu_a M{-}N$	$\nu_s M{-}N$	νCo-Cl	$\nu Co{-}OH_2(?)$	other
5	sal 1 amnap	3384	1618	1281	-	-	-	-	-	-	-
5C	$Co(sal\ 1\ amnap)_2 \cdot 2H_2O$	3345	1604	1316	593	543	527	405	-	255	-

Table 4:42 Infrared frequencies (cm^{-1}) of the pvan1amnap-based complexes

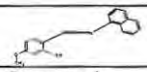

	Compound	νO-H	$\nu C{=}N_{(imine)}$	νC-O	$\nu_a M{-}O$	$\nu_s M{-}O$	$\nu_a M{-}N$	$\nu_s M{-}N$	νCo-Cl	$\nu Co{-}OH_2(?)$
6	pvan 1 amnap	3442	1613	1289	-	-	-	-	-	-
6A	$Co(p\text{-}van\ 1\ amnap)_2Cl_2 \cdot \frac{1}{2}H_2O$	3395	1636	1303	612	-	500	399	333(?)	273
6C	$Co(p\text{-}van\ 1\ amnap)_2 \cdot 2H_2O$	3420	1609	1308	596	539	-	-	-	268

Table 4:43 Infrared frequencies (cm^{-1}) of the ovan1amnap-based complex

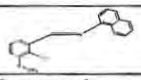

	Compound	νO-H	$\nu C{=}N_{(imine)}$	νC-O	$\nu_a M{-}O$	$\nu_a M{-}N$	$\nu_s M{-}N$	$\nu Co{-}OH_2(?)$	other
7	ovan 1 amnap	3447	1616	1254	-	-	-	-	-
7A	$Co(o\text{-}van\ 1\ amnap)_2.3H_2O$	3439	1627	1242	621	439	430	270	308

Table 4:44 Infrared frequencies (cm^{-1}) of the van1amnap complexes

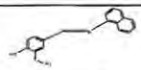

	Compound	νO-H	$\nu C{=}N_{(imine)}$	νC-O	$\nu_a M{-}O$	$\nu_s M{-}O$	$\nu_a M{-}N$	$\nu_s M{-}N$	νCo-Cl	$\nu Co{-}OH_2(?)$
8	van 1 amnap	3439	1621	1284	-	-	-	-	-	-
8A	$Co(van\ 1\ amnap)Cl \cdot 2H_2O$	3351	1648	1275	623	592	485	393	292	249
8C	$Co(van\ 1\ amnap)_2 \cdot 5H_2O$	3437	1620	1282	634	600	489	-	-	279, 251

Table 4:45 Infrared frequencies (cm^{-1}) of the sal4amp-based complexes

	Compound	νO-H	$\nu C{=}N_{(imine)}$	$\nu C{=}N_{(py)}$	νC-O	$\nu_a M{-}O$	$\nu_s M{-}O$	$\nu_a M{-}N$	$\nu_s M{-}N$	$\nu M{-}N_{(py)}$
9	sal4amp	3432	1630	1576	1280	-	-	-	-	-
9A	$Co(sal4amp)_2Cl_2$	3460	1610	1578	1276	584	518	415	389	255(?)
9B	$Co(sal4amp)_2$	3441	1622	1602	1281	585	517	441	318	226(?)
9C	$Co(sal4amp)_2 \cdot 2H_2O$	3460	1627	-	1280	585	516	441	318	224(?)

Table 4:46 Infrared frequencies (cm^{-1}) of the pvan4amp-based complexes

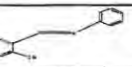

	Compound	νO-H	$\nu C{=}N_{(imine)}$	$\nu C{=}N_{(py)}$	νC-O	$\nu_a M{-}O$	$\nu_s M{-}O$	$\nu_a M{-}N$	$\nu_s M{-}N$	$\nu M{-}N_{(py)}$	other	
10	pvan4amp	3407	1633	1601	1267	-	-	-	-	-	-	-
10A	$Co(pvan4amp)_2Cl_2.2H_2O$	3446	1609	1603	1304	594	562	501	360	207(?)	383(?)	-
10B	$Co(pvan4amp)_2.6H_2O$	3480	1628	1609	1319	574	558	492	367	247(?)		303
10C	$Co(pvan4amp)_2.7H_2O$	3490	1629	1615	1320	575	555	491	363	-		302

Table 4:47 Infrared frequencies (cm^{-1}) of the ovan4amp-based complexes

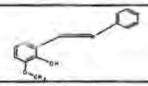

	Compound	νO-H	$\nu C{=}N_{(imine)}$	$\nu C{=}N_{(py)}$	νC-O	$\nu_a M{-}O$	$\nu_s M{-}O$	$\nu_a M{-}N$	$\nu_s M{-}N$	$\nu M{-}N_{(py)}$	other
11	o-van4amp	3358	1645	1603	1278	-	-	-	-	-	-
11A	$Co(ovan4amp)_2Cl_2 \cdot 3H_2O$	3427	1631	1539	1237	594, 560	543	-	415	240	387(?)
11B	$Co(ovan4amp)_2 \cdot 5H_2O$	3435	1615	1564	1238	557	531	450	413	-	-
11C	$Co(ovan4amp)_2 \cdot 3H_2O$	3331	1614	1563	1238	551	530	448	413	-	-

Table 4:48 Infrared frequencies (cm^{-1}) of the van4amp-based complexes

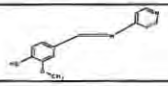

	Compound	νO-H	$\nu C{=}N_{(imine)}$	$\nu C{=}N_{(py)}$	νC-O	$\nu_a M{-}O$	$\nu_s M{-}O$	$\nu_a M{-}N$	$\nu_s M{-}N$	$\nu M{-}N_{(py)}$	other
12	van4amp	3444	1652	1588	1264	-	-	-	-	-	-
12A	$Co_2(van4amp)_3Cl_2{\cdot}5H_2O$	3456	1660	1625	1304	594,558	532	438	402	masked	345, 298
12B	$Co(van4amp)_2{\cdot}\frac{1}{2}H_2O$	3166	1646	1582	1272	554	-	448	357	278	-
12C	$Co(van4amp)_2{\cdot}\frac{1}{2}H_2O$	3166	1645	1581	1274	554	-	450	356	278	-

Table 4:49 Infrared frequencies (cm^{-1}) of the sal3amp-based complexes

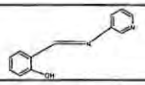

	Compound	νO-H	$\nu C{=}N_{(imine)}$	$\nu C{=}N_{(py)}$	νC-O	$\nu_a M{-}O$	$\nu_s M{-}O$	$\nu_a M{-}N$	$\nu_s M{-}N$	$\nu M{-}N_{(py)}$	other	
13	sal3amp	3442	1616	1568	1283	-	-	-	-	-	-	-
13A	$Co(sal3amp)_2Cl_2$	3440	1619	1566	1277	597	560, 536	436	342(?)	-	342(?)	309
13B	$Co(sal3amp)_2{\cdot}\frac{1}{2}H_2O$	3444	1604	1584	1317	597	547, 525	491	334	254	-	309
13C	$Co(sal3amp)_2{\cdot}\frac{1}{2}H_2O$	3443	1604	1575	1317	598	548	491	348	253	-	309

Table 4:50 Infrared frequencies (cm^{-1}) of the pvan3amp-based complexes

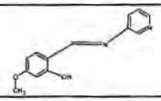

	Compound	νO-H	$\nu C{=}N_{(imine)}$	$\nu C{=}N_{(py)}$	νC-O	$\nu_a M{-}O$	$\nu_s M{-}O$	$\nu_a M{-}N$	$\nu_s M{-}N$	other	
14	p-van3amp	3442	1610	1586	1297	-	-	-	-	-	-
14A	$Co(pvan3amp)_2Cl \cdot H_2O$	3441	1609	1568	1207	591, 572	545	497, 430	413, 393	340	366
14B	$Co(pvan3amp)_2 \cdot ½H_2O$	3440	1615	1574	1210	576	521	496	409	-	365, 318
14C	$Co(pvan3amp)_2 \cdot 3H_2O$	3438	1615	1575	1211	576	520	496	409	-	364, 318

Table 4:51 Infrared frequencies (cm^{-1}) of the ovan3amp-based complexes

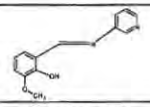

	Compound	νO-H	$\nu C{=}N_{(imine)}$	$\nu C{=}N_{(py)}$	νC-O	$\nu_a M{-}O$	$\nu_s M{-}O$	$\nu_a M{-}N$	$\nu_s M{-}N$	$\nu M{-}N_{(py)}$	other	
15	o-van3amp	3440	1615	1565	1259	-	-	-	-	-	-	-
15A	$Co(ovan3amp)_2Cl_2 \cdot 3H_2O$	3439	1608	1541	1235	566	530	494	447	255(?)	287	316
15B	$Co(ovan3amp)_2 \cdot ½H_2O$	3441	1614	1539	1234	541	520	470	347	271	-	306
15C	$Co(ovan3amp)_2 \cdot ½H_2O$	3442	1614	1563	1245	546	523	478	350	278	-	308

Table 4:52 Infrared frequencies (cm^{-1}) of the van3amp-based complexes

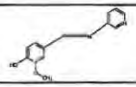

	Compound	νO-H	$\nu C{=}N_{(imine)}$	$\nu C{=}N_{(py)}$	νC-O	$\nu_a M{-}O$	$\nu_s M{-}O$	$\nu_a M{-}N$	$\nu_s M{-}N$	$\nu M{-}N_{(py)}$	other	
16	van3amp	3432	1623	1569	1286	-	-	-	-	-	-	-
16A	$Co\ (van3amp)_2Cl_2 \cdot 5H_2O$	3321	1665	1631	1285	591	559	509	428, 406	-	361	382
16C	$Co(van3amp)_2 \cdot ½H_2O$	3166	1645	1581	1274	590	541	463	425	-	-	353, 345

Table 4:53 Infrared frequencies (cm^{-1}) of the sal3pico-based complexes

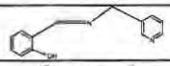

	Compound	νO-H	$\nu C{=}N_{(imine)}$	$\nu C{=}N_{(py)}$	νC-O	$\nu_a M{-}O$	$\nu_s M{-}O$	$\nu_a M{-}N$	$\nu_s M{-}N$	other	
17	sal3pico	3432	1628	1576	1274	-	-	-	-	-	-
17A	$Co(sal3pico)_2Cl_2 \cdot ½H_2O$	3441	1608	1531	-	590	504	421	352	325	302
17B	$Co(sal3pico)_2 \cdot H_2O$	3441	1619	1599	-	588	502	422	347	-	314
17C	$Co(sal3pico)_2 \cdot 1½H_2O$	3440	1621	1596	-	589	500	418	344	323	

Table 4:54 Infrared frequencies (cm^{-1}) of the pvan3pico-based complexes

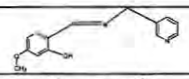

	Compound	νO-H	$\nu C{=}N_{(imine)}$	$\nu C{=}N_{(py)}$	νC-O	$\nu_a M{-}O$	$\nu_s M{-}O$	$\nu_a M{-}N$	$\nu_s M{-}N$	other	
18	p-van3pico	3425	1626	1515	1294	-	-	-	-	-	-
18A	$Co(pvan3pico)_2Cl_2$	3435	1617	1604	1305	591	502	445	420	325, 302	375,
18B	$Co(pvan3pico)_2 \cdot H_2O$	3428	1620	1602	1314	590	501	467	420	-	375, 302
18C	$Co(pvan3pico)_2 \cdot H_2O$	3442	1619	1603	1315	591	498	467	420	-	375, 302

Table 4:55 Infrared frequencies (cm^{-1}) of the ovan3pico-based complexes

	Compound	νO-H	$\nu C{=}N_{(imine)}$	$\nu C{=}N_{(py)}$	νC-O	$\nu_a M{-}O$	$\nu_s M{-}O$	$\nu_a M{-}N$	$\nu_s M{-}N$	other	
19	o-van3pico	3440	1615	1565	1259	-	-	-	-	-	-
19A	$Co(ovan3pico)_2Cl_2 \cdot 1½H_2O$	3439	1608	1541	1235	545	493	472	429	325, 302	375,
19B	$Co(ovan3pico)_2 \cdot H_2O$	3441	1614	1539	1234	533	502	470	425	-	375, 302
19C	$Co(ovan3pico)_2 \cdot H_2O$	3442	1614	1563	1245	530	502	465	426	-	375, 302

Table 4:56 Infrared frequencies (cm^{-1}) of van3pico-based complexes

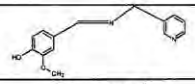

	Compound	νO-H	$\nu C{=}N_{(imine)}$	$\nu C{=}N_{(py)}$	νC-O	$\nu_a M{-}O$	$\nu_a M{-}N$	$\nu_s M{-}N$	$\nu M{-}N_{(py)}$	other	
20	van3pico	3432	1634	1580	1286	-	-	-	-	-	-
20A	Co $(van3pico)_2Cl_2 \cdot 3H_2O$	3378	1637	1555	1286	(b)	-	-	-	-	-
20B	$Co(van3pico)_2 \cdot 5H_2O$	3358	1642[a]	1553	1292	590	428	384	272	-	364

(a) Split band

(b) Far IR data not publishable

Table 4:57 Infrared frequencies (cm^{-1}) of the sal2pico-based complexes

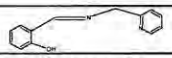

	Compound	νO-H	$\nu C{=}N_{(imine)}$	$\nu C{=}N_{(py)}$	νC-O	$\nu_a M{-}O$	$\nu_s M{-}O$	$\nu_a M{-}N$	$\nu_s M{-}N$	other	
21	sal2pico	3417	1625	1584	1303	-	-	-	-	-	-
21A	$Co(sal2pico)_2$	3439	1620	1589	1273	-	487	-	387	-	340
21B	$Co(sal2pico)_2 \cdot 4H_2O$	3440	1620	1565	1264	552	-	418	384	-	-
21C	$Co(sal2pico)_2 \cdot 4H_2O$	3442	1619	1562	1268	554	-	420	384	-	-

Table 4:58 Infrared frequencies (cm^{-1}) of the pvan2pico complexes

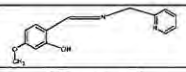

	Compound	νO-H	$\nu C{=}N_{(imine)}$	$\nu C{=}N_{(py)}$	νC-O	$\nu_a M{-}O$	$\nu_s M{-}O$	$\nu_a M{-}N$	$\nu_s M{-}N$	$\nu M{-}N_{(py)}$	other	
22	pvan2pico	3442	1614	1586	1271	-	-	-	-	-	-	-
22A	$Co(pvan2pico)_2Cl_2 \cdot 2H_2O$	3368	1629	1597	1302	591	556	-	428	-	360	335, 311
22B	$Co(pvan2pico)_2 \cdot 4H_2O$	3435	1598	1562	1290	591	553	463	423	283	-	270, 260
22C	$Co(pvan2pico)_2 \cdot 4½H_2O$	3445	1598	1561	1300	595	550	463	419	-	-	273, 260

Table 4:59 Infrared frequencies (cm^{-1}) of the ovan2pico complexes

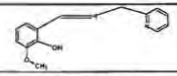

	Compound	νO-H	$\nu C{=}N_{(imine)}$	$\nu C{=}N_{(py)}$	νC-O	$\nu_a M{-}O$	$\nu_s M{-}O$	$\nu_a M{-}N$	$\nu_s M{-}N$	$\nu M{-}N_{(py)}$	other
23	ovan2pico	3440	1615	1565	1259	-	-	-	-	-	- -
23A	$Co(ovan2pico)_2Cl_2 \cdot 3H_2O$	3439	1608	1541	1235	545	493	472	429	-	- -
23B	$Co(ovan2pico)_2 \cdot 1½H_2O$	3441	1614	1539	1234	533	502	470	425	-	- 311
23C	$Co(ovan2pico)_2 \cdot 2H_2O$	3442	1614	1563	1245	530	502	465	426	-	- 308

Table 4:60 Infrared frequencies (cm^{-1}) of the van2pico complexes

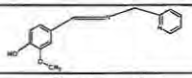

	Compound	νO-H	$\nu C{=}N_{(imine)}$	$\nu C{=}N_{(py)}$	νC-O	$\nu_a M{-}O$	$\nu_s M{-}O$	$\nu_a M{-}N$	$\nu_s M{-}N$	$\nu M{-}N_{(py)}$	other
24	van2pico	3432	1634	1580	1286	-	-	-	-	-	- -
24A	$Co_2(van2pico)_3Cl_2 \cdot H_2O$	3378	1637	1555	1286	-	-	-	-		
24B	$Co(van2pico)_2 \cdot 4H_2O$	3358	1642[a]	1553	1292	590	-	428	384	272	364

(a) Split band

(b) Far IR data not publishable

4.5 Electronic and diffuse reflectance spectra data for the ligands

Table 4:61 UV/visible and diffuse reflectance spectral data for the aniline-based Schiff bases

No.	Compound	Solvent	200-240 nm		250-300 nm		305-350 nm	>360 nm	
1	saani	Methanol	206	226	272	300	315	337	-
		DMF	-	-	272	300	318	334	-
		Solid state	-	273	286	304	326, 354	363	374
2	pvaani	Methanol	220	235	290	-	315, 335, 355	-	410
		DMF	-	-	279	-	308	-	-
		Solid state	-	-	289	302	307	367	457
3	ovaani	Methanol	220	235	275	290	305, 315	-	450
		DMF	-	-	-	304	308	-	540
		Solid state	-	-	270	-	324, 333, 344	373	398
4	vaani	Methanol	205	-	285	-	325, 345		418
		DMF	-	-	284	-	305, 344, 355		-
		Solid state	-	-	282	287	309, 379		-

Table 4:62 UV/visible and diffuse reflectance spectral data for the 1-aminonaphthalene-based Schiff bases

No.	Compound	Solvent	200-240 nm		250-300 nm		305-350 nm	>360 nm	
5	sallamnap	Methanol		230	260	-	354	-	
		DMF		-	-	300	346	-	
		Solid state		-	274	-	333	379	
6	pvanlamanap	Methanol	215	230	287		353	-	-
		DMF	-	-	278		322, 349	-	-
		Solid state	-	-	-		310	370	420 sh
7	ovanlamnap	Methanol	215	225	275	-	345		-
		DMF	-	-	274	296	336		-
		Solid state	-	-	290	-	333		509
8	vanlamnap	Methanol	226	234	-	-	-	364	
		DMF	-	-	290	300	336	-	
		Solid state	-	-	-	-	-	-	

Table 4:63 UV/visible and diffuse reflectance spectral data for the 4-aminopyridine-based Schiff bases

No.	Compound	Solvent	200-240 nm		250-300 nm		305-350 nm	>360 nm	
9	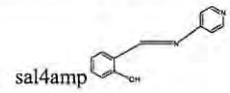 sal4amp	Methanol	215	-	257		319	-	408
		DMF	-	-	-		312	-	-
		Solid state	-	237	299		-	366	553
10	pvan4amp(2½$H_2$0) 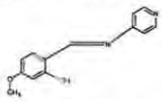	Methanol	206	246	280		339	-	
		DMF	-	-	274		328	-	
		Solid state	-	232	271		323, 332	361	
11	ovan4amp(H_2O) 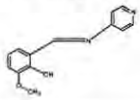	Methanol	209	250	-		-	391	
		DMF	-	-	274		340	-	
		Solid state	-	-	261		323	-	
12	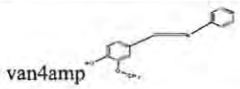 van4amp	Methanol	-	247	-		350		
		DMF	278	-	-		306, 314, 334		
		Solid state	-	236	278		318		

Table 4:64 UV/visible and diffuse reflectance spectral data for the 3-aminopyridine-based Schiff bases

No.	Compound	Solvent	200-240 nm		250-300 nm		305-350 nm	>360 nm	
13	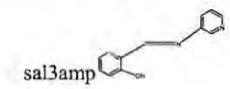 sal3amp	Methanol	-	226	277	-	340		-
		DMF	-	-	280	-	339		-
		Solid state	-	-	279	294	321, 348		418
14	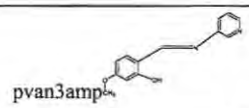 pvan3amp	Methanol	210	225	245	285	335	-	
		DMF	-	-	-	276	312	-	-
		Solid state	-	-	-	297	313, 353	365	-
15	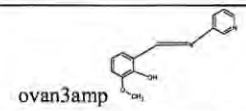 ovan3amp	Methanol		225	275	-	-	-	416
		DMF		-	278	298	-	-	-
		Solid state		-	267	302	309, 324, 343	367	392
16	van3amp 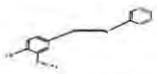	Methanol	210	240		-	345	365	380
		DMF	-	-		297	328	-	-
		Solid state	224	-		294	343	373	378

Table 4:65 UV/visible and diffuse reflectance spectral data for the 3-aminomethylpyridine-based Schiff bases

No.	Compound	Solvent	200-240 nm		250-300 nm		305-350 nm	>360 nm	
17	sal3pico 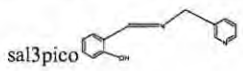	Methanol	225	250	260		315		401
		DMF	-	-	272		318		-
		Solid state	-	-	260		331		430
18	pvan3pico 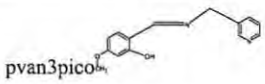	Methanol	220	235	265	300	-	380	
		DMF	-	-	278	-	318	-	
		Solid state	-	-	275	-	322	-	
19	ovan3pico 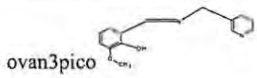	Methanol	225		265	-	335		420
		DMF	-		272	279	332		-
		Solid state	-		264	-	342		-
20	van3pico 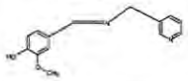	Methanol	225	275	290	300	310, 340	-	400
		DMF	-	-	272	-	302	360	-
		Solid state	-	-	273	-	309	-	-

Table 4:66 UV/visible and diffuse reflectance spectra data for the 2-aminomethylpyridine-based Schiff bases

No.	Compound	Solvent	200-240 nm		250-300 nm		305-350 nm	>360 nm	
21	sal2pico 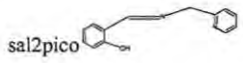	Methanol	217	230	260		317	365	
		DMF	-	292	300		318	365	
		Solid state	-	-	263		319	-	
22	pvan2pico 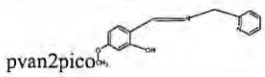	Methanol	221	230	260	-	-	-	
		DMF	-	294	302		315	365	
		Solid state	-		259		320, 331, 340	-	
23	ovan2pico 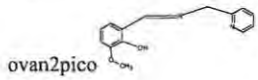	Methanol		220	265		325, 335	-	425
		DMF		-	272		330	-	-
		Solid state		-	269		319	371	-
24	van2pico 	Methanol		238	-		342		
		DMF		-	300		341		
		Solid state		-	290		345		

4.6 Electronic and diffuse reflectance spectral data for the complexes (UV/vis region)

Table 4:67 UV/visible and diffuse reflectance spectral data for the saani complexes

No.	Compound	Solvent	200-240 nm		250-300 nm		305-350 nm	360-700 nm	
1	saani	Methanol	206	226	272	300	315, 337	-	-
		DMF	-	-	272	300	318, 334	-	-
		Solid state	-	273	286	304	326, 354	363	374
1A	$Co(saani)_3Cl_2.1½H_2O$	Methanol	205	230		290	335	-	-
		DMF	-	-	275	295	-	385	592
		Solid state	-	-	276	-	365	625	676
1B	$Co(saani)_2.½H_2O$	Methanol	205	230	290		335	382	
		DMF	-	-	281		349	400	
		Solid state	-	-	282		309, 330, 352	469	
1C	$Co(saani)_2$	Methanol	205	230	290		345	380	-
		DMF	-		288		-	398	-
		Solid state	225		279		314	350	535

Table 4:68 UV/visible and diffuse reflectance spectral data for the pvaani complexes

No.	Compound	Solvent	200-240 nm		250-300 nm		305-350 nm	360-700 nm	
2	pvaani	Methanol	220	235	290		315, 335	355	410
		DMF	-	-	279		308	-	-
		Solid state	-	-	289		302, 307	367	457
2A	$Co(pvaani)_2Cl_2$	Methanol	205	245	290	315	-	365	-
		DMF	-	-	289	-	347	373	-
		Solid state	-	-	262	-	334	-	671
2B	$Co(pvaani)_2$	Methanol	210	235	245	280	295	305	365
		DMF	-	-		293	349	373	-
		Solid state	-	-	284	-	354	494	-
2C	$Co(pvaani)_2.½H_2O$	Methanol	205	245	-		305	365	-
		DMF	-	-	295		-	370	-
		Solid state	-	-	292		-	359	490

Table 4:69 UV/visible and diffuse reflectance spectral data for the ovaani complexes

No.	Compound 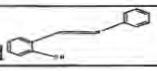	Solvent	200-240 nm		250-300 nm		305-350 nm	360-700 nm	
3	ovaani	Methanol	220	235	275	290	305	315	450
		DMF	-	-	-	-	304, 308	-	540
		Solid state	-	270	-	324	333, 344	373	398
3A	$Co(ovaani)_2Cl_2.½H_2O$	Methanol	210		245	300	-	365	-
		DMF	-		-	287	-	362	-
		Solid state	-		267	298	372	459	668
3B	$Co(ovaani)_2.½H_2O$	Methanol	205	235	-	300	-	395	-
		DMF	-	274	284	-	341	395	-
		Solid state	-	-	-	292	322	374	465
3C	$Co(ovaani)_2.½H_2O$	Methanol	205	215	240	280	-	395	-
		DMF	-	-	-	297	312	-	-
		Solid state	-	-	287	-	319	361, 372	464

Table 4:70 UV/visible and diffuse reflectance spectral data for the vaani complex

No.	Compound 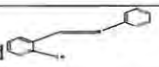	Solvent	200-240 nm		250-300 nm		305-350 nm	360-700 nm	
4	vaani	Methanol	205		285	-	325, 345	418	
		DMF	-		284	-	305, 344	355	
		Solid state	-		282	287	309	379	
4A	$Co(vaani)Cl_2$	Methanol	205	230	280		335	-	-
		DMF	-	-	275		316, sh 335	-	-
		Solid state	-	-	269		322, 346	618	665

Table 4:71 UV/visible and diffuse reflectance spectral data for the sal1aminonaphthalene-based complexes

No.	Compound 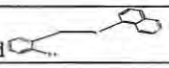	Solvent	200-240 nm		250-300 nm		305-350 nm	360 -700 nm
5	sal1amnap	Methanol		230	260	-	354	-
		DMF		-	-	300	346	-
		Solid state		-	274	-	333	379
5C	$Co(sal1amnap)_2.2H_2O$	Methanol		231	-		346	-
		DMF		-	285		332, 344	-
		Solid state		-	271		306	353

Table 4:72 UV/visible and diffuse reflectance spectral data for the pvanlaminonaphthalene-based complexes

No.	Compound	Solvent	200-240 nm		250-300 nm		305-350 nm	360 -700 nm	
6	pvanlamnap	Methanol	215		230	285	345	355	-
		DMF	-		-	278	322	349	-
		Solid state	-		-	-	310	370	sh420
6A	$Co(pvanlamnap)_2Cl_2.½H_2O$	Methanol		228		288	347	-	-
		DMF		-		293	346	-	-
		Solid state		231		299	354	374	667
6C	$Co(pvanlamnap)_2.2H_2O$	Methanol		235		-	352	-	
		DMF		-		287	345	-	
		Solid state		-		280	308, 320, 348	376	

Table 4:73 UV/visible and diffuse reflectance spectral data for the ovanlaminonaphthalene-based complexes

No.	Compound	Solvent	200-240 nm		250-300 nm		305-350 nm	360-700 nm	
7	ovanlamnap	Methanol	215	225	275	-	345	407	-
		DMF	-	-	274	296	336	-	-
		Solid state	-	-	-	290	333	-	509
7A	$Co(ovanlamnap)_2.3H_2O$	Methanol		220	280		335		-
		DMF		-	274		343		-
		Solid state		-	269		326, 343		667

Table 4:74 UV/visible and diffuse reflectance spectral data for the vanlaminonaphthalene-based complexes

No.	Compound	Solvent	200-240 nm		250-300 nm		305-350 nm	360-700 nm	
8	Vanlamnap	Methanol		226	234	-	364	-	
		DMF		-	290	300	336	-	
		Solid state		259	-	328	-	448	
8A	$Co(vanlamnap)Cl.2H_2O$	Methanol	210	230	280		335	355	-
		DMF	-	-	280		316	-	-
		Solid state	-	-	266		333	445	614
8C	$Co(vanlamnap)_2.5H_2O$	Methanol		228	-	-	359	-	-
		DMF		-	284	292	-	-	-
		Solid state		-	261	-	316, 337, 354	490	611

Table 4:75 UV/visible and diffuse reflectance spectral data for the sal4aminopyridine-based complexes

No.	Compound 	Solvent	200-240 nm		250-300 nm		305-350 nm	360-700 nm	
9	sal4amp	Methanol	225	255	-		315	400	-
		DMF	-	-	276		349	-	-
		Solid state	-	237	299		-	366	553
9A	$Co(sal4amp)_2Cl_2$	Methanol	225	235	250		345	375	-
		DMF	-	-	274		325	-	-
		Solid state	-	-	262		311, 319, 366	577	640
9B	$Co(sal4amp)_2$	Methanol	215	225	235	-	340, 375	-	-
		DMF	-	-	276	-	324, 371	-	-
		Solid state	-	-	271	301	314, 350	363	374
9C	$Co(sal4amp)_2.2H_2O$	Methanol	210		250		325, 340	-	375
		DMF	-		274		342	-	370
		Solid state	224		277		304, 312, 353	363	373

Table 4:76 UV/visible and diffuse reflectance spectral data for the pvan4aminopyridine-based complexes

No.	Compound 	Solvent	200-240 nm		250-300 nm		305-350 nm	360-700 nm	
10	pvan4amp	Methanol	210	240		280	335	-	
		DMF	-	-		274	328	-	
		Solid state	-	232	271	323	332	361	
10A	$Co(pvan4amp)_2Cl_2.2H_2O$	Methanol	215	230	245	280	335	355	-
		DMF	-	-	274	284	307, 346	359	-
		Solid state	-	-	266	-		361	378
10B	$Co(pvan4amp)_2.6H_2O$	Methanol	230	245	280	-	315, 345	355	
		DMF	-	-	280	284	-	359	
		Solid state	227	-	273	-	317, 328	368	
10C	$Co(pvan4amp)_2.7H_2O$	Methanol		245	280		345	355	
		DMF		-	290		-	359	
		Solid state		-	272		324, 333	373	

Table 4:77 UV/visible and diffuse reflectance spectral data for the ovan4aminopyridine-based complexes

No.	Compound 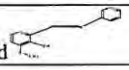	Solvent	200-240 nm		250-300 nm		305-350 nm	360-700 nm
11	ovan4amp	Methanol	215	250	-	-	340	
		DMF	-	-	282	295	348	
		Solid state	-	-	261	-	323	
11A	$Co(ovan4amp)_2Cl_2.3H_2O$	Methanol	220		265	-	340	-
		DMF	-		-	275	347	-
		Solid state	-		-	273	324	362
11B	$Co(ovan4amp)_2.5H_2O$	Methanol	210	225	240	-	315	355
		DMF	-	-	-	271	344	-
		Solid state	226	-	-	273	324	367
11C	$Co(ovan4amp)_2.3H_2O$	Methanol	210		245	-	335, 345	-
		DMF	-		-	272	341, 345	-
		Solid state	-		-	274	308	367

Table 4:78 UV/visible and diffuse reflectance spectral data for the van4aminopyridine-based complexes

No.	Compound 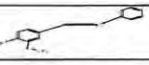	Solvent	200-240 nm		250-300 nm		305-350 nm	360-700 nm	
12	van4amp	Methanol	-	247			350		
		DMF	278	-			306, 314, 334		
		Solid state	-	-			-		
12A	$Co_2(van4amp)_3Cl_2.5H_2O$	Methanol	210	250	-	-	340	355	-
		DMF	-	-	276	303	343, 347	-	-
		Solid state	-	-	-	299	366	463	579
12B	$Co(van4amp)_2.2½H_2O$	Methanol	205		250	-	340	355	-
		DMF	-		276	-	308, 349	-	-
		Solid state	-		-	295	365	498	594
12C	$Co(van4amp)_2.3H_2O$	Methanol		215	235	245	330	345	360
		DMF		-	276	-	307, 340	-	-
		Solid state		-	-	-	306	477	578

Table 4:79 UV/visible and diffuse reflectance spectra data for the sal3aminopyridine-based complexes

No.	Compound	Solvent	200-240 nm		250-300 nm		305-350 nm	360-700 nm	
13	sal3amp	Methanol	225		275	-	335	-	-
		DMF	-		273	301	-	-	-
		Solid state	-		279	294	321, 348	-	418
13A	$Co(sal3amp)_2Cl_2$	Methanol	220	235	275		-	380	-
		DMF	-	-	276		320	370	-
		Solid state	-	-	263		349		646
13B	$Co(sal3amp)_2.\ ½H_2O$	Methanol	205		275		335	410	-
		DMF	-		277		320	-	-
		Solid state	-		268		309	365	370
13C	$Co(sal3amp)_2.\ ½H_2O$	Methanol	205		270		340	405	
		DMF	-		277		322	351	
		Solid state	-		267		-	366	

Table 4:80 UV/visible and diffuse reflectance spectral data for the pvan3aminopyridine-based complexes

No.	Compound	Solvent	200-240 nm		250-300 nm		305-350 nm	360-700 nm	
14	pvan3amp	Methanol	210	225	245	285	335	-	
		DMF	-	-	-	278	319	-	
		Solid state	-	-	-	297	313, 353	365	
14A	$Co(pvan3amp)_2Cl.H_2O$	Methanol	205	240	285		-	360	-
		DMF	-	-	278		318	-	-
		Solid state	-	-	269		361	584	627
14B	$Co(pvan3amp)_2.\ ½H_2O$	Methanol			280		338	-	373
		DMF			272		326	363	sh571
		Solid state			284		-	360	-
14C	$Co(pvan3amp)_2.3H_2O$	Methanol	207	-	275		-	377	
		DMF	-	-	-		318	368	
		Solid state	-	239	281		-	354	

Table 4:81 UV/visible and diffuse reflectance spectral data for the ovan4aminopyridine-based complexes

No.	Compound 	Solvent	200-240 nm		250-300 nm		305-350 nm	360-700 nm	
15	ovan3amp	Methanol		225	275	-	-	-	416
		DMF		-	278	298	-	-	-
		Solid state		-	267	302	309, 324, 343	367	392
15A	Co(ovan3amp)Cl.H_2O	Methanol	211	240	270	285		-	391
		DMF	-	-	272	-	324	-	-
		Solid state	-	-	273	-	398	585	637
15B	Co(ovan3amp)$_2$.½H_2O	Methanol	205	245	280		335	-	401
		DMF	-	-	283		318	-	-
		Solid state	279	-			324	364	-
15C	Co(ovan3amp)$_2$.½H_2O	Methanol	205	241	279		-	-	400
		DMF	-	-	280		321	-	-
		Solid state	-	-	283		310	377	-

Table 4:82 UV/visible and diffuse reflectance spectral data for the van4aminopyridine-based complexes

No.	Compound 	Solvent	200-240 nm		250-300 nm		305-350 nm	360 -700 nm	
16	van3amp	Methanol	210	240		-	345	365	380
		DMF	-	-		297	328	-	-
		Solid state	224	-		294	343	373	378
16A	Co(van3amp)Cl_2.H_2O	Methanol	205	235		285	315, 325, 335		
		DMF	-	-		-			
		Solid state	-	-		-			
16C	Co(van3amp).2H_2O	Methanol	210	240	-	-	345	355	-
		DMF	-	-	280	-	315	345	-
		Solid state	-	-	271	297	341, 353	367	376

Table 4:83 UV/visible and diffuse reflectance spectral data for the sal3pico-based complexes

No.	Compound 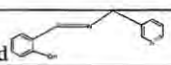	Solvent	200-240 nm		250-300 nm		305-350 nm	360-700 nm	
17	sal3pico	Methanol	225		250	260	315		401
		DMF	-		272	-	318		-
		Solid state	-		260	-	331		430
17A	Co(sal3pico)$_2$$Cl_2$.½$H_2O$	Methanol	215	240	-		-	390	-
		DMF	-	-	-		-	-	-
		Solid state	-	-	276		316 , 360	375	621
17B	Co(sal3pico)$_2$.H_2O	Methanol	205		270		335	385	-
		DMF	-		280		315	380	-
		Solid state	-		276		349	353	585
17C	Co(sal3pico)$_2$.1½H_2O	Methanol	205		265		335	385	-
		DMF	-		280		-	369	-
		Solid state	-		275		338	355	588

Table 4:84 UV/visible and diffuse reflectance spectral data for the pvan3pico-based complexes

No.	Compound	Solvent	200-240 nm		250-300 nm		305-350 nm	360-700 nm	
18	pvan3pico	Methanol	220	235	265	300	-	380	
		DMF	-	-	278	-	318	-	
		Solid state	-	-	273	-	-	365	
18A	$Co(pvan3pico)_2Cl_2$	Methanol	205		265	-	325, 340	-	-
		DMF	-		280	291	317	364	-
		Solid state	-		283	303	330, 363	539	622
18B	$Co(pvan3pico)_2.½H_2O$	Methanol	205		260		-	365	
		DMF	-		279		318	364	
		Solid state	-		285		-	365	
18C	$Co(pvan3pico)_2.½H_2O$	Methanol	205		260			365	
		DMF	-		278			362	
		Solid state	-		273			357	

Table 4:85 UV/visible and diffuse reflectance spectral data for the ovan3pico-based complexes

No.	Compound	Solvent	200-240 nm		250-300 nm		305-350 nm	360-700 nm	
19	ovan3pico	Methanol	225		265	-	335		420
		DMF	-		272	279	332		-
		Solid state	-		264	-	342		-
19A	$Co(ovan3pico)_2Cl_2.1½H_2O$	Methanol	210	240	265		-	385	-
		DMF	-	-	284		316	374	-
		Solid state	-	-	286		313, 360	381	596
19B	$Co(ovan3pico)_2.H_2O$	Methanol	205	215	265		335	405	-
		DMF	-	-			347	-	363
		Solid state	-	-	268		346	355	367
19C	$Co(ovan3pico)_2.H_2O$	Methanol	205		270		340	-	410
		DMF	-		280		-	356	-
		Solid state	-		268		-	367	377

Table 4:86 UV/visible and diffuse reflectance spectral data for the van3pico-based complexes

No.	Compound	Solvent	200-240 nm		250-300 nm		305-350 nm	360 -700 nm	
20	van3pico	Methanol	225	275	290	300	310	340	400
		DMF	-	-	272	-	302	360	-
		Solid state	-	-	273	-	309	-	-
20A	$Co(van3pico)_2Cl_2.1½H_2O$	Methanol		249	-		343		
		DMF		-	289		303		
		Solid state		-	-		-		
20B	$Co(van3pico)_2.5H_2O$	Methanol		246	-	-	345		565
		DMF		-	286	306	346		564
		Solid state		-	-	-	-		-

Table 4:87 UV/visible and diffuse reflectance spectral data for the sal2pico-based complexes

No.	Compound	Solvent	200-240 nm		250-300 nm		305-350 nm	>360 nm	
21	sal2pico	Methanol	217	230	260	-	317	365	
		DMF	-	292	-	300	318	365	
		Solid state	-	-	263	-	319	-	
21A	$Co(sal2pico)_2$	Methanol	215	220	255		-	-	
		DMF	-	-	292		328, 345	-	
		Solid state	-	-	-		351	394	
21B	$Co(sal2pico)_2.4H_2O$	Methanol	227	246	260		-	390	-
		DMF	-	-	289		342	-	-
		Solid state	-	-	272		-	-	618
21C	$Co(sal2pico)_2.4H_2O$	Methanol	225	245	260		-	390	-
		DMF	-	-	285		344	-	-
		Solid state	-	-	-		328	-	620

Table 4:88 UV/visible and diffuse reflectance spectral data for the pvan2pico-based complexes

No.	Compound	Solvent	200-240 nm		250-300 nm		305-350 nm	360-700 nm	
22	pvan2pico	Methanol	221	230	285	-	345	355	
		DMF	-	-	294	302	315	365	
		Solid state	-	-	259	320	331, 340	-	
22A	$Co(pvan2pico)_2\ Cl_2.2H_2O$	Methanol	223		252		348	-	-
		DMF	-		290		345	-	-
		Solid state	-		-		-	356	384
22B	$Co(pvan2pico)_2.4H_2O$	Methanol	210		255	-	340		
		DMF	-		280	303	344		
		Solid state	-		260	-	-		
22C	$Co(pvan2pico)_2.4½H_2O$	Methanol	215		255	-	340		-
		DMF	-		283	300	353		-
		Solid state	-		-	-	345		518

Table 4:89 UV/visible and diffuse reflectance spectral data for the ovan2pico-based complexes

No.	Compound 	Solvent	200-240 nm		250-300 nm		305-350 nm	360 -700 nm	
23	ovan2pico	Methanol	220		265		325, 335	425	
		DMF	-		272		330	-	-
		Solid state	-		269		319	371	482
23A	$Co(ovan2pico)_2Cl_2.3H_2O$	Methanol	235	245	-	-	-	395	630
		DMF	-	276	286	291	344	-	-
		Solid state	-	-	-	-	306	402	630
23B	$Co(ovan2pico)_2.1½H_2O$	Methanol	215	230	245	255	-		-
		DMF	-	-	276	284	344		-
		Solid state	-	-	-	-	350		483
23C	$Co(ovan2pico)_2.2H_2O$	Methanol	215	230	245	-	-	400	
		DMF	-	-	284	298	344	-	
		Solid state	-	-	-	-	331	480	

Table 4:90 UV/visible and diffuse reflectance spectral data for the van2pico-based complexes

No.	Compound 	Solvent	200-240 nm		250-300 nm		305-350 nm	360 -700 nm	
24	van2pico	Methanol	215	230	285		345	355	
		DMF	-	-	300		342	-	
		Solid state	-	-	290		345	-	
24A	$Co(van2pico)_2Cl_2.H_2O$	Methanol		250			-	352	-
		DMF		-	300		344	-	-
		Solid state		-	289		342	-	500
24B	$Co(van2pico)_2.4H_2O$	Methanol		253		-	350		-
		DMF		-		303	345		-
		Solid state		-		-	341		504

4.7 NMR spectroscopy spectra data for the ligands

Table 4:91 ^{1}H and ^{13}C chemical shift of the aniline-based ligands

No.	compound		HC=N	C-OH	O-CH_3	LFER Σσ
1	saani	^{1}H ^{13}C	8.63(s, 1H) 162.7	13.25 (br,1H) 161.1	- -	1.22[1]
2	pvaani	^{1}H ^{13}C	8.56 (s, 1H) 161.4	13.80 (br,1H) 164.0	3.88 (s, 3H) 55.4	0.95[1]
3	ovaani	^{1}H ^{13}C	8.64(s, 1H) 162.6	13.70 (br,1H) 151.5	3.94 (s, 3H) 56.2	1.34[1]
4	vaani	^{1}H ^{13}C	8.36 (s, 1H) 160.5	6.14 (br,1H) 147.2	3.99 (s, 3H) 55.2	-0.25[2]

Table 4:92 ^{1}H and ^{13}C chemical shift of the 1-aminonapthalene-based ligands

No.	compound		HC=N	C-OH	O-CH_3	LFER Σσ
1	sal1amnap	^{1}H ^{13}C	8.71(s, 1H) 162.6	13.41 (s,1H) 161.2	-	1.22[1]
2	pvan1amnap	^{1}H ^{13}C	8.62 (s, 1H) 162.6	13.88 (s,1H) 163.9	3.88 (s, 3H) 55.7	0.95[1]
3	ovan1amnap	^{1}H	8.73(s, 1H) 163.3	13.94 (s,1H) 151.4	3.94 (s, 3H) 56.16	1.34[1]
4	van1amnap	^{1}H ^{13}C	8.43 (s, 1H) 160.0	7.76 (1H) 147.2	4.00 (s, 3H) 56.1	-0.25[2]

Table 4:93 ^{1}H and ^{13}C chemical shift of the 4-aminopyridine-based ligands

No.	compound		HC=N	C-OH	H-$N_{(py)}$	N-C(H)=C	O···H-$N_{(amine)}$	C=$O_{(quinoid)}$	C-OMe	O-CH_3	LFER Σσ
9	sal4amp	^{1}H ^{13}C	8.49(s, 1H) 166.5	13.04 (br,<1H) 160.9	3.96 (s,<1H) -	- -	- -	- -	- -	- -	1.22[1]
10	pvan4amp	^{1}H ^{13}C	- -	- -	4.1 (br,<1H) -	9.72 (s,<1H) 151.0	13.11 (br,<1H) -	- 194.4	- 164.3	3.47 (d, 3H) 55.7 (d)	0.95[1]
11	ovan4amp	^{1}H -	- -	- -	4.15 (br,<1H) -	10.00(s1H) 151.4	13.11 (br,<1H) -	- 196.6	- 165.7	3.94 (d, 3H) 55.7 (d)	1.34[1]
12	van4amp	^{1}H ^{13}C	(Insoluble) (Insoluble)								-0.25[2]

Table 4:94 ^{1}H and ^{13}C chemical shift of 3-aminopyridine-based ligands

No.	compound		HC=N	C-OH	O-CH_3	LFER Σσ
13	sal3amp	^{1}H ^{13}C	8.64(s, 1H) 161.1	12.75 (s,1H) 164.5	-	1.22[1]
14	pvan4amp	^{1}H ^{13}C	8.54 (s, 1H) 163.6	13.20 (s,1H) 164.4	3.86 (s, 3H) 55.5	0.95[1]
15	ovan4amp	^{1}H ^{13}C	8.63(s, 1H) 164.6	13 08 (s,1H) 151.2	3.92 (s, 3H) 56.2	1.34[1]
16	van4amp	^{1}H ^{13}C	8. 34 (s, 1H) 160.2	2. 17 (1H) 152.6	3.99 (s, 3H) 56.1	-0.25[2]

Table 4:95 ^{1}H and ^{13}C chemical shift of 3-aminomethylpyridine-based ligands

No.	compound		HC=N	C-OH	O-CH_3	=N-CH_2	LFER Σσ
17	sal3pico	^{1}H ^{13}C	8.49(s, 1H) 160.9	13.04 (s,1H) 166.45	- -	4.82(s, 2H) 60.7	1.22[1]
18	pvan3pico	^{1}H ^{13}C	7.99 (s, 1H) 164.8	13.80 (br,1H) 163.0	3.50 (s, 3H) 54.6	4.34 (s,2H) 59,1	0.95[1]
19	ovan3pico	^{1}H	8.09(s, 1H) 165.9	13.08 (s,1H) 150.5	3.48 (s, 3H) 55.3	4.39 (s,2H) 59.5	1.34[1]
20	van3pico	^{1}H ^{13}C	8.06 (s, 1H) 162.5	9.81 (br,1H) 149.1	3.92(s, 3H) 55.9	4.79 62.1	-0.25[2]

Table 4:96 ^{1}H and ^{13}C chemical shift of 2-aminomethylpyridine-based ligands

No.	compound		HC=N	C-OH	O-CH_3	=N-CH_2	LFER Σσ
21	sal2pico	^{1}H ^{13}C	(Insoluble) (Insoluble)				1.22[1]
22	pvan2pico	^{1}H ^{13}C	8.39 (s, 1H) ~161	13.77 (br,1H) 165.7	3.47 (s, 3H) 55.4	4.81(s, 2H) 64.0	0.95[1]
23	ovan2pico	^{1}H ^{13}C	7.23(s, 1H) 166.5	12.29 (br,1H) 151.2	3.46 (s, 3H) 56.1	4.88 (s, 2H) 64.6	1.34[1]
24	van2pico	^{1}H ^{13}C	(Insoluble) (Insoluble)				-0.25[2]

4.8 References

1. C. Hansch, A. Leo, R. W. Taft, Chem. Rev.; 1991, **91**, 165-195.
2. E. M. Hodnett, W. J. Dunn, III, J. Med. Chem.; 1970, **13**, 768-71.

5 DISCUSSION (PHYSICAL AND CHEMICAL STUDY)

5.1 Preliminary comment

This chapter is used to discuss the results obtained from all the techniques used in characterizing the isolated Schiff bases and their corresponding Co(II) complexes. The discussion will focus on some of the observed striking behaviours of the various synthesized ligands and complexes.

The analytical data of the twenty-four ligands isolated are listed in Tables 4:1 – 4:6. The ligands are subdivided into six groups based on the type of amine that was condensed with salicylaldehyde, vanillin, *ortho*-vanillin or *para*-vanillin. The effect of having hydroxy and methoxy groups in different position is observed in the colours, rate of reactions as well as in all the physicochemical and spectroscopic data.

The analytical data of all the isolated complexes of the various Schiff bases are listed in Tables 4:7 – 4:30. The complexes are grouped according to the type of amine used in preparing their Schiff bases. In all, we have six categories based on the six groups of amine ligands.

5.1.1 Colours and structures of the synthesized ligands

Six categories of Schiff bases have been synthesized as a result of using different amines for the formation of the ligands. Each of the different categories has four different types of Schiff bases because they have been produced from the condensation of salicylaldehyde, *para*-vanillin, *ortho*-vanillin or vanillin with the various amines. The resulting Schiff bases are intensely coloured and are of varying colours.

The colour intensities as well as the various colours can be attributed to the different amines as well as the positions of the methoxy and the hydroxy groups on the phenyl attached to the carbon of the C=N. These auxochromic groups at different positions resulted in the observed varying colours of the Schiff bases. The presence of the hydroxy and or methoxy in the conjugated system resulted in the enhancement of the delocalization of the π-electrons in the molecule, consequently resulting in the different colours. It must be noted that the studies revealed that the hydroxy group in the *ortho*- position is the cause of the high colour intensity. While all the *ortho*-hydroxylated or and *meta*- or *para*- methoxy containing ligands are intensely coloured, most of the ligands obtained from vanillin are cream-like, less intense, because the OH is *para* -

substituted. The effect of using different amines is seen in the varying colours of the ligands and their corresponding complexes.

While *ortho-* hydroxyl ligands are coloured, the presence of methoxy in *meta-* or *para-* position resulted in more intense coloured ligands. For instance, while ligand 1 and 2 are yellow, the presence of methoxy group in the *para-* position of ligand 2 resulted in more intense yellowish compound. This phenomenon is also shown by ligand 13 and 15 respectively. The two are orange in colour with ligand 15 having more intense colour because of the presence of the *meta-* methoxy substituent.

The structures of Schiff bases and their analogues have been thoroughly studied and summarized.[1,2] The molecular structure of Schiff bases is determined by the possibilities for tautomeric transformation, formation of different types of hydrogen bond as well as by conformational effects.[3] These properties, as shown in the IR, UV/vis/ NIR and NMR sections, are responsible for the factors influencing the structure of Schiff base complexes.

In this work, the results obtained from the UV/vis in methanol and DMF as well as from the NMR in chloroform have been used to explain the phenomenon of tautomerism in Schiff bases. Some information in the literature regarding the stereochemistry of Schiff bases have been considered while drawing the tentative structures of the synthesised Schiff bases as well as while discussing some of their behaviour. For instance, it has been established that non-planar form of Schiff base is the energetically preferred conformation.[1,3] IR, UV and NMR have been used to explain hydrogen bonding in Schiff bases. The strength of hydrogen bond has been used to determine the preferred Z- to E- isomerization. In some cases, the formation of intramolecular hydrogen bond is an alternative to the formation of intermolecular hydrogen bond. Intramolecular hydrogen bonds in Schiff bases may form six- or five-membered cycles. The hydrogen bonds participating in six-membered rings are essentially stronger than those of five-membered rings due to the acquisition of a quasi-aromatic type in the former case;[3] this can be supported by spectroscopic data.

5.1.2 Some physical trends across the different groups of Schiff bases

The general trend observed for each group was that Schiff base with methoxy substituent have higher melting points than those without. It was also observed that ligands with OH in the para-

position melt at higher temperature than others. All the ligands are stable in air. The Schiff bases are soluble in all organic solvents but poorly soluble in water. A literature search employing SciFinder revealed that most of the compounds reported here are novel. The few ones that have been reported are referenced in this work. Worthy of mentioning is the rate of formation of the ligands in Table 4:1 – 4:6. The formation of Schiff base decreases as the amine used was changed from aniline to aminopyridines to aminomethylpyridines. While some of the ligands formed after 2 – 12 hours of refluxing, other remained in solution for days, while others were isolated as oily liquids. For instance, while crystalline ligand 7 was obtained immediately after refluxing, ligand 6 took days to crystallized, ligand 5 was an oily liquid until ammonium hydroxide added to solidify it. These behaviors are attributable to the presence, absence or position of the methoxy as well as the hydroxyl groups in each of the ligands. Earlier workers refluxed the amine with aldehydes or ketones for 12 – 18 hours.[4] The first sets of ligands synthesised were refluxed for 18, 12, 6, 3 and 2 hours respectively. It was observed that there was no much difference in the yields when the reaction time was reduced; consequently, most of the ligands were later refluxed for 2 hours. The observation was supported by the syntheses of Schiff bases by Al-Allaf and Sheet,[5] Cimerman et al.,[6] Guofa et al.,[7] Yeap et al.,[8]

5.1.3 Structure of the complexes

The reactions of Schiff bases with transition-metal compounds can lead to three types of complexes. The most common of these is the inner-chelate complex in which the Schiff base is bonded to the metal through the oxygen atoms of its deprotonated hydroxy groups and the nitrogen atoms of its C=N groups.[9] That is, those in which the ligand binds as a dianionic N_2O_2 donor system. Schiff bases have also been known to coordinate via nitrogen atoms only.[9] This is the system in which the ligands act as a neutral N_2 donor binding via the imine groups. This occurs when transition-metal halides are used. The third possibility involves the hydrogenation of the C=N group, and formation of an inner-chelate complex between the secondary amine ligands and the metal in a higher oxidation state.[9]

All the complexes obtained from cobalt chloride are denoted as "A", those of cobalt acetate as "B" while those in which triethylamine was added to cobalt chloride are represented as "C". In the work reported here, the first two coordination types have been formed. These conclusions are based on both vibrational and electronic spectra, diffuse reflectance spectra and microanalysis results. The two types of complexes isolated are: the $CoL_2.nH_2O$ complexes, which were

synthesized by reaction of Schiff base with cobalt(II) acetate in methanol or by the reaction of triethylamine added to cobalt chloride before combining with the Schiff base and the $Co(HL)_2Cl_2.nH_2O$, containing neutral ligands, obtained from the reaction of cobalt(II) chloride in methanol with HL_2. Simply put, the formulae for isostructural series 'A' complexes are anticipated to be $ML_2X_2.nH_2O$, (L = Schiff base, X = chloride) while those of series 'B' and 'C' are anticipated to have $ML_2.nH_2O$. There are few of the complexes that do not follow the general formulae highlighted above. These are: 1A $[M(HL)_3Cl_2]$, 4A = $(MLCl_2)$, 7A and 21A (ML_2), 8A = (MLCl), 12A = $(M_2L_3Cl_2)$, 15A (MLCl).

Efforts were made to synthesized three complexes from each of the twenty-four ligands. However, it was only possible to synthesised sixty-one out of the expected seventy-two complexes. The complexes 4B, 4C, 5A, 5B, 6B, 7B, 7C, 8B, 16B, 20C and 24C were unable to be made with success. The bulkiness of the aminonaphthalene and small ionic radius of 3d cobalt might be ascribed for the reason why complexes 5A, 5B, 6B, 7B, 7C and 8B cannot be made. This may account for the reason while most of the complexes that have been obtained from this ligand are made from rare earth elements.[10,11] The presence of hydroxy in the *para*-position of the phenyl ring favours bridging instead of chelation, hence might be the reason why the complexes 4B, 4C, 16B, 20C and 24C were not formed.

While most of the complexes synthesized from *ortho*-hydroxylated or and *para-* or *meta*-methoxy Schiff bases with cobalt chloride are green, those produced from cobalt acetate or cobalt chloride with triethylamine added are brown, reddish brown or yellowish green. The presences of auxochromic groups in the ligands have striking effects on the color of the resulting complexes. For instance, while all the complexes obtained from cobalt chloride are green, the intensity of the green depends on the position of methoxy group in addition to the *ortho*-hydroxy group.

Only the complexes synthesized from 2-aminomethylpyridine (Tables 4:27 – 4:30) are soluble in water, all others are soluble or slightly soluble in non-aqueous solvents (DMF, methanol, ethanol, hexane, etc). They are all stable in air.

The microanalysis data for all the isolated ligands and their corresponding cobalt(II) complexes are listed in Tables 4:1 – 4:30. The elemental analyses are in good agreement with the chemical formulae proposed for the compounds.

The complexes made from cobalt acetate were found to be akin in properties to those obtained from triethylamine-stripped cobalt chloride. The addition of triethylamine to $CoCl_2.6H_2O$ prevents chlorine from coordinating, therefore resulting in products that have exact properties as those from cobalt acetate.

5.2 Infrared spectroscopy of the Schiff bases and their corresponding complexes

The infrared frequencies of various diagnostic bands for the various Schiff bases isolated are listed in Tables 4:31 – 4:36. Few of the Schiff bases have previously been synthesized and characterized using IR. Analyses of the Schiff bases and their corresponding chelates are based on previous assignment of similar Schiff bases.[12,13]

In the mid-IR, assignments are based on typical group frequencies. For the aniline-based and 1-aminonaphthalene- based Schiff bases, stretching frequencies of OH, $C=N_{(imine)}$, and C–O are used as the diagnostic bands while $C=N_{(pyridine)}$ band was included for the other four groups .[14-16] The exact positions of the characteristic bands vary from one Schiff base or complex to another since the position of the substituents and the amines used are different. For the analyses of all the Schiff bases, the effect of the varying the positions of methoxy as well as the hydroxy substituents on the stretching frequencies of OH, C=N and C-O will be discussed later. Reported assignments are largely empirical and generally restricted to the ligands bands highlighted above.

To derive the assignments for the metal-ligand stretching frequencies, far infrared spectroscopy was used. This study examines the effect of substituents in the phenyl ring as well as the substitution of amine with azine on the vibrational stretching frequencies of the complexes.

5.2.1 The OH stretching vibration

The IR band arising from the O-H valence vibration is one of the earliest known and most studied of any. Bellamy[17] reported that Aschkinass and Ransohoff in 1895 were the first to observe the OH vibration. It has been observed that when hydrogen bonding occurs, there is an increase in the bond-length of the OH, causing the absorption band to shift to a lower frequency.[17] Badger and Bauer[18] showed that the magnitude of the shift of the OH fundamental,

due to hydrogen bonding, could be used as a measure of the strength of the hydrogen bond formed, being about 35 cm^{-1} per kilo calorie.

Intramolecular hydrogen bonding effects have been used to measure the basicity of certain π-orbitals.[19] In such π-orbitals, it has been observed that as the electron environment adjacent to the double bond is altered, the basicity of the π-electrons changes, hence causing corresponding change in the strength of the hydrogen bonding. The changes in the strength of the intramolecular hydrogen bonds in the Schiff bases have been attributed to transmission due to inductive and resonance effects from the substituent through a comparatively large number of intermediate atoms.

In order to discuss the observed OH stretching frequencies, associated properties have been considered.[20] In considering their properties, two types of functional groups in the molecule have been put into consideration. One is the hydroxy group, while the other is the lone pair of the C=N group.

Three different types of hydroxyl group bonding are known. These are, intermolecular, intramolecular, chelation in which resonance structures are involved. The absorption range of the OH valence-stretching vibration of an unbounded[17] hydroxyl group is usually 3700-3500 cm^{-1}. Medium and broad ν(OH) stretching bands with a frequency range of 3445-3209 cm^{-1} are the observed characteristic features for all the Schiff bases reported here. The results indicate associated properties since the ν(OH) frequencies are below 3700-3500 cm^{-1}. This implies there is association between the OH and C=N group or intermolecular association between the *para*-substituted OH containing Schiff bases.

It was difficult to give precise evaluation of ν(OH) frequencies because of broadened frequencies caused by hydrogen bonding. Though the nature of the perturbed hydroxy band of the conjugated-chelate ring involving the O–H-----N=C hydrogen bond does allow for the assignment of an exact frequency, it was however, assumed that the band is roughly symmetrical, hence the center has been used to obtain the ν(OH) data listed in all the mid-IR Tables.

The observation was that the position of the ν(OH) bands are affected by concentration in the mull, consequently, it is of the opinion that the associated property in most of the ligands is

intermolecular and or intramolecular hydrogen bonding. Since the stretching frequencies are broad, it implies that the H atom from the O-H group in the Schiff bases has a tendency to migrate to azomethine N atom via the O-H-------N intramolecular hydrogen bonding.[8,14,19,21] The probable structure for most of the ligands have been postulated as enol-imino tautomer. However, stabilization of the enol-imino tautomer may vary depending on the position of the substituents in the phenyl rings. Nevertheless, a few of the Schiff bases may be in keto form because of the appearance of a characteristic strong band at 1733 cm^{-1}. The position of the tautomeric equilibrium is strongly determined by the type of solvent used.[3] Protonic and aprotonic solvents with high dielectric constants shift the equilibrium towards the quinonoid tautometer.[3]

An examination of Tables 4:31 – 4:36 showed the extreme breadth and complexity of the hydroxyl band typical of salicylidineanilines and other Schiff bases, consequently making it difficult, if not impossible, to observed the effect of electron-donating ring substituent on the stretching frequency. Consequently, using the data for correlation analyses becomes dubious.

5.2.2 The C=N stretching vibration

A good deal of work has been done on the position of the $C=N_{(imine)}$ stretching absorption in various classes of compounds.[22] Factors affecting the position of the $C=N_{(imine)}$ stretching absorption within this band include the physical state of the compound, the position and nature of the substituent group, conjugation with either carbon or nitrogen, or both, and hydrogen bonding.

5.2.2.1 Group 1: The mid IR spectra of aniline-based Schiff bases

The characteristic group frequencies of aniline - based Schiff bases are listed in Table 3:31. Fabian et al.[23] found a frequency range of 1650–1638 cm^{-1} for the compounds of the type Ar–CH=N–R, when Ar is unsubstituted phenyl group. Clougherty et al.,[24] reported the stretching frequencies for seventeen aniline based ligands, and found a frequency range of 1631–1613 cm^{-1}. They observed that a frequency shift of about minus 8 cm^{-1} occurs when hydroxy is substituted in the 2-position of the benzylidine phenyl ring. Using *N*-benzylideneaniline as a reference, the stretching frequencies for the four ligands obtained from condensation of aniline with salicylaldehyde or its derivatives are listed in Table 4:31. The $C=N_{(imine)}$ stretching frequencies

for this ligands appeared at lower frequency when compared with the $C=N_{(imine)}$ benzylideneaniline stretching frequency. The explanation for the shift to lower frequency is two-fold. It is known that increase in mass always resulted in shifting to lower frequency. This reason is insufficient to account for the appearance of ligands 2 and 3 at slightly lower frequencies than ligand 1. The presence of hydroxy in the 2-position of ligands 1, 2 and 3 is the dominant reason for the shift to lower frequency. There is interaction between $C=N_{(imine)}$ and the *ortho*-hydroxyl resulting in the observed relative low frequencies. While mass effect and interaction between $O–H------C=N_{(imine)}$ have been used to explain the possible scenarios, other factors such as inductive and mesomeric effect (resonance), conjugation, π-cloud interaction have an effect on the shifts. For instance, the $C=N_{(imine)}$ of ligand 2 is lower than 3, even though they both have methoxy group substituent. There is resonance contribution more to ligand with 4-position methoxy substituent than the *meta*-methoxy substituted ligand 3 (Scheme 5:1 and 5:2)

Scheme 5:1 resonance stabilization in *para*-methoxy substituted Schiff base

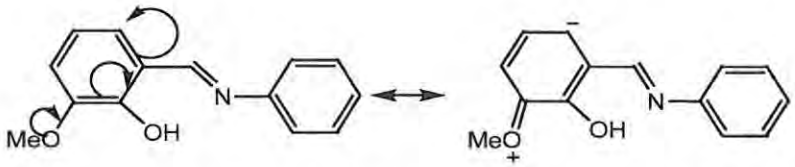

Scheme 5:2 Resonance stabilization in *meta*-methoxy substituted Schiff base

Substituents that enhances mesomeric shift decreases the bond order, hence lead to lower frequency.[25] However, the stretching frequency of ligand 4 is shifted to higher wavenumber. This implies that the hydroxy bonding association between OH and $C=N_{(imine)}$ does not exist or was weak in this compound, since its OH is attached at the 4-position, hence confirming the observed $C=N_{(imine)}$ stretching frequencies for ligands 1, 2 and 3. The presence of methoxy group in 3-position, allows the pushing of electrons into the phenyl ring, hence shortening the length of $C=N_{(imine)}$, hence, resulting in the observed frequency.

From the listed data in Table 4:31, the effect of having methoxy group coupled with hydroxy in different positions is also seen in the C–O frequencies of the four Schiff bases.

While the C–O stretching frequencies of compounds 1 and 4 appeared at 1284 cm^{-1}, the effect of methoxy in 3- or 4- positions shifted the C–O stretching frequencies of the ligands 2 and 3 to 1290 cm^{-1} and 1254 cm^{-1} respectively. This is an indication that the presence of methoxy in the 3-position of the phenyl ring resulted in lengthening the phenolic bond while the phenolic bond is shortened in the other three. The effect is well noticeable in ligands 2 and 3 respectively.

The appearance of medium and broad absorption bands in the 3440 cm^{-1} – 3444 cm^{-1} can be used to further substantiate the presence of hydrogen bonding between the *ortho*-hydroxy and $C{=}N_{(imine)}$. For ligand 4, the association is most likely intermolecular as the *para*-substituted hydroxy does not favour intramolecular associating between the OH and the $C{=}N_{(imine)}$.

5.2.2.2 Group 2: The mid IR spectra of 1-aminonaphthalene-based Schiff bases

The diagnostic stretching frequencies of 1-aminonaphthalene-based ligands are listed in Table 3:32. The trend observed for this group is almost the same as in group 1. The increase in mass certainly has an effect on the frequencies of the compounds. When compared with the benzylideneaniline, it is apparent that appearance of the bands at lower frequencies relative to the first group is partly due to changing of amine from aniline to aminonaphthalene. The absorbance band of ligand 5 appeared at 1618 cm^{-1}, while those of ligand 6 and ligand 7 shifted to 1613 and 1609 cm^{-1} respectively, as a result of methoxy donating electron density into the rings, hence affecting the length of C=N bond. The presence of methoxy in 3-position seems to have more effect on both $C{=}N_{(imine)}$ and C–O stretches as shown by spectra data of ligands 3 and 7, than the presence of methoxy in 4-position.

Conjugation with phenyl and a + M group like *p*-methoxy or *m*-methoxy is expected to lead to lower frequencies.[25] However, the appearance of ligand 7 at much lower frequency than ligand 6 implies that other factors may have contributed to the observed vibrations. Ligand 5, like ligand 1, had broad OH band shifted enormously to low wavenumber. This is an indication of strong hydrogen bond involving the hydroxy group. The introduction of methoxy group in 3- or 4-positions shifted the νOH to slightly higher frequency.

Skorokhod et al.[16] are reported to have synthesized ligand 5. They found the νC=N and νC–O appearing at 1600 and 1190 cm^{-1} respectively. However, ligand 5 reported here does not show bands at those wavenumbers, thus, it was suspected that the spectrum of either our or their

sample had been influenced by the method of sample preparation. The difference in properties lies in the preparation of the ligand it was observed. The addition of NH_4OH to the reaction mixture using the procedure highlighted by Skorokhod et al.[16] resulted in the oily Schiff base solidifying. The Schiff based reported by Skorokhod et al.[16] resulted in the formation of ammonium salt of the ligand while ligand 5 reported in this work is a free ligand as confirmed by the microanalysis and the mass spectrometry.

As noted earlier, the presence of methoxy in 3- or 4 positions causes noticeable increase in the melting point of synthesized Schiff bases. Skorokhod et al.[16] reported 180° C for the salt of ligand 5. This is surprising, because ligand 7 melted at 90-92 ° C while the melting point of ligand 9 was 100-101 ° C.

Guofa et al.[7] reported the preparation and vibrational spectra for ligand 7 and complexes with rare earth nitrates. Their infrared assignments of the ligand agree with the present work.

The substitution of aniline with 1-aminonaphthalene have pronounce effect only on the $C=N_{(imine)}$ stretch but less effect on the C-O and OH stretching frequencies as listed in the data in Table 4:32. The appearance of the OH absorption of ligand 8 at lower wavenumber than ligand 4 may imply that the intermolecular bonding is more pronounce in ligand 8 than in ligand 4. The C-O stretching frequencies for this series of ligands appeared in the same region as those of group 1 analogues.

5.2.2.3 Group 3: The mid IR spectra of 4-aminopyridine-based Schiff bases

Nelson et al.[26] believed pyridine and its derivatives should have spectra similar to those of benzene and its derivates. The C=C and C=N vibrations appear in the 1660 – 1590 cm^{-1} and 1500 cm^{-1} region. However, while agreeing with them to some extent, the results obtained from this work proved otherwise. The spectra data for 4-aminopyridine-based Schiff bases are listed in Table 4:33. The vibrational frequencies appeared at much higher wavenumber on substitution of aniline with 4-aminopyridine. When compared with group 1, the only difference is the presence of nitrogen in the pyridine ring.

The plausible explanation for this behavior is ascribed to the changes which occur in the nitrogen orbitals of the $C=N_{(imine)}$ due to its interaction with the nitrogen of the pyridine ring. This impart

more s-character to these orbitals resulting in C=N shortened and hence frequency rise. While $C=N_{(imine)}$ stretching frequency of ligand 1 appeared at 1620 cm^{-1} that of ligand 9 appeared at much higher frequency. The presence of methoxy in 3- or 4-position of the phenyl ring on the carbon of the $C=N_{(imine)}$, increases the s-character of the nitrogen, consequently leading to the decrease in bond length, and hence the observed high frequencies for ligands 10, 11 and 12 in that order. Ligand 12 has the highest frequency because of no hydroxyl association with the $C=N_{(imine)}$ bond.

The $C=N_{(pyridine)}$ bands appeared in the 1576 – 1603 cm^{-1} region. They are known to appear in this region.[26] The $C=N_{(pyridine)}$ band for this series of ligands will be compared with those of the other groups and examine the effect of varying the nitrogen of the pyridine ring or substituting aminopyridine with aminomethylpyridines.

The phenolic stretching frequencies of the ligands in this group appeared 1264 – 1278 cm^{-1} region. Except for ligand 3, the phenolic stretching frequencies for the ligands in this group appeared at lower frequency when compared with the group 1 analogues. This observation is attributed to resonance effects due to the substituents in the phenyl ring which pushes electron into the ring and the 4-nitrogen in the pyridine ring which withdraws electron density, hence lengthening the C-O bond and consequently lowering stretching frequencies.

The medium and broad absorptions in the 3348 – 3432 cm^{-1} region for the ligands in this series substantiate the association between the *ortho*-hydroxyl and the $C=N_{(imine)}$. The appearance of OH band at 3348 cm^{-1} in ligand 4 may be an indication that the intermolecular hydrogen bond in the *para*-hydroxy substituent might be more than the intramolecular hydrogen bond in the other three ligands. When compared with the group 1 analogues, the OH stretching frequency for the ligands in this series appeared to be more affected by the association hydrogen bonding.

5.2.2.4 Group 4: The mid IR spectra of 3-aminopyridine-based Schiff bases

The spectra of 3-aminopyridine-based Schiff bases isolated are listed in Table 4:34. The spectra data of this group differs to both group 1 and 3. Their behavior has to do with position of nitrogen of the pyridine ring. The greater electronegativity of nitrogen (relative to carbon) suggests that such canonical forms may contribute to a significant degree of their chemistry. Basic chemistry of pyridine and its derivatives reveals that they are weak bases and that the

nitrogen in the ring is sp^2 hybridized. Since polar canonical structures are possible, having electron donating substituents will increase the basicity of pyridine or its derivates, and those substituents on the 2 and 4-positions will influence this basicity more than an equivalent 3-substituent. The nitrogen in the pyridine ring acts like an electron withdrawing substituent, having it in the 3-position impart less s character on the orbitals, consequently increasing the length of the bonds, which eventually leads to the observed $C{=}N_{(imine)}$ stretching frequencies listed in Table 4:34. Another plausible explanation for the observed frequencies for this group is that the pyridine ring is in conjugation with the substituted phenyl ring; consequently leading to lower bond order in the C=N bond, weakening the bond, and hence causing a shift to lower frequency (Scheme 5:3). However, the presence of nitrogen in the 2- or 4-position of pyridine should probably enhance mesomeric shift more than when the nitrogen is in 3-position, hence should result in lower frequencies relative to group 3. The fact that the spectral data for groups 3 and 4 are contrary to that expected implies that the mesomeric effect is not the only factor that determine the $C{=}N_{(imine)}$ frequency. Support for some conjugation is however indicated by a comparison with group 5, the aminomethylpyridine derivatives.

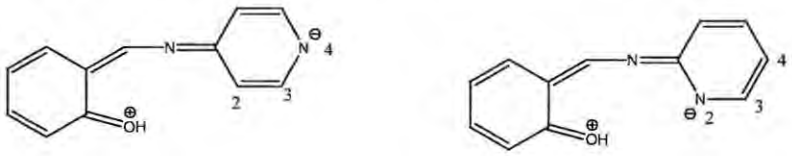

A B

Scheme 5:3 2- or 4- nitrogen contributing to resonance stabilization in aminopyridine Schiff base

Like the $C{=}N_{(imine)}$, the $C{=}N_{(pyridine)}$ also appeared at lower wavenumber than $C{=}N_{(pyridine)}$ of the 4-aminopyridine-based analogues. The explanations given above for the $C{=}N_{(imine)}$ stretching frequencies holds for the $C{=}N_{(pyridine)}$ stretching frequencies observed.

As expected, the decrease in the C=N stretching frequency always leads to corresponding increase in the C-O stretching frequency. The C-O of ligand 15 appeared at lower wavenumber than the other three ligands. This implies that the presence of the electron donating methoxy in the phenyl ring of ligand 15 lengthened the C-O bond while it was shortened in the other three ligands, hence the observed wavenumbers. The C-O stretching frequencies for this series of ligands are similar to those of group 1 ligands but appeared at slightly higher wavenumbers. However, C-O absorptions for the 3-aminopyridine-based ligands appeared at higher wavenumbers than those of the 4-aminopyridine-based analogues.

The medium and broad absorption bands for ligands 13, 14 and 15 appeared in the 3440 – 3442 cm^{-1} region while that of ligand 16 appeared at 3432 cm^{-1}. This indicate that the association between the *ortho*-hydroxy and the $C=N_{(imine)}$ in ligands 13, 14 and 15 are almost the same as the group 1 ligands but less than the group 3 analogues. The appearance of the OH band at 3432 cm^{-1} in ligand 4 implies that the intermolecular hydrogen bond in the *para*-hydroxy is more than the intramolecular hydrogen bond in the other three ligands.

5.2.2.5 The mid IR spectra of 3-aminomethylpyridine-based Schiff bases

The infrared frequencies for the isolated 3-aminomethylpyridine-based Schiff bases are listed in Table 4:35. This group showed another interesting vibrational property, particularly when compared with group 4. The only difference between group 4 and this group is extra methylene between the $C=N_{(imine)}$ bond and the pyridine ring. The additional methylene is expected to cause the frequency shift slightly to lower frequency if mass effect has any effect on the spectra of the Schiff bases in this group. However, the appearance of $C=N_{(imine)}$ vibrational bands at much higher frequencies for this group relative to group 4 confirms the assertion that combination of factors determines the position of vibrational and electronic bands. The explanation for the observed frequencies is that, the insertion of a methylene group between the $C=N_{(imine)}$ bond and the pyridine ring, isolates the pyridine ring from conjugated π system of the rest of the molecule. The methylene makes it impossible for the pyridine ring to conjugate with the rest of the molecule. (Scheme 5:4)

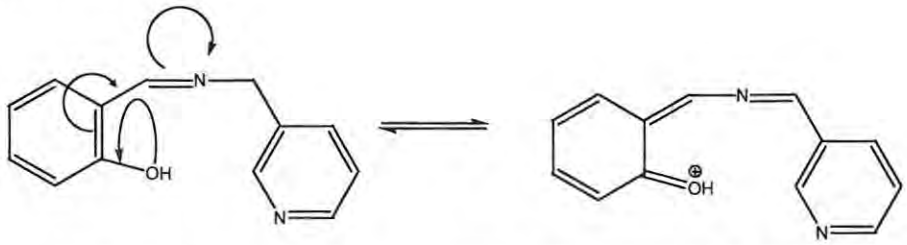

Scheme 5:4 Methylene insertion isolates pyridine ring from conjugating with the phenyl ring

Absence of such conjugation leads to higher bond order in the C=N bond, which consequently strengthens the bond; the increase in force constant resulted in the observed high frequencies (Scheme 5:4). Nevertheless, the $-OCH_3$ substituent at the 3- or 4- position shifted the $C=N_{(imine)}$ frequencies of ligands 18 and 19 to lower frequencies as expected. The $C=N_{(imine)}$ band of compound 20 appeared at much higher frequency than the other three because of the absence of intramolecular hydrogen bonding between it and the O–H bond. The strong intramolecular and

or intermolecular hydrogen bonding present in all the ligands leads to very broad and weak hydroxyl absorption, hence IR is not that informative with respect to the nature of O–H bonding. As expected, the C–O stretches were all affected, with increase or decrease depending on the absence or the position of the substituent $-OCH_3$ and hydroxy in the ligand.

5.2.2.6 The mid IR spectra of 2-aminomethylpyridine-based Schiff bases

The vibrational data of 2-aminomethylpyridine-based Schiff bases are listed in Table 4:36. The frequencies appeared at lower frequencies than the 3-aminomethylpyridine analogues. There are two functional groups in this series of ligands, which are able to form intramolecular hydrogen-bond with the imino nitrogen. These are the *ortho* hydroxyl group, and the 2-pyridine nitrogen. While it may be assumed that the 2-nitrogen in the pyridine ring in addition to the $C{=}N_{(imine)}$ nitrogen could participate in the hydrogen bonding with the *ortho* hydroxyl of the phenyl ring if existed in Z- form or only the azomethine hydrogen if in E-configuration, because of its proximity (Scheme 5:5), such association should lead to a decrease in vibrational frequencies, hence the observed frequencies.

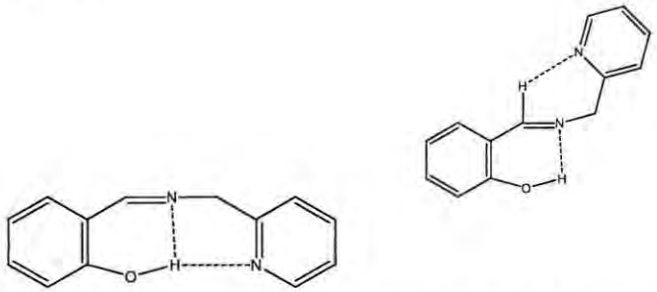

Scheme 5:5 Hydrogen bonding formation in Z- and (E) -2-((pyridine-2-ylmethylimino)methyl)phenol

If O-H did hydrogen bond to $C{=}N_{(pyridine)}$, then the $C{=}N_{(imine)}$ will be more double bond in character, and therefore appear at higher frequency. However, the fact that $C{=}N_{(pyridine)}$ appeared at lower frequency in the 2-aminomethylpyridine-based ligands than the 3-aminomethylpyridine analogue implies a less double character. The appearance of stretching frequency of ligands 22 and 23 at lower frequency than ligands 18 and 19 is an evidence to corroborate less double character in the 2-aminomethyl analogue, hence the observed C=N stretching frequencies. However, in ligand 24 where the hydroxy is in the *para*-position in the phenyl ring, the inability of the OH to hydrogen bond with the C=N resulted in the higher frequency of the 2-aminomethylpyridine analogue relative to the 3-aminomethylpyridine analogue.

The appearance of the C=N stretching frequencies of ligands 22 and 23 at lower frequencies relative to the other may be as a result of methoxy substituents which have the ability to push delocalise electron density into the phenyl ring, thereby increasing the bond order of C=N bond and lead to the observed $C=N_{(imine)}$ stretch frequency.

The evidence of intramolecular hydrogen bonding is observed in the OH absorption frequency of ligand 24 which appeared at lower wavenumber relative to the other three ligands.

Cimerman et al.[6] compared the values of OH stretching frequencies of the 3-aminomethylpyridine-based ligand with the two analogues. They observed a lower frequency value for the former. Barring other effects, a shift of OH to lower values reflects a strong intramolecular hydrogen bond. They postulated that an increase in imino nitrogen basicity as a result of insertion of methylene results in a strengthening of the intramolecular hydrogen bond OH-----N=C, hence shifting the tautomeric equilibrium to ketoenamine form.[6]

While the C–O stretching frequency of ligands 21 and 22 appeared at 1303 and 1287 cm^{-1} respectively, those of ligands 23 and 24 shifted to much more lower frequency. The reason for shift to lower frequency can be ascribe to the effect of 3-methoxy which cause the lengthening of the C–O bond, and eventually lead to the observed lower frequency in ligands 23 and 24 respectively.

5.2.3 The spectra of the isolated complexes

In order to ascertaining the binding mode of the Schiff bases to cobalt in the new complexes, the infrared spectra of the free ligands were compared with those of their corresponding isolated complexes. The discussion has been restricted to those complexes that have been confirmed by microanalysis. The complexes have been numbered according to the groupings of the Schiff base from which they are made.

While most of the complexes agreed with the proposed structures, few show differences in trends of composition to the rest of the sequence. These have been highlighted in section 4.1.3 above. When a comparison is done within the group, the general empirical formulae for the isostructural "A" series complexes are $MH_2L_2Cl_2$, while ML_2 is the formulae for "B" and "C" series.

The following sections will discuss the ligand coordination in the complexes from the position of the bands of stretching vibrations of the donor C=N, C-O and the OH groups. These will be followed by the far infrared discussions of the various isolated complexes with the aim of assigning geometry for the complexes.

5.2.3.1 Group 1: The mid IR spectra of the complexes of the aniline-based ligands

It is well known that the ligand bands are shifted to lower or higher frequencies with simultaneous variation in intensity when a chelate is formed.[3, 27-29] The magnitude of the shift depends on the type of the Schiff base, the substituents and other factors. Tables 4:37 – 4:40 shows the list of all the aniline-based ligands compared with their isolated complexes. The general trend observed is that $C=N_{(imine)}$ stretching frequencies increased to higher wave number for all the complexes produced from cobalt chloride while all the complexes produced from cobalt acetate or stripped cobalt chloride (cobalt chloride combined with triethylamine) have their stretching frequencies shifted to lower wavenumbers, relative to their various ligands.

This suggests that for the complexes 1A, 2A, 3A and 4A, coordination to the metal increases electron density from the phenyl ring into the imine C=N bond, resulting in increased double bond character. This implies that there is no metal-ligand back bonding. In contrast, the corresponding B and C series of the complexes differs with the lowering of the $\nu C=N_{(imine)}$ suggesting significant back bonding from the cobalt into the antibonding orbital of the $C=N_{(imine)}$.

Thus, coordination of the Schiff base to the metal through the azomethine nitrogen reduces the electron density in the azomethine link, consequently, lowering the C = N stretching frequency. This account for the negative shifts observed in all the cobalt acetate and stripped cobalt chloride derived complexes.

The C–O stretching frequencies for all the complexes with the exception of ligand 3 (ovaani), increased to higher wavenumbers relative to the ligands. The presence of a peak at 1635 cm^{-1} has been attributed to the characteristic of a quinonoid system.[30] With the exception of the ligand 3 complexes, the increase in the absorption frequencies of the phenolic C–O band in the complexes confirms that phenolic oxygen is also involved in the coordination with increase double bond character. It has previously been established that when electron density is pushed into the ring system by the substituents on the phenyl ring, the N–M stretch decreases while the M–O stretch increases.[31, 32]

The observed C-O frequency for ligand 3 implies that the methoxy in the *meta-* position donates electron to the OH, hence lengthening the phenolic bond, and resulting in the shift to lower wavenumber.

The vibrational spectra of the complexes in this group showed in most cases, broad and weak band in the region 3434-3447 cm^{-1} which confirms the intramolecular hydrogen-bonded OH. The presence of these absorptions can be used to substantiate the presence of water in most of the complexes.

5.2.3.2 Group 2: The mid IR spectra of the complexes of the 1-aminonaphthalene-based ligands

The spectra information for the 1-aminonaphthalene–based ligands and their isolated complexes are listed in Table 4:41–4:44. The trend in this group is almost similar to that observed for the aniline- based complexes. However, there are instances where the $\nu C{=}N_{(imine)}$ shifts are smaller, which is attributed to the bulkiness of the aminonaphthalene group. While the $C{=}N_{(imine)}$ stretching frequencies for complexes 5C, 6C, 7C shifted to lower frequencies, suggesting back bonding from the metal into the antibonding orbital of the $C{=}N_{(imine)}$, those of 6A, 7A and 8A shifted to higher frequencies relative to their respective ligands, implying increased double bond character and suggesting there is no metal-ligand back bonding. The position of these bands undergoes variation depending on the type of Schiff base from which the complex is made. These shifts suggest that the ligands coordinate with the metal ions through the azomethine nitrogen.

In the complexes 5C, 6A and 6C, the phenolic C–O stretching vibrations appeared at higher value than the observed wavenumber for the ligands, while it appeared at lower value in the complexes of 7A, 8A and 8C. The observed shifts for complexes 7A, 8A, and 8C are ascribed to the electron donating effect of the 3-methoxy substituent and the bulkiness of aminonaphthalene. The C–O stretching vibration shift to lower frequency, hence confirms the participation of the phenolic oxygen atom in the complex formation. This suggests that the p-hydroxy group in complexes 8A and 8C must be involved in bonding to an alternate metal, thus acting as a bridging ligand.

The vibrational spectra of the ligands showed in most cases, broad and weak band in the region 3350-3445 cm^{-1} which confirms the intramolecular hydrogen-bonded OH. The shifting of these broad and weak bands to lower frequencies confirms the presence of water in most of the complexes. The presence of water is also corroborated by the presence of peaks at about 860 cm^{-1} in most of the complexes, the OH_2 rock.[33]

5.2.3.3 Group 3: The mid IR spectra of the complexes of the 4-aminopyridine-based ligands

The spectra data of 4–aminopyridine Schiff bases and their cobalt(II) complexes are listed in Tables 4:45–4:48. As a result of changing amine type from the aniline and 1-aminonaphthalene to aminopyridine or aminomethylpyridine, the diagnostic bands that will be focused increases to four. These bands are the stretching frequencies of OH, C–O, $C=N_{(imine)}$ and $C=N_{(pyridine)}$. The infrared spectra indicate whether the Schiff bases bond with cobalt in a bidentate or tridentate manner. It is possible to use the stretching frequencies νOH, $\nu C=N_{(imine)}$ and $\nu C=N_{(pyridine)}$ to determine the site of coordination of the Schiff bases to metal in the formation of the complexes.

It is interesting to note that the behavior of the complexes of Schiff base 9 and 10 are similar to the aniline-based complexes above. The only difference between the two ligands is the presence of 4-methoxy substituent in Schiff base 10. The C=N stretch for their respective complexes (9A – C and 10A – C) shifted to lower frequencies. The A series complexes obtained from cobalt chloride are significantly affected by coordination, that is, the stretching frequency shifted more to low frequency. The shifts of the A series are bigger than those of the "B" and "C" series, suggesting different extent of the M-L back bonding. The "A" complexes are different from the aniline-based complexes; they have opposite shifts, that is, the pyridine increases the M-L back bonding for the "A" series complexes. The IR of these complexes suggests that they unlikely to be isostructural with the amine based complexes.

The C–O stretching frequencies are relatively unchanged for the three complexes of ligand 9 relative to the ligand, while they shifted to higher frequencies in all the complexes of ligand 10. The appearance of the C-O stretching frequency for 10A, 10B and 10C at above 1300 cm^{-1} might be an indication of their existence in quinonoid form.

Tentatively, the presumption is that the complexes are coordinated in a chelating fashion via the azomethine nitrogen and the phenolic oxygen. The orientation does not favor the use of pyridine 4-nitrogen as coordination site unless in a bridged form, hence the Schiff bases 9 and 10 are likely to be bidentate.

The complexes of Schiff bases 11 and 12 also showed interesting properties. They both have a 3-methoxy substituent but differ by having OH in 2- and 4- positions respectively. As expected, the $C=N_{(imine)}$ stretching frequencies are shifted to lower frequencies. However, the complexes obtained from cobalt chloride (11A and 12A) appeared at higher frequency than 11B, 11C and 12B, 12C complexes. This may be attributed to the presence of 3-methoxy as well as the coordination of chlorine as shown in the microanalysis. The effect of resonance as well as inductive effect due to the aminopyridine 4-nitrogen cannot be ruled out. The fact that 12A is a polynuclear or polymeric complex accounts for the reason why its $C=N_{(imine)}$ stretching frequency does not follow the trend of the isostructural compounds observed in the rest of the series. There were also noticeable changes in the C–O stretching frequencies of all the complexes relative to the ligand. This also implies that the metal coordinated also through the phenolic oxygen.

The observation again is that the o-vanillin-based complexes have the opposite trend for νC–O relative to the other complexes in this group. The behaviour of νC–O is varied with the o-vanillin-based complexes (11A – C) showing a shift to lower frequency in contrast to the increased quinoidal contribution on coordination found in the rest of the complexes.

The $C=N_{(pyridine)}$ stretch suggest there is varied behaviour in the complexes, showing shifts to both higher and lower frequencies, depending on whether the synthesis is for the "A" series or "B", and "C" series, depending on the nature of substitution of the phenyl ring. For example, 11A – C all show negative shift. The latter behaviour suggests there is conjugation between the phenyl and the azine rings.

Where analytical data suggest the presence of water molecules, broad and weak absorptions in the region 3331-3490 cm^{-1} substantiate these evidences. The fact that the OH stretching frequency of complexes 12B and 12C appeared at 3366 cm^{-1} might implies stronger intermolecular hydrogen bonding in these complexes than the others in the series.

5.2.3.4 Group 4: The mid IR spectra of the complexes of 3-aminopyridine-based ligands

The spectra data for complexes obtained from 3-aminopyridines are listed in Tables 4:49 – 4:52. There is not much difference in the spectra of ligand 13 and complex 13A. However, slight shift in the stretching frequencies were observed with the exception of νC–O, which may be used as confirmation for the coordination of the ligand to the metal ion. These indicate that the phenolic oxygen is involved in the complex formation. For the pseudo-octahedral complexes, 13B and 13C, the C=N stretching frequencies observed at 1616 cm^{-1} in the ligand shifted to 1604 cm^{-1}. Another band at 1653 cm^{-1} was also observed. This is indicative of quinoidal contribution.[30] These may also be regarded as $\nu C–O_{(assymmetric)}$ and $\nu C–O_{(symmetric)}$ stretches.

The C–O stretching frequencies for the complexes 13B and 13C shifted to higher frequencies in contrast to that found for the cobalt chloride synthesis. This is an indication that the phenolic oxygen may have participated in the complex formation. There are a noticeable changes in the $\nu C=N_{(pyridine)}$, of the two complexes relative to the ligand, hence there is possibility that coordination might have taken place through the pyridine nitrogen. This would suggest the ligand acts in a bridging arrangement.

It is noted that the metal to ligand complex 15A is 1:1, and thus it differs to the rest of the 3-aminopyridine-based Schiff base complexes.

The complexes of ligands 14 and 15 showed another interesting behavior. There was no noticeable change in the $C=N_{(imine)}$ stretching frequency of complexes 14A, 15B and 15C, whereas, their $C=N_{(pyridine)}$ and C-O stretching frequencies shifted to lower wavenumber. This might be an indication that coordination does not take place at the azomethine nitrogen for these complexes but through the phenolic oxygen and the pyridine nitrogen in a bridging arrangement.

The reverse is the case for complexes 14B, 14C and 15A. While the $C=N_{(imine)}$ stretching frequency for complex 14B and 14C shifted to higher wavenumber, their $C=N_{(pyridine)}$ and C-O stretching frequencies shifted to lower wavenumbers as expected. This might be an indication that the ligand is tridentate. These observed frequencies are ascribed to the substituent effects of 3- or 4- methoxy in their respective Schiff bases.

The stretching frequencies νC–O for the complexes 14A – C and 15A – C is shifted to lower frequencies. This observation might be as a result of the delocalization of electron into the ring by the 3- or 4- methoxy via mesomeric shift, consequently leading to the shifting of the frequencies negatively or positively as the case may be. This is because the methoxy at the *para or meta* position shortens or lengthens the C = N bond, consequently, leading to the shift of frequencies to higher or lower absorption frequencies.

Unlike the 4-aminopyridine-based complexes, and in contrast to the salicylaldimine, the *para*-vanillin complexes with 3-aminopyridine shows the reverse trends for $\nu C{=}N_{(imine)}$, suggesting the position of the nitrogen in the azine ring plays an important role in controlling the back bonding into the $\nu C{=}N_{(imine)}$.

A comparison of the spectra of complexes in Tables 4:45–4:48 with those of Tables 4:49 – 4:52 revealed the effects of having nitrogen in different positions in the pyridine ring. The frequencies of the 4-aminopyridine ligands appeared at much higher frequencies than those of the 3-aminopyridine.

The presence of a broad and weak band in the region 3444-3166 cm^{-1} confirms the intramolecular or intermolecular hydrogen-bonded OH. The presence of these absorptions can be used to substantiate the presence of water in most of the complexes. The OH stretching frequency for complex 16C appeared at 3166 cm^{-1}. This is an indication that intermolecular hydrogen bonding is greater in this complex than the other complexes in this series.

5.2.3.5 Group 5: The mid IR spectra for the complexes of the 3-aminomethyl-based ligands

The spectral data for 3-aminomethylpyridine-based Schiff bases are listed in Tables 4:53 – 4:56. The vibrational data for all the complexes in this group suggested that coordination takes place through either the N-imine or the N-pyridine or both. This is confirmed by the significant changes in the $\nu C{=}N_{(imine)}$ and the $\nu C{=}N_{(pyridine)}$ values listed in Tables 4:53 – 4:56.

For instance, the $\nu C{=}N_{(imine)}$ at 1628 cm^{-1} of ligand 17 shifted to 1606 cm^{-1} in complex 17A while it appeared at 1619 cm^{-1} and 1621 cm^{-1} in complexes 17B and 17C respectively. It is important to note that the C–O stretching frequency seen in the spectra of the ligand could not be

clearly identified in all the complexes 17A, 17B and 17C. This observation might be an indication that on coordination, there is a change in coupling within the ligand modes of vibration.

With the exception of 19B and 19C, there was substantial shift in the $\nu C{=}N_{(pyridine)}$ bands in all the three complexes relative to their respective ligand band. The complexes obtained from Schiff bases 18 and 19 (18A - C, 19A - C), all have their $\nu C{=}N_{(imine)}$ shifted to lower frequencies indicating metal to ligand back bonding occur while their C–O stretches were shifted to higher frequencies as expected. The presence of 3- or 4- methoxy in the ligands 18 and 19 resulted in complexes that showed a reduction in the frequency gap between $\nu C{=}N_{(imine)}$ and $\nu C{=}N_{(pyridine)}$ that was observed in the complexes 17A, 17B and 17C.

While the $\nu C{=}N_{(imine)}$ for most of the complexes shifted to lower frequency, that for 19A and 20A shifted to higher frequencies, again reflecting the different behaviour of the 3- methoxy substitution.

The ligand band $\nu C{=}N_{(imine)}$ seen at 1634 cm^{-1} for compound 20 shifted to 1637 cm^{-1} while the $\nu C{=}N_{(pyridine)}$ shifted from 1580 cm^{-1} to 1555 cm^{-1}. The C–O stretching frequency remains the same. This implies that the N-imine and N-pyridine is involved in the coordination processes. The coordination also shifted the broad νOH to lower frequency suggesting hydrogen bonding; hence the Schiff base may be bidentate.

5.2.3.6 Group 6: The mid IR spectra of the complexes of the 2-aminomethylpyridine-based ligands

The spectral data for the 2-aminomethylpyridine-based complexes are listed in Tables 4:57 – 4:60. The vibrational spectra data for this group is varied. The varied behaviour is ascribed to the azine nitrogen in the 2-position. It allows for chelation as indicated by the composition of 21A, which differs to the to the rest of the sequence of complexes synthesized from cobalt(II) chloride.

For the complexes of ligands 21, 22 and 24, the $\nu C{=}N_{(imine)}$stretch shifted to lower frequency while the shift of $\nu C{=}N_{(pyridine)}$ depended on the type of substituent. However, the observation is

that complexes 23A – C and 24A and B showed a shift to higher frequency relative to others as a result of 3-position methoxy substitution.

The C–O stretching frequency for the complexes shifted higher, hence confirming that the complexes might have been formed by tridentate ligands.

The $\nu C{=}N_{(imine)}$ stretching frequency for Schiff base 23, appeared at 1618 cm^{-1} while that of $\nu C{=}N_{(pyridine)}$ appeared at 1589 cm^{-1}. On coordination, the $\nu C{=}N_{(imine)}$ shifted to higher frequencies in all the three complexes. The C–O stretching frequency also shifted to higher frequency showing that the ligand may be tridentate, and may have coordinated through the N-imine, N-pyridine and the phenolic oxygen.

They are slightly different from the 3-aminomethylpyridine. The difference may be ascribed to the position of the pyridine nitrogen in the two ligands used in forming the various complexes.

The existence for Schiff bases that contain a hydroxyl substituent of the keto-amine and hydroxy-imine tautomer allows for a study of the role of nature of the parent amine and the influence of additional substituents on the parent phenyl on the equilibrium position of the tautomer.

5.3 Correlation analysis of mid infrared bands

Percy and Thornton [34,35] made use of the correlation, both of the Hammett substituent parameters for a variously substituted-aniline ring and various metal ions in a series of isostructural complexes. In these studies they astutely selected a single amine for their Schiff base synthesis to examine the role of the electronic substituent effects. Their focus, however, was on the influence of these factors on the complexes, and they did not discuss the effect on tautomer equilibrium of the free ligands. Similarly, their study on the effect of substitution on the phenyl ring [36] focused on the metal complexes, rather than the free ligand.

For the present set of ligands, the equilibrium should be dependant on the basicity of the parent amine. In addition, two of the ligands have structural features that ought to stabilize proton transfer from the hydroxyl moiety, favouring the keto form. For the 2-aminomethylpyridine-based ligands, the keto-amine tautomer is stabilized by hydrogen bonding, involving the azine

nitrogen (Scheme 5:6). Thus, νC-O (observed at 1303 cm^{-1}) possesses the greatest double bond character in the present set of salicylaldimine ligands.

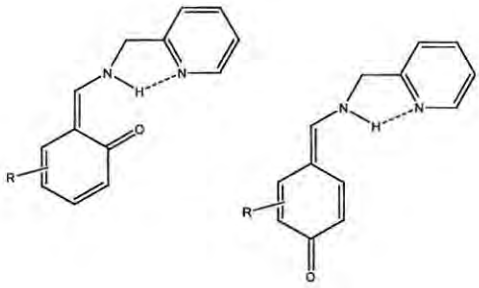

Scheme 5:6 Keto-amine tautomer stabilized by hydrogen bonding to azine nitrogen

For the 4-aminopyridine derivatives the keto form is stabilized by extensive conjugation throughout the molecule when the azine nitrogen is the receptor of the proton (Scheme 5:7). This is seen in the high frequency of νC=N (1630 cm^{-1} for the salicylaldimine ligand), reflecting the extensive conjugation.

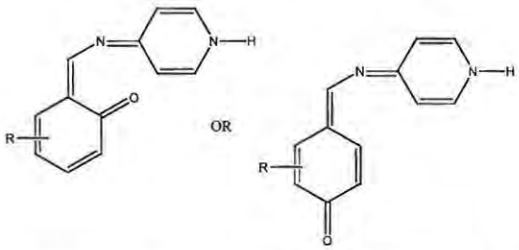

Scheme 5:7 Keto-amine tautomer resonance stabilized by proton transfer to azine nitrogen

Table 5:1 Correlation of the $pK_{a(amine)}$ for the parent amine against the frequencies of νC=N and νC-O of the ligands.

	aniline-based	1-aminonaphthalene-based	4-amino pyridine-based	3-amino pyridine-based	3-aminomethylpyridine-based	2-aminomethylpyridine-based
pK_a	4.74	4.16	6.1	1.5	9.2	
νC=N	1621	1618	1630	1616	1626	1627
νC-O	1285	1281	1275	1285	1274	1303

When considering the influence of substituents on the parent phenyl on the equilibrium position of the tautomer a comment of caution is required, particularly for the behaviour of the νC-O fundamental. Moieties bound to a benzene ring undergo significant vibrational coupling with the fundamental vibrations of the benzene ring. The extent of the coupling is dependant both on the mass of the substituent, and the position of binding. Such behaviour has been elaborated by the

prime work of Varsányi and his coworkers.[37] An important criterion is that the behaviour or the coupling is very different for light substituents (eg. C, O, N, F atoms) than for heavy substituents (eg. Cl, Br. I). In their study,[36] Percy and Thornton employed a mixture of light and heavy substituents (H, OCH_3, Cl and Br). They were able to note frequency changes in relation to the substituent parameters, but did not undertake a regression analysis. In the present work, only light substituents were selected. The coupling is position dependant,[37] and according to Varsányi's classification salicylaldehyde is ortho di-light substituted, o-vanillin is vicinal tri-light substituted (ie. 1, 2, 3- substituted), and p-vanillin and vanillin are both asymmetric tri-light substituted (ie. 1, 2, 4- substituted). Since the νC-O is being employed as a diagnostic vibration, of interest for this work is the behaviour of the C-X stretches. Wilson modes 7a and 7b describe two of the C-X for all three categories,[37] thus the coupling experienced will be similar. The third C-X stretch in vicinal substituted benzene (mode 2) cannot couple with the ring breathing vibration (mode 1) since it is already coupled with mode 7a.[37] Thus, only electronic effects should be observed for νC-O going from salicylaldehyde to o-vanillin. However, for asymmetric tri-substititution the third C-X is described by mode 13. This has the correct symmetry to introduce additional coupling with the 'Star of David' ring breathing vibration, mode 12, [37] depending on the energies of the two modes of vibration. Consequently, the frequencies for νC-O for both p-vanillin and vanillin derivatives may reflect both electronic effects and changes in the extent of the vibrational purity of the band. This would result in a poor regression analysis. The influence of symmetry in changes in coupling within a molecule is nicely seen in the study of various methyl-substituted benzene by Draeger.[38] The C=N stretch, being further removed from the phenyl ring should not be as strongly influenced by the situation described above. However, this vibration will be influenced by the nature of the amine parent, which should also influence the regression analysis.

Plots of the Hammett substituent parameters for the substituents on the phenyl ring of the Schiff bases against νC=N and νC-O were carried out. The statistical validity of the correlations was determined by regression analysis using Q tests[39] at the 99% (and/or 95%) level. The outlier in each correlation shows that at both the 95% and 95% level, the outliers must be retained. For four samples, the Q test at 95% is (0.829) and at 99% is (0.926). The values in Table 5.2 is

Table 5:2 Correlation of the Hammett subsituent parameters for substituents on the phenyl ring on the frequencies of νC=N and νC-O of the ligands.

	aniline-based	1-aminonaphthalene-based	4-amino pyridine-based	3-amino pyridine-based	3-aminomethylpyridine-based	2-aminomethylpyridine-based
νC=N (R^2)	0.4690	0.5475	0.4533	0.5643	0.9973	0.8407
Q test (99%/95% confidence)	0.331	0.492	0.371	0.701	0.300	0.212
νC-O (R^2)	0.1649	0.2149	0.7203	0.1383	0.3473	0.5412
Q test (99%/95% confidence)	0.501	0.251	0.232	0.311	0.353	0.561

statistically acceptable since $Q_{exp} < Q_{crit}$.[39] The imine stretches all have negative slopes, indicating that electron donating substituents (negative σ) result in an increase in C-N double bond character. The behaviour of νC-O, however, varies. Positive slopes occur for the 2-pico- and 4-aminopyridine substituents, negative slopes occur for the rest. The negative slopes again indicating that electron donating substituents result in an increase in C-O double bond character. Surprisingly, with the first two sets of ligands, it appears that stabilizing of the C=N may occur at the expense of the C-O. This would suggest that, with increased electron withdrawal away from the phenyl ring, the keto-amine and hydroxy-imine tautomer shifts towards the keto form. Since these two series of ligands are the ones that have structural features introducing additional stabilization factors, it is not surprising their behaviour differs from the others ligands.

Extending the examination of Free Energy Relationships to the complexes, a precondition to allow the electronic parameters to be compared consistently is that the complexes be isostructural. Thus, for coordination to the anionic ligand, νC=N shifts to lower frequencies in the order of 15 to 40 cm^{-1}, while coordination to the neutral ligand causes smaller (5 to 1 cm^{-1}) shift to higher frequencies.[33,40] Consequently comparisons can only be made separately within the two general series $M(HL)_2Cl_2$ and ML_2, excluding those complexes that fail to fit.

Percy and Thornton[34,35] noted that, in as much as metal coordination in *N*-arylsalicylaldimine complexes leads to stabilization of νC=N, it occurs at the expense of νC-N and νC-O. However, even when examining νC=N and νC-O within the two general series $M(HL)_2Cl_2$ and ML_2, it is clear that for the present series of complexes this is not necessarily always the case, and that the trend in the behaviour of νC=N and νC-O is influenced by both the nature and position of

substituents on the phenyl ring , as well as the nature of the substituent on the imine nitrogen; that is, the nature of the original amine used to produce the Schiff base.

5.4 The far infrared

Ligand vibrations occur in the high frequency (wavenumber) region, while the low frequency region originates from both ligand vibrations and from metal-ligand coordinate bonds. The high frequency vibrations are generally expected to be predominantly ligand-sensitive, while low frequency vibrations are likely to be metal sensitive. However the nature of the ligand is also extended to the behaviour of this metal-ligand vibrations.[33] It is known that the transmission of electronic effects of the substituent through a molecule may occur by a mesomeric (resonance) or an inductive effect, or a combination thereof. It is also known that an electron releasing substituent may increase the M-L bond order by a combination of the two.[33]

Direct information about the coordinate bond and the coordination number can be obtained from the far infrared spectrum. In this work efforts were directed at comparing the effect of the substituents on the phenyl ring, as well as that of the amine substitution on the metal-ligand bonds. An empirical basis was employed for the interpretation by comparing the free ligand against the complexes, as done for the high frequency region. Recall that the complexes obtained from cobalt(II) chloride are denoted "A", while "B" and "C" are those obtained from cobalt(II) acetate and triethylamine stripped cobalt(II) chloride, respectively. Comparisons can thus be made between complexes across the group as well as within the groups. A precondition for the electronic parameters to be compared consistently is that the complexes are isostructural. In the present range of Schiff bases this is unlikely due to the differing sites of hydroxyl group on the phenyl ring (in vanillin the OH position para to the imine precludes chelation, favouring bridging, contrary to the other three substituents), and due to the different sites of the azine nitrogen in the pyridine ring (the 2-aminomethylpyridine-based amine is the only one that permits chelation - all the others favour bridging). When comparing within the group the general empirical formulae are $MH_2L_2Cl_2$' for series "A" complexes, and ML_2 for series "B" and "C". There are, however, notable exceptions for which the far infrared assists in establishing the most likely structure (for example the polynuclear complex 12A). These are described in detail below.

The metal-ligand frequencies are expected to occur below 600 cm^{-1}. In *N*-arylsalicylaldimine complexes both M-O and M-N bands are associated with the imine and hydroxyl groups. Percy

and Thornton[34,35] noted vibrational coupling between νM-O and νM-$N_{(imine)}$ occurs extensively; encountering as many as five M-L bands below 600 cm^{-1}. By employing both correlations of the Hammett substituent parameters for a variously substituted aniline ring and using various metal ions in a series of isostructural complexes, they noted that both the electronic factors associated with the amine substitution as well as the Crystal Field Stabilizing Energy of the metal determines the extent of this coupling [34,35]. Based on these correlations, Percy and Thornton characterised three frequency series for the Co(II) complexes: a broad range of 529-380 cm^{-1} (identified as νM-O); 523-497 cm^{-1} and 465-411 cm^{-1} (both identified as νM-N).[35] Attention is drawn to the possibility of the reversal of the assignment of the lowest band as either M-N or M-O, depending on the exact nature of substitution on the amine moiety. Percy and Thornton [35,36] further noted that, in as much as the crystal field stabilisation is reflected in the ligand vibrations νC=N, νC-N (not unambiguously identified in the different series of ligands presently being investigated) and νC-O, so too is the behaviour seen in the νM-O and νM-N. Specifically, where metal ion substitution leads to stabilisation of the M-N and the C=N, it is accomplished at the expense of M-O and of C-N and C-O, respectively.[36]

In a supplementary study Percy and Thornton showed that substitution of the phenyl ring introduces additional variations to the extent of the coupling between M-O and M-N.[36] Based on ^{15}N-isotope labelling of *N*-p-tolysalicylaldimine, two to four bands between 550-490 cm^{-1} were identified as being variably strongly coupled νM-O/νM-N, the extent of coupling being dependant on the phenyl ring substitution.[36] But there constantly exists, below 450 cm^{-1}, an additional band that is the purest νM-N.[36] They also noted that the M-L vibrations shift to higher frequency in correlation with the π resonance parameter of the substituent on the phenyl ring, with the exception of the ortho-methoxy substituent, which they explain as differing because of steric hindrance due to the bulkiness of the substituent .[36]

For some of the ligands in the present study there exists the presence of additional donor sites. Further more the use of cobalt(II) chloride salts introduces the possibility of halide coordination. Both introduce the possibility of coordination numbers larger than four for the metal complexes, consequently the far infrared spectra have the potential for greater complexity than those experienced by the isostructural distorted tetrahedral *N*-arylsalicylaldimine cobalt(II) complexes.

An increase in coordination number causes a lower frequency shift of νM-L.[33] The size of the shift is a reflection of the strength of the additional donor atom. For example, the stronger ligand

field effect of the azine nitrogen donor in the pyridine adducts of cobalt(II) salicylaldehyde complexes results in larger decreases in νM-O than those for oxygen adducts.[41] This is similarly seen in the frequencies of νCo-Cl observed in octahedral and tetrahedral complexes. For the tetrahedral complexes two bands are observed at approximately 340 and 300 cm^{-1}, while for the octahedral complexes two bands occur at approximately 230 and 222 cm^{-1}.[42]

In an apparent contradiction to this observation, bonding of the azine nitrogen in pyridine complexes with octahedral Co(II) should be observed by two νM-N bands[43] at 260 and 130 cm^{-1}, but at 248 and 208 cm^{-1} for tetrahedral Co(II).[42] While these authors did not discuss this behaviour, a possible explanation may lie in the different extent of M→L back bonding into the pyridine ring according to the symmetry constraints. A greater back bonding will be reflected in a stronger force constant, and thus in a higher frequency.

Coordination of a water molecule gives rise to three new sets of infrared active M-OH_2 fundamentals, the rock (weak band 800-600 cm^{-1}), the wag (a medium to weak band 650-400 cm^{-1}), and the M-OH_2 stretches and bends.[33] There is some question as to the expected frequency of the M-OH_2 stretch for M(II) complexes, with deuteration studies supporting both regions of 345-280 cm^{-1} [44,45] and 440-360 cm^{-1} [46]

5.4.1 Group 1: The far infrared spectra of the complexes of the aniline-based ligands

Table 4:37 - 4:40 lists selected characteristic group frequencies for the spectral data for the isolated aniline-based ligands and their cobalt(II) complexes. Complexes 1A and 4A have compositions that are outside the general formulae of $MH_2L_2Cl_2$ and ML_2.

The far infrared region, when compared with the free ligand, identifies activated bands, which reflects additional complexity on coordination. These will include the M-L bands for the Schiff base. Recognising the probability of extensive coupling and in the absence of isotope labelling (beyond the scope of this work), based on the previous work of Thornton and his co-workers two bands in the higher region 561-504 cm^{-1} are tentatively assigned as νM-O, while two in the lower region 498-400 cm^{-1} have been assigned to νM-$N_{(imine)}$. (This is also consistent with the identification of the M-O assignment in salicylaldehyde complexes,[41] and that the metal-imine bands are found lower than metal-amine.[43] The lowest M-N can be expected to be the most pure M-L. For the salicylaldimine complexes two of the three higher frequency bands may better

describe chelate ring modes of vibration rather than being identified as the asymmetric/symmetric M-L pair which are expected with the bridging ligands, such as vaani. However, for the sake of consistency and simplicity in describing the assignments of all the complexes investigated in this work, the higher M-O is considered as the asymmetric stretch and the lower as the symmetric stretch; similarly the description of the asymmetric and symmetric M-N stretches is used.

Compound 1A is most likely octahedral involving C-O and C-$N_{(imine)}$ chelation of the Schiff base. The higher coordination number is evident by the lower ν_sM-O and ν_aM-$N_{(imine)}$ when compare with the distorted tetrahedral compound 1B and 1C, which similarly involves chelation of the Schiff base. [34,35]

The presence of chloride means that compound 2A is not isostructural with 2B and 2C. There is no clear spectroscopic evidence that the chlorides in 2A are coordinated. The presence of bands at 365 and 289 cm^{-1}, which could suggest tetrahedral coordinated chlorides also appear in other spectra, suggesting they are activated ligand vibrations. For the compound to be tetrahedral with Co-Cl binding, the Schiff base cannot be chelating. The frequencies of M-O and M-N are inconclusive in establishing the coordination in the solid state. The behaviour of 3A, 3B and 3C is identical to the pvaani series, suggesting that 2A and 3A are isostructural, while the others are similarly isostructural. Both ligands 2 and 3 are able to chelate. The most probable geometry for all these complexes in the solid state is distorted tetrahedral.

The ligand vaani (4), in which the hydroxyl group is para to the imine does not permit chelation, but does permit bridging. It is thus not surprising that suitable complexation does not occur in the absence of halides. With an empirical formula of $MLCl_2$, 4A must be polynuclear, possibly a tetrahedral dimer involving bridged Schiff base ligands and terminal Co-Cl. The band at 352 cm^{-1} is tentatively identified as tetrahedral Co-Cl.

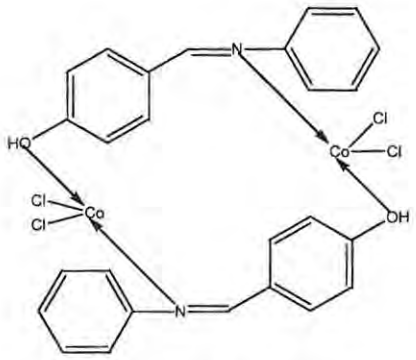

5:6 The tentative structure of vaani (4A) complex

5.4.2 Group 2: The far infrared spectra of the complexes of the 1-aminonaphthalene-based ligands

Table 4:41 – 4:44 lists selected characteristic group frequencies for the spectral data for the isolated 1-aminonaphthalene-based ligands and their cobalt(II) complexes. For this series of complexes there is very little compliance with the general formulae ML_2Cl_2 and ML_2. Formation of cobalt complexes with 1-aminonaphthalene-based Schiff bases is very restrictive, no doubt due to the bulkiness of the amine. This could also be expected to favour formation of the tetrahedral complex, involving M-O and M-$N_{(imine)}$ chelation. For 6A the band at 333 cm^{-1} might describe as a tetrahedral Co-Cl, in which case the ligand cannot be chelating. 6C, 7A and 8C might all possibly octahedral, with coordinated water. With the bridging nature of van-1-amnap 8A must be tetrahedral bridged polymer. The medium or weak band at 292 cm^{-1} is tentatively identified as a Co-Cl, this would necessarily need to be bridged for tetrahedral coordination if the water is not coordinated. The latter is possible given the band at 249 cm^{-1}. The identification of this as coordinated water would also agree with 8C likely being octahedral, with coordinated water.

5.4.3 Group 3: The far infrared spectra of the complexes of the 4-aminopyridine-based ligands

Tables 4:45-4:48 lists selected characteristic group frequencies for the spectral data for the isolated 4-aminopyridine-based ligands and their cobalt(II) complexes. The introduction of the pyridine ring adds a donor site. The position of the nitrogen does not permit coordination, but will allow for the possibility of bridging to a different metal centre.

The possible structure of the complexes 9A, 10A and 11A is ambiguous from the far infrared spectra. The bands between 210 and 280 cm^{-1} may be identified as either $\nu M\text{-}N_{(py)}$, or as $\nu M\text{-}OH_2$. The absence of waters of crystallisation in the complexes 9A and 9B supports the former assignment. The band found between 385-390 cm^{-1}, while a little high in frequency, could possibly be ascribed to a tetrahedral Co-Cl stretch. However in an apparent conflict, for 9A the band observed at 255 cm^{-1} is suggestive of octahedral coordinated azine nitrogen, and 9A could be either tetrahedral or octahedral. The assignment of $\nu M\text{-}N_{(py)}$ for 10A and 11A are indicative of tetrahedral coordination, however this can only be possible if the Schiff base is not involved in chelation. The second series – 9B+C to 11B+C – are most likely octahedral, generally the $\nu_a M\text{-}O$ lies lower than the A series and the tentative assignment of $\nu M\text{-}N_{(py)}$ is suitable for octahedral coordination. The exception is that for 9B and 9C for which $\nu M\text{-}N_{(py)}$ is typical of tetrahedral cobalt azine binding. The assignment of the $\nu_s M\text{-}N$ at 318 cm^{-1} for 9B and 9C is very tentative, as it is the lowest in the series of complexes under investigation. However assignments of $\nu M\text{-}O$ as low as 307 cm^{-1} were noted for *N*-arylsalicylaldimine Cu(II) complexes, the frequency reflecting both the coupled nature of the vibration, and the mesomeric effect of the substituent.[35]

The ligand van4amp does not permit chelation, but allows for possible bridging employing the hydroxyl group, the imine nitrogen and azine nitrogen. 12A does not conform to the general formula. It appears to be a dinuclear polymer, possibly containing both an octahedral and a tetrahedral centre involving both bridging Schiff base ligands (with observation of $\nu_a M\text{-}O$ at both 594, and 558 cm^{-1}, respectively) and bridged halogens (with tetrahedral Co-Cl at 345 and 298 cm^{-1}). Identification of any $\nu M\text{-}N_{(py)}$ binding is not possible, being masked by the tetrahedral Co-Cl vibrations. The complex 12B and 12C appears to octahedral, the bands at 278 cm^{-1} being interpreted as being either $\nu M\text{-}N_{(py)}$, or with the existence of extensive solvation, as $\nu M\text{-}OH_2$.

When compared with the group one ligands, the introduction of the methoxy group into positions 3- or 4- of the phenyl ring and the presence of the nitrogen in the 4-position of the pyridine ring results in shift in the bands assigned to $\nu M\text{-}O$ and $\nu M\text{-}N$, as noted by Thornton's group,[34-36] indicating subtle changes in the nature of the vibrational coupling. This shift is in the order 4-OH < 4-OMe < 3-OMe. For this group, it is believed $\nu(M - N)$ and $\nu(M - O)$ depend on inductive effect and not on resonance and it is suggested that inductive effect on the substituents predominate in determining the bond order. It is likely that the transmission of the inductive effect might depend on interligand conjugation. It is likely that metal-ligand sigma bonding plays a significant role in stabilizing these complexes. 9A – 12A appeared at slightly higher

frequencies than their Bs and Cs analogue. This substantiate that the coordination states for these series of complexes are not the same.

5.4.4 Group 4: The far infrared spectra of the complexes of the 3-aminopyridine-based ligands

Table 4:49-4:52 lists selected characteristic group frequencies for the spectral data for the isolated 3-aminopyridine-based ligands and their cobalt(II) complexes. The introduction of the pyridine ring adds a donor site. Again, the position of the nitrogen does not permit coordination, but will allow for the possibility of bridging to a different metal centre. All the complexes in this set appear to follow the standard formulae of $MH_2L_2CL_2$ and ML_2, with the exception of 14A which, like 8A contains only one chloride ion

In comparing the 4-aminopyridine- and 3-aminopyridine-based Schiff base complexes, it is interesting to note that the M-L bands, in particular the ν_aM-O and ν_aM-$N_{(imine)}$, appear to be shifted slightly to higher frequencies on changing the position of the azine nitrogen from 4 to 3. This would suggest that delocalization occurs over the entire Schiff base.

Complexes 13A, 14A, 15A and 16A all possess vibrations that may indicate tetrahedral coordinated chloride. In the case of the salicylaldimine (13A), however, the band at 342 cm^{-1} may better describe a low frequency ν_sM-N. An additional caution is that the appearance of possibly the νM-$N_{(py)}$ at 255cm^{-1} in 15A would suggest octahedral coordination through bridging, reflecting the ambiguity of coordination assignment noted above for 9A.

Complexes 13B and 13C are probably octahedral involving both chelation of the Schiff base, and bridging through the azine nitrogen (the 255cm^{-1} band reflecting octahedral coordination). This is similarly seen in 15B and 15C; in the latter case the shift of ν_aM-O by 20 cm^{-1} and ν_sM-O by 10 cm^{-1} when compared to 15A supports such a conclusion. 14B, 14C and 16C do not show bands in the region of the νM-$N_{(py)}$. They may instead be octahedral as the result of coordination of water, with the bands at approximately 350-360 cm^{-1} being suitable candidates for octahedral νM-OH_2.

5.4.5 Group 5: The far infrared spectra of the complexes of the 3-aminomethylpyridine-based ligands

Selected characteristic group frequencies for the spectral data for the isolated 3-aminomethylpyridine-based ligands (3-pico) and their cobalt(II) complexes are listed in Tables 4:53-4:56. All the complexes in this set appear to follow the standard formulae of $MH_2L_2Cl_2$ and ML_2. The position of the azine nitrogen does not favour its involvement in forming a chelate ring, but it does offer a site for potential bridging. The insertion of the methylene group between the C=N and the pyridine ring increases the basicity of the azomethine nitrogen, but destroys the conjugation between the pyridine ring and the rest of the molecule. The effect of this insertion was noted in the mid-infrared, and it similarly influences the far infrared. It appears that the Co-O and Co-N stretches in general occur at much lower frequencies than their 3-aminopyridine analogues.

Complexes 17A, 18A, 19A show tetrahedral coordinated chlorides are present. The complexes 17B, 17C, 18B, 18C, 19B and 19C may all be octahedral with coordinated water, with all possessing bands suitable as candidates for octahedral $\nu M\text{-}OH_2$. However they are all monohydrates only and consequently there must be bridging of some sort to satisfy the coordination requirements. Unfortunately no suitable $\nu M\text{-}N_{(py)}$ could be detected in the vibrational spectrum, and the assigned coordination must be tentative. For van3pico there is no possibility of chelation, and the bridged complex involves both the hydroxyl and imine groups, and in addition the coordinated azine nitrogen is cautiously identified at 272 cm^{-1} indicates octahedral coordination of the metal.

5.4.6 Group 6: The far infrared spectra of the complexes of the 2-aminomethylpyridine-based ligands

Tables 4:57-4:60 lists selected characteristic group frequencies for the spectral data for the isolated 2-aminomethylpyridine-based ligands (2-pico) and their cobalt(II) complexes. Containing no chlorides, compound 21A does not fit the standard formula. The aminopyridine based ligands with sal, p-van and o-van would allow for both a six membered chelate ring (C-O, $C\text{-}N_{(imine)}$) and a five membered ring ($C\text{-}N_{(imine)}$, $C\text{-}N_{(py)}$). Only the second chelate ring is possible with van2pico, and the hydroxyl group may only be involved in bridging.

The far infrared spectra for this group of complexes are very poorly resolved, being strongly masked by internal ligand vibrations. Consequently it is very difficult to make satisfactory

analyses from the data. However possible assignment of tetrahedral coordinated chloride in 22A suggests that, with the exception of 21A, they follow the general tetrahedral coordination found for this group. The geometry of 21A remains ambiguous, as the anhydrous compound there remains the potential of being octahedral, bound by the azine nitrogen. However the resolution of the spectrum is too poor to identify a $\nu M\text{-}N_{(py)}$. The "B" and "C" complexes are very cautiously suggested to be octahedral based on the assignment of $\nu M\text{-}N_{(py)}$ at 283 cm^{-1} (22B) and 274 cm^{-1} (24B).

5.5 Electronic spectra of Schiff bases

Before interpretation of the UV-visible-NIR spectra can be made several issues need to be clarified. The first is that there are different regions of the spectra to be considered. These are: the UV region (below 300nm), the visible region (ranging from blue through to red, 430 nm to 750 nm) and the near infrared region (800 nm to 2000 nm). Each region introduces its own considerations when interpreting the spectra.

When running solution spectra, the nature of the solvent may interfere with the spectrum of the sample. Solvents containing lone pairs such as water, alcohols, amines and chloroform will possess $n \rightarrow \sigma^*$ transitions that limit the interpretation of the sample spectrum, especially in the UV region. In addition solvents may induce shifts of the ligand bands (solvochromatism), particularly with polar solvents, and may also cause other changes as a result of solvent coordination, or even dissociation of the complex. The behaviour of protic (eg. MeOH) and nonprotic (eg. DMF) polar solvents may also be a factor – protic solvents can stabilise cations by unshared electron pairs, and can stabilise anions by hydrogen bonding. In summary, for keto-enone tautomers (and by extension, to the keto-imine tautomers in the present series of ligands), removal of lone pairs from possible conjugation will induce a blue shift, while enhancement of the phenolate ion will induce a red shift.

The electronic spectra of the Schiff bases and their corresponding cobalt(II) complexes are summarized in Tables 4:61-4:90. To enable easy comparison, the information obtained from the diffuse reflectance and solution electronic spectra in the UV/vis region using DMF and methanol have been put together in each of the Table for all the isolated ligands of the same series. In addition, the information obtained from the diffuse reflectance and solution electronic spectra of the ligands and their corresponding cobalt(II) complexes in the UV/vis region are also listed.

Assessment of the electronic behaviour of each ligand and their isolated cobalt complexes were done. The ligands and their complexes were studied in DMF and methanol respectively to enable a brief prying into the effect of solvents on their electronic properties. The work done here is qualitative and not quantitative; hence the molar absorptivity (formerly called the molecular extinction coefficient) was not calculated for the spectra data of the Schiff bases and their complexes.

The section is divided into two main parts: the first part is focused on looking at the effect of substitution on the phenyl ring as well as replacement of aniline with aminopyridine or aminomethylpyridine within and across the groups. The subsection also looked at the effect of solvents on the electronic spectra of the synthesised Schiff bases. The section is concluded by briefly looking at the differences that was observed in the electronic spectra of ligands in solution as well as in solid state using diffuse reflectance technique.

The second part of this section examines the electronic spectra of the corresponding cobalt(II) complexes of the Schiff bases discussed in part one of the section. Using the information from the diffuse reflectance, the geometry of the various complexes is assigned where possible.

5.5.1 Examination of the effect of substitution on the phenyl ring

The effect of substitution on phenyl ring is examined at this point. The interest is to determine what influences the shifting of position of equilibrium to imine-enol or keto-amine tautomer formation. For the brief examination, substitution and solvents effects are discussed. Thereafter, the effect of substitution of the different amines used for the syntheses is examined on the electronic spectra.

5.5.1.1 Group 1: The electronic spectra of the aniline-based Schiff bases

The electronic spectra of aniline-based ligands in methanol are shown overlap in Figure 5:1. The wavelengths are tabulated in Table 4:61. The most striking difference observed is the effect of methoxy group on the electronic spectra of ligands 1 - 4. A band above 400 nm was observed in ligands 2, 3 and 4. The presence of a band above 400 nm is an indication of predominance of keto-amine tautomers in solution.[21,50,51] The absence of this band in ligand 1 reveals the predominance of O-H.....N=C form of the Schiff base.[21,47-8]

It's noted that the position of the methoxy group in the phenyl ring determines the position of the band above 400 nm. In ligand 2, the keto-amine band occurred at much lower wavelength than in ligands 3 and 4; Figure 5:2. The red shift is due to the nature of the substituent and position, which shift the equilibrium towards the keto-amine tautomer. Such equilibrium will also be favoured by the polar nature of the solvent. The spectral changes observed as a function of solvent composition is an indication that an equilibrium exit in solution between two tautomeric forms of the Schiff bases.[49] Scheme 5: 8 is used to depict the effect of substituent and solvent on the tautomers of the various Schiff bases in this series and the series of the other five groups studied. While the 3-methoxy substituent stabilizes the structure of ligand 3, and hence favoured keto-amine tautomer, solvent would probably favoured the shift of ligands 2 and 4 to the right.

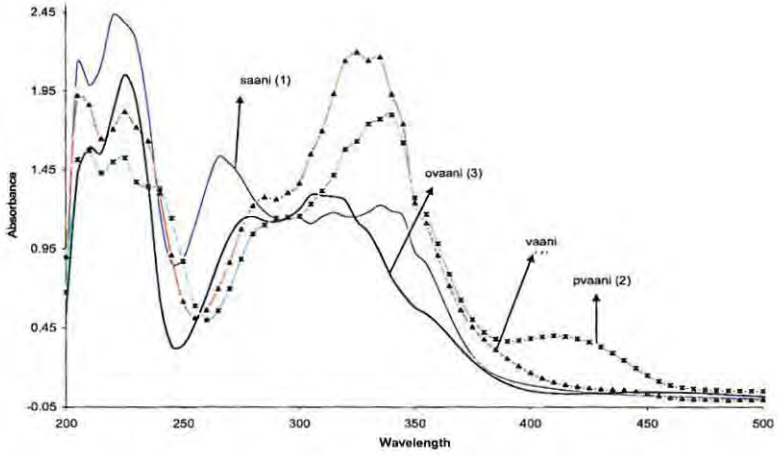

Figure 5:1 UV/vis absorption spectra of ligands 1, 2, 3 and 4 in methanol

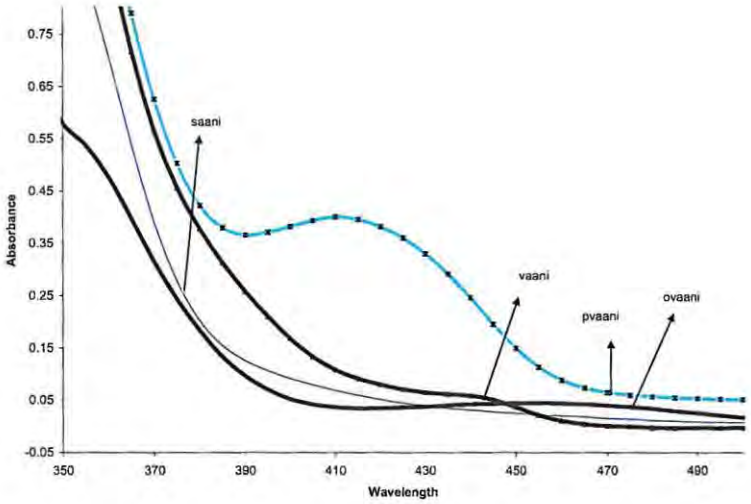

Figure 5:2 UV/vis absorption spectra of ligands 1, 2, 3 and 4 showing keto-amine band in methanol

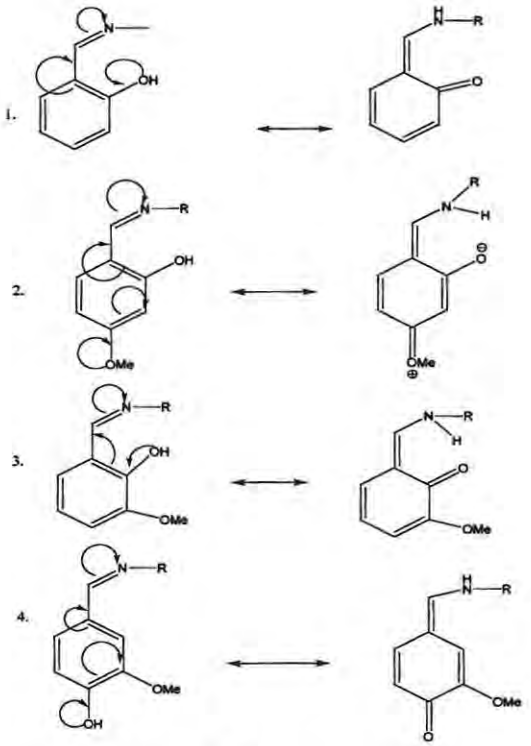

Scheme 5:8 Tautomerism in Schiff bases

The composite bands at 315 nm and 335 nm observed in ligand 1, blue shifted in ligand 3, because of the presence of methoxy in meta-position while it red shifted in ligands 2 and 4. The benzenoid band around 265 nm exhibited by ligand 1 red shifted in all the other three ligands showing the effect of the methoxy substituent.

As observed in methanol, ligands 1 - 4 followed similar trends in DMF, Figure 5:3 refers. However, the keto-amine band above 400 nm that was observed for ligands 2 and 4 in methanol were not seen while a weak band at 540 nm was observed for ligand 3. It was not possible comparing wavelengths below 270 in DMF since the solvent absorb in this region. The general trend is that the bands shifted to lower energy in DMF. This observation is ascribed to the solvent polarity.[49,50] The enol-imine predominance in DMF implies that a strong intermolecular hydrogen bond exit between the solvent and the ligands. The polar structures of the ligands are destabilized by the DMF polarity, resulting in the blue shifting of the bands.[50] Similar changes have been observed for some salicylideneimines.[51-3]

For the aniline-based ligands, the extent of the red or blue shifting of the four focused bands (200-240 nm, 250-300 nm, 310-340 nm and above 400 nm) differs for each band and is depended on the position of the substituent(s), solvent or combination of both. For instance, while the absence of methoxy resulted in the formation of imine-enol ligand 1, the presence of 3-methoxy substituent resulted in the formation of a keto-amine tautomer.

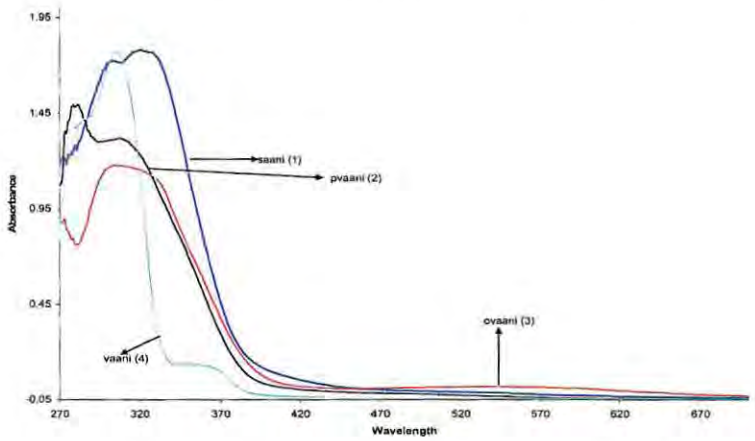

Figure 5:3 UV/vis absorption spectra of ligands 1, 2, 3 and 4 in DMF

5.5.1.2 Group 2: The electronic spectra of the 1-aminonaphthalene-based Schiff bases

The wavelengths of aminonaphthalene-based ligands in methanol, DMF and solid state are tabulated in Table 4:62. In methanol, the band above 400 nm which suggest keto-amine tautomers predominance was not seen or very weak (if present) in all the four ligands of this series. The keto-amine band above was also absent when the ligands were studied in DMF. Figures 5:4 showed spectra of aminonaphthalene-based ligands in methanol. The fine structure observed in the spectra of the ligands in methanol was lost in DMF as expected. This is attributable to higher polarity of DMF relative to methanol.[50]

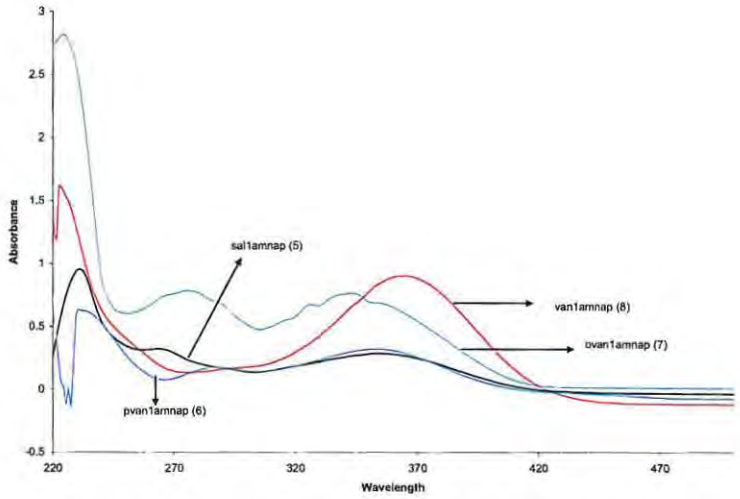

Figure 5:4 UV/vis absorption spectra of ligands 5, 6, 7 and 8 in methanol

The replacement of aniline with 1-aminonaphthalene caused a shift to higher wavelengths, typified by Figures 5:5 and 5:6 respectively. This is associated with increased conjugation, and the smaller energy gap between $\pi \rightarrow \pi^*$ and $n \rightarrow \pi^*$ orbitals of the aminonaphthalene. However, while increase in conjugation caused the shift of the band observed at 340 nm for the aniline-based to higher wavelength on replacement of aniline with aminonaphthalene, it effect resulted in the formation of less of the keto-amine tautomer in the equilibrium mixture.

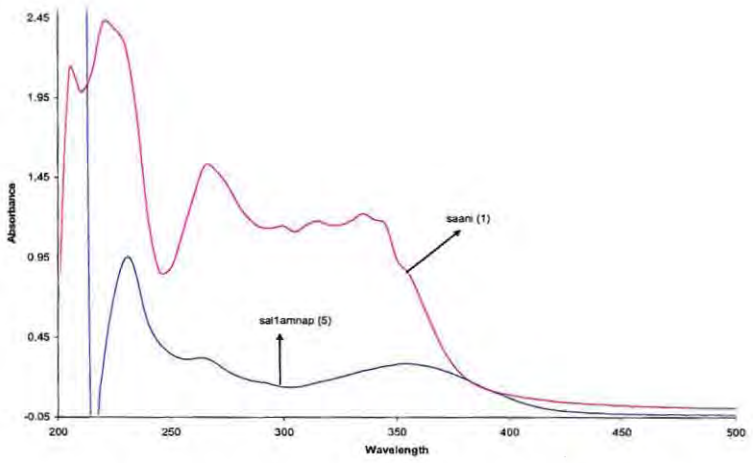

Figure 5:5 UV/vis absorption spectra of ligands 1 and 5 in methanol showing the effect of increased aromatic amine on the enol-imine tautomer

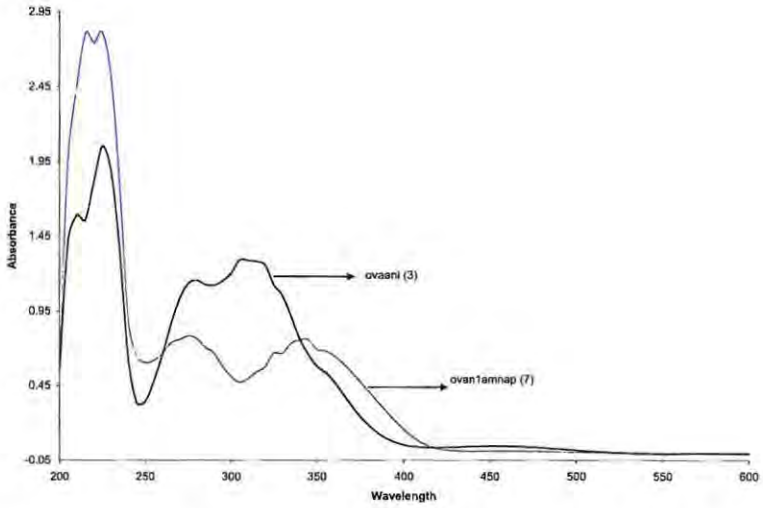

Figure 5:6 UV/vis absorption spectra of ligands 3 and 7 in methanol showing the effect of increased aromatic amine on the keto-amine tautomer.

5.5.2 Examination of the effect of substitution of the amine with aminopyridine

The next section will be dedicated to discussing the effect of replacing aniline with aminopyridine on the electronic spectra of the synthesised ligands. Where applicable the solvent as well as substituent effects will be discussed.

5.5.2.1 Group 3: The electronic spectra of the 4-aminopyridine-based Schiff bases

The electronic spectra of 4-aminopyridine are given in Table 4:63. The Schiff bases were dissolved in methanol and DMF respectively. The spectra are shown in Figures 5:7 and 5:8 respectively. The effect of having the methoxy in different positions was also apparent in behaviour of these ligands. The band at 319 nm that was seen in ligand 9, the Schiff base without a methoxy substituent, was shifted to 339 nm in the *p*-methoxy substituted ligand 10 while the *meta*-methoxy substituted ligand 11, is further red shifted to 391 nm in methanol. The reason for the red shifting of *m*-methoxy substituted compound relative to the *p*-methoxy substituted compound can be ascribed to resonance structures. The *p*-substituted compound has more canonical structures which stabilize more than the m-substituted ligand. The more the resonance structures, the more the possibility of shifting wavelength to lower energy.

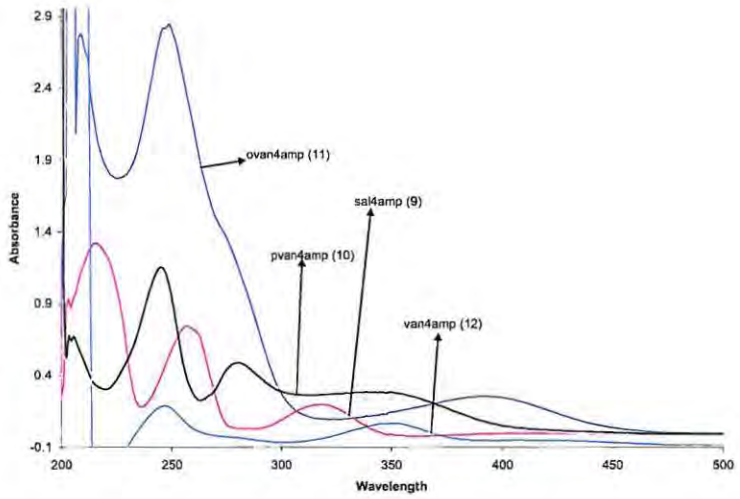

Figure 5:7 UV/vis absorption spectra of ligands 9, 10, 11 and 12 in methanol showing substituent effects

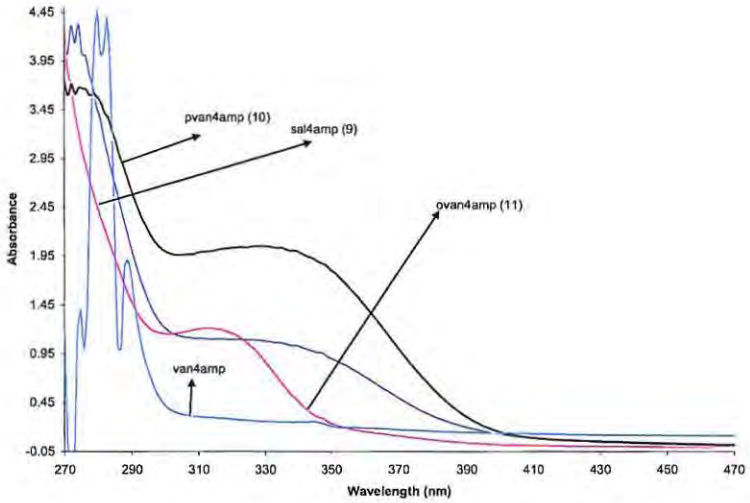

Figure 5:8 UV/vis absorption spectra of ligands 9, 10, 11 and 12 in DMF

The effect of solvent is also demonstrated by this set of ligands. Solvents are known to affect the fine structure of absorption curves as well as the wavelengths of the maxima.[50] It is well known that vibrational fine structure is lost when there is increase in solvent polarity.[50] A blue shift of the keto-amine band caused by increasing the polarity of the solvent implies a decrease in the polar quinoid resonance forms.[50] A band of ligand 9 that appeared at 257 nm in DMF blue shifted in ligands 10, 11 and 12 as a result of the presence of a methoxy group. Since the methoxy group is an electron donor, the unshared electron pairs may interact with the solvent or

with other molecules in solution. This may account for the blue shift as the polarity of the solvent increases, since the solvation with the polar solvents contributes to the stability of the ground states more than the excited states.[50] With the exception of other effects; the blue shift is expected to increase gradually with solvent polarity. There was shift of wavelength to lower energy as the solvent polarity increases. This account for the significant blue shift observed as DMF is used to substitute methanol.

The comparison of ligands 9, 10, 11 and 12 with the aniline-based ligands revealed that the replacement of aniline with the 4-aminopyridine caused the wavelength shift towards lower wavelength. Figures 5:9 is used to depict these observations. This implies that substitution of aniline with pyridine shifted the wavelengths to higher energy. The general trend observed is that replacement of aniline with pyridine lead to the predominance formation of enol-imine tautomers. This effect is ascribed to the presence of nitrogen in the pyridine ring which probably pushes its nonbonding electron into the conjugated ring, and consequently affecting the electron density around the azomethine nitrogen.

However, while keto-amine band was absent in ligands 10, 11 and 12, a band at above 400 nm was observed for ligand 9. This is an indication that keto-amine may be predominance. The presence of the keto-amine band in ligand 9 may be ascribed to the absence of methoxy, hence a weak intermolecular hydrogen bonding of the imine, which resulted in the red shifting of the keto-amine band on solvation with the solvent molecule. There may be predominant contributions of the polar structure to the excited state, hence making the excited state more polar than the ground state.[49,50]

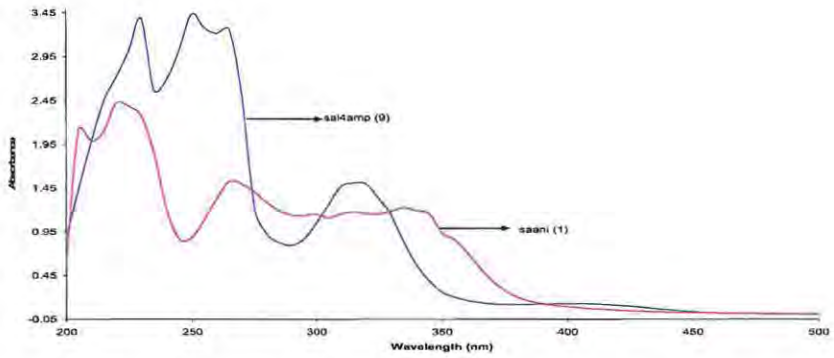

Figure 5:9 Comparison of UV/vis absorption spectra of saani (1) and sal4amp (9)

5.5.2.2 Group 4: The electronic spectra data of the 3-aminopyridine-based Schiff bases

This section examines the effect of solvent and substituents on the electronic spectra of the 3-aminopyridine-based ligand. Thereafter, this group of Schiff bases is compared with the 4-aminopyridine-based ligands. The analyses also look at the effect of substitution of aniline with 3-aminopyridine on the keto-amine or enol-imine formation.

Data for the ultraviolet and visible absorption spectra of 3-aminopyridine ligands in methanol, DMF and solid state are summarized in Table 4:64. The spectra for 3-aminpyridine-based ligands 13, 14, 15, 16 in methanol and DMF are shown in Figures 5:10 and 5:11 respectively. As observed for the groups that have previously been discussed, the absorption maxima of all the ligands suffered large hypsochromic shifts more in DMF than methanol. These shifts are typical of compounds with strong intramolecular hydrogen bond. It is interesting to note that the ligands having methoxy group substituent in the meta- position suffered larger hypsochromic shifts in the more polar solvent, DMF. The blue shift in more polar solvent is characteristic of dipolar species.[52] This behavior is ascribed to the stabilization of the ground state by the solvent.[49] When the ligands are compared in each of the solvents, it was observed that the presence of the nonbonding pair substituents shifted the absorption substantially to longer wavelength. For instance, the band at 340 nm observed for sal3amp (13) shifted to longer wavelength in ovan3amp (15) and van3amp (16) when dissolved in methanol because of the presence of methoxy in the 3-position. Even in DMF, the absorption band of o-van3amp, (15) still appeared at higher wavelength than sal3amp (13) due to the methoxy group in the meta-position.

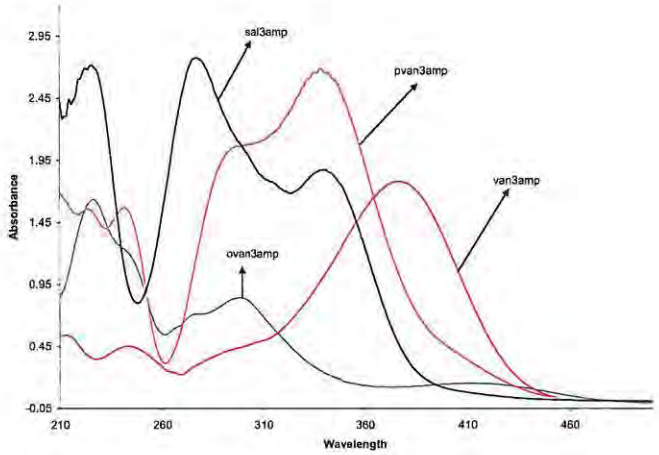

Figure 5:10 UV/vis absorption spectra of ligands 13, 14, 15 and 16 in methanol

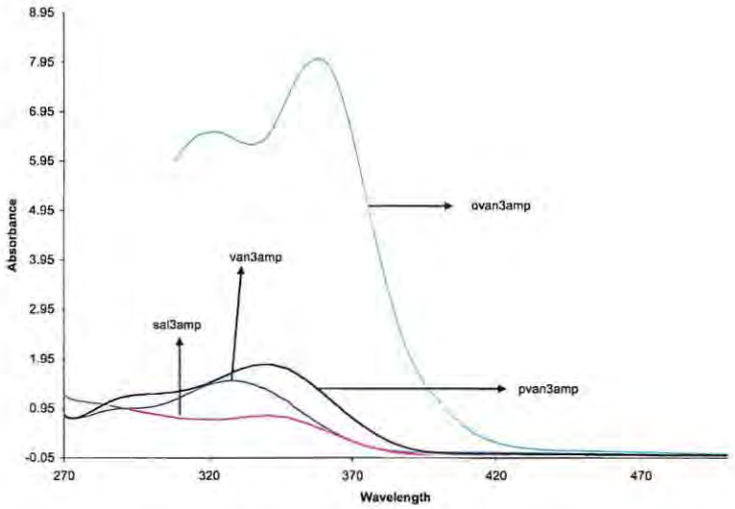

Figure 5:11 UV/vis absorption spectra of ligands 13, 14, 15 and 16 in DMF

The methoxy group is believed to stabilize the polar structure to the excited state, making the ground state less polar than the excited state. In DMF, the electronic band observed at 340 nm in sal3amp (13) shifted to much lower absorption in van3amp (16). The reason for shifting to higher energy may be attributed to intermolecular hydrogen bond. Since its OH is in the para-position, the possibility of coordinating with the solvent molecules is high. The absorption bands for sal3amp (13) and pvan3amp (14) appeared almost the same in both solvents. However, the observation is that there was decrease in fine structures and intensity as DMF is used to substitute methanol.[50]

A comparison of the 4-aminopyridine Schiff bases with the 3-aminopyridines Schiff bases revealed that the 3-aminopyridines absorbed at higher wavelength than the 4-aminopyridines in both solvents. A tentative explanation of the experimental results is ascribed to the strength of the pyridine base stabilizing the keto-amine tautomer through it H-acceptor ability. The 3-aminopyridine is a better proton-acceptor than the 4-aminopyridine, Scheme 5:9 refers.

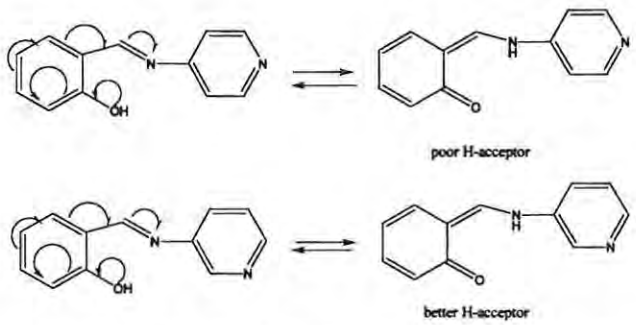

Scheme 5:9 Structures showing the 3-aminopyridine-based Schiff base as a better proton acceptor than the 4-aminopyridine analogue

Angyal and Angyal[54] noted that protonation constants of the amino group of aminopyridines depend on its substitution site on the pyridine ring. The log K of the 2-aminopyridne is -7.6, while those of 3-aminopyridine and 4-aminopyridine is -1.5 and -6.1 respectively.[55] Similar characteristics can be predicted for the corresponding Schiff bases. According to the published work of Cumper and Singleton,[56] two types of intermolecular hydrogen bonding can be envisaged with solvents. In hydrogen bonding by solvents, the amine acts as a proton acceptor and electronic interactions between the lone pair electrons of the amino-nitrogen atom and the π-electrons of the aromatic ring is decreased, leading to hypsochromic shifts as a result of decrease in electron density on the nitrogen atom.[56] In the same vein, Pimentel[57] proposed that excitation places a nodal plane through the electron-donating amino group, consequently reducing its electron density in the excited state and hence, making it poorer proton acceptor. This would also lead to the hypsochromic shift observed in the 4-aminopyridine analogues. The second hydrogen bonding effect is by the solute. According to Pimentel, there is electron migration from the electron donating amino group in the excited state, resulting in stronger hydrogen bonding and hence bathrochromic displacements ensue.[57] The relative order of the bathochromic shifts is, 4-aminopyridines > 3-aminopyridines > aniline ~ 2-aminopyridines.[57] However, the presence of the methoxy as well as the hydroxy groups in different positions in the phenyl ring of the series of Schiff bases studied coupled with the effects of nitrogen in different position in the pyridine ring resulted in the observed absorption bands illustrated in Figure 5:12 below.

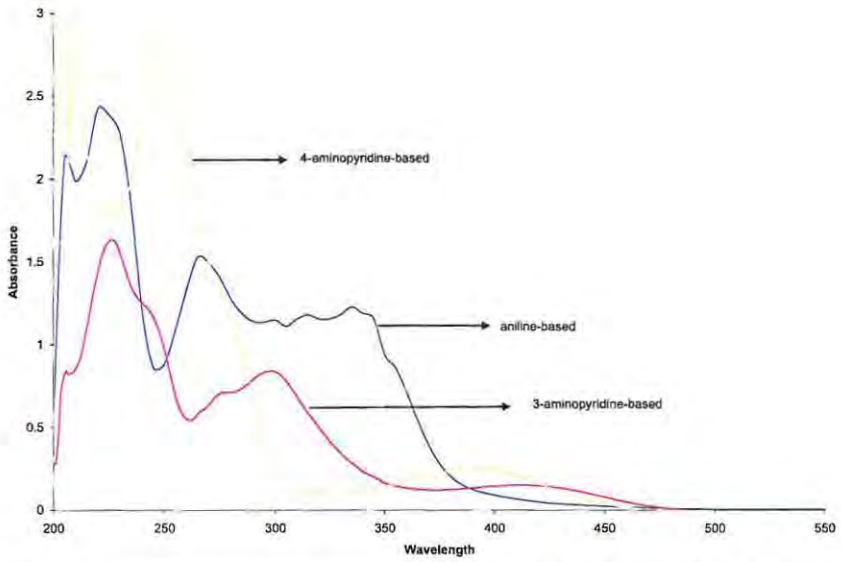

Figure 5:12 Bathrochromic band shift in the aniline-based, the 3- and the 4-aminopyridine-based Schiff bases

Unlike sal3amp (13), pvan3amp (14) and ovan3amp (15), all the bands of van3amp (16) are red shifted. This agrees with the basicity of the pyridine stabilizing the keto-amine tautomer. Such behaviour indicates the influence of the pyridine ring and the nature of the phenyl ring acting concomitantly. The absence of the keto-amine band (a band above 400 nm) for ligands 13, 14 and 16 might be an indication that that O-H------N=C form predominate.

A comparison of 3-aminopyridine-based ligands (group 4) with the aniline-based ligands (group 1) revealed that the spectra of the two groups are similar. However, it was observed that the benzenoid bands were affected, with a red shift of 10 nm when the aniline is substituted with 3-aminopyridine. The keto-amine band observed at 450 nm in ovaani (3) also shifted to lower wavelength in ovan3amp (15), as a result of the substitution of aniline with 3-aminopyridine, Figure 5:12 refers.

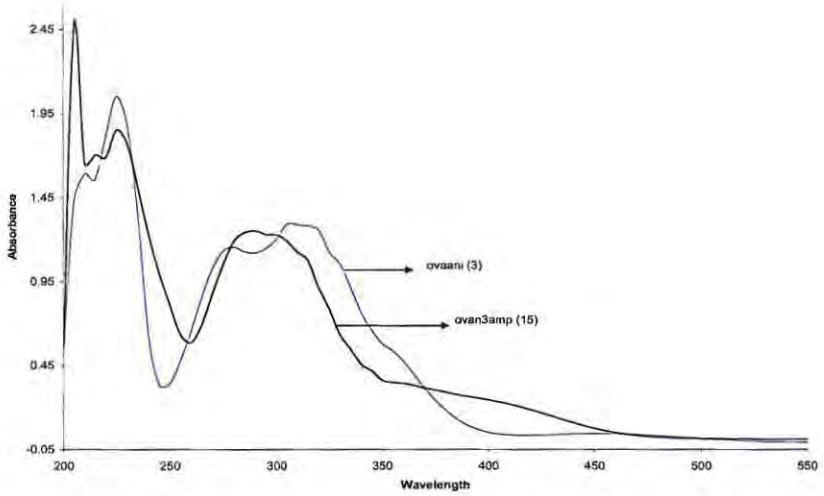

Figure 5:13 Comparison of UV/vis absorption spectra of ovaani (3) and ovan3amp (15)

5.5.3 Examination of the effect of substitution of amine with methylaminopyridine

The following section discusses the effect of the introduction of methylene (CH_2) between pyridine and the imine. The analysis examines the solvents and substitution effects on the electronic spectra of these sets of ligands. Thereafter, their electronic effect is compared with the 3-aminopyridine- and the aniline-based ligands. This section also looks at the effect of insertion of methylene on the enol-imine or keto-amine formation.

5.5.3.1 Group 5: The electronic spectra of 3-aminomethylpyridine-based Schiff bases

Schiff bases obtained from the condensation of amino- and aminoalkylpyridines with salicylaldehyde have been found to be predominantly in the enolimine tautomeric form in solid state and in the solutions of non-polar solvents.[58,59,60] Galic et al.[55] have also shown that the Schiff bases derived from aminoalkylpyridines readily convert to ketoamines in polar, protic solvents, like methanol, ethanol, or alcohol/water mixtures.[6,55] They claimed that the tendency of tautomeric inter-conversion is much less pronounced in the case of the Schiff bases derived from the aminopyridines.[6,55] They ascribed this behaviour to the reduced basicity of the amino nitrogen caused by the proximity of the pyridine ring and the delocalization of the imino nitrogen electron pair.[60]

The list of electronic spectra data for the 3-aminomethylpyridine-based ligands is listed in Table 4:65. Only the salicylaldimine of the 3-aminomethylpyridine has previously been reported.[5,6]

Trends of events in this group are almost the same as what has been discussed for the earlier groups. In methanol, it is interesting to observe that all except *para*-methoxy substituted ligand, pvan3pico (18) exhibited bands at above 400 nm. The appearance of the band at 400 nm and above may be due to the formation of the keto-amine tautomers. The bathochromic shift is determined by the position of the methoxy substituent in the phenyl group. In methanol, comparison of sal3pico (17), ovan3pico (19) and van3pico (20) showed that the weak band observed at 430 nm for Schiff base 17, shifted in ligand (20) to 309 nm or disappeared while ligand 19 has a broad band at above 430 nm.

The spectra of the ligands in methanol and DMF are shown in Figures 5:14 and 5:15 respectively. In DMF, the diagnostic band is seen around 300 nm. The band at 318 nm that was observed for sal3pico (17), appeared the same in pvan3pico (18), red shifted to 332 nm in ovan3pico (19), but blue shifted in van3pico (20) to 301 nm with a weak band at 360 nm. The hypsochromic shift observed for van3pico (20) can be ascribed to the interactions between the lone-pair electrons of the *para*-hydroxy group and the polar solvent leading to the decrease in π-electrons of the aromatic ring, and hence the observed blue shifts in wavelength.[56]

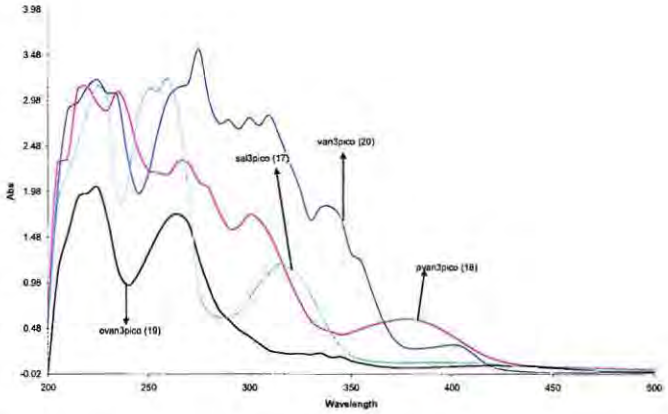

Figure 5:14 UV/vis absorption spectra of ligands 17, 18, 19 and 20 in methanol

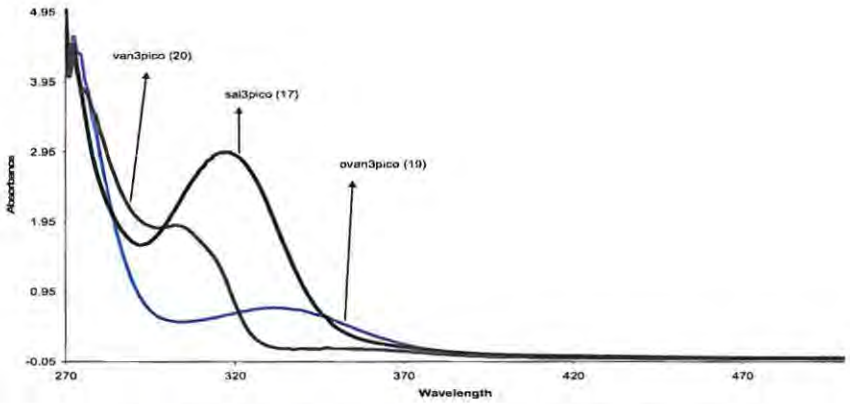

Figure 5:15 UV/vis absorption spectra of ligands 17, 19 and 20 in DMF

When the ligands in this series are compared with the 3-aminopyridine-based Schiff bases, it was observed that bands shifted to higher energy. This blue shifting is ascribed to the insertion of methylene group between the C=N and the pyridine ring and reduction of resonance into the pyridine ring.

With the exception of pvan3pico (18), it was observed that the insertion of the methylene between imine and the pyridine ring resulted in the predominance formation of keto-amine tautomers. However, when compared with the aniline based-ligands, the observation is that the keto-amine bands blue shifted.

5.5.3.2 Group 6: The electronic spectra data of 2-aminomethylpyridine-based Schiff bases

This section examines the effect of the insertion of the methylene group and the changing of the location of the pyridine nitrogen from position 3 to position 2 on the electronic spectra of these ligands.

The synthesis and structure of Schiff base of salicylaldehyde with 2-aminomethylpyridine has been previously reported.[6,61] The electronic spectra data of 2-aminomethylpyridine ligands are listed in Table 4:66 while their spectra in methanol are shown in Figure 5:16. It was observed that the absorption curves of 3-aminomethypyridine-based ligands are similar to the absorption curves of the 2-aminopyridine-based ligands. However, 2-aminomethylpyridine-based ligands appeared at lower energy than their 3-aminomethylpyridine analogues (Figure 5:17). This is

attributable to the higher basicity of the imine nitrogen in the 2-aminomethylpyridine than its 3-aminomethylpyridine analogue.

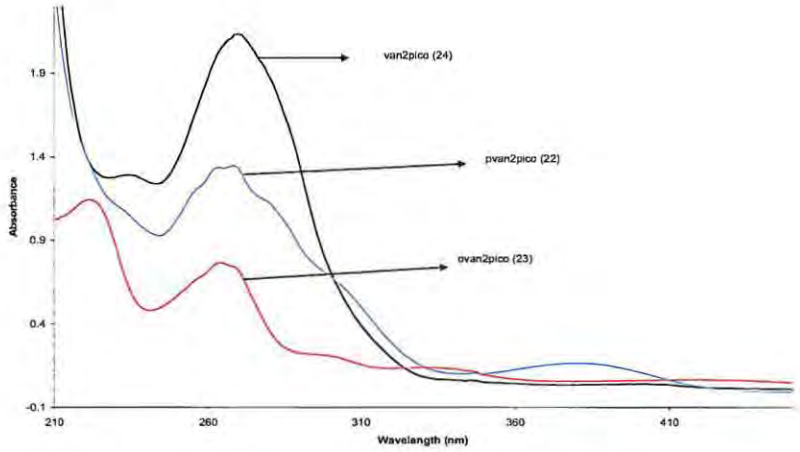

Figure 5:16 UV/vis absorption spectra of ligands 22, 23 and 24 in methanol

The insertion of methylene between the C==N bond and the pyridine isolates the pyridine from the conjugated phenyl ring, hence increasing the basicity of the azomethine nitrogen. However, it appeared that the insertion of the methylene is not what determines the enol-imine or keto-amine formation for this series but the position of the pyridine nitrogen or the functional groups. There are two functional groups which is able to form an intramolecular hydrogen bonding with the imino nitrogen: the ortho hydroxy, and the 2-aminopyridine if the ligand takes the Z-configuration or azomethine hydrogen and the 2-aminopyridine if the ligand exists in E-conformation as depicted previously in Scheme 5:5.

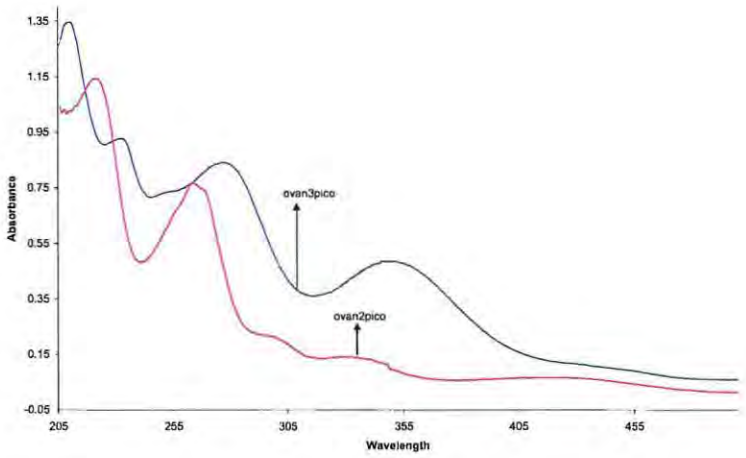

5:17 Comparison of UV/vis absorption spectra of ovan3pico (19) and ovan2pico (23)

Competition between these two groups to form hydrogen bond with imine nitrogen could be the reason why keto-amine is not formed in ligands 21, 22 and 24. The formation of keto-amine tautomer is due to solvation and resonance stabilization.[62] The absence of keto-amine band in the electronic spectra of ligands 21, 22, and 24 implies that loss of a large amount of resonance energy which is possible only if the ground state is stabilized by contribution of polar resonance forms did not take place.[62] For ligand 23, the loss in resonance energy resulted in the appearance of the band at 425 nm.

5.5.4 Solid state UV/vis (Diffuse reflectance spectra)

The solid state UV/vis for the ligands was carried out using diffuse reflectance technique. The spectra obtained from the diffused reflectance technique showed marked differences from those obtained from solution UV/vis using DMF and methanol respectively. The UV/Vis absorption bands in solid state are broad and not symmetrical with solution electronic spectra. This implies that different electronic transition occurs in the solid state.[63] These results are attributable to the formation of aggregates; implying strong dipolar interactions in the solid state.[63] Additional UV/vis maxima which bathrochromically shifted were observed using diffuse reflectance. Figure 5:18 is used to typify this observation.

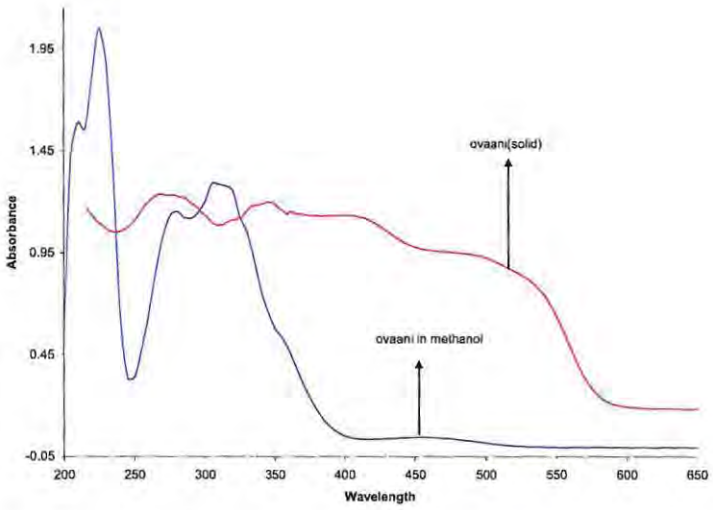

Figure 5:18 UV/vis absorption spectra of ligand 3 (ovaani) in solution (methanol) and solid state (diffuse reflectance)

5.6 The electronic spectra of cobalt(II) complexes

Having discussed the effects of substitution on the phenyl ring, the effects of using different amines as well as the effect of solvents on the electronic spectra of the synthesised Schiff bases, the specifics Schiff base complexes of cobalt(II) will now be addressed. The information from the spectra curves will be used to assigned metal ligand charge transfer or ligand metal charge transfer. Thereafter, the diffuse reflectance data will be used to assign geometry to the various complexes using previously assigned methods.

The electronic spectra data of the complexes listed in Tables 4:67 – 4: 90 does not include near infrared region spectra data. It is believed spectra curves conveys the required stereochemistry information needed for geometry assignments more than just spectra data. In addition, combination and overtone bands complicate band assignment in the near infrared region.[64] Consequently, few spectra curves and relevant metal transitions in the near infrared and visible regions have been used to illustrate the wealth of information obtained from the diffused reflectance technique.

The presence of a metal centre in the complexes may result in metal to ligand charge transfer (MLCT), or in ligand to metal charge transfer (LMCT). These involve the transfer of electrons from a full orbital to an empty orbital, in short-lived excited states, consequently no net oxidation-reduction occurs. Such charge transfers are La Porte-allowed and consequently may mask weaker ligand bands or d-d transitions. The bands due to d-d transitions are determined by symmetry considerations and by both metal and ligand characteristics (the ligand field parameters). They may occur any where from the UV, through the visible region, and into the near infrared region, reflecting the wide range of energies involved. They also have different intensities, reflecting the probability (or "allowedness") of the transition. Exact details may be found in standards text books.[65,66] Interpretation of the bands in the near-infrared may be complicated by the appearance in this region of overtones of, in particular, C-H, N-H, and O-H vibrational modes. Because of vibrational overtones, it is difficult to use solvents in the near infrared region.[64]

Cobalt(II) as the free ion has the spectroscopic term symbols ^4F, ^4P and ^2H, ^2G, ^2F, $^2D_{(2)}$, ^2P. In a cubic field the degeneracies of the states will be lifted into states described by the molecular term symbols $^4A_{2(g)}$, $^4T_{1(g)}(F)$ and $^4T_{2(g)}$ for the ^4F term, and the $^4T_{1(g)}(P)$ for the ^4P term (where $_{(g)}$ reflects the octahedral fields, and its absence reflects the tetrahedral field). The doublet F and P

terms are similarly lifted into the analogous Mulliken symbols, while the ^2D are lifted into the $^2E_{(g)}(D)$ and $^2T_{2(g)}(D)$ terms, and ^2G is lifted into $^2A_{1(g)}$, $^2E_{(g)}(G)$, $^2T_{1(g)}$ and $^2T_{2(g)}(G)$ molecular terms.[65]

For high spin complexes the ground state terms are $^4T_{1g}(F)$ for O_h symmetry and $^4A_2$ for T_d symmetry. In the simplified interpretation, making use of the Orgel diagram for the d^7 ion, the three spin allowed transitions will be the $^4T_{1g}(F) \rightarrow {}^4T_{2g}$ (ν_1); the $^4T_{1g}(F) \rightarrow {}^4A_{2g}$ (ν_2)and the $^4T_{1g}(F) \rightarrow {}^4T_{1g}(P)$ (ν_3) for an octahedral complex. The crystal field stabilisation energy ($10Dq_{oct}$) may be determined by the difference in the energies of the first two transitions. This is however complicated by the fact that there is mixing between the wave functions of the $^4T_{1g}(F)$ and the $^4T_{1g}(P)$ terms (according to the non-crossover rule for species of similar symmetry), and in addition that for stronger field ligands the $^4T_{1g}(F) \rightarrow {}^4A_{2g}$ and $^4T_{1g}(F) \rightarrow {}^4T_{1g}(P)$ transitions are of similar energies, and may even cross.[65]

For the simplified interpretation of tetrahedral Co(II) complexes the three spin allowed transitions will the $^4A_2 \rightarrow {}^4T_1(P)$ (ν_1), the $^4A_2 \rightarrow {}^4T_1(F)$ (ν_2) and the $^4A_2 \rightarrow {}^4T_2$ (ν_3). While there is mixing of the $^4T_1(F)$ and the $^4T_1(P)$ terms, the crystal field stabilisation energy ($10Dq_{tet}$) is defined by the $^4A_2 \rightarrow {}^4T_2$ transition. There is no mixing of these two terms, but the $^4T_1(F)$ and $^4T_1(P)$ terms do mix.[65]

Distortion from perfect octahedral or tetrahedral symmetry for the molecule towards that for square planar geometry causes a lowering of the overall symmetry in pseudo- octahedral and pseudo tetrahedral- geometries, and results in further lifting of the triple degenerate T states. For the square planar general molecular system MA_2B_2, in the cis- molecule (C_{2v} symmetry) the $^4T_{1(g)}$ is lifted to $^4A_2$, the $^4B_1$ and the $^4B_2$ states, the $^4T_{2(g)}$ is lifted to $^4A_1$, the $^4B_1$ and the $^4B_2$ states, while the $A_{2(g)}$ is the A_2 state; for the trans- molecule (C_{2h} symmetry) the $^4T_{1(g)}$ is lifted to ^4A_g and two ^4B_g states, the $^4T_{2(g)}$ is lifted to two ^4A_g and one ^4B_g states, while the $A_{2(g)}$ is the B_g state.[65] For any transition involving a T term, in either the ground state or the excited state, for the d-d transitions the electronic spectrum could display band broadening, the appearance of shoulders, or even distinct band separation, depending on the extent of distortion towards the square planar geometry.

Spin forbidden d-d transitions from the quaternary ground states to doublet excited states are extremely weak, and should not have much bearing on the interpretation of the electronic

spectra, unless deconvolution of the band envelopes is being undertaken.[67] Energy diagrams including the spin forbidden transitions are described by Tanabe-Sugano diagrams, which express their energies in terms of the Racah parameters. That for octahedral Co(II) (d^7) highlights the possibility for a change in the ground state from $^4T_{1g}(F)$ for spin free or high spin complexes, to $^2E_g(G)$ for spin paired or low spin complexes, once the energy of the crystal field splitting exceeds the pairing energy. For Co(II) this would be when strong field ligands result in $10Dq_{oct}$ exceeding 9 300 cm^{-1}.[66] Since Dq_{tet} is $^4/_9$ths that of Dq_{oct}, this is peculiar to octahedral complexes. Consequently, with octahedral low spin complexes the spin-allowed transitions occur between the doublet states, and there are four such transitions expected. The ligands in the present work are not expected to be sufficiently strong enough to cause low spin complexes.

An additional comment may be made on the band shapes associated with the d-d transitions. These often have "fine structure" associated with them, distorting them from a Gaussian form. This may be ascribed to the distortion from perfect symmetry as discussed above, but in addition spin-orbit coupling is said to account for some lifting of degeneracies.[66] Spin-orbit coupling is associated with the T terms, but not the A terms, and could thus be reflected in excitations involving the $^4T_{1(g)}$ or $^4T_{2(g)}$ states.

The intensities of the bands is a reflection of the probability (or "allowedness") of the transition. The d-d transitions of octahedral and square planar complexes of C_{2v} symmetry (cis-configuration) will not only be La Porte orbitally forbidden, they will also be La Porte parity forbidden (both use terms inclusive of the gerade subscript). As such, their intensities will be 100 fold less intense than those associated with tetrahedral and square planar complexes of C_{2h} symmetry (trans-configuration).

A general comment on the wavelength of the transitions can also be made. The energy associated with the crystal field splitting is determined by the nature of the metal, the ligand, and by the geometry of the complex. Since Dq_{tet} is $^4/_9$ths that of Dq_{oct}, the energies of the transitions for the octahedral complexes will be larger than those of the tetrahedral complexes. Consequently for octahedral complexes the high energy (ν_3) is expected to occur in or towards the UV region, while (ν_2) and (ν_1) are expected in the lower wavelength regions of the visible spectrum, the exact wavelength being determined by the ligand field parameter. For tetrahedral complexes (ν_3) and (ν_2) are anticipated in the higher wavelength regions of the visible spectrum, while the low

energy (ν_1) is expected to occur in the near-infra red or even the infra red region, again depending on the ligand field parameter.

5.6.1 Group 1: The electronic spectra of the complexes of the aniline-based ligands

5.6.1.1 The electronic spectra of the complexes of ligand 1

The electronic spectra data of ligand 1 cobalt complexes are listed in Table 4:67. A detailed interpretation has been previously reported of the UV-visible-near infrared spectrum for the cobalt(II) complex with one of the ligands used in this work, namely *N*-phenylsalicylaldimine.[70] ,Kuźniarska-Biernacka et al. [67] commented on the previously[68] noted observation that, in polar solvents with strong donor strength (such as EtOH, DMF, DMSO) and at dilute concentrations (less than 5 x 10^{-4} M) bis(*N*-phenylsalicylaldiminato)cobalt(II) exhibits a UV spectrum similar to the free ligand. This behaviour was ascribed to dissociation of the complexes below this concentration, revealing the only ionised ligand spectrum. West[68] also compared the absorption spectra of [Co(salan)$_2$] with the ligand in absolute ethanol. He observed that electronic spectrum of the ligand is similar to that of the complex. This was the observation in the present work when the complex 1B was dissolved in acetone at 3 X 10^{-5} M. This can be attributed to complete dissociation in very dilute solutions. It was observed that while the spectral curves are similar, the benzenoid bands are slightly shifted to higher wavelength in the complex.

While this was only observed for complex 1B in acetone, 1A, the complex obtained from hexaaquocobaltous chloride in ethanol gave essentially similar curve in virtually all the solvents used. 1A has been previously studied by Bamfield.[69] The complex is paramagnetic, octahedral and was found to conduct in DMF solution. The tentative explanation for the observed similarity in spectra curves is that the complex ionizes when dissolved in solvents at certain concentration. West's[68] explanation was that the complex ionized in the presence of water. An alternative explanation might be possible in view of the work of Mellor and his co-worker, which West reported.[68] They investigated the spectra of nickel complexes of the chelate type, and showed that complexes possessing paramagnetic susceptibilities (and hence tetrahedral ionic structures) show absorption spectra similar to those of the base from which are they are obtained.

While agreeing with the explanations given for the similarity in spectrum of the dissociated complex and its ligand by West,[68] Kuzniarska-Biernacka et al.,[67] Mellor and his co-worker,[68] we

would like to add that the solvent, the ratio of the ligand to metal as well as the quantity of complex dissolved might have major roles in determining the type of electronic spectra that would be produced. Figures 5:19, 5:20 are used in buttressing these observations and suggestions.

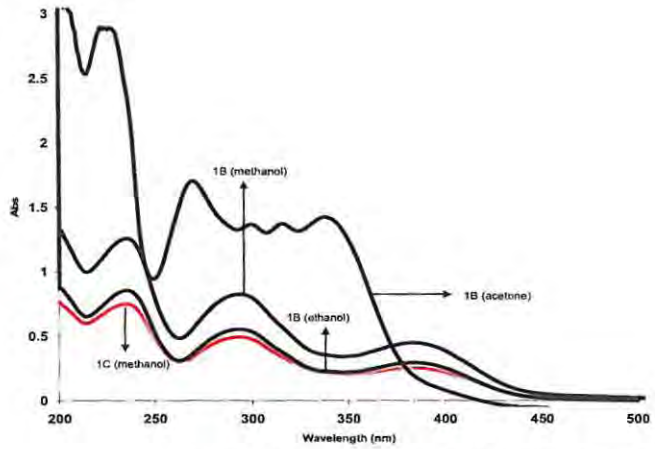

Figure 5:19 Complex 1B and 1C in different solvents

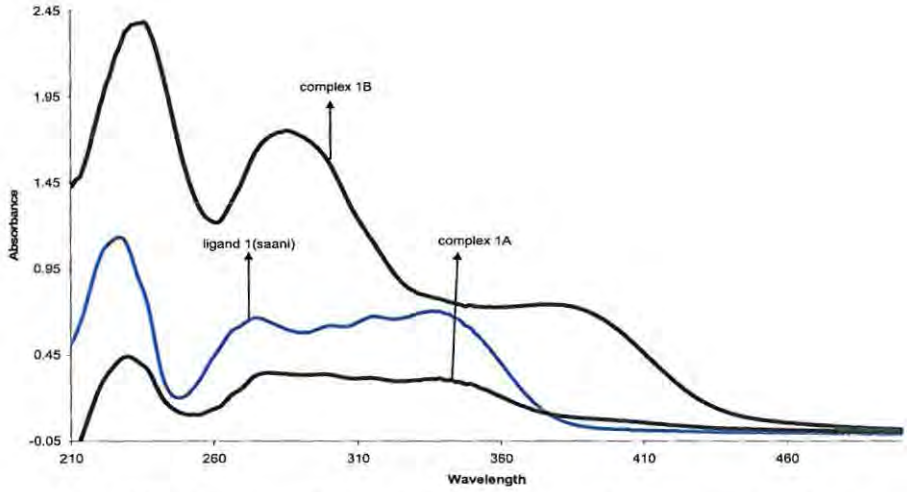

Figure 5:20 Comparison of the ligand 1(saani), and the complexes 1A and 1B in methanol

At higher concentrations the presence of the complex results in the appearance of two additional bands that mask these internal ligand bands. These are the appearance of a Co→O MLCT (a metal to ligand charge transfer involving electron transfer from the full $t_{2\ (tetrahedral)}$ d orbital to an empty π^* ligand orbital involving predominantly the oxygen donor) at about 390 nm,[67] and a Co→N MLCT (a metal to ligand charge transfer involving electron transfer from the full $t_{2\ (tetrahedral)}$ d orbital to an empty π^* ligand orbital involving predominantly the nitrogen donor) at about 290 nm.[67] In polar solvents of intermediate strength, such as dioxane the latter is only

observed as a shoulder against the stronger intramolecular absorbance at 230 nm assigned to $\pi \rightarrow \pi^*$ benzenoid band. The information as listed in this paragraph extracted from the work of Kuzniarska-Biernacka et al[67] will be used in assigning the bands in this work.

The spectra of undissociated 1A in both methanol and DMF showed the effect of solvent on the electronic spectra. In methanol, the Co→O band observed as a shoulder at 375 nm was almost not seen in DMF while Co→N observed at 290 nm blue shifted to 280 nm. The hypochromic shifts in the charge transfer band is attributed to the effect of changing from methanol to DMF. A band observed at 335 nm in methanol blue shifted to 327 nm in DMF.

In benzene, a shoulder band at 588 nm has been observed for bis(salicylaldehyde-aniline)cobalt(II) complex.[67] In the present work, a band at 592 nm was observed when 1A was dissolved in DMF. This band may be attributed either to intra-ligand transitions or charge transfer between the ligand and the cation.

Electronic absorption spectra of complexes 1B and 1C are similar but different from that of the complex formed from cobalt chloride, 1A. In methanol, three well resolved bands at 234 nm, 292 nm and 380-2 nm were observed in the spectra of 1B and 1C. The bands at 292 nm and 382 nm have been previously assigned as metal-ligand charge transfer arising from π-electron interaction between the metal and the ligand. This assignment has been made because Laporte-allowed transition occurs only on complex formation and is absent in the free Schiff bases.[67] The band around 382 nm has been assigned to Co→O,[67,70] while the band at 292 nm is assigned to Co→N.[67,70] In DMF, the absorption band at 234 nm was not observed because DMF absorbed in the region below 270 nm. However, the Co→O observed in methanol at 382 nm red shifted to about 400 nm while the Co→N at 292 nm blue shifted to 282 nm. Both the $CT_{Co\rightarrow O}$ and the $CT_{Co\rightarrow N}$ do not have the same position in the two solvents used for this study, as was similarly observed by Kuzniarska-Biernacka et al.[67]

5.6.1.2 Electronic spectra of complexes of ligands 2, 3 & 4

Having discussed the spectra results of ligand 1 and its complexes, the effect of introduction of a methoxy group into the 4- or 3- position of the phenyl ring is to be discussed. The effects of the aprotic and protic solvents on the spectra of the complexes are also discussed where applicable. Thereafter, the reflectance results are used to determine the geometry of the complexes.

The electronic spectra and diffuse reflectance data of ligand 2 and its complexes are listed in Table 4:68. In methanol, there are four clearly defined bands in the spectra of these complexes. The Co→O band appeared at 365 nm for complexes 2A, 2B and 2C respectively while the Co→N was observed at 290 nm in 2A but red shifted in B & C to 305 nm respectively. In addition to the metal-ligand charge transfer bands, two additional bands assigned as intramolecular bands appeared between 205-210 nm and 235-245 nm in the three complexes.[67] In DMF, the positions of the absorption maxima of the $CT_{Co\rightarrow O}$ band for three complexes are similar to their positions in methanol. The Co→N bands blue shifted in DMF. As observed by Kuzniarska-Biernacka et al.[67] this implies that the Co→N bands are more affected by the solvent; hence are depend on the acceptor number whereas the Co→O band does not depend on any solvent parameters. The shift in the electronic band is ascribed to the effect of the methoxy in the 4- position in these complexes. The results implies that addition of cobalt(II) to ligand 2 blue shifted the metal-ligand charge transfer bands, which signifies the driving of the systems towards enol-imine form.

The electronic spectra and the diffuse reflectance data of o-vaani (ligand 3) and its complexes are listed in Table 4:69. Four distinct bands are apparent in the spectra of the three complexes of ligand 3 in methanol. The $CT_{Co\rightarrow O}$ band for 3A appeared at 365 nm while those of 3B and 3C are seen at 395 nm respectively. The difference in $CT_{Co\rightarrow O}$ band is ascribed to the difference in geometry of these complexes. The $CT_{Co\rightarrow N}$ band appeared at 300 nm in complex 2A, while those of complexes 3B and 3C are seen at 300 nm and 285 nm respectively. The other two bands assigned to intramolecular ligand bands appeared at 205-210 nm and 235-245 nm respectively.

In DMF, two bands assigned to metal-ligand charge transfer are seen. The $CT_{Co\rightarrow O}$ band appeared at 362 nm while those of 3B and 3C were observed at 395 nm respectively. The $CT_{Co\rightarrow N}$ band blue shifted in the three complexes. While Co→N band for 3A appeared at 287 nm, those of 3B and 3C appeared at 290 nm and 294 nm respectively. This implies that the Co→N bands are more affected by the solvent; hence depend on the acceptor number[70] whereas the Co→O band does not depend on any solvent parameters.

Comparing the complexes of ligand 1 with those of ligand 2 and 3, the spectra results showed that the introduction of a methoxy into the 4-position blue shifted the Co→O bands while it red shifted the same band when the methoxy substituent was changed from 4-position to 3-position.

Complex 4A is an exception to the general formula of $M(HL)_2Cl_2$. It is a 1:1 ratio complex. In methanol, four bands were also seen. While the band at 280 nm is assigned the Co→N band, the band at 335 nm is assigned with less confidence because the complexes is not likely to chelate through the hydroxy group except by bridging. This implies that the azomethine nitrogen may be involved in the complexes formation. The other two bands at 230 nm and 205 nm are assigned as intramolecular bands. As expected, the change in solvent polarity saw the wavelength observed at 335 nm in methanol shifting to 316 in DMF.

Making use of component Gaussian band analysis, Kuźniarska-Biernacka, et al.[67] were able not only to deconvolute the charge transfer bands from intramolecular (i.e. the ligand) bands in the UV region, but were also able to deconvolute the components for the weaker spin forbidden transitions to doublet states from those for the spin-allowed d-d transitions in the near-infrared-visible region. For $Co(saani)_2$ in a tetrahedral environment the three spin allowed transitions occur at about 585 nm, at about 885 nm and at about 1 290 nm.[67] These are, respectively, the $^4A_2 \rightarrow {}^4T_1(P)$, the $^4A_2 \rightarrow {}^4T_1(F)$ and (possibly) the $^4A_2 \rightarrow {}^4T_2$ (or alternatively a low symmetry component of the $^4A_2 \rightarrow {}^4T_1(F)$ excitation).[40] The d-d absorbance at 585 nm is observed as a shoulder on the Gaussian arms of the first and second band (the charge transfer bands) in the UV,[67] and thus can be masked by the more intense intramolecular ligand transitions associated with the *N*-phenylsalicylaldimineato ion at 496 nm and 464 nm respectively.

In another development, Ashmawy et al. investigated cobalt(II) complexes with *N, N'*-ethylenebis(1-hydroxy-2-naphthylalkyleneimine) Schiff bases.[40] Three categories of complexes were determined: square-planar cobalt(II) species (based on the characteristic square planar band at 1 200nm);[71] pseudo-tetrahadral cobalt(II) complexes (based on absorption bands at 1 400 – 1 200nm, assigned to 'low symmetry' components of the second tetrahedral transition, 600 – 500 nm, assigned to $^4A_2 \rightarrow {}^4T_1(F)$ and 400 nm, assigned to $^4A_2 \rightarrow {}^4T_1(P)$, assignments similar for known tetrahedral bis(saliylidineiminato cobalt(II) complexes)[75] and pseudo-octahedral cobalt(II) complexes (based on absorption bands at 880-800 $^4T_{1g}(F) \rightarrow {}^4T_{2g}$ and 600-500 nm, assignment unable to be done with any degree of confidence).[72]

On the basis of the information from the reflectance spectra, it is possible to categorize all the isolated complexes into (pseudo)-tetrahedral, (pseudo)-octahedral geometry or even square planar. The assignments of the geometries is tentative, consequently, the use of octahedral or

tetrahedral is reserved for complexes that have been well studied, belonging to O_h and T_d point group, hence, the term pseudo-tetrahedral, pseudo-octahedral or distorted square-planar is used in describing the assignment.

Bamfield[69] reported the synthesis of cobalt chloride complex of *N*-phenylsalicylideneimine, the properties of which agrees with the properties of the complex designated 1A in this study. The microanalysis indicates that the complex comprises of three molecules of the ligand, two atoms of chlorine and one of cobalt. Based on the magnetic susceptibility and molar conductivity, the complex has previously been formulated as an octahedral cobalt(II) complex.[69] While agreeing with him that the complex can have octahedral geometry in solution because it ionizes and even far infrared results discussed in section 5.2.4.1 can be tentatively assigned an octahedral geometry to the complex, the diffuse reflectance spectra result discussed in this section proved otherwise. The diffuse reflectance spectra Figure 5:21 are used to illustrate this observation.

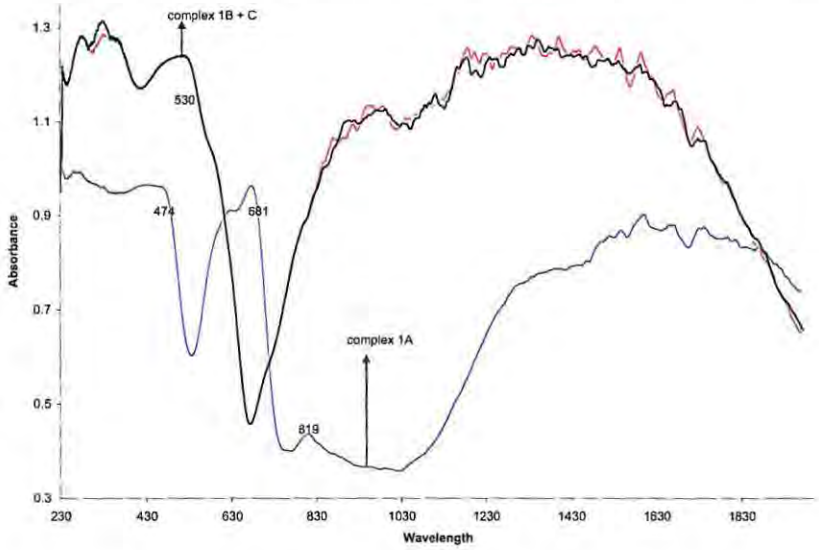

Figure 5:21 Diffuse reflectance spectra of complexes 3A and 3B + C

$[Co(salan)_2]$, 1B is widely studied and have been known to adopt tetrahedral coordination geometry.[67] The microanalysis, IR and the reflectance spectra reported here supported this geometry. The spectra of complex 1A and 1B + 1C show absorption bands at 1400-1200 nm, 600-500. The band at 1400-1200 can be assigned to low symmetry components of the second tetrahedral transition $^4A_2 \rightarrow {}^4T_1(F)$,[40] while the band at 600-500 nm is assigned to the $^4A_2 \rightarrow {}^4T_1(P)$ transition.[40] When the reflectance spectra of complexes 1B and 1C are compared with complex 1A, the observation was that the spectra curves are similar. The band shift in complex 1A shifted to higher wavelength. This is expected since chlorine is a weaker ligand relative to water. As a

result of this observation, in solid state, it is believed that 1A is pseudo-tetrahedral while in solution it can exist as octahedral because it ionizes as discussed earlier. A band at 819 nm was observed in ligand 1A. The appearance of a band in this region has been ascribed to octahedral complexes. Since the bands at 1400-1200 nm and 600-500 nm coupled with bands with considerable breadth and fine structure signify tetrahedral structure for this complex, the band at 819 nm may probably be a spin forbidden band.[64] Field of lower symmetry as well as large spin-orbit coupling of Co(II) are some of the reasons for the splitting observed in their spectra.[73] The band at ~ 819 nm has also been assigned to $^4A_2 \rightarrow {}^4T_1(F)$ by Shivankar et al.[74] using Orgel's publication[75] as a reference. In the same vein, Sacconi[76] et al. reported reflectance data for some tetrahedral complexes. One of their complexes showed three bands at 1299 nm, 892 nm and 556 nm. They claimed the bands are indicative of tetrahedral configuration. They further calculated the dipole moments of the complexes with the spectra to confirm the geometry.[76] Multiple absorptions do occur in the visible and near infrared region. This has been attributed to the low symmetry components of the crystal field and transitions to the doublet states.[77]

The complexes of ligands 2, 3 and 4 showed similar pattern of spectra curves as the complexes 1A, 1B and 1C signifying also distorted tetrahedral geometries. The ligand field splitting parameter varies systematically with the identity of the ligand, consequently slight shifts were observed as the ligands are varied. The appearance of band at 1140–1250 nm might be an indication of tendency of complexes 2A, 3A and 4A changing to square planar. The band at ~ 1176 nm was tentatively assigned as a spin-forbidden transition, and is said to be characteristic of the presence of planar low-spin cobalt(II).[78] The presence of 3- or 4-methoxy substituents probably contributed to the shift of the bands in the observed geometry. As observed in the reflectance spectra of the complexes of ligand 1 (saani), the reflectance spectra of 2A, 3A and 4A appeared at higher wavelength than those of the "B" and the "C" series. The band shift is expected since chlorine is a weaker field relative to water. For the complexes of the aniline-based ligands, the presence of a 3- or 4- methoxy substituent does not affect the tetrahedral geometry of the complexes but rather resulted in noticeable band shift.

5.6.2 Group 2: The electronic spectra of the complexes of the 1-aminonaphthalene-based ligands

This section discusses the effect of increasing the aromaticity on the electronic spectra of the complexes. From the spectra data of the group two ligands, it was observed that the wavelength

is red shifted relative to the group 1 ligands as a result of decrease in the difference energy level(s).

The electronic spectra and the reflectance data for the aminonaphthalene complexes isolated are listed in Tables 4:71- 4:74.

The solution UV for these series of complexes is similar to the ligands from which they are synthesised. Consequently, it is impossible assigning the few broad bands that are seen from their spectra curves. However, the effect of solvent was observed when methanol was replaced with DMF. There was blue shift of bands in DMF and lost of fine structures as observed earlier.

While the solution UV failed to produce distinct bands that can be used to differentiate the ligands from their respective complexes to enable easy characterization, the reflectance spectra provided useful information and the wealth of the information has been used to differentiate the geometries of the complexes. For instance, the presence of well structure absorption bands in the visible region with high intensity is an indication of tetrahedral geometry.[79]

Complexes 6A, 7A, 8A and 8C show absorption bands between 1400-1200 nm, 600-500 nm. The first band has also been assigned to low symmetry components of the second tetrahedral transition $^4A_2 \rightarrow {}^4T_1(F)$, while the well structured absorption band at 700-500 nm is assigned to the $^4A_2 \rightarrow {}^4T_1(P)$ transition. These bands with considerable breadth as well as the fine shape of the spectra are typical of distorted tetrahedral complexes.[79] The band at 820-835 nm present in these complexes may be assigned to spin forbidden transition or may also be assigned to $^4A_2 \rightarrow {}^4T_1(F)$ as discussed earlier. The spectra curves are similar to curves shown in Figure 5:21. The band around 800 nm may be used as a diagnostic band between a tetrahedral and a pseudo-tetrahedral complex.

Complexes 5C and 6C have been characterized as distorted square-planar as a result of a band at 1200 nm and the absence of any visible bands in the visible region or band at 880-800 nm which could be assigned to the low symmetry components of the octahedral $^4T_{1g}(F) \rightarrow {}^4T_{2g}(F)$ transition. The bands below 400 nm observed has been previously assigned to charge transfer band and internal ligand band.[76,80]

5.6.3 Group 3: The electronic spectra of the complexes of the 4-aminopyrdine-based ligands

The electronic spectra and the reflectance data for the 4-aminopyridine ligands and their corresponding isolated cobalt complexes will be discussed in this section. The effect of substitution of aniline with 4-aminopyridine will be examined. The discussion will also look at the effect of protic and aprotic solvent on the electronic spectra of the complexes. The diffuse reflectance data will be used to assign the geometry of the various complexes where possible

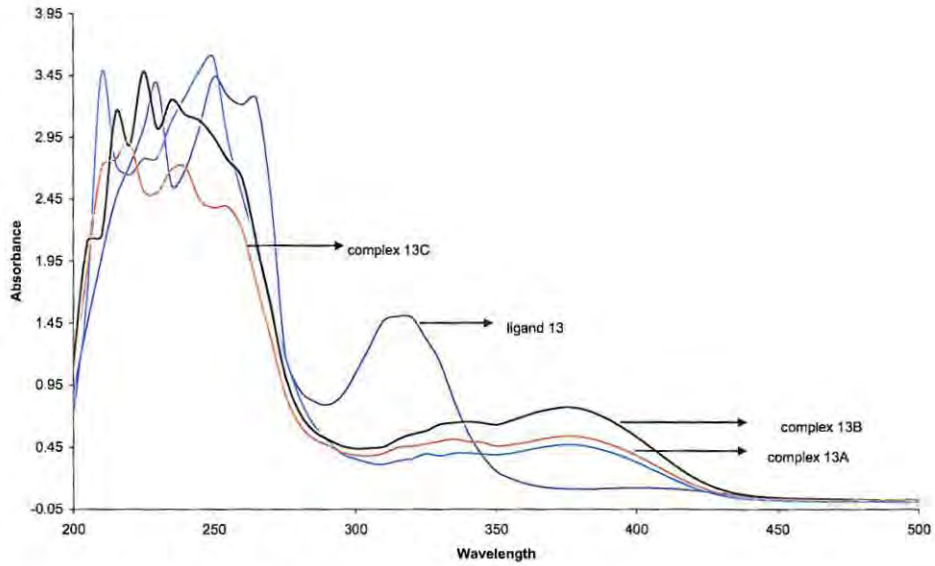

Figure 5:22 Sal4amp (ligand 9) and its complexes in methanol

The electronic spectra data of sal4amp (ligand 9) and its isolated complexes are listed in Table 4:75, while the spectra in methanol and DMF are shown in Figures 5:22 and 5:23 respectively. In DMF, two major bands are seen. The band at 382 nm is assigned to Co→O band and a weaker band at 328 nm assigned to Co→N band. In methanol, the Co→O band blue shifted and appeared at 375 nm while the Co→N band red shifted and was observed at 335 nm. It is interesting to note that the Co→N band red shifted by 7 nm when the solvent was changed from DMF to methanol while the Co→O band blue shifted also by 7 nm indicating less keto and more imine character. This observation is as a result of changing from strong aprotic solvent to strong polar protic solvent. In methanol, the higher energy region (below 260 nm) is the only region that has bands which differentiates the complex obtained from cobalt chloride, 9A from those of 9B and 9C complexes.

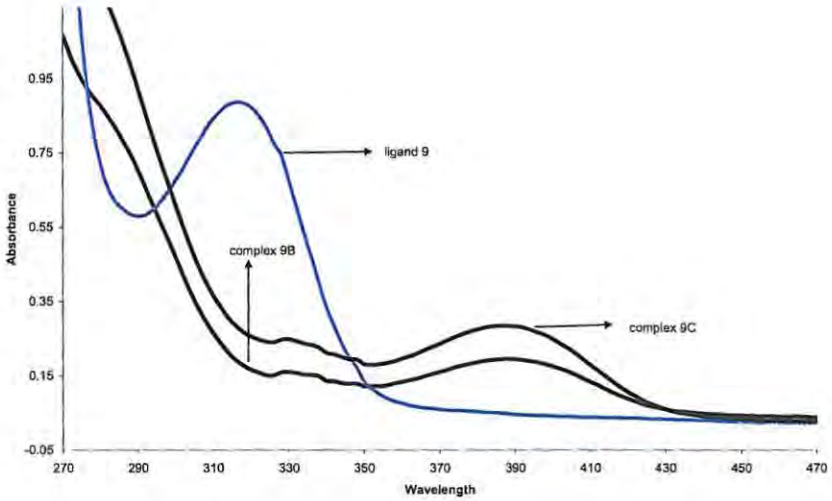

Figure 5:23 Sal4amnap (ligand 13) and its complexes in DMF

The electronic spectra and reflectance spectra data for p-van4amp and the complexes obtained from it are tabulated in Table 4:76. In methanol, there are four well resolved bands in the spectra curves of the three complexes of ligand 10 (pvan4amp). The bands at 360 nm and 355 nm have been assigned as the Co→O for 10A and 10B, 10C respectively. Other maxima observed at 240-5 nm and 205-15 nm may be assigned to intramolecular bands.[67]

The electronic spectra and the reflectance data of o-van4amp and is complexes are tabulated in Table 4:77. In methanol, three bands are seen at 220 nm, 265 nm and a broad band at 340 nm are seen from the spectrum of complex 11A. The absorption band at 340 nm is assigned to Co→O while the band at 265 nm is assigned to Co→N. In DMF, the Co→O appeared in the same region as in methanol but well resolved and was seen at 347 nm while the Co→N band red shifted. It shifted from 265 nm to 280 nm. This suggests methanol donates proton to ketone and causes blue shift of the band. For complexes 11B and 11C in methanol, a band assignable to Co→O appeared at 395 nm, while the Co→N was observed at 240-5 nm. The Co→N red shifted to 272 nm in DMF.

The electronic spectra and reflectance data of van4amp and its complexes are listed in Table 4:78. Four bands were observed in methanol for the complexes of ligand 12. The Co→O for the three complexes appeared at 355 nm while the Co→N bands were observed at 280-5 nm. In

addition to the charge transfer bands, two additional bands were seen in methanol at 340 nm and 305-315 nm. These bands may be due to intramolecular bands. In DMF solution, three bands were observed for all the three complexes. The Co→O appeared at ~ 345 nm while the Co→N appeared at 276 nm. The complexes 12A, 12B and 12C can not be differentiated using solution spectra.

The comparison of these series of complexes with aniline-bases complexes revealed that the replacement of aniline with the 4-aminopyridine shifted the absorption bands to higher energy, hence less keto-amine tautomers.

The general trends after chelation are that the complexes have almost the same absorption bands in both solvents. The similarities in wavelengths are evidence of complex formation. Chelation is known to considerably reduce the polarity of the metal ion because of partial sharing of its positive charge with the donor groups (Schiff bases) and possible π electron delocalization over the whole chelation ring. This idea is known as Tweedy's chelation theory.[81]

The reflectance spectra for the 4-aminopyridines-based complexes presented interesting geometric information. On the basis of the information from their reflectance spectra, the complexes have been characterised into three categories. The spectrum of complex 9A exhibits two bands in the visible region at 641 nm and 572 nm. This has been assigned to the $^4A_2 \rightarrow {}^4T_1(P)$ tetrahedral transition. The absorption bands at 1 400-1 200 nm is also assigned to low symmetry components of the second tetrahedral transition $^4A_2 \rightarrow {}^4T_1(F)$. While 9A is pseudo-tetrahedral, 9B and 9C may be distorted square-planar due to the presence of a band at 1200 nm and the absence of well-structured band in the visible region.[71] The spectra of these complexes is shown in Figure 5:24.

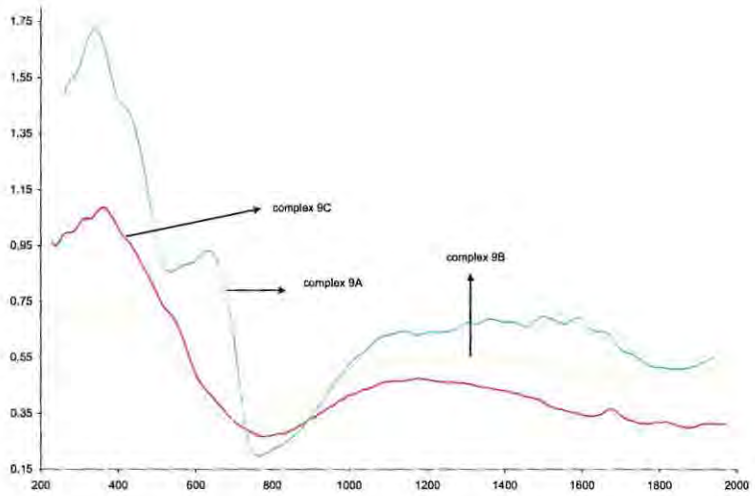

Figure 5:24 Diffuse reflectance spectra of ligand 9 (sal4amp) complexes

Complex 10A exhibits a band at 1 200 nm. This band is characteristic of a square-planar cobalt(II) complexes.[71] The band at 822 nm is assigned to spin forbidden band. However, Sacconi[82] assigned a square-pyramidal structure to a complex with bands at 1493 nm, 877 nm and 595 nm. Since octahedral and square planar complexes have a center of symmetry, coupling of vibrational and electronic motions may be blamed for the intensity observed at 822 nm. The slightly distorted octahedral and square planar metal complexes may have a fractional part of a d-d transition "allowed" which may be responsible for intensity in many cases.[83] The absence of well structured bands in the visible region couple with the appearance of weak band at 815 nm has been used as evidence for assigning pseudo-octahedral complexes to10B and 10C respectively. The band at 812 nm may be assigned to the low symmetry components of the octahedral $^4T_{1g}(F) \rightarrow {}^4T_{2g}(F)$ transition.

The reflectance spectra data for the complexes 11A, 11B and 11C indicate a pseudo-octahedral geometry. The appearance of bands at 380-390 nm, 1008 – 1078 nm, 1453-1477 nm and a weak band at 500 nm may be used as evidence for the geometry suggested.

The reflectance spectrum data for 12A indicate that the complex also has tetrahedral geometry. Two well-structured bands in the visible region at 602 nm and 489 nm were observed. This band have been assigned to the $^4A_2 \rightarrow {}^4T_1(P)$ tetrahedral transition because they are well structured and have high intensities. The band at 373 nm can be assigned to metal-ligand charge transfer[84] while the band at 1 400-1 200 nm is assigned to the second tetrahedral transition $^4A_2 \rightarrow {}^4T_1(F)$. For the

B and C analogues, the appearance of two well structured bands at 578 nm and 498 nm in the visible region, coupled with the band at 1 400-1 200 nm assigned to the second tetrahedral transition $^4A_2 \rightarrow {}^4T_1(F)$ can be use as evidence for the suggested tetrahedral geometries for the complexes. The band observed below 360 nm has been assigned to charge transfer.[84] Although 12A, B and C are tetrahedral, the absorptions of complex 12A appeared at higher wavelength than those of the B and C analogues. This is expected since chlorine is a weaker ligand relative to water in the spectrochemical series.

5.6.4 Group 4: The electronic spectra of the complexes of the 3-aminopyridine-based ligands

The solution and diffuse reflectance spectra data of 3-aminopyridine-based complexes are listed in Tables 4:79-4:82. This section examines the effects of replacement of aniline with 3-aminopyridine. The behaviour of these complexes is compared with the 4-aminopyridine analogues where necessary.

In methanol, four bands are apparent in the spectra of the three complexes of ligand 13 (sal3amp). While the Co→O for 13A appeared at 380 nm, those of 13B and 13C appeared at 410 nm and 405 nm respectively. The Co→N for 13A appeared at 285 nm while those of 13B and 13C blue shifted. This result implies that the geometry for 13A is different from the geometry of 13B and 13C respectively. The other bands in seen below 260 nm in methanol have been assigned as intramolecular bands.

In methanol, the Co→O for 14A appeared at 360 nm while 14B and 14C show Co→O absorption band at 375 nm. The Co→N appeared at 285 nm for complex 14A while Co→N for the B and C analogue appeared at 275 nm respectively.

For the complex 15A, the Co→O band appeared at 390 nm in methanol, while those of the B and C analogue red shifted. The Co→O band for complexes 15B and 15C appeared at 400 nm respectively. While the Co→N band appeared at 285 nm for complex 15A, it appeared at 275 nm and 280 nm for complexes 15B and 15C respectively. The other bands at 205 nm and 240 nm have been assigned to intramolecular bands.

For the complexes 16A and 16C in methanol, the Co→O band appeared at higher energy relative to the other complexes in this series. The Co→O absorption band for 16A appeared at 335 nm while that of 16C appeared at 345 nm. The Co→N band for complexes 16A and 16B appeared at 285 nm and 265 nm respectively.

The general trend observed in the solution spectra for the 3-aminopyridine complexes is that the Co→O absorption bands for the "A" complexes appeared at lower energy while their Co→N bands appeared at higher wavelength relative to the "B" and "C" analogues. It was also observed that replacement of aniline favours keto-amine formation. However, the presence of a methoxy substituent in 4-position (complexes 14A, 14B and 14C) of the phenyl ring cause the shift to higher energy, hence less of the keto-amine tautomers. The shift to higher energy was more pronounced in complexes 16A and 16C due to the hydroxy and methoxy substituent in 4- and 3-positions respectively.

When this series of complexes are compared with aniline-based complexes, the observation is that their Co→O appeared at higher wavelength than those of aniline-based while Co→N appeared at lower energy. There appearance of Co→N at higher energy relative to the aniline-based complexes can be attributed to the effect of the withdrawing ability of the pyridine nitrogen. The Co→O band for this series of complexes appeared at higher wavelength that those of the 4-aminopyridine. This observation is ascribed to the different effects of pyridine nitrogen in 4- or 3-position respectively. In DMF, fine structures were lost as expected due to polarity. In addition to the lost in fine structures, slight shifts of bands to lower energy were observed.

From the reflectance spectra curves, it was possible to differentiate the tetrahedral complexes 13A, 14A, 15A and 16A from their octahedral complexes "B" and "C" analogues. The presence of well-structured bands in the visible region of compounds 13A, 14A, 15A and 16A at 646 nm – 602 nm assigned to the $^4A_2 \rightarrow {}^4T_1(P)$ tetrahedral transition is used as a characteristic band that differentiates them from their B and C analogues. In addition, the appearance of bands at 1400-1200 nm assigned to the second tetrahedral transition $^4A_2 \rightarrow {}^4T_1(F)$ is also another evidence for this assignment of this geometry.

The complexes 13B and C have a low intensity shoulder band at 520 nm typical of pseudo-octahedral complexes and another band at 1065 nm while the charge transfer band appeared at 372 nm.

The reflectance spectra of 14B+C, 15B+15C and 16C are similar to the spectra of all the other "B+C" complexes that have been discussed. The characteristic low intensity in the near infrared region coupled with the absence of well-structured bands in the visible region as well as the presence of a band around 370 nm are used as the evidence to support their pseudo-octahedral geometries. In addition to the mentioned area of absorptions, they all have a band at around ~1067 nm, a region assignable to spin-forbidden, and a characteristic of planar low-spin cobalt(II).[78] The band at ~ 1067 nm may be one of the expected transitions of cobalt(II) ion or fractional part of a d-d transition "allowed".[83]

When the complexes 13A, 14A, 15A are compared with 1A, 2A, 3A, we observed that the well-structured bands for the complexes in this group appeared at lower wavelength that those of aniline-based complexes. The reason for the shifting of the absorbance to higher energy can be ascribed to the effect of the nitrogen in the pyridine ring. It is evident that the presence of nitrogen in the pyridine ring makes the Schiff bases interact more with the d-orbitals and hence cause a greater energy difference between the e_g and the t_{2g} orbitals than the electrons of the aniline-based Schiff bases. This also implies that aniline is weaker ligand relative to the 3-aminopyridine. From the spectrochemical data, it has been shown that orbital contributions in tetrahedral Co(II) complexes decrease as the ligands vary from I^- toward CN^-, i.e., as the intensity of the ligand field increases.[84]

5.6.5 Group 5: The electronic spectra of the complexes of the 3-aminomethylpyridine-based ligands

This section and the following section examine the effect of inserting methylene between the azomethine and the pyridine ring on the electronic spectra of 2- or 3-aminomethylpyridine. The ligands obtained from this series contain three atoms capable of coordinating to cobalt, but the steric condition does not favour them binding in this arrangement. The reflectance spectra are used to determine the geometry of the various complexes.

The list of solution as well as the reflectance spectra data for 3-aminomethylpyridine-based complexes is presented in Tables 4:83– 4:86.

In methanol, the Co→O for 17A appeared at 390 nm while those of 17B and 17C appeared at 380 nm respectively. The Co→N for 17A was seen at 240 nm while those of 17B and 17C red shifted and appeared at 270 nm. The behaviour of these complexes in DMF is similar to their behaviour in methanol. This may imply that protonation is not important in determining the keto-imine tautomer in these complexes. The curves from the diffuse reflectance spectra were used to further differentiate 17A from 17B and 17C. Like most of the complexes obtained from cobalt chloride, 17A has well-structured bands with high intensity in the visible region. 17A has well structured band at 620 nm. This band has been assigned to the $^4A_2 \rightarrow {}^4T_1(P)$ tetrahedral transition. A band at 1400-1200 nm assigned to the second tetrahedral transition $^4A_2 \rightarrow {}^4T_1(F)$ was also observed. The information from the diffused reflectance showed that they may be tetrahedral or distorted tetrahedral in nature while 17B and 17C may be octahedral complexes. The geometry of 17B and 17C may be octahedral because of the absence of well structure bands in the visible region.[79] This is shown using the spectra in Figure 5:25 below.

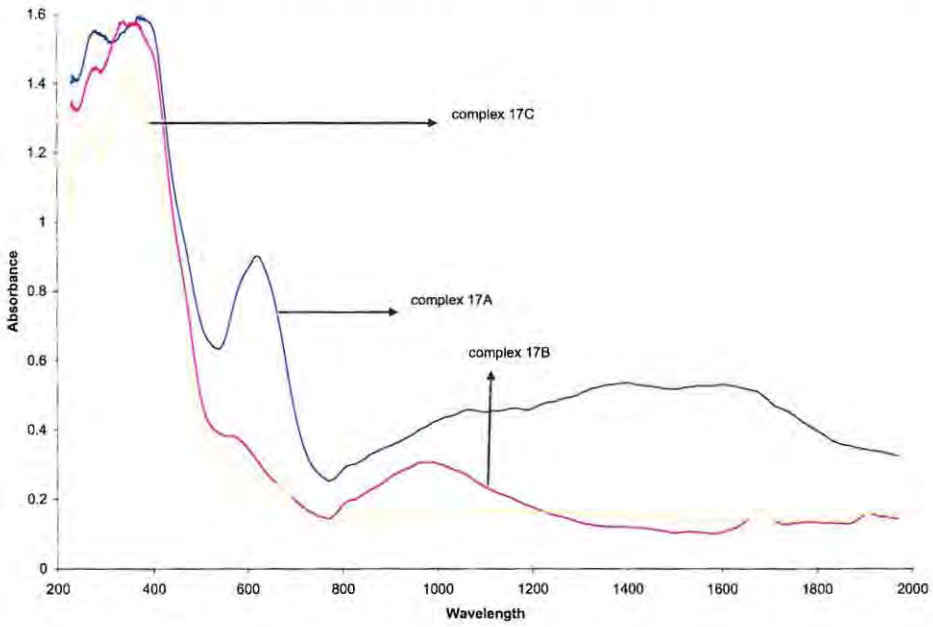

Figure 5:25 Reflectance spectra of ligand 17 (sal3pico) complexes

In methanol, the Co→O for 18A appeared at 360 nm while those of the 18B and 18C were seen at 365 nm. The Co→N appeared at 245 nm in complex 18A while it was seen at 265 nm in the complexes. On comparison of these three complexes with 17A, 17B and 17C respectively, it was observed that absorption bands blue shifted. This effect is ascribed to the effect of methoxy in the *para*-position of the Schiff base of the complexes. The effect of the methoxy is well pronounced on the Co→O absorption bands.

The reflectance spectra for 18A showed five well resolved bands. The absorption band at 330 nm is assigned to charge transfer while two bands appeared in the visible region. The bands at 622 nm and 538 nm in the visible region are well structured. These bands have been assigned to the $^4A_2 \rightarrow {}^4T_1(P)$ tetrahedral transition. The band at 913 nm and 1400-1200 nm may be assigned to the second tetrahedral transition $^4A_2 \rightarrow {}^4T_1(F)$. The absence of the well structured bands in the visible region, presence of a band at 375 nm and a band at 998 nm is an indication that 18B and 18C might be octahedral or distorted octahedral. The band at 998 nm is assigned to $^4T_{1g} \rightarrow {}^4T_{2g}$.

The solution spectra of 19A, 19B and 19C in methanol showed four bands in the UV region. The Co→O for complex 19A appeared at 385 nm while those of the 19B and 19C appeared 395 nm. While the Co→O for 19B and 19C are red shifted relative to the Co→O of 19A, their Co→N appeared at higher energy at 245 nm. The Co→O for 19A appeared at 265 nm. Other absorbance maxima have been assigned to intramolecular bands.

The reflectance spectra data showed that complex 19A may be tetrahedral due to the presence of well-structured band at 597 nm in the visible region. The band at 373 nm is assigned to charge transfer. However, the insertion of methylene between pyridine ring and the azomethine probably resulted in the second tetrahedral $^4A_2 \rightarrow {}^4T_1(F)$ transition appearing at 1000-1400 nm instead of 1400-1200 nm. A band at 816 nm was also observed. The reflectance data of 19B and 19C revealed that the complexes have octahedral geometry. This is due to the absence of well-structured band in the visible region as well as the presence of low intensity bands in the near infrared region as illustrated by the reflectance spectra of the complexes depicted in Figure 5:26.

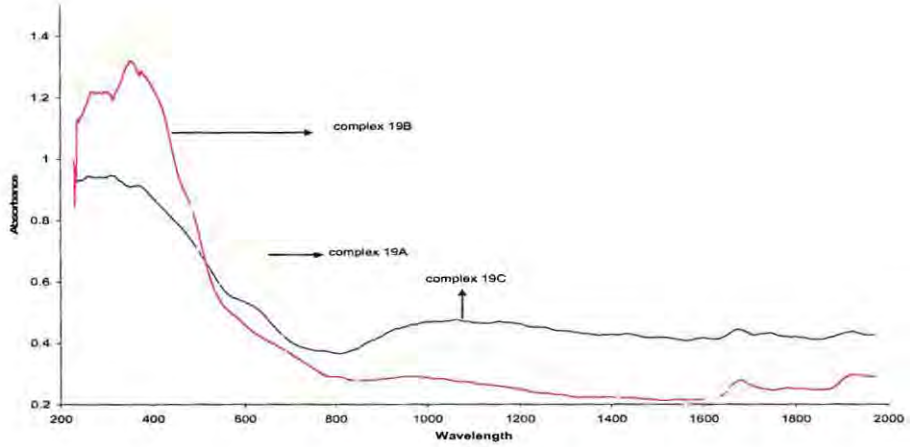

Figure 5:26 Diffuse reflectance spectra of ligand 19 (ovan3pico) complexes

The solution spectra of 20A showed the Co→O appearing at 342 nm while that of 20B appeared at 344 nm. The Co→N for 20A appeared at 246 nm while that of the "B" analogue appeared at 243 nm. The appearance of the absorption bands at higher energy is ascribed to the effect of *para*-hydroxy or the *meta*- methoxy substituents. In DMF, the fine structure observed in methanol was lost. It was not well resolved, hence difficult making good comparison with the methanol spectra. The reflectance spectra data of 20A indicate a tetrahedral geometry while that of 20B showed distorted octahedral geometry using the evidences discussed above.

The comparison of complexes 1A, 9A, 13A and 17A, Figure 5:27 showed the effect of using various ligands. The band in the visible region shifted to lower energy when aniline was substituted by the 3 or 4 amino- or 3-aminomethylpyridine. This was the general trend observed within and across the groups. This is an indication that the aminopyridines and the aminomethylpyridines are stronger ligands than the aniline.

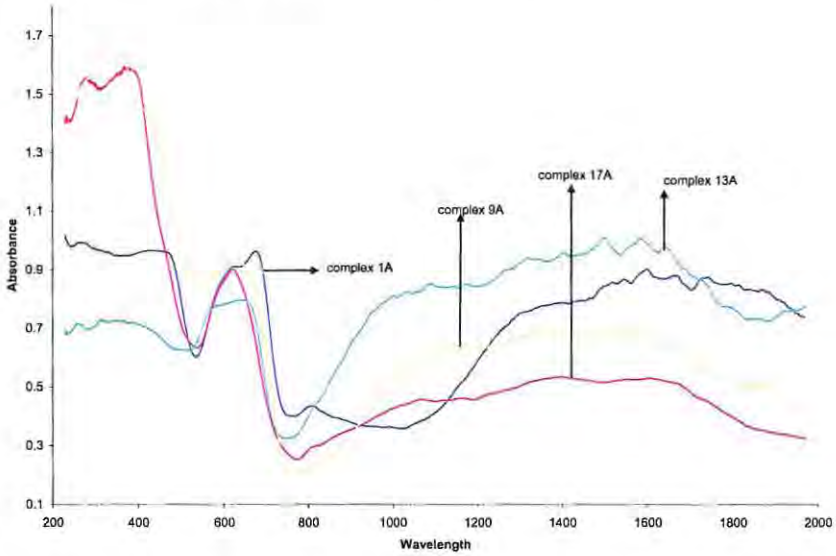

Figure 5:27 comparison of diffuse reflectance spectra of some tetrahedral complexes

5.6.6 Group 6: The electronic spectra of the complexes of the 2-aminomethylpyridine-based ligands

This section examines the effect on the electronic spectra of the isolated complexes of replacing 3-aminomethylpyridine with 2-aminomethylpyridine. The spectra data will be use to confirm whether introducing the 2-aminopyridine shift the equilibrium to enol-imine or keto-amine tautomer. Thereafter, the reflectance spectra data will be used to assign geometries where possible.

Yamada and Yamanouchi[85] synthesised metal complexes of Schiff bases obtained from substituted salicylaldehyde and 2-aminopyridine derivatives. The complexes were found to be mostly tetrahedral irrespective of the nature of the substituent on the phenyl ring. This was our observation for the complexes obtained from salicylaldehyde or its derivatives with aniline. The insertion of methylene between the C=N and pyridine rings probably makes the behaviour of 2-aminopyridine complexes reported by Yamada and Yamanouchi[85] to be slightly different from the complexes of the 2-aminomethylpyridine-based reported in this work.

The spectra of the complexes in this series showed the Co→O absorption maxima for the "A" series of complexes appearing at slightly higher energy than the "B" and "C" analogues. For instance, the Co→O for 21A appeared at 380 nm while those of 21B and 21C appeared at 395 nm respectively. The Co→N for 21A was observed at 243 nm while those of "B" and "C" appeared at 250 nm respectively. The observed trend is in line with the orderly variation in energy differences upon changing the ligand in metal complexes.

The Co→O for 22A, 23A and 24A appeared at 352 nm, 400 nm and 345 nm while their Co→N were observed at 251 nm, 240 nm and 248 nm respectively. While the replacement of 2-aminomethylpyridine shifts the equilibrium towards the formation of keto-amine tautomers, substituents on the phenyl ring as well as the geometry of the complexes determines the position of the equilibrium. For instance, the presence of a methoxy in the *meta*-position shifted the absorption bands above 400 nm with the "B" and "C" analogues appearing at slightly higher wavelength than their "A" analogue. The presence of hydroxy or methoxy groups in the 4-position of the phenyl ring resulted in the shifting of the absorption maxima to enol-imine tautomer. The Co→O for the 22B and 22C appeared at 390 nm, while those of 23A and 23B red shifted and was observed at 405 nm. The Co→O for complex 24B appeared at 365 nm. The observed wavelength is determined by the ability of ligands with have appreciable π –donor properties. Most ligands have similar sigma-bonding abilities, while possessing widely ranging π-donor and π-acceptor properties. The difference in energy is largest for strong π-acceptor ligands and vice versa.

The Co→N for the complexes in this series appeared between 255-240 nm. The absence of well-resolved spectra from DMF coupled with absorbance of DMF in the region below 270 nm made it impossible for us to discuss solvent effect on this series of complexes. However, it was

observed that the absorption maxima observed around 400 nm in methanol were absent or too weak to be seen in DMF.

This series of complexes when compared with 3-aminomethylpyridine revealed that replacement of 3-aminomethypyridine with 2-aminomethylpyridine causes red shifting of the bands. This implies that the insertion of the methylene allows the protonation of the azomethine nitrogen more in 2- aminomethylpyridine than the 3- analogues.

The two series of the aminomethylpyridine (group 5 and 6) complexes absorbed at higher wavelength than the aniline-based ligands. This is attributable to the insertion of methylene between the pyridine and the azomethine nitrogen, which resulted in the destruction of the conjugation between the pyridine ring and the substituted phenyl ring.

The reflectance spectra for this series of complexes is ambiguous, as the complexes have potential of being octahedral, tetrahedral or other geometry due to the presence of azine nitrogen in the 2-position. The resolution of the spectra agrees with the octahedral geometry as a result of the presence of absorption bands between broad 500-700 nm. However, the high intensity of these bands creates a doubt in assigning the octahedral geometry for the complexes in this series. The presence of bands at 826-860 nm may also suggest octahedral geometry, since that region as be assigned to the low symmetry components of the octahedral $^4T_{1g}(F) \rightarrow {}^4T_{2g}(F)$ transition.[40] As highlighted above, the high intensity of the bands for these complexes might also indicate a tetrahedral geometry.

5.7 NMR spectroscopy of the Schiff bases

The keto-amine enol-imine tautomer equilibrium is sensitive to the physical state, the nature of solvent and to the electronic effects of substituents. The azomethine proton and enol proton chemical shifts can be used to evaluate the position of the keto-amine enol-imine tautomer equilibrium of Schiff bases. Any significant presence of the keto-amine tautomer is expected to split the methine proton, with the concomitant loss of the OH proton. The positions of the chemical shifts are also sensitive to the electronic effects of substituents, and these may be correlated with the Hammett substituent parameters[35,86-7] Any significant presence of the keto-amine tautomer is also expected to be reflected in the aromatic protons, with the quinoidal form undergoing down field shifts.[88] However, with the pyridyl protons undergoing down field

shifts,[88] the aromatic region is not as simple in interpreting the tautomer equilibria as is the previously mentioned chemical shifts. Similar differentiation between the aromatic and quinoid forms should be noticeable in the ^{13}C NMR spectra.[88] The NMR spectra were all run in$CDCl_3$ to permit the examination of a possible correlation between the Linear Free Energy Relationship (σ) and the chemical shifts.

5.7.1 Group 1: The aniline-based Schiff bases

For salicylaldimines the alkyl amine derivatives have been known to present more keto-amine in polar solutions than do the aryl derivatives[89] Indeed, the aryl based salicylaldimines have long been recognised as containing the enol-imine tautomer only, even in polar solvents.[6,90-1] For various substituted *N*-aryl salicylaldimines the chemical shifts for O<u>H</u> were observed between δ13.46 – 11.83, and singlets for N=C<u>H</u> occur between δ8.70-8.35.[42] With the benzalanilines the aniline moiety is not planar with the *trans*-benzalamino skeleton.[87] This means that there is not complete π conjugation throughout the whole molecule, and that substitution on either ring will influence the azomethine proton to different extents, both in terms of the chemical shifts, and in terms of the tautomer equilibrium. Two groups of researchers[86-7] have shown that the electronic structure of the azomethine group is more sensitive to substitution in the benzaldehyde ring than in the aniline ring, with an electron donating substituent causing a small shift to higher field of the azomethine proton by increasing electron density on the carbon atom. [86-7]

Using the solid state NMR it was observed that electron donating groups favour the enol-imine tautomer, while electron withdrawing favour the keto-amine[92] This effect however was considered less significant in solution[92] accounting for the dominance of the enol-amine in solution at room temperature for the aryl salicylaldimines. In contrast, the presence in the solid state of both the enol-imine and keto-amine tautomers were identified for salicylideneaniline derivatives, for example by the appearance of both the phenol ring *C*-2 at δ149 (enol) and its down field shifted companion at δ 168 (quinoid).[92]

For aryl salicylaldimines the dominance in solution, at room temperature, of the enol-amine is regarded by Dudek and Dudek[90] to be the exception rather than the rule. They state that the better approximation would be to regard all phenols with strong hydrogen bonds as quinoids, rather than as benzene derivatives.[90] This could make the behaviour of the vanillin-based Schiff bases investigated in this work different in polar solvents to those in which the hydroxyl moiety occurs in position 2.

The NMR data for the four aniline based Schiff bases studied in this work are presented in Table 4:91 Only the NMR data for *N*-salicylideneaniline (saani) was found to have been previously reported in the literature.[93] The reported ^{1}H NMR ($CDCl_3$) shows a singlet (1H) at 8.75 for the ketimine C<u>H</u>, and a singlet (1H) at δ 13.2 for the O<u>H</u>.[93] For the ^{13}C NMR, the ketimine H*C*=N has been reported at δ 162.8 ($CDCl_3$).[93] These agree with this study's findings.

Additional comments can be made; the salicylaldimine hydroxyls are generally broad. The relative acidity of the hydroxyl proton can be judged by its chemical shift. Introduction of the methoxy group to the salicylaldimine results in a slight increased acidity and a downfield shift for the O<u>H</u> by δ = 0.45 – 0.55. The vanillin based Schiff base is the least acidic (δ = 6.14), and intramolecular proton transfer to the imine is not favoured for the hydroxyl group in the *para* position. As a consequence the ^{13}C chemical shift for the hydroxyl containing carbon is noticeably up-field compared with that for the deshielded p-vanillin salicylaldimine derivative (δ =164.0). This difference is similarly noticeable in the parent aldehydes (*C*-4: δ = 152.3 for vanillin *cf.* *C*-2: δ = 164.99 for p-vanillin.[94] There is a noticeable correlation between the Linear Free Energy Relationship (σ) and the ^{1}H chemical shift. This is discussed in more detail below.

5.7.2 Group 2: The 1-aminonaphthalene-based Schiff bases

While several studies have made use of a naphthalene ring system for the aldehyde precursor of the Schiff base[62, 95-6] there appears to be no study in the literature that employs it for the amine precursor.

The NMR data for the four 1-aminonaphthalene based Schiff bases studied in this work are presented in Table 4:92

Due to steric factors the naphthyl moiety is unlikely to be planar with the benzene ring. Consequently delocalisation of the benzene π system is unlikely to extend into the naphthyl system. It is possible though that it could extend as far as the imine system. For this to occur, the position of keto-amine/ enol-imine tautomer equilibrium will depend on the relative acidity of the hydroxyl group, and on the basicity of the imine nitrogen and its ability to act as a suitable proton acceptor. In the absence of a literature value of pK_a for the Schiff base, comparison of the aromatic amine values will give an idea as to the relative basicity of the imine nitrogen. The

reported pK_a (at 20°) for aniline is 4.74 and for 1-aminonaphthalene is 4.16, very similar.[97] Consequently the naphthyl derivatives should follow the behaviour of their aryl analogues, and be predominantly in the enol-amine form. The present study shows this to be true.

A basic side chain moiety in azole condensed quinoxalines alters the tautomeric ratio between the enamine and methylene imine forms in favour of the enamine.[98] The present study investigates the role of the nature of the amine on the keto-amine/ enol-imine tautomer equilibrium in the present series of Schiff bases. The presence of the pyridine ring makes the imine nitrogen a stronger base. This induces stronger hydrogen bonding, and a possible shift in the tautomer-equilibrium compared to the aromatic amines.[95] In addition, substituents on the amine component of the Schiff base can have a greater electronic influence on the azomethine group when compared with those of the aromatic amines, with strongly electron donating groups stabilizing the keto-amine tautomer. [95] The occurrence of the keto-amine tautomer for pyridine based salicylaldehydes has been inferred form the UV spectra.[99] In a series of substituted 3-[(2-pyridinylimino)methyl]-2-naphthalenol, the keto-amine tautomer dominates in all except the strongly electron withdrawing NO_2 substituted analogues. In $CDCl_3$ the keto-amine (^1H NMR) occurs as a doublet (with a coupling constant, which is solvent dependant, of 6-8Hz) at δ 9.96 ± 0.06, and the OH is observed as broad at δ 15.56± 0.15.[95]

5.7.3 Group 3: The 4-aminopyridine based Schiff bases

The synthesis of only the Schiff-base of salicylaldehyde with 4-aminopyridine has been previously reported.[6]

Aminopyridines are weak bases and they can exist in neutral and protonated form at physiological pH.[101] They are bioactive *N*-heterocyclic tertiary amines, and act by increasing the strength of the nerve signal through blocking of the voltage-dependent K^+ channel. The protonated form is the active species.[100] With $pK_{a(py)}$ for the free 2-, 3-, and 4-aminopyridine of 6.82, 5.94, and 9.29, respectively,[101] the 4-aminopyridine is the most likely of the pyridine-based Schiff bases investigated here to be protonated at the pyridine nitrogen site.

With a $pK_{a(NH2)}$ of 6.1 for 4-aminopyridine,[6] the 4-aminopyridine based salicylaldimine is expected to have an equilibrium more shifted to the ketoenamine than the aryl amines. For the delocalisation of the π system to occur over the whole molecule the pyridine ring needs to be

planar with the benzene ring. If the pyridine is non-planar, the delocalisation extends only as far as the imine nitrogen. There is no reported crystal structure of any of the 4-aminopyridine based Schiff bases, and possible conformers that may exist in solution are shown below.

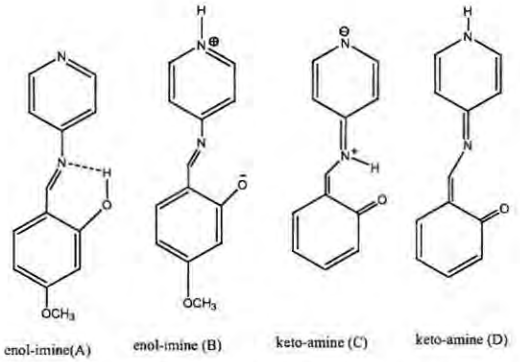

Scheme 5:10 The possible conformers of the 4-aminopyridine

The NMR data for the four 4-aminonpyridine based Schiff bases studied in this work are presented in Table 4:93

Császár et al.[100] have reported the ^{1}H NMR for, amongst others, the various aminopyridines of salicylaldehyde. They noted that they did not observe the existence of tautomers in solution by IR and NMR, but ascribed this to the solvents employed.[99] In the present work, the enol-imine tautomer is observed to dominate as indicated by the azomethine proton chemical shift (δ = 8.49, singlet, integrating for1H). The integration of the hydroxyl proton, however, suggests that there exists in solution an equilibrium between the protonated hydroxyl (A) and protonated pyridine nitrogen (B) species. In the methoxy-substituted salicylaldimines the presence of the electron donor appears to favour the keto-amine tautomer, as evident by the appearance of the deshielded quinoid carbon at δ = 194.4 (p-vanillin) and at δ = 196.6 (o-vanillin) and the relatively shielded azomethine carbon {N-*C*(H)=C} at about δ = 151. Again there appears to be an equilibrium between the protonated imine and pyridine nitrogens. The existence of the conformers is reflected in the splitting of NMR chemical shifts for both the methoxy proton and carbon (O-*C*H$_3$). The vanillin based Schiff base with 4-aminopyridine is insoluble in $CDCl_3$. This means that no valid correlation can be made of the chemical shift, δ against the substituent parameter σ. The present NMR study suggests that the 4-aminopyridine salicylaldimines may offer an opportunity to examine, by NMR spectroscopy, the tautomer equilibria in a variety of solvents. Such a study, though, is beyond the scope of the present work.

5.7.4 Group 4: The 3-aminopyridine based Schiff bases

With a $pK_{a(NH2)}$ of 1.5 for 3-aminopyridine[6] the 3-aminopyridine based salicylaldimine is expected to have an equilibrium less shifted to the keto-amine than their 4-aminopyridine based analogues. With $pK_{a(py)}$ of 5.94 for 3-aminopyridine,[101] in the Schiff bases the pyridine nitrogen site would likely be the receptor site in any proton transfer.

The NMR data for the four 3-aminopyridine based Schiff bases studied in this work are presented in Table 4:94

The ^{1}H NMR of 3-aminopyridine based salicylaldimine only, has previously been reported; the chemical shifts δ 8.9 (s, C<u>H</u>=N) and 12.75 (s, O<u>H</u>)(acetone-d_6) suggests that only the enol-imine tautomer exists in solution. The present study supports this conclusion, and finds this to be true for all of the Schiff bases with 3-aminopyridine.

5.7.5 Group 5: The 3-aminomethylpyridine-based Schiff bases

Only the 3-aminomethylpyridine-based salicylaldimine has previously been reported.[6,55] For the 3-aminomethylpyridine-based salicylaldimine in the solid state the pyridine is non planar with the benzene ring, and the delocalised benzene π involves only the imine and the methane groups.[6] Unlike 2-aminopyridine based salicylaldimine discussed below, on forming the Schiff base the basicity of the pyridine nitrogen decreases and the basicity of the hydroxyl increases, suggesting that the non-planar conformation exists predominantly in solution.[55] As has also been noted for the free pyridine[102] for the Schiff base the pyridine nitrogen $\{pK_{a(py)} = 5.91$ [55] is in fact less basic than the imine nitrogen$\{pK_{a(NH2)} = 9.23\}$[55]. This means that the imine nitrogen would be the receptor site in any proton transfer, allowing the splitting of the methine proton to be used to indicate any presence of the keto-amine tautomer. The <u>H</u>C=N chemical shift was reported in $CDCl_3$ as a singlet at δ 8.48, the OH at δ 13.06 indicating[6] the predominance of the enol-imine. This was confirmed by the lack of displacement of the aromatic protons typical of the quinoid form.[6] Using UV spectroscopy, Galić et al.[55] noted that for salicylaldehyde Schiff bases with 2-aminopyridine and 3-aminomethylpyridine (amongst others) in non-polar solvents the enol-imines were predominantly present. However, in polar solvents rapid tautomeric interconversion of enol-imines to keto-amines as well as slow hydrolysis were noted.[55] The tendency to tautomeric interconversion was significant in the case of the 3-aminomethylpyridine-base Schiff base, whereas in the case of other Schiff bases it was very low.

The NMR data for the four 3-aminomethylopyridine based Schiff bases studied in this work are presented in Table 4:95.

5.7.6 Group 6: The 2-methylpyridine-based Schiff bases

The structure of the 2-aminomethylpyridine-based salicylaldimine has previously been reported.[6] No NMR studies were found in the literature.

For the 2-aminomethylpyridine-based salicylaldimine in the solid state the pyridine is planar (within 4°) with the benzene ring,[6] however lack of the quinoid ring skeletal stretches (1530 cm^{-1}) in the infrared spectra indicates the enol-imine tautomer dominates, even in polar solvents.[6]

The NMR data for the four 3-aminometylpyridine based Schiff bases studied in this work are presented in Table 4:96.

Only the 2-aminopyridine based salicylaldimine has previously been reported. [55]
With a $pK_{a(NH2)}$ of 7.6 for 2-aminopyridine, [55] the equilibrium is expected to be most shifted to favour the keto-amine of the pyridine based systems. The pyridine nitrogen $\{pK_{a(py)} = 7.09\}$[58] is more basic than the free pyridine $\{pK_{a(py)} = 5.34\}$[55], and is protonated before the imine nitrogen.[58]
For the 2-aminopyridine based salicylaldimine, in the solid state the pyridine ring is planar with the benzene ring, stabilised by hydrogen bonding with the imine proton in the E conformation. This would permit the delocalisation of the π system over the whole molecule. However, Cimerman and his coworkers [6,59]caution the conclusion made by Csasaszar and Balog;[61] based on the UV spectral data, of the presence of keto-amine for all salicylideneaminopyridines. Instead they maintain that for the 2-aminopyridine-based salicylaldimine the keto-amine tautomer doesn't exist even in polar solutions.[6]

5.8 Correlation analysis of the chemical shift of the HC=N and C=N of the Schiff bases

Table 5:3 Correlation of the Hammett subsituent parameters for substituents on the phenyl ring on the frequencies of HC=N and C=N of the ligands.

	aniline-based	1-aminonaphthalene-based	3-amino Pyridine-based	3-aminomethylpyridine-based
HC=N (R^2)	0.9951	0.9815	0.9783	0.134
Q test (99%/95% confidence)	0.200	0.667	0.286	0.08
C=N (R^2)	0.8514	0.9735	0.4815	0.0865
Q test (99%/95% confidence)	0.429	0.611	0.220	0.068

Plots of the Hammett substituent parameters for the substituents on the phenyl ring of the Schiff bases against HC=N and C=N were carried out. The statistical validity of the correlations was determined by regression analysis using Q tests[39] at the 99% and 95% level. A plot of the HC=N chemical shifts of the aniline-based, 1-aminonaphthalene-based and the 3-aminopyridine-based gave a reasonable correlation with the Hammett parameters, whereas 3-aminomethylpyridine-based does not give a reasonable correlation. In the same vein, while the C=N of aniline and 1-aminonapthalene correlate reasonably well with the Hammett substituents, those of 3-aminopyridine and the 3-aminomethyl pyridine azomethine carbon do not give a reasonable correlation. Good correlation might imply that the azomethine carbon and proton are essentially dependent on the perturbation of the aldimine π-bond whereas those that correlate poorly probably indicate a second order effect. However, while the correlation might be poor for some of them (as indicated by a low R^2 value) the rejection quotient test (Q test) at 99% and 95% (0.926 and 0.829 respectively) is greater than the Q_{exp} for all the correlation carried out, hence the outliers are retained.[39]

5.9 References

1. M. Calligaris and L. Randaccio, *Comprehensive coordination chemistry*, Vol. 2, G. Wilkinson, (Ed.), Pergamon Press, Oxford, 1987.
2. J. Costamanga, J. Vargas, R. Latorre, A. Alvarado, G. Mena, Coord. Chem. Rev.; 1992, **119**, 67-.
3. A. D. Garnovskii, A. L. Nivorozhkin and V. I. Minkin, Coord. Chem. Rev.; 1993, **126**, l-69.
4. N. Raman, Y. Pitchaikani, A. Kulandaisamy, Proc. Indian Acad. Sci. (Chem. Sci.); 2001, **113**, 183-89.
5. T. A. K. Al-Allaf, A. Z. M. Sheet, Polyhedron; 1995, **14**, 2, 239-248.
6. Z. Cimerman, R. Kiralj, N. Galic, J. Mol. Struc.; 1994, **323**, 7-14.
7. L. Guofa, S. Tongshun, Z. Yongnian, J. Mol. Struc.; 1997, **412**, 75-81.
8. G. Y. Yeap, S.T. Ha, N. Ishizawa, K. Suda, P. L. Boey, W. A. K. Mahmood, J. Mol. Struc.; 2003, **658**, 87-99.
9. F. L. Bowden, D. Ferguson, J. Chem. Soc., Dalton Trans.; 1974, 460-62.
10. L. Guofa, Z. Yongnian, L. Xiaoxun, Huaxue Xuebao; 1992, 50, 473-8, (CAN 117:82354)
11. Z. Li, X, Xuexiang, L. Guofa, S. Tongshun, Synth. React. Inorg. Met.-Org. Chem.; 1999, 29, 233-244, (CAN 130:261015)
12. O. Berkesi, T. Kortvelyesi, C. Hetenyi, T. Nemeth, I. Palinko, Phys. Chem. Chem. Phys.; 2003, 5, 2009-2014.
13. K. Wozniak, H. He, J. Klinowski, W. Jones, T. Dziembowska, E. Grech, J. Chem. Soc. Faraday Trans.; 1995, **91**, 3926-32.
14. H. H. Freddman, J. Am. Chem. Soc., 1961, 83, 2900-2905.
15. S. Patai, *The chemistry of carbon-nitrogen double bond*, Wiley, NY, 1970.
16. L. S. Skorokhod, I. I. Seifullina, S. A Dzhambek, Russ. J. Coord. Chem.; 2002, **28**, 643-646.

17. L. J. Bellamy, *The infra-red spectra of complex molecules*, Chapman and Hall, London, 3rd ed., 1975.

18. R. M. Badger, S. H. Bauer, J. Chem. Phys., 1937, **5**, 839-51, (CAN 32:350).

19. A. W. Baker, A. T. Shulgin; J. Am. Chem Soc.; 1958, **80**, 5358-63.

20. O. Berkesi, T. Kortvelyesi, C. Hetenyi, T. Nemeth, I. Palinko, Phys. Chem. Chem. Phys.; 2003, **5**, 2009-14.

21. Z. Popovic, G. Pavlovic, D.M. Calogovic, V. Rohe, I. Leban, J. Mol. Struct. 2002, 615, 23-31.

22. J.A. Faniran, K. S. Patel, J. C. Bailar Jr., J. Inorg. Nuc. Chem., 1974, 36, 1547-51.

23. J. Fabian, M. Legrand, Bull. Soc. Chim, France; 1956, 1461-3.

24. L. E. Clougherty, J. A. Sousa, G. M. Wyman, J. Org. Chem.; 1957, **22**, 462-9.

25. W. Kemp, *Organic Spectroscopy*, English Language Book Society/Macmillan, London, 1975.

26. N. L. Alpert, W. E. Keiser, H. A. Szymanski, *IR theory and practice of infrared spectroscopy*, 2nd ed. Plenum press, New York, 1970.

27. F. Dianzhong, W. Bo, Trans. Met. Chem.; 1993, **18**, 101-3.

28. A. Seminara, S. Giuffrida, A. Musumei, I. Fragala, Inorg. Chim. Acta.; 1984, 201-5.

29. M. Tumer, C. Celik, H. Koksal, S. Serin, Trans. Met. Chem.; 1999, **24**, 525-32

30. P. Bamfield, J. Chem. Soc. (A); 1967, 804-8.

31. G. C. Percy, D. A. Thornton, J. Inorg. Nucl. Chem.; 1972, **34**, 3369-76.

32. R. D. Hancock, D. A. Thornton, J. Mol. Struc. ; 1969, **4**, 361-7

33. Nakamoto, K.; *Infrared and Raman spectra of inorganic and coordination compounds* 3rd Ed, Wiley-Interscience, New York (1978)

34. G. C. Percy and D. A. Thornton, J. Inorg. Nucl. Chem.; 1971, **34**, 599-604.

35. G. C. Percy and D. A. Thornton, J. Inorg. Nucl. Chem., 1972, **34**, 3357-6.

36. G. C. Percy and D. A. Thornton, J. Inorg. Nucl. Chem., 1973, **35**, 2319-27.

37. G. Varsányi, S. Zöke, *vibrational spectroscopy of benzene derivatives*, Academic Press, New York, USA, 1969.

38. J. A. Draeger, Spectrochim. Acta, 39A (1983) 809-25.

39. D. A. Skoog, D. M. West, F. J. Holler, *Fundamentals of analytical chemistry*, 7th ed, Saunders College Publishing, Philadelphia, USA, 1995.

40. M. Ashmawy, R.M. Issa, S.A. Amer, C.A. McAuliff, R.V. Parish; J. Chem. Soc.Dalton, 1986, 421-426

41. G.C. Percy and D.A. Thornton, J. Inorg. Nucl. Chem., 35 (1973) 2719-2726.

42. J.E. Ruede and D.A. Thornton, J. Mol. Struct., 34 (1976) 75-81.

43. M.L. Niven, G.C. Percy and D.A. Thornton, J. Mol. Struct., 68 (1980) 73-80.

44. T. P.E. Auf der Heyde, C. S. Green, D. E. Needham, D. A. Thornton and G. M. Watkins, J. Mol. Struct.. 70 (1981) 121-6.

45. D. M. Adams, P. J Lock, J. Chem. Soc. A; 1971, 2801-6.

46. I. Nakagawa, T. Shimanouchi, Spectrochim. Acta, 1964, **20**, 429-39.

47. M. Yildiz, Z. Kilic, T. Hokelec, J. Mol. Struct.; 1998, 441, 1-10.

48. H. Nazir, M. Yildiz, H. Yilmaz, M.N. Tahir, D. Ulku, J. Mol. Struct.; 2000, 524, 241-50.

49. P.W. Alexander, R.J. Sleet, Aust. J. Chem.; 1970, **23**, 1183-90.

50. H. E. Ungnade, J. Am. Chem. Soc.; 1953, **75**, 432-4.

51. D. Heinert, A. E. Martell, ibid.; 1963, **85**, 183-4.

52. L. N. Ferguson, I. J. Kelly, ibid.; 1951, **73**, 3707-9.

53. M. D. Cohen, S. Flavian, J. Chem Soc. (B), 1967, 321-8.

54. S. J. Angyal, C. L. Angyal, J. Chem. Soc.; 1952, 1461-66.

55. N. Galic, Z. Cimerman, V. Tomisic, Anal. Chim. Acta; 1997, **343**, 135-143.

56. C. W. N. Cumper, A. Singleton, J. Chem. Soc. (B), 1968, 649-51.

57. G. C. Pimentel, J. Am. Chem. Soc.; 1957, **79**, 3323-6

58. Z. Cimerman, Z. Stefanac, Polyhedron 1985, **4**, 1755–1760.

59. Z. Cimerman, N. Gale˘si´c, B. Bosner, J. Mol. Struct.; 1992, **274**,131–144.

60. N. Gali´c, D. Matkovic-Calogovic, Z. Cimerman, Struct. Chem. 2000, **11**, 361-5.

61. J. Csaszar, J. Balog, Acta. Chim. Acad. Sci. Hung.; 1975, **87**, 321-30; CAN 84:173169

62. G. O. Dudek, J. Am. Chem. Soc.; 1963, **85**, 694-7.

63. S. Spange, M. El-Sayed, H. Muller, G. Rheinwald, H. Lang, W. Poppitz, Eur. J. Org. Chem.; 2002, 4159-68.

64. A.B.P. Lever, Chapter 6, *Inorganic electronic spectroscopy*, 2nd Ed. (1984) Elsevier, Amsterdam.

65. B. Douglas, D. McDaniel, J. Alexander; Chapter 10, *Concepts and models of inorganic chemistry* 3rd Ed (1993) John Wiley & son, New York.

66. Nicholls; Chapter 6 *Complexes and first-row transition elements*, (1974) MacMillan Press, London.

67. I. Kuźniarska-Biernacka, A. Bartecki, K. Kurzak; Polyhedron, 2003, **22**, 997-1007.

68. B. West, J. Chem. Soc.; 1952, 3123-9.

69. P. Bamfield, J. Chem. Soc. (A), 1967, 804-8.

70. T. Tanaka, J. Am. Chem. Soc.; 1958, **80**, 4108-10.

71. H. Nishikawa, S. Yamada, Bull. Chem. Soc. Jpn.; 1964, **37**, 1154-60.

72. M. Hariharam, F. Urbach, Inorg. Chem.; 1969, **8**, 556-9.

73. R. L. Carlin, J. Chem. Edu.; 1963, **40**, 135-143.

74. V. S. Shivankar, R. B. Vaidya, S. R. Dharwadkar, N. V. Thakkar, Synth. React. Inorg. Met-Org. Chem., 2003, **33**, 1597-1622.

75. L. E. Orgel, J. Chem. Phys.; 1955, **23**, 1004-14, CAN 49:68007.

76. P. L Orioli, L. Sacconi, M. D. Vaira, Chem. Commun., 1965, 103

77. J. Ferguson, J. Chem. Phys.; 1963, **39**, 116-28, CAN 59:12894.

78. M.A. Hitchman, Inorg. Chem.; 1977, **16(8)**, 1985-93.

79. R. L. Carlin, *Stereochemistry of cobalt(ii) in transition metal chemistry*, vol. 1, Edward Arnold (Publisher) Ltd., London, 1965.

80. L. Sacconi, M. Ciampolini, F. Maggio, F. P. Cavasino, J. Am. Chem. Soc.; 1947, **69**, 1886-.

81. B.G. Tweedy, Phytopath.; 1964, 55, 910.

82. L. Sacconi, Coord. Chem. Rev.; 1966, **1**, 192-204

83. H. B. Gary, J. Chem. Edu.; 1964, **41**, 2-12

84. L. Sacconi, M. Ciampolini, F. Maggio, F. P. Cavasino, J. Am. Chem. Soc.; 1962, **84**, 3246-8.

85. S. Yamada, K. Y.amanouchi, Bull. Chem. Soc. Jpn.; 1969, **42**, 2562-66

86. K. Tabei, E. Saitou, Bull. Chem. Soc. Jpn., 1969, **42**, 1440-1443.

87. L. E. Khoo, Spectrochim. Acta; 1979, **35A**, 993-995.

88. E. Pretsch, P Bühlmann , C. Affolter, *Structure determination of organic compounds* (3rd Ed.) (2000) Springer, New York.

89. G. Dudek, E. P. Dudek' J. Chem. Soc. B; 1971, 1356-1360.

90. G. O. Dudek, E .P. Dudek, Chem. Comm. 1964, **19**, 464-466.

91. D. J. Darensbourg, P. Rainy, J. Yarbourgh, Inorg. Chem.; 2001, **40**, 986-993.

92. H. Pizzala, M. Carles, W. E. E. Stone, A. Thevand, J. Chem. Soc. Perkin Trans. 2, 2000, 935-939.

93. A. K. Jain, A. Gupta, R. Bohra, I. P. Lorenz,and P. Mayer, Polyhed., 2006, **25**, 654-662.

94. A. Pelter, R. S. Ward, T. I. Gray, J. Chem. Soc. Perkin Trans. 1; 1976, 2475-83.

95. H. Ranganathan, D. Ramaaswamy, T. Ramasami, M. Santappa, Chem. Letters 1979, 1201-02.

96. G. O. Dudek, Spectrochim. Acta; 1963, **19**, 691-700.

97. P. H. Gorre, A. M., Lubiensky, J. Chem. Soc. 1963, 6056-7.

98. Y. Kurasawa, Y. Matsumoto, A. Ishikura, K. Ikeda, T. Hosaka, A. Takada, H. S. Kim, Y. Okamoto, J. Heterocyc. Chem.; 1993, **30**, 1463, (CAN 120:244966).

99. J. Császár, J. Balog and A. Makary, Acta Phys.Chem. 24 (1978), 471-84, (CAN 91:156919).

100. N. A. Caballero, F.J. Melendez, C. Muñoz-Caro, A. Niño, Biophysical Chemistry, 2006, **124**, 155-160.

101. B. Kamienski , M. Paluch, Bull. Acad. Pol. Sci. Chim. , 1967, **15**, 345-8, CAN 68:6598.

102. G. Anderegg, K. Popov, P. S. Pregosin, Helv. Chim. Acta; 1986, **69**, 329-32, (CAN 104:185886).

6 REVIEW OF THE BIOLOGICAL STUDY

6.1 Introduction

Fungal and bacterial infections persist as a threat to worldwide health, costing the world billions of dollars each year, especially with the increasing emergence of drug[1] resistance pathogens. Consequently, drug companies collaborating with scientists continue to focus on the development of new antimicrobial drugs to take care of the many microorganisms which are resistant to the currently used antibiotics. Most antibiotics used in the treatment of microbial infections have side effects,[2,3] hence the need for research to development new antibiotics or improve the existing ones. The new drug requires several relevant bioassays before it can be recommended for use.

6.1.1 Identifying a bioassay

Choosing the right bioassay is essential to the success of a drug research program.[4] The test should be simple, quick, reproducible, and relevant, as there is usually a large number of compounds to be analyzed. The test is done *in vitro* (i.e. on isolated cells, tissues, enzymes, or receptors) or *in vivo* (on animals). Generally, *in vitro* bioassays are preferred[4] because they are cheaper, easier to carry out, less controversial, and they can be automated. In modern medicinal chemistry, both *in vitro* and *in vivo* are used to determine not only whether the candidate drugs are acting at the desired target, but also whether they have activity at other undesired targets. The final decision is usually to find drugs that have the best balance of good activity at the desired and minimal activity at other targets.

6.1.2 Biological methods

Several methods are available for testing the biological activity of newly synthesized or isolated natural compounds. Antioxidant assays or free radical scavenging, antimicrobial susceptibility tests, brine shrimp lethality assay, cytotoxicity assay, potato disc assay, lemna assay, are some of the methods[5, 6] used for detecting biological activities. In most or all of these tests, a compound with known biological activity, (e.g. vitamin C is known to have antioxidant property, hence used as control), or a test that does not include the test sample, is used for the assessment. Schiff bases and cobalt complexes have been shown to have antitumor, antibacterial and antifungal

activities, consequently, the Schiff bases, and their cobalt(II) complexes synthesised in this work were accompanied with two different biological testing methods.

The two methods employed in the present work for the biological studies are antimicrobial susceptibility testing and brine shrimp lethality assay. Consequently, this chapter has been subdivided into two major sections, covering the overview of the two biological studies used to evaluate the Schiff bases, and their corresponding cobalt complexes. The experimental procedures followed are also presented in chapter 7, while the results for each of the biological studies in tabular forms are listed in chapter 8. The discussions of all the results of the biological work are presented in chapter 9 while chapter 10 is reserved to give the general summary and to indicate future work.

6.2 Microorganism

Microbe (microorganism) is the term used to describe an organism[7] that cannot be seen without the aid of a microscope. This includes virus, bacteria, archaea, fungi, and protista. Bacteria and archaea have prokaryotic cell structure while fungi are eukaryotes.[7] The prokartotes cells lack a distinct nuclear membrane; do not have complex internal organelles, such as mitochondria or chloroplasts which are associated with energy generation in eukaryotes. Prokaryotes have neither reticulum, endoplasmic nor Golgi apparatus membranes. On the other hand, the eukaryotes have a nucleus and complex internal organelles.

6.2.1 Bacteria

Bacteria are a major group of living organisms. They are prokaryotes, microscopic and unicellular. As prokaryotes, bacteria have relatively simple cell structure lacking a cell nucleus, cytoskeleton, and organelles such as mitochondria and chloroplasts. They contain all the machinery required for growth and self-replication at the expense of food stuffs.[8] Bacteria are the most abundant of all organisms. They are presence in the soil, water, and serve as symbionts of other organisms. Like plant and fungal cells, they have cell walls but with a very different composition.[7,9,10] The cell walls of bacteria are made out of peptidoglycan while that of fungi and plants are made of chitin and cellulose respectively. The cell wall is used in characterizing bacteria into groups.

Bacteria have been grouped as Gram-positive and Gram-negative respectively. This grouping is based on differences in cell wall structure as revealed by Gram staining. The cell wall of Gram-positive bacteria contains a thick peptidoglycan or murein layer and teichoic acids. Gram-negative bacteria have an outer, lipopolysaccharide-containing membrane and a thin peptidoglycan layer located in the periplasm. The search for differences between bacteria and animal cells that could provide the basis for a selective antibacterial attack lies in their general structure.[7] Many of them use a flagellum to move around. The flagella of bacteria are different in structure from the flagella of other groups. The vigor of movement in variety of bacteria depends on the number of flagella they possess. [7,9,10]

Bacteria reproduce by asexual reproduction which results in cell division. This leads to the formation of two identical cloned daughter cells. Solid growth media such as agar plates and liquid growth media are the methods used in the laboratory to grow bacteria. Bacteria are both valuable and detrimental to the environment and animals, including humans. Many bacteria are pathogens;[8,10,11] in humans they cause tetanus, typhoid fever, pneumonia, food–borne illness, leprosy, tuberculosis, etc. Leaf spot, fireblight, and wilts are detrimental effects of bacteria on plants.

Contact, air, food, water, and insect-borne microorganisms are the modes of infection. Antibiotics, classified as bactericidal and bacteriostatic, are used to treat bacteria infections. Bactericidal are antibacterial agents that kill bacteria while those that inhibit the growth of bacteria are referred to as bacteriostatic.

In the present study, *Escherichia coli*, *Pseudomonas aeruginosa*, *Staphylococcus aureus* and the fungus, Aspergillus *niger*, were used as test organisms for the antimicrobial susceptibility testing, consequently, the following sections are dedicated to brief general information about bacteria and fungus.

6.2.1.1 *Escherichia coli* (*E. coli*)

Escherichia coli (*E. coli*) is a species of bacteria that lives in the lower intestines of warm blooded animals. They are important for the proper digestion of food. Fecal contamination is used to determine its presence in ground–water; hence tests for its presence are widely used in public health laboratories.[8] It belongs to the group enterobacteriaceae. It is commonly used as a

model organism for bacteria in general. It is Gram-negative. *E. coli*, is usually harmless. However, three situations are known in which harmless *E. coli* causes illness.[12] When *E .coli* leaves intestinal tract and enters urinary track. An infection called "honeymoon erstitis" occurs because the bacteria are introduced into the bladder through intercourse.[12] It is known also to cause an infection called "peritonitis" when it gets out of the intestinal tract through a hole or tear and into abdomen.[12] Certain strains of *E. coli* are toxigenic and can cause food poisoning when contaminated meats are consumed.[8] Treatment with antibiotics is usually effective. Most strains of *E. coli* are sensitive to sulfonamides, aminoglycosides, chloramphenicol, ampicillin, streptomycin, etc.[8]

E. coli is frequently studied in cellular biology, because of its ubiquity. Its structure is clear, hence makes for an excellent target for the life science novice.[9]

6.2.1.2 *Staphylococcus aureus (S. aureus)*

Staphylococcus aureus (a.k.a. golden staph) is a bacterium that lives as a commensal in the nose and on the skin of healthy person. It has ability to infect other tissues when normal barriers have broken down. Infections caused by staph can spread through contact with pus from an infected wound, skin to skin contact with an infected person, and contact with an object used by an infected person.

It can cause illness ranging from skin infection such as pimples, boils, wound infections and deep abscesses, to life–threatening diseases such as pneumonia, meningitis, endocarditis, purulent arthritis and septicemia. [13-15] It also causes food poisoning. It is an important pathogen for domestic animals. *Staphylococcus aureus* is known to be the cause of many eye infections such as blepharitis and dacrocystitis.[16] Inflammation of the eyelid (blepharitis) and chronic blepharoconjunctivitis are both caused by *Staphylococci*.[17]

It appears as a Gram-positive coccus, and appears in grape-like clusters when viewed through a microscope. When grown out on agar plates, large golden-yellow colonies are seen.

The therapeutic problem posed by drug–resistant *Staphylococci* is self-evident. As a result of prevalence of *Staphylococci* resistance to one or more antimicrobial agents, there is always the

need to determine the drug sensitivity of the infecting organism. Agents such as oxacillin, methicillin or a cephalosporin are the first line antistaphylococal antibiotics.[8]

The resistance to antibiotics may be connected to the vivid yellow pigmentation. It is believed that drugs that inhibit the bacterium's production of the carotenoids responsible for the yellow coloration may weaken it and renew its susceptibility to antibiotics.[18]

6.2.1.3 *Pseudomonas aeruginosa (P. aeruginosa)*

Pseudomonas is found primarily in the soil or waters, or on plants, and they are known to attack a variety of organic compounds. It is a Gram-negative, aerobic rod. It belongs to the bacterial family *Pseudomonadaceae.*

Pseudomonas aeruginosa is seen as epitome of an opportunistic pathogen of humans.[19] The bacteria infect tissues if the tissue defenses are compromised in some manner. Consequently, *P. aeruginosa* infection is uncommon in normal individuals, except for minor infections such as chronic external otitis. However, *P. aeruginosa* infection is common in those with compromised host defenses.[20] Urinary tract infections, respiratory system infections, dermatitis, soft tissue infections, bacteremia, gastrointestinal infections, bone and joint infections, a variety of systemic infections are infections common to *P. aeruginosa.*[20]

Optimum temperature for growth is 37 degrees, and it is able to grow at temperatures as high as 42 degrees. *Pseudomonas aeruginosa* is a dreaded pathogen, it is known for its resistance to antibiotics. Fluorquinolones, gentamicin, amikacin, and carbenicillin have proved useful.[20] The aforementioned antibiotics are not effective against all strains, and resistance to these agents has been observed.

6.2.2 Microbial growth control

Chemical agents (antimicrobial agents) can be used to control the growth of microorganisms.[21] An antimicrobial agent is a chemical that kills or inhibits the growth of microorganisms. An antimicrobial agent may be synthetic chemical or natural product. The term bactericidal or fungicidal is used for antimicrobial agents that kill bacteria or fungi while bacteriostatic or fungistatic is the term used for those that inhibit the growth of the microorganisms.

6.2.2.1 Measuring antimicrobial activity

Antimicrobial activity is measured by determining the smallest amount of agent needed to inhibit the growth of a test organism. This value is called the minimum inhibitory concentration (MIC).

One of the commonly used procedures for studying antimicrobial action is the agar diffusion method.[22] A Petri dish containing an agar medium evenly inoculated with the test organism is prepared. Known amounts of the antimicrobial agent (synthetic or natural) are added to sterile antibiotic assay discs, which are then placed firmly on the surface of the agar. The inoculated agar plate and antimicrobial agent containing assay discs are incubated at a specific temperature for 10-24 hours or more. During the incubation, the agent diffuses from the assay disc into the agar; a zone of inhibition is created. The diameter of the zone is used to determine the effectiveness of the agent. This method is routinely used to test for antibiotic sensitivity in pathogens.[21]

Another method of testing of antimicrobial activity is the tube / broth dilution technique.[22] Disc diffusion susceptibility testing offers a simple, rapid, and cost -effective method for susceptibility testing and is thus employed in the present study.[22]

6.2.2.2 Enumeration of microorganisms

In order to ascertain the quantity of bacteria in a given sample, it is often necessary to determine the number of bacteria as well as to compare the amount of growth under various conditions.[23] Plate count, direct microscopic method and turbidity using spectrophotometer are some of the techniques used in determining the number as well as the growth of bacteria in a given sample.

6.2.2.3 Plate count (viable count) technique

The quantity of bacteria in a given sample is usually too great to be counted; hence, serial dilution of the sample is plated out on an agar surface. This is to enable the formation of single isolated visible colonies; the number of viable cells can then be measured from the number of the colonies in that known dilution. [23,24]

Colony-Forming Units (CFUs) are used in plate count technique to express the quantity of viable bacteria numbers. The colony-forming unit may contain organisms that clump together or forms

multiple cell arrangements. By extrapolation, this number can be used to calculate the number of CFUs in the original sample.

Note that a plate having 30-300 colonies is chosen because this range is considered statistically significant.[23]

Number of CFUs per ml of sample = number of colonies (30-300) X the dilution factor of the plate counted

The bacteria sample is diluted by factor of 10 and plated on agar. For a more accurate count, each dilution is done in duplicate or triplicate and average count calculated. [23,24]

Figures 6:1 shows representatives of the plates used in calculating the colony-forming unit (CFU) for all the bacteria used as test organisms. The plates have less than 300 but more than 30 colonies, hence were counted. The attempt at calculating the colony-forming units for the fungus tested, *Aspergillus niger*, proved abortive as the hairy structure of the fungus made absolute counting impossible.

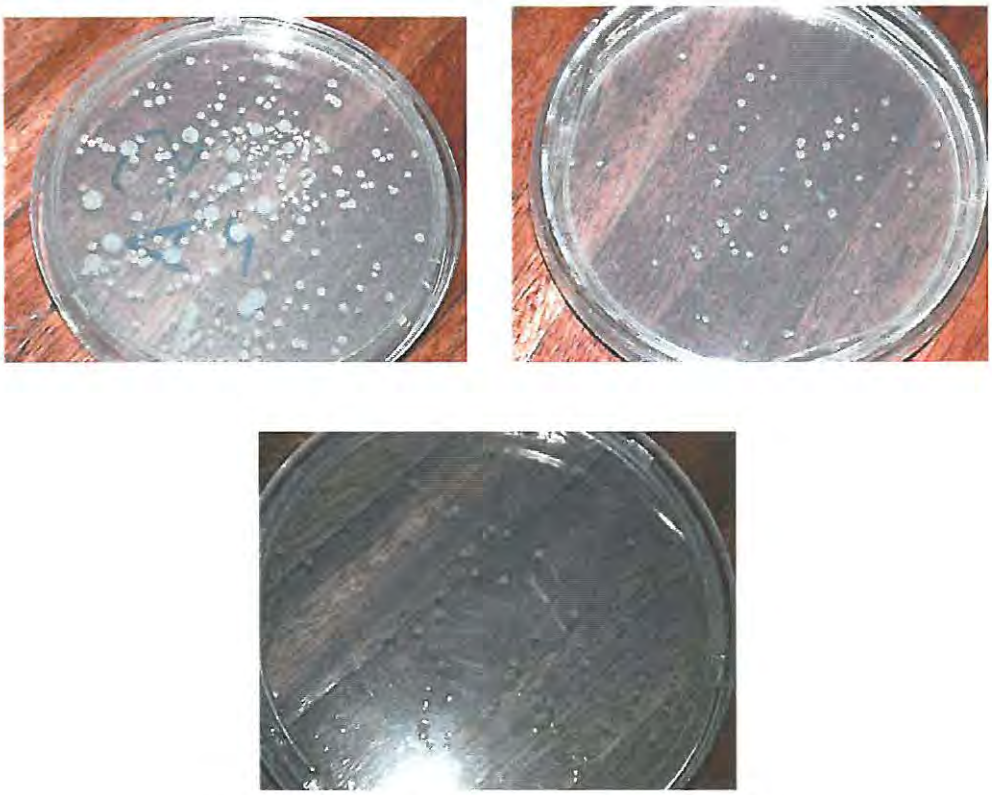

Figure 6:1 The colony forming unit of some of the bacteria studied

6.3 Fungi

Fungi are filamentous, non-photosynthetic, eukaryotic microorganisms. They have heterotrophic nutrition. Their basic cellular unit is described as a hypha, a tubular compartment which is surrounded by a rigid, chitin-containing wall.[7] Fungi may be single-celled, e.g. yeasts, or multicellular filamentous colonies, e.g. molds and mushrooms. The multicellular fungi have no leaves, stems, or roots, and thus are much less differentiated than higher plants, but are much more differentiated than bacteria.[24] In addition to yeast, mushrooms and molds; the lineages of fungi also include rusts, smuts, puffballs, truffles, and morels. This class of organism is important in terms of their ecological and economic roles. While some fungi provide numerous drugs and food, others serve as mycorrhizae, which dwell in the roots of most vascular plants and supply essential nutrients.

Fungi are also known to cause a number of plant and animal diseases: in humans, ringworm, athlete's foot, and several more serious diseases. Fungi are chemically and genetically more similar to animal than other organisms, consequently, fungal diseases are difficult to treat.[25] As a result of the substantial physiologic differences between bacteria and fungi, it is not surprising that they respond to different drugs.[24] Polyene agents and grisefulvin are among the first effective antifungal chemotherapy drugs developed.

6.3.1 *Aspergillus niger*

Aspergillus niger is one of the commonest of the genus *Aspergillus*. It causes black mold on certain types of fruit and vegetables, and is a common contaminant of food.[26] *A. niger*, *A. fungatus*, and *A. terreus*, have been identified as important pathogens for immuno-compromised humans.

Unlike other *Aspergillus* species, *Aspergillus niger* is less likely to cause disease. However, serious lung disease called the aspergillosis can occur if large amounts of spores are breathed in. Aspergillosis is a disease common among horticultural workers. Unlike other aspergillus, some stains are used in the industrial production of citric acid,[26] (E330), gluccoric acid (E574) and glucoamylase and α-galactosidase.

6.3.2 Susceptibility testing methods of antifungal agents

Like in bacteria, methods used in comparing activities begin with selection of organisms and determining the minimum inhibitory concentrations. The activity of an antifungal agent is evaluated by its ability to kill a pathogen or by its capacity to simply inhibiting the growth of fungi.

The ability of an antifungal agent to kill a pathogen as opposed to simply inhibiting its growth is a desirable quality, particularly in setting of decreased immunity. Antifungal susceptibility testing methods approved by the Clinical and Laboratory Standards institutes (CLSI), of New York, include disk diffusion method,[22] broth dilution,[22] colorimetric testing,[27] flow cytometry,[28] and spectrophotometric testing.[29] These and other approved methods have revolutionized methods used to standardized yeast and filamentous fungi. However, there is still more work to be done as standardization lags behind that for susceptibility testing.[22]

At present, successful antifungal drugs used clinically for general infections affect four general biological processes:[22] ergosterol synthesis or function (allylamines, azole, and polyenes), deoxyribonucleic acid (DNA) and protein synthesis (5-flucytosine), and glucan synthesis (caspofungin). The ideal antifungal drug target is one that inhibits an essential process in a broad spectrum of pathogenic fungi and has no analogue counterpart in humans.[30]

6.4 Brine shrimp assay

The search for bioactive compounds has greatly been enhanced by phytochemical research. The method of bioassay is the most critical and trouble aspect of phytochemical studies once isolation or synthesis and structural elucidation have been carried out. In order to be able to design or isolate a variety of novel, chemically diverse, bioactive compounds, a method that should be simple to perform, fast, economical, in-house and having valid statistical correlation must be used.[5] Brine shrimp assay is one of the assays that has probably been able to satisfy the aforementioned criteria. The brine shrimp lethality is said to be superior to or as equally predictive as the solid tumor cytotoxicities.[5]

Brine shrimp are crustaceans that live in saline environment. Their eggs are readily available from pet stores and hatched quickly in salty water. The larvae are termed nauplii, they are sensitive to small doses of biologically-active chemicals.

Michael et al., proposed brine shrimp lethality assay.[31] Vanhaecke et al., and Sleet and Brendel were reported by Carballo et al. to later develop the method.[32] It is based on the ability to kill laboratory cultured *Artemia* nauplii, brine shrimp. In 1982, Meyer et al.,[33] introduced the brine shrimp lethality test as a simple, general, in-house bioassay for natural products. The assay has been utilized in a number of laboratories for diverse purposes. For instance, it has been used for the detection of fungal toxins,[34] heavy metals,[35] pesticides,[36] cytotoxicity testing of dental materials,[37] etc. hence it is considered a useful tool for preliminary assessment of toxicity.[38] In pharmacological testing, a correlation has been found between brine shrimp lethality test and antitumor compounds found in terrestrial plant extracts.[33, 38,39] McLaughlin et al.[40] showed that the brine shrimp assay has strong correlation with the 9KB cytotoxicity assay. They also observed that brine shrimp assay as well as the human lung carcinoma and human colon adenocarcinoma demonstrate very strong correlations to the P-388 marine leukemia assay. Since early 1980s, the emphasis at the National Cancer Institute (NCI) shifted from leukaemia to solid tumor bioassays and from *in vivo* to *in vitro* screens.[5]

As proposed by Meyer et al.,[33] the brine shrimp lethality test has been employed in this study to determine the toxicity of the various Schiff bases and their cobalt(II) complexes, hoping to find a correlation between this assay and cytotoxicity. The decision to use this assay is based on the premise that pharmacology is simply toxicity at lower dose, and also because it is known that most antitumor compounds are cytotoxic. The simple procedure, low cost and correlation to cytotoxicity and antitumor assays make brine shrimp assay a routine, in–house prescreen method of detecting antitumor compounds.[5,32,33]

6.4.1 Toxicology

Toxicology is defined as "the study of the nature and mechanism of toxic effects of substances on living organisms and biologic systems".[41]

The science of toxicology is based on the theory that there is a relationship linking a toxic reaction (the response) and the amount of poison received (the dose).[42] An important assumption in this relationship is that there is almost always a dose below which no response occurs or can be measured. A second assumption is that once a maximum response is reached any further increases in the dose will not result in any increased effect.

The degree of effects a poison produces is determined by the dose of a poison administered. The dose is the amount of exposure to a potentially toxic agent and is usually measured in milligrams per kilogram (mg/kg) or mg per liter (mg/l) where mg is the amount of chemical present, kg refers to the weight of the person or animal exposed.

6.4.2 LD_{50} and LC_{50}

The LD_{50} and LC_{50} are standardized measures for comparing and expressing the toxicity of chemicals. LD denotes "Lethal Dose" while LC stands for "Lethal Concentration".[43] The LD_{50} is the amount of material (dose), which kills half (50%) of the animals, while LC_{50} refer to concentration of a chemical in air or concentration of a chemical in water (used in environmental studies). Many kinds of animals are used by toxicologists for testing, but rat and mice are often used. The LD_{50} is usually expressed in milligrams of chemical per kilogram of body weight (mg/kg) while LC_{50} is often expressed as mg of chemical per volume of medium the organism is exposed to. The LD_{50} of different poisons may be easily compared; however, it is always necessary to know which species was used for the tests and how the poison was administered (the route of exposure), since the LD_{50}/LC_{50} of a poison may vary considerably based on the species of animal and the exposure patterns. Toxicity assessment is quite complex, many factors can affect the results of toxicity tests. Some of these factors include variables like temperature, food, light, and stressful environmental conditions. Other factors related to the animal itself include age, sex, health, and hormonal status. The lower the LD_{50}/LC_{50}, the more toxic is the chemical. Chemicals are practically non-toxic when the LD_{50}/LC_{50} is large.[42,]

Meyer et al.,[33] Solis et al.,[38] MacLaughlin et al.,[44] Chowdhury et al.,[45] Mohammad and Islam,[46] etc. expressed the results of the brine shrimp assay as LC_{50}, while Machado et al.,[47] Lee et al.[48] and others expressed their results as LD_{50}. The LD_{50}/LC_{50} and 95 % confidence were determined using probit analysis method described by Finney.[49] Standardized computational procedures with good statistical backing have been used to fit data obtained from the brine shrimp lethality test.[49] Consequently, the lengthy calculations of the classical probit analysis have been replaced by a method giving far greater accuracy in very little time.[49] Data analysis computer software such as R, SAS, Statistical, and even Microsoft excel have been used to fit the numerical data obtained from biological assays. For the brine shrimp analysis results presented in chapter 8, R analysis software[50] has been used to calculate the LD_{50}.

6.5 References

1. A. Persidis, Nat. Biotechnol.; 1999, **17**, 1141-1142.
2. M. H. Goldstein, R. P. Kowaski, Y. J. Gorden, Ophthalmol.; 1999, **106**, 1313–1318.
3. T. Lancaster, A. M. Swart, Brit. Med. J.; 1998, **316**, 667, (CAN : PubMed ID 9522812.
4. P. L. Graham, *An introduction to medicinal chemistry*, 3rd ed.; Oxford University Press, New York, 2005.
5. J. E. Anderson, C. M. Goetz, J. L. McLaughlin, Phytochem. Analys.; 1991, **2**, 107-111.
6. J. L. McLaughlin, L. Lingling, M. S. Rogers, J. E. Anderson, Drug Info. J.; 1998, **32**, 513-524.
7. J. Nicklin, K. Graeme-Cook, R. Killington, *Instant notes microbiology*, 2nded.BIOS Scientific Publishers Limited, Oxford, 2002.
8. B. D. Davis, R. Dulbecco, H. N. Eisen, H. S. Ginsberg, *Microbiology including immunology and molecular genetic,* 3rd ed. Harper and Row, Hagerstown, 1980.
9. http://en.wikipedia.org/wiki/bacterium, date accessed, 14/06/2006.
10. I. E. Alcamo, *Fundamentals of microbiology*, 5th ed. Benjamine Cumming, California, U.S.A, 1997.
11. T. J. Franklin, G. A. Snow, *Biochemistry of antimicrobial action*, 2nd ed. Chapman and Hall, London, 1975.
12. http://en.wikipedia.org/wiki./*E.Coli*, date accessed, 14/06/2006.
13. S. I. Morse, *Microbiology including immunology and molecular genetic*, 3rd ed. B.D. Davis, R. Dulbecco, H. N. Eisen, H. S. Ginsberg, Eds. Harper and Row, Hagerstown, 1980.
14. http://textbookofbacteriology.net/staph.html, date accessed, 14/01/2006.

15. http://en.wikipedia.org/wiki/staphylococcus_aureus, date accessed, 14/06/2006.

16. J. H. Miller, *Disease of the eye*, Churchill Livingstone, New York, 1990, 127–165.

17. F. C. Blodi, C. F. Blodi, *Differential Diagnosis of Eye Disease*, Gerorg Thieme Verlage, New York, 1998, 84–116.

18. M. P. Jevons, Brit. Med. J.; 1961, **1**, 124-5.

19. http://textbookofbacteriology.net/pseudomonas.html, date accessed, 16/06/2006.

20. A. C. Sonnenwirth, *Microbiology Including Immunology and Molecular Genetic*, 3rd ed. B. D. Davis, R. Dulbecco, H. N. Eisen, H. S. Ginsberg, Eds. Harper and Row, Hagerstown, 1980.

21. M. T. Madigan, J. M. Martinko, J. Parker, *Biology of microorganism*, 8th ed. Prentice Hall Upper Saddle River, New York, 1998.

22. E.J. Ernst, P.D. Rogers, *Antifungal agents methods and protocols*, Human Press, Totowa, New Jersey, 2005.

23. J. G. Cappuccino, N. Sherman, *Microbiology: a laboratory manual*, 3rd ed. Benjamin/Cumming and Publishing Company, California, U.S.A. 1992.

24. G. S. Kobayashi, *Fungi: Microbiology Including Immunology and Molecular Genetic*, Eds. B.D. Davis, R. Dulbecco, H. N. Eisen, H. S. Ginsberg, 3rd ed. Harper and Row, Hagerstown, 1980.

25. http://www.ucmp.berkeley.edu/fungi/fungi.html, date accessed, 22/06/2006.

26. http://en.wikipedia.org/wiki/Aspergillus_niger, date accessed, 22/06/2006.

27. A. Espinel-Ingroff, M. Pfaller, S. A. Messer, C. C. Knap, N. Holliday, S. B. Killiam , J. Clin. Microbiol.; 2004, **42**, 718-721.

28. C. Wenisch, K. F. Linnau, B. Parschalk, K. Zedtwitz-Liebenstein, A. Georgopoulos, J. Clin. Microbiol., 1997, **35**, 5-10.

29. M. A. Pfaller, S. A. Messer, S. Coffmann, J. Clin. Microbiol. 1995, **33**, 1094-1097.

30. B. Monk, R. Cannon, Curr. Drug Targets infect. Disord.; 2002, **2**, 309-329.

31. A. S. Michael, C. G. Thompson, M. Abramovitz,. Science 1956, **123,** 464, CAN 50:50384).

32. J. L. Carballo, Z. L. Hernandez-Inda, P. Perez, M. D. Gravalos, Bio. Med. Cent. Biotech.; 2002, **2**, 17-21.

33. B. N. Meyer, N. R. Ferrigni, J. E. Putnam, L. B. Jacobsen, D. E. Nichols, J. L. McLaughlin, Plant med. 1982, **45**, 31-34.

34. J. Harwig, P. Scott, Appl. Microbiol. 1971, **21,** 1011-1016.

35. M, Martínez, J. Del ramo, A. J. Torreblanca, J. Díaz-Mayans, Aquacul. 1998, **172,** 315-325.

36. M. V. Barahona, S. Sánchez-Fortún, Env. Pollut.; 1999, **104,** 469-476.

37. M. Pelka, W. Danzl, W. Distler, A. Petschelt, J. Dent.; 2000, **28**, 341-345.

38. P.N. Solís, C.W. Wright, M.M. Anderson, M.P. Gupta, J.D. Phillipson, Plant Med. 1993, **59**, 250-252.

39. M. M. Mackeen, A. M. Ali, N. H. Lajis, K. Kawazu, Z. Hassan, M. Amran, M. Habsah, L. Y, Mooi, S. M. Mohamed, J. Ethnopharmacol., 2000, **72,** 395-402.

40. J. E. Andeson, C. J. Chang, J. L. McLaughlin, J. Nat. Prod.; 1988, **51,** 2, 307-309.

41. M. Kemple, J. Pest. Ref.; 2001, **21**, 4.

42. Extension Toxicology Network, Dose-response relationships in toxicology, 1993.

43. http://www.ccohs.ca/oshanswers/chemicals/ld50.html, 16/06/2005

44. J. L. MacLaughlin, C. J. Chang, D. L.Smith, *Studies in natural products chemistry*, Ed. A.U. Rahman, Elsevier, Amsterdam, 1991.

45. S. C, Nargis, K. Rezaul, R. Sohel, Pharm. J.; 2005, **4**, 1-4.

46. M. Al-Amin, R. Islam, Dhaka Uni. J. Pharm. Sci.; 2005, **4**, 1-9.

47. S. L. Machado, L. V. Santos, W. F. Costa, B. P. Filho, M. H. Sarragiotto, Acta. Sci. Technol. Maringa; 2005, **27**, 107-110.

48. S. Lee, B. Min, Y. Kho, Arch. Pharm. Res.; 2002, **25**, 652-4.

49. D. J. Finney, *Probit analysis*, 3rd ed., Cambridge University Press, Cambridge, 1971.

50. www.r-project.org, R : Copyright 2001, The R Development Core Team Version 1.3.1 (2001-08-31)

7 EXPERIMENTAL (BIOLOGICAL STUDY)

7.1 Antimicrobial assay

7.1.1 Methodology

The antimicrobial susceptibility testing of the Schiff bases and their corresponding cobalt complexes were carried out by the agar well diffusion method, using *Escherichia coli*, *Pseudomonas aeruginosa*, *Staphylococcus aureus* and *Aspergillus niger*, as test organisms. The concentration of the compounds dissolved in pure DMF or methanol ranged from 4 mg/ml to 0.5 mg/ml.

7.1.2 Materials used for the antimicrobial testing

The three bacteria (*P. aeruginosa*, *S. aureus*, and *E. coli*), as well as the fungus (*A. niger*), were supplied by the microbiology department, Rhodes University. Nutrient agar and broth, malt extracts were supplied by Biolab, (Biolab Cat. # HG000C1.500). Antibiotic assay discs, 12.7 mm diameter and sterile 0.45 μm membrane filters were purchased directly from Sigma- Aldrich, Steinheim, Germany. Other standard materials used were small stainless steel forceps, bacteria loop, glass spreaders, sterile Petri dishes, disposable gloves, protective mask, and Eppendorf research adjustable volume setting pipettes, autoclave and a 37°C constant environment room.

7.1.3 Preparation of nutrient agar plates

A solution of the nutrient agar powder was prepared in accordance with the manufacturer's instructions. The quantity required to prepare the needed plates were put in Erlenmeyer flask, dissolved in double distilled water, aluminum foiled was used to cover the flask and the solution autoclaved for 20 minutes at 121°C. The solution was cooled and 15-20ml was aseptically poured into each of the required number of sterile Petri dished and the dishes covered with their lids. The plates were allowed to set, then inverted and incubated for 24 hours. The incubated plates were checked after 24 hours to ensure that bacteria free plates were used for the antimicrobial testing.

7.1.4 Antibacterial susceptibility screening, inoculation and incubation

The agar disc diffusion technique was employed for the antibacterial susceptibility screening. These tests were performed in triplicate and thereafter, activities of the compounds were checked. 10^7- 10^8 colony-forming units (CFU)/ml were spread on the surface of the nutrient agar using a glass spreader. The plates were inoculated with 100 µl of the bacteria strain cultured that has been diluted to a known concentration colony forming unit. To enable even distribution of bacteria on the inoculated plates, glass spreaders were used. The Schiff bases and their corresponding complexes were prepared by dissolving 4mg of each in DMF and a series of dilutions were prepared from each. The concentrations of the sample solutions used throughout these biological studies are 4 mg/ml, 1 mg /ml and 0.5 mg/ml of solvent. A blank (DMF/methanol) was used, while respective metal salts and the starting materials were also dissolved in DMF/methanol. Ampicillin, the reference antibiotics, was dissolved in water. The discs having a diameter of 12.7 mm were soaked in each of the solutions, air dried in the lamina flow, before placing firmly on the Petri plates that had been previously seeded with bacteria to be tested. All these operations were carefully performed under aseptic conditions. The plates and the compounds soaked assay disc were allowed to stand for another 15 minutes before incubating at 37±1 °C for 10–14hrs. At the end of the incubation period, the diameters of the zones of inhibition around the assay discs were measured. Plates were incubated at 37±1 °C for 10–14 hrs. At the end of the incubation period, the diameter of the zones of inhibition around the discs was measured.

7.1.5 Preparation of malt extracts agar plates

A solution of the malt extracts agar powder was prepared in accordance with the manufacturer's instructions. The quantity required to prepare the needed plates were put in Erlenmeyer flask, dissolved in double distilled water, aluminum foiled was used to cover the flask and the solution autoclaved for 20 minutes at 121°C. The solution was cooled and 15-20ml was aseptically poured into each of the required number of sterile Petri dished and the dishes covered with their lids. The plates were allowed to set, then inverted and incubated for 24 hours. The incubated plates were checked after 24 hours to ensure that fungi free plates are used for the antifungal testing.

7.1.6 Antifungal susceptibility, screening, inoculation and incubation

The antifungal activities of the compounds were determined using malt extract agar plates prepared using the procedure highlighted above. Malt agar medium was also used to maintain pure fungal cultures. Tween and sterile distilled water were used to loosen the spores of the cultured fungus used. The plates were inoculated with 100 µl of the diluted fungus strain cultured. To enable even distribution of fungus on the inoculated plates, glass spreaders were used. Solutions of the Schiff bases and their complexes and the metal salts were prepared in DMF, while solution of benomyl, the reference antifungal compound used was dissolved in water and in DMF respectively. The active ingredient in benomyl is benzimidazole. Antibiotic assay disc of 12.7 mm diameter were soaked in 4, 2, and 1 mg/ml DMF or methanol solution of the Schiff bases, the complexes, metal salts, starting material, antifungal as well as DMF or methanol. The soaked antibiotic assay discs were air dried under a lamina flow hood and placed on each of the inoculated malt extracts plates with the help of forceps flamed from time to time. All the procedures highlighted above were done aseptically under a lamina flow hood. The plates and the compounds soaked assay disc were allow to stand for another 15 minutes before incubating at 37±1 °C for 10 – 14hrs. At the end of the incubation period, the diameters of the zones of inhibition around the assay discs were measured. The results obtained are contained are tabulated and discussed in chapter 6.

7.2 Brine shrimp assay

7.2.1 Hatching of the shrimps

Brine Shrimp eggs (*Artemia salina*) (PRO 100, Ocean Star, International Inc., Snowville, Utah, 84336, USA) were hatched by incubation in filtered seawater at room temperature (approx 25°C) under constant aeration in light for 24 hours. A plastic divider with several 2mm holes was clamped in the dish to make two unequal compartments. The eggs (ca. 50 mg) were sprinkled into the large compartment which was darkened, while the smaller compartment was illuminated. Oil-free oxygen was passed continuously through an aquarium pump. After 48 hours the phototropic nauplii were collected by pipette from the lighted side, having been separated by the divider from their shells.

7.2.2 Preparation of test compounds and incorporation of the shrimps

Samples were prepared by dissolving 1 mg of each of the Schiff bases and their cobalt(II) complexes in 100 µl methanol. 650 µl of filtered sea water was added to provide a bioassay stock solution of 1 mg per 750 ml. In 96 micro-well plates, 75 µl of filtered seawater was

pipetted into wells B-D and 150 µl (200 µg) of the mixture of each of compounds were carefully pipetted into the "A" rows of the 96-well microplates. 75 µl was removed from well A, added to well B and mixed thoroughly. 75 µl was transferred from well B to C, and from C to D. The final 75 µl from wells D was discarded. Serial dilutions of eight were made for very reactive Schiff bases and complexes while four dilutions were made for the less reactive ones. Thereafter, 75 µl of seawater was added to all the wells, making a total of 150 µl seawater plus the test solution. Lastly, 100 µl of shrimps-containing seawater was added, making a total of 250 µl per well. The serial dilution allowed for toxicity ranges between 400 to 3.12 ppm to be examined. A minimum of 10 organisms were added to each of the wells. Adding equal amount of nauplii inside the wells of the microplates was not possible. However, the 'R' data analysis computer program used for the analysis of the numerical data was used to address the problems of disparity. The control was also made using the steps outlined above except that the addition of test compounds was left out. The wells were maintained under illumination.

After 24 hours, each well was examined under a Leica dissecting microscope and the numbers of dead (non-motile) as well as live nauplii were counted. The percent death at each dose was determined. Figure 7:1 show some of the brine shrimp under microscope after 24 hours treatment with the test samples.

Figure 7:1 Some brine shrimps treated with a test sample in one of the wells of a 96 micro-well plate.

Applying the data analysis "R" software, using a program written by the Statistics department of the Rhodes University, the Probit and logit linear regression analyses were used to fit the data, hence, the LD_{50} calculated. Consequently, it was possible to compare the toxicity of each of the ligands and their complexes.

8 RESULT (BIOLOGICAL STUDY)

8.1 Antimicrobial assay results

Table 8:1 Antimicrobial activities of the aniline-based ligands

No.	Chemotherapeutic agent	Concn. mg/ml	Gram-negative		Gram-positive	Fungus
			E. coli	*P. aeruginosa*	*S. aureus*	*A. niger*
			Average zone size	*Average zone size*	*Average zone size*	*Average zone size*
1	saani	*4*	*15*	*16*	*13*	*27*
		1	*13*	*14*	*13*	*23*
		0.5	*13*	*13*	*13*	*15*
2	pvaani	*4*	*17*	*18*	*14*	*27*
		1	*15*	*15*	*13*	*25*
		0.5	*13*	*13*	*13*	*14*
3	ovaani	*4*	*21*	*24*	*16*	*30*
		1	*19*	*20*	*16*	*29*
		0.5	*14*	*16*	*14*	*16*
4	vaani	*4*	*15*	*18*	*15*	*27*
		1	*14*	*15*	*14*	*25*
		0.5	*13*	*13*	*13*	*13*
	DMF (control)	*4*	*14*	*14*	*14*	*14*
		1	*13*	*13*	*13*	*14*
		0.5	*13*	*13*	*13*	*13*
	Ampicillin (standard antibacterial)	*4*	*30*	*30*	*32*	-
		1	*27*	*27*	*25*	-
		0.5	*21*	*20*	*22*	-
	Benomyl (standard antifungal) in water	*4*	-	-	-	*25*
		1	-	-	-	*20*
		0.5	-	-	-	*18*
	Benomyl (standard antifungal) in DMF	*4*	-	-	-	*40*
		1	-	-	-	*36*
		0.5	-	-	-	*30*

Table 8:2 Antimicrobial activities of the aniline-based ligand 1 and its complexes

No.	Chemotherapeutic agent	Concn. mg/ml	Gram-negative		Gram-positive	Fungus
			E. coli	*P. aeruginosa*	*S. aureus*	*A. niger*
			Average zone size	*Average zone size*	*Average zone size*	*Average zone size*
1	saani	*4*	*15*	*16*	*13*	*27*
		1	*13*	*14*	*13*	*23*
		0.5	*13*	*13*	*13*	*15*
1A	$Co(saani)_3Cl_2.1½H_2O$	*4*	*16*	*20*	*15*	*32*
		1	*14*	*17*	*13*	*25*
		0.5	*13*	*14*	*13*	16
1B	$Co(saani)_2.½H_2O$	*4*	*16*	*20*	*18*	*35*
		1	*14*	*18*	*16*	*20*
		0.5	*13*	*13*	*13*	*13*
1C	$Co(saani)_2$	*4*	*17*	*20*	*18*	*38*
		1	*14*	*17*	*17*	*19*
		0.5	*13*	*13*	*13*	*14*
	DMF (control)	*4*	*14*	*14*	*14*	*14*
		1	*13*	*13*	*13*	*14*
		0.5	*13*	*13*	*13*	*13*
	Ampicillin (standard antibacterial)	*4*	*30*	*30*	*32*	-
		1	*27*	*27*	*25*	-
		0.5	*21*	*20*	*22*	-
	Benomyl (standard antifungal) in water	*4*	-	-	-	*25*
		1	-	-	-	*20*
		0.5	-	-	-	*18*
	Benomyl (standard antifungal) in DMF	*4*	-	-	-	*40*
		1	-	-	-	*36*
		0.5	-	-	-	*30*

Table 8:3 Antimicrobial activities of the aniline-based ligand 2 and its complexes

No.	Chemotherapeutic agent	Concn. mg/ml	Gram-negative		Gram-positive	Fungus
			E. coli	*P. aeruginosa*	*S. aureus*	*A. niger*
			Average zone size	*Average zone size*	*Average zone size*	*Average zone size*
2	pvaani	*4*	*17*	*18*	*14*	*27*
		1	*15*	*15*	*13*	*25*
		0.5	*13*	*13*	*13*	*14*
2A	$Co(pvaani)_2Cl_2$	*4*	*17*	*20*	*17*	*21*
		1	*15*	*16*	*14*	*21*
		0.5	*13*	*14*	*13*	17
2B	$Co(pvaani)_2$	*4*	*21*	*16*	*20*	*21*
		1	*19*	*14*	*18*	*18*
		0.5	*15*	*13*	*14*	*18*
2C	$Co(pvaani)_2.½H_2O$	*4*	*22*	*20*	*20*	*23*
		1	*18*	*19*	*17*	*18*
		0.5	*15*	*13*	*13*	*17*
	DMF (control)	*4*	*14*	*14*	*14*	*14*
		1	*13*	*13*	*13*	*14*
		0.5	*13*	*13*	*13*	*13*
	Ampicillin (standard antibacterial)	*4*	*30*	*30*	*32*	-
		1	*27*	*27*	*25*	-
		0.5	*21*	*20*	*22*	-
	Benomyl (standard antifungal) in water	*4*	-	-	-	*25*
		1	-	-	-	*20*
		0.5	-	-	-	*18*
	Benomyl (standard antifungal) in DMF	*4*	-	-	-	*40*
		1	-	-	-	*36*
		0.5	-	-	-	*30*

Table 8:4 Antimicrobial activities of the aniline-based ligand 3 and its complexes

No.	Chemotherapeutic agent	Concn. mg/ml	Gram-negative		Gram-positive	Fungus
			E. coli	*P. aeruginosa*	*S. aureus*	*A. niger*
			Average zone size	*Average zone size*	*Average zone size*	*Average zone size*
3	ovaani	*4*	*21*	*24*	*16*	*30*
		1	*19*	*20*	*16*	*29*
		0.5	*14*	*16*	*14*	*16*
3A	$Co(ovaani)_2Cl_2$	*4*	*17*	*18*	*17*	*23*
		1	*14*	*17*	*15*	*23*
		0.5	*13*	*13*	*13*	17
3B	$Co(ovaani)_2$	*4*	*17*	*20*	*20*	*22*
		1	*15*	*19*	*16*	*14*
		0.5	*13*	*14*	*14*	*19*
3C	$Co(ovaani)_2.\ ½H_2O$	*4*	*16*	*18*	*17*	*25*
		1	*14*	*16*	*15*	*26*
		0.5	*13*	*13*	*14*	*16*
	DMF (control)	*4*	*14*	*14*	*14*	*14*
		1	*13*	*13*	*13*	*14*
		0.5	*13*	*13*	*13*	*13*
	Ampicillin (standard antibacterial)	*4*	*30*	*30*	*32*	-
		1	*27*	*27*	*25*	-
		0.5	*21*	*20*	*22*	-
	Benomyl (standard antifungal) in water	*4*	-	-	-	*25*
		1	-	-	-	*20*
		0.5	-	-	-	*18*
	Benomyl (standard antifungal) in DMF	*4*	-	-	-	*40*
		1	-	-	-	*36*
		0.5	-	-	-	*30*

Table 8:5 Antimicrobial activities of the aniline-based ligand 4 and its complex

No.	Chemotherapeutic agent	Concn. mg/ml	Gram-negative		Gram-positive	Fungus
			E. coli	*P. aeruginosa*	*S. aureus*	*A. niger*
			Average zone size	*Average zone size*	*Average zone size*	*Average zone size*
4	vaani	*4*	*15*	*18*	*15*	*27*
		1	*14*	*15*	*14*	*25*
		0.5	*13*	*13*	*13*	*13*
4A	$Co(vaani)_2Cl_2$	*4*	*18*	*20*	*15*	*36*
		1	*15*	*15*	*14*	*24*
		0.5	*13*	*13*	*13*	*14*
	DMF (control)	*4*	*14*	*14*	*14*	*14*
		1	*13*	*13*	*13*	*14*
		0.5	*13*	*13*	*13*	*13*
	Ampicillin (standard antibacterial)	*4*	*30*	*30*	*32*	-
		1	*27*	*27*	*25*	-
		0.5	*21*	*20*	*22*	-
	Benomyl (standard antifungal) in water	*4*	-	-	-	*25*
		1	-	-	-	*20*
		0.5	-	-	-	*18*
	Benomyl (standard antifungal) in DMF	*4*	-	-	-	*40*
		1	-	-	-	*36*
		0.5	-	-	-	*30*

Table 8:6 Antimicrobial activities of the 1-aminonaphthalene-based ligand

No.	Chemotherapeutic agent	Concn. mg/ml	Gram-negative		Gram-positive	Fungus
			E. coli	*P. aeruginosa*	*S. aureus*	*A. niger*
			Average zone size	*Average zone size*	*Average zone size*	*Average zone size*
6	pvan1amnap	*4*	*16*	*19*	*24*	*27*
		1	*15*	*17*	*20*	*25*
		0.5	*13*	*13*	*14*	*13*
7	ovan1amnap	*4*	*27*	*19*	*27*	*36*
		1	*24*	*17*	*25*	*24*
		0.5	*22*	*14*	17	*14*
	DMF (control)	*4*	*14*	*14*	*14*	*14*
		1	*13*	*13*	*13*	*14*
		0.5	*13*	*13*	*13*	*13*
	Ampicillin (standard antibacterial)	*4*	*30*	*30*	*32*	-
		1	*27*	*27*	*25*	-
		0.5	*21*	*20*	*22*	-
	Benomyl (standard antifungal) in water	*4*	-	-	-	*25*
		1	-	-	-	*20*
		0.5	-	-	-	*18*
	Benomyl (standard antifungal) in DMF	*4*	-	-	-	*40*
		1	-	-	-	*36*
		0.5	-	-	-	*30*

Table 8:7 Antimicrobial activities of the ovanlamnap and its complex

No.	Chemotherapeutic agent	Concn. mg/ml	Gram-negative		Gram-positive	Fungus
			E. coli	*P. aeruginosa*	*S. aureus*	*A. niger*
			Average zone size	*Average zone size*	*Average zone size*	*Average zone size*
7	ovanlamnap	*4*	*20*	*27*	*19*	*27*
		1	*19*	*24*	*17*	*25*
		0.5	*16*	*22*	*14*	*17*
7A	$Co(ovanlamnap)_2.3H_2O$	*4*	*22*	*23*	*21*	*24*
		1	*20*	*20*	*18*	*23*
		0.5	*17*	*16*	*14*	*16*
	DMF (control)	*4*	*14*	*14*	*14*	*14*
		1	*13*	*13*	*13*	*14*
		0.5	*13*	*13*	*13*	*13*
	Ampicillin (standard antibacterial)	*4*	*30*	*30*	*32*	-
		1	*27*	*27*	*25*	-
		0.5	*21*	*20*	*22*	-
	Benomyl (standard antifungal) in water	*4*	-	-	-	*25*
		1	-	-	-	*20*
		0.5	-	-	-	*18*
	Benomyl (standard antifungal) in DMF	*4*	-	-	-	*40*
		1	-	-	-	*36*
		0.5	-	-	-	*30*

Table 8:8 Antimicrobial activities of the 4-aminopyridine-based ligands

No.	Chemotherapeutic agent	Concn. mg/ml	Gram-negative		Gram-positive	Fungus
			E. coli	*P. aeruginosa*	*S. aureus*	*A. niger*
			Average zone size	*Average zone size*	*Average zone size*	*Average zone size*
9	sal4amp	*4*	*13*	*17*	*13*	*28*
		1	*13*	*15*	*13*	*23*
		0.5	*13*	*14*	*13*	*18*
10	pvan4amp(2½ H_2O)	*4*	*14*	*17*	*13*	*22*
		1	*13*	*15*	*13*	*22*
		0.5	*13*	*13*	*13*	*15*
11	ovan4amp(H_2O)	*4*	*17*	*14*	*13*	*23*
		1	*15*	*13*	*13*	*23*
		0.5	*13*	*13*	*13*	*16*
	DMF (control)	*4*	*14*	*14*	*14*	*14*
		1	*13*	*13*	*13*	*14*
		0.5	*13*	*13*	*13*	*13*
	Ampicillin (standard antibacterial)	*4*	*30*	*30*	*32*	-
		1	*27*	*27*	*25*	-
		0.5	*21*	*20*	*22*	-
	Benomyl (standard antifungal) in water	*4*	-	-	-	*25*
		1	-	-	-	*20*
		0.5	-	-	-	*18*
	Benomyl (standard antifungal) in DMF	*4*	-	-	-	*40*
		1	-	-	-	*36*
		0.5	-	-	-	*30*

Table 8:9 Antimicrobial activities of the 4-aminopyridine-based ligand 9 and its complexes

No.	Chemotherapeutic agent	Concn. mg/ml	Gram-negative		Gram-positive	Fungus
			E. coli	*P. aeruginosa*	*S. aureus*	*A. niger*
			Average zone size	*Average zone size*	*Average zone size*	*Average zone size*
9	sal4amp	*4*	*13*	*17*	*13*	*28*
		1	*13*	*15*	*13*	*23*
		0.5	*13*	*14*	*13*	*18*
9A	$Co(sal4amp)_2Cl_2$	*4*	*16*	*16*	*18*	*22*
		1	*14*	*14*	*15*	*19*
		0.5	*13*	*13*	*13*	*15*
9B	$Co(sal4amp)_2$	*4*	*14*	*16*	*16*	*24*
		1	*14*	*14*	*16*	*24*
		0.5	*13*	*13*	*13*	*16*
9C	$Co(sal4amp)_2.2H_2O$	*4*	*19*	*16*	*20*	*24*
		1	*16*	*14*	*18*	*22*
		0.5	*14*	*13*	*14*	*14*
	DMF (control)	*4*	*14*	*14*	*14*	*14*
		1	*13*	*13*	*13*	*14*
		0.5	*13*	*13*	*13*	*13*
	Ampicillin (standard antibacterial)	*4*	*30*	*30*	*32*	-
		1	*27*	*27*	*25*	-
		0.5	*21*	*20*	*22*	-
	Benomyl (standard antifungal) in water	*4*	-	-	-	*25*
		1	-	-	-	*20*
		0.5	-	-	-	*18*
	Benomyl (standard antifungal) in DMF	*4*	-	-	-	*40*
		1	-	-	-	*36*
		0.5	-	-	-	*30*

Table 8:10 Antimicrobial activities of the 4-aminopyridine-based ligand 10 and its complexes

No.	Chemotherapeutic agent	Concn. mg/ml	Gram-negative		Gram-positive	Fungus
			E. coli	*P. aeruginosa*	*S. aureus*	*A. niger*
			Average zone size	*Average zone size*	*Average zone size*	*Average zone size*
10	pvan4amp	*4*	*14*	*17*	*13*	*22*
		1	*13*	*15*	*13*	*22*
		0.5	*13*	*13*	*13*	*15*
10A	$Co(pvan4amp)_2Cl_2.2H_2O$	*4*	*17*	*18*	*18*	*31*
		1	*15*	*16*	*16*	*26*
		0.5	*14*	*14*	*15*	*21*
10B	$Co(pvan4amp)_2.6H_2O$	*4*	*20*	*18*	*19*	*32*
		1	*18*	*17*	*17*	*26*
		0.5	*14*	*13*	*13*	*20*
10C	$Co(pvan4amp)_2.7H_2O$	*4*	*20*	*20*	*18*	*33*
		1	*16*	*18*	*15*	*26*
		0.5	*13*	*13*	*13*	*21*
	DMF (control)	*4*	*14*	*14*	*14*	*14*
		1	*13*	*13*	*13*	*14*
		0.5	*13*	*13*	*13*	*13*
	Ampicillin (standard antibacterial)	*4*	*30*	*30*	*32*	-
		1	*27*	*27*	*25*	-
		0.5	*21*	*20*	*22*	-
	Benomyl (standard antifungal) in water	*4*	-	-	-	*25*
		1	-	-	-	*20*
		0.5	-	-	-	*18*
	Benomyl (standard antifungal) in DMF	*4*	-	-	-	*40*
		1	-	-	-	*36*
		0.5	-	-	-	*30*

Table 8:11 Antimicrobial activities of the 4-aminopyridine-based ligand 11 and its complexes

No.	Chemotherapeutic agent	Concn. mg/ml	Gram-negative		Gram-positive	Fungus
			E. coli	*P. aeruginosa*	*S. aureus*	*A. niger*
			Average zone size	*Average zone size*	*Average zone size*	*Average zone size*
11	ovan4amp	*4*	*17*	*14*	*13*	*23*
		1	*15*	*13*	*13*	*23*
		0.5	*13*	*13*	*13*	*16*
11A	$Co(ovan4amp)_2Cl_2.3H_2O$	*4*	*15*	*16*	*18*	*33*
		1	*14*	*15*	*17*	*22*
		0.5	*13*	*13*	*14*	*18*
11B	$Co(ovan4amp)_2.5H_2O$	*4*	*18*	*16*	*20*	*31*
		1	*16*	*14*	*19*	*22*
		0.5	*13*	*13*	*14*	*14*
11C	$Co(ovan4amp)_2.3H_2O$	*4*	*23*	*16*	*22*	*28*
		1	*21*	*14*	*19*	*24*
		0.5	*17*	*13*	*14*	*18*
	DMF (control)	*4*	*14*	*14*	*14*	*14*
		1	*13*	*13*	*13*	*14*
		0.5	*13*	*13*	*13*	*13*
	Ampicillin (standard antibacterial)	*4*	*30*	*30*	*32*	-
		1	*27*	*27*	*25*	-
		0.5	*21*	*20*	*22*	-
	Benomyl (standard antifungal) in water	*4*	-	-	-	*25*
		1	-	-	-	*20*
		0.5	-	-	-	*18*
	Benomyl (standard antifungal) in DMF	*4*	-	-	-	*40*
		1	-	-	-	*36*
		0.5	-	-	-	*30*

Table 8:12 Antimicrobial activities of the 4-aminopyridine-based ligand 12 complexes

No.	Chemotherapeutic agent	Concn. mg/ml	Gram-negative		Gram-positive	Fungus
			E. coli	*P. aeruginosa*	*S. aureus*	*A. niger*
			Average zone size	*Average zone size*	*Average zone size*	*Average zone size*
12A	$Co_2(van4amp)_3Cl_2.5H_2O$	*4*	*14*	*16*	*21*	*18*
		1	*13*	*14*	*17*	*17*
		0.5	*13*	*13*	*14*	*15*
12B	$Co(van4amp)_2.2½H_2O$	*4*	*20*	*18*	*19*	*18*
		1	*18*	*15*	*16*	*17*
		0.5	*14*	*14*	*13*	*15*
12C	$Co(van4amp)_2.3H_2O$	*4*	*13*	*13*	*18*	*23*
		1	*13*	*13*	*16*	*18*
		0.5	*13*	*13*	*13*	*14*
	DMF (control)	*4*	*14*	*14*	*14*	*14*
		1	*13*	*13*	*13*	*14*
		0.5	*13*	*13*	*13*	*13*
	Ampicillin (standard antibacterial)	*4*	*30*	*30*	*32*	-
		1	*27*	*27*	*25*	-
		0.5	*21*	*20*	*22*	-
	Benomyl (standard antifungal) in water	*4*	-	-	-	*25*
		1	-	-	-	*20*
		0.5	-	-	-	*18*
	Benomyl (standard antifungal) in DMF	*4*	-	-	-	*40*
		1	-	-	-	*36*
		0.5	-	-	-	*30*

Table 8:13 Antimicrobial activities of the 3-aminopyridine-based ligands

No.	Chemotherapeutic agent	Concn. mg/ml	Gram-negative		Gram-positive	Fungus
			E. coli	*P. aeruginosa*	*S. aureus*	*A. niger*
			Average zone size	*Average zone size*	*Average zone size*	*Average zone size*
13	sal3amp	*4*	*16*	*18*	*16*	*25*
		1	*14*	*17*	*16*	*21*
		0.5	*13*	*13*	*14*	*18*
14	pvan3amp	*4*	*15*	*20*	*14*	*23*
		1	*14*	*18*	*13*	*24*
		0.5	*13*	*14*	*13*	*18*
15	ovan3amp	*4*	*15*	*22*	*14*	*28*
		1	*15*	*20*	*14*	*25*
		0.5	*13*	*17*	*13*	*15*
16	van3amp	*4*	*13*	*16*	*13*	*22*
		1	*13*	*14*	*13*	*20*
		0.5	*13*	*13*	*13*	*14*
	DMF (control)	*4*	*14*	*14*	*14*	*14*
		1	*13*	*13*	*13*	*14*
		0.5	*13*	*13*	*13*	*13*
	Ampicillin (standard antibacterial)	*4*	*30*	*30*	*32*	-
		1	*27*	*27*	*25*	-
		0.5	*21*	*20*	*22*	-
	Benomyl (standard antifungal) in water	*4*	-	-	-	*25*
		1	-	-	-	*20*
		0.5	-	-	-	*18*
	Benomyl (standard antifungal) in DMF	*4*	-	-	-	*40*
		1	-	-	-	*36*
		0.5	-	-	-	*30*

Table 8:14 Antimicrobial activities of the 3-aminopyridine-based ligand 13 and its complexes

No.	Chemotherapeutic agent	Concn. mg/ml	Gram-negative		Gram-positive	Fungus
			E. coli	*P. aeruginosa*	*S. aureus*	*A. niger*
			Average zone size	*Average zone size*	*Average zone size*	*Average zone size*
13	sal3amp	*4*	*16*	*18*	*16*	*25*
		1	*14*	*17*	*16*	*21*
		0.5	*13*	*13*	*14*	*18*
13A	$Co(sal3amp)_2Cl_2$	*4*	*18*	*19*	*18*	*16*
		1	*16*	*16*	*16*	*14*
		0.5	*13*	*14*	*15*	*18*
13B	$Co(sal3amp)_2.½H_2O$	*4*	*20*	*19*	*15*	*16*
		1	*19*	*16*	*14*	*14*
		0.5	*14*	*14*	*13*	*16*
13C	$Co(sal3amp)_2.½H_2O$	*4*	*20*	*16*	*16*	*19*
		1	*18*	*15*	*14*	*14*
		0.5	*14*	*13*	*13*	*16*
	DMF (control)	*4*	*14*	*14*	*14*	*14*
		1	*13*	*13*	*13*	*14*
		0.5	*13*	*13*	*13*	*13*
	Ampicillin (standard antibacterial)	*4*	*30*	*30*	*32*	-
		1	*27*	*27*	*25*	-
		0.5	*21*	*20*	*22*	-
	Benomyl (standard antifungal) in water	*4*	-	-	-	*25*
		1	-	-	-	*20*
		0.5	-	-	-	*18*
	Benomyl (standard antifungal) in DMF	*4*	-	-	-	*40*
		1	-	-	-	*36*
		0.5	-	-	-	*30*

Table 8:15 Antimicrobial activities of the 3-aminopyridine-based ligand 14 and its complexes

No.	Chemotherapeutic agent	Concn. mg/ml	Gram-negative		Gram-positive	Fungus
			E. coli	*P. aeruginosa*	*S. aureus*	*A. niger*
			Average zone size	*Average zone size*	*Average zone size*	*Average zone size*
14	pvan3amp	*4*	*15*	*20*	*14*	*23*
		1	*14*	*18*	*13*	*24*
		0.5	*13*	*14*	*13*	*18*
14A	$Co(pvan3amp)_2Cl.H_2O$	*4*	*22*	*21*	*20*	*25*
		1	*20*	*20*	*20*	*14*
		0.5	*17*	*18*	*17*	*15*
14B	$Co(pvan3amp)_2.½H_2O$	*4*	*19*	*16*	*18*	*15*
		1	*17*	*14*	*16*	*14*
		0.5	*14*	*13*	*14*	*18*
14C	$Co(pvan3amp)_2.3H_2O$	*4*	*19*	*16*	*18*	*22*
		1	*17*	*14*	*15*	*15*
		0.5	*13*	*13*	*14*	*14*
	DMF (control)	*4*	*14*	*14*	*14*	*14*
		1	*13*	*13*	*13*	*14*
		0.5	*13*	*13*	*13*	*13*
	Ampicillin (standard antibacterial)	*4*	*30*	*30*	*32*	-
		1	*27*	*27*	*25*	-
		0.5	*21*	*20*	*22*	-
	Benomyl (standard antifungal) in water	*4*	-	-	-	*25*
		1	-	-	-	*20*
		0.5	-	-	-	*18*
	Benomyl (standard antifungal) in DMF	*4*	-	-	-	*40*
		1	-	-	-	*36*
		0.5	-	-	-	*30*

Table 8:16 Antimicrobial activities of the 3-aminopyridine-based ligand 15 and its complexes

No.	Chemotherapeutic agent	Concn. mg/ml	Gram-negative *E. coli* Average zone size	Gram-negative *P. aeruginosa* Average zone size	Gram-positive *S. aureus* Average zone size	Fungus *A. niger* Average zone size
15	ovan3amp	*4*	*15*	*22*	*14*	*28*
		1	*15*	*20*	*14*	*25*
		0.5	*13*	*17*	*13*	*15*
15A	Co(ovan3amp)Cl.H_2O	*4*	*16*	*20*	*16*	*22*
		1	*14*	*18*	*14*	*20*
		0.5	*13*	*14*	*13*	*18*
15B	Co(ovan3amp)$_2$.½H_2O	*4*	*20*	*14*	*16*	*24*
		1	*17*	*13*	*14*	*18*
		0.5	*14*	*13*	*13*	*16*
15C	Co(ovan3amp)$_2$.½H_2O	*4*	*14*	*14*	*17*	*19*
		1	*13*	*13*	*14*	*17*
		0.5	*13*	*13*	*13*	*15*
	DMF (control)	*4*	*14*	*14*	*14*	*14*
		1	*13*	*13*	*13*	*14*
		0.5	*13*	*13*	*13*	*13*
	Ampicillin (standard antibacterial)	*4*	*30*	*30*	*32*	-
		1	*27*	*27*	*25*	-
		0.5	*21*	*20*	*22*	-
	Benomyl (standard antifungal) in water	*4*	-	-	-	*25*
		1	-	-	-	*20*
		0.5	-	-	-	*18*
	Benomyl (standard antifungal) in DMF	*4*	-	-	-	*40*
		1	-	-	-	*36*
		0.5	-	-	-	*30*

Table 8:17 Antimicrobial activities of the 3-aminopyridine-based ligand 16 and its complexes

No.	Chemotherapeutic agent	Concn. mg/ml	Gram-negative		Gram-positive	Fungus
			E. coli	*P. aeruginosa*	*S. aureus*	*A. niger*
			Average zone size	*Average zone size*	*Average zone size*	*Average zone size*
16	van3amp	*4*	*13*	*16*	*13*	*22*
		1	*13*	*14*	*13*	*20*
		0.5	*13*	*13*	*13*	*14*
16B	$Co(van3amp).2H_2O$	*4*	*16*	*14*	*13*	*17*
		1	*14*	*13*	*13*	*15*
		0.5	*13*	*13*	*13*	*14*
16C	$Co(van3amp).2H_2O$	*4*	*20*	*14*	*13*	*18*
		1	*18*	*14*	*13*	*15*
		0.5	*14*	*13*	*13*	*14*
	DMF (control)	*4*	*14*	*14*	*14*	*14*
		1	*13*	*13*	*13*	*14*
		0.5	*13*	*13*	*13*	*13*
	Ampicillin (standard antibacterial)	*4*	*30*	*30*	*32*	-
		1	*27*	*27*	*25*	-
		0.5	*21*	*20*	*22*	-
	Benomyl (standard antifungal) in water	*4*	-	-	-	*25*
		1	-	-	-	*20*
		0.5	-	-	-	*18*
	Benomyl (standard antifungal) in DMF	*4*	-	-	-	*40*
		1	-	-	-	*36*
		0.5	-	-	-	*30*

Table 8:18 Antimicrobial activities of the 3-aminomethylpyridine-based ligands

No.	Chemotherapeutic agent	Concn. mg/ml	Gram-negative		Gram-positive	Fungus
			E. coli	*P. aeruginosa*	*S. aureus*	*A. niger*
			Average zone size	*Average zone size*	*Average zone size*	*Average zone size*
17	sal3pico	*4*	*13*	*13*	*13*	*19*
		1	*13*	*13*	*13*	*18*
		0.5	*13*	*13*	*13*	*15*
18	pvan3pico	*4*	*13*	*17*	*13*	*23*
		1	*13*	*15*	*13*	*15*
		0.5	*13*	*13*	*13*	*14*
19	ovan3pico	*4*	*13*	*14*	*13*	*20*
		1	*13*	*13*	*13*	*17*
		0.5	*13*	*13*	*13*	*15*
20	van3pico	*4*	*15*	*13*	*13*	*18*
		1	*14*	*13*	*13*	*18*
		0.5	*13*	*13*	*13*	*17*
	DMF (control)	*4*	*14*	*14*	*14*	*14*
		1	*13*	*13*	*13*	*14*
		0.5	*13*	*13*	*13*	*13*
	Ampicillin (standard antibacterial)	*4*	*30*	*30*	*32*	-
		1	*27*	*27*	*25*	-
		0.5	*21*	*20*	*22*	-
	Benomyl (standard antifungal) in water	*4*	-	-	-	*25*
		1	-	-	-	*20*
		0.5	-	-	-	*18*
	Benomyl (standard antifungal) in DMF	*4*	-	-	-	*40*
		1	-	-	-	*36*
		0.5	-	-	-	*30*

Table 8:19 Antimicrobial activities of the 2-aminomethylpyridine-based ligands

No.	Chemotherapeutic agent	Concn. mg/ml	Gram-negative		Gram-positive	Fungus
			E. coli	*P. aeruginosa*	*S. aureus*	*A. niger*
			Average zone size	*Average zone size*	*Average zone size*	*Average zone size*
21	sal2pico	*4*	*13*	*13*	*13*	*14*
		1	*13*	*13*	*13*	*14*
		0.5	*13*	*13*	*13*	*13*
22	pvan2pico	*4*	*17*	*15*	*15*	*15*
		1	*14*	*14*	*13*	*14*
		0.5	*13*	*13*	*13*	*14*
23	ovan2pico	*4*	*13*	*14*	*13*	*15*
		1	*13*	*13*	*13*	*14*
		0.5	*13*	*13*	*13*	*14*
24	van2pico	*4*	*15*	*13*	*13*	*18*
		1	*14*	*13*	*13*	*18*
		0.5	*13*	*13*	*13*	*17*
	DMF (control)	*4*	*14*	*14*	*14*	*14*
		1	*13*	*13*	*13*	*14*
		0.5	*13*	*13*	*13*	*13*
	Ampicillin (standard antibacterial)	*4*	*30*	*30*	*32*	-
		1	*27*	*27*	*25*	-
		0.5	*21*	*20*	*22*	-
	Benomyl (standard antifungal) in water	*4*	-	-	-	*25*
		1	-	-	-	*20*
		0.5	-	-	-	*18*
	Benomyl (standard antifungal) in DMF	*4*	-	-	-	*40*
		1	-	-	-	*36*
		0.5	-	-	-	*30*

Table 8:20 Antimicrobial activities of the 3-aminomethylpyridine-based ligand 17 and its complexes

No.	Chemotherapeutic agent	Concn. mg/ml	Gram-negative		Gram-positive	Fungus
			E. coli	*P. aeruginosa*	*S. aureus*	*A. niger*
			Average zone size	*Average zone size*	*Average zone size*	*Average zone size*
17	sal3pico	*4*	*13*	*13*	*13*	*19*
		1	*13*	*13*	*13*	*18*
		0.5	*13*	*13*	*13*	*15*
17A	$Co(sal3pico)_2Cl_2½H_2O$	*4*	*13*	*13*	*17*	*21*
		1	*13*	*13*	*15*	*22*
		0.5	*13*	*13*	*13*	*15*
17B	$Co(sal3pico)_2.H_2O$	*4*	*13*	*13*	*13*	*23*
		1	*13*	*13*	*13*	*20*
		0.5	*13*	*13*	*13*	*15*
17C	$Co(sal3pico)_2.1½H_2O$	*4*	*13*	*16*	*13*	*19*
		1	*13*	*15*	*13*	*15*
		0.5	*14*	*13*	*13*	*14*
	DMF (control)	*4*	*14*	*14*	*14*	*14*
		1	*13*	*13*	*13*	*14*
		0.5	*13*	*13*	*13*	*13*
	Ampicillin (standard antibacterial)	*4*	*30*	*30*	*32*	-
		1	*27*	*27*	*25*	-
		0.5	*21*	*20*	*22*	-
	Benomyl (standard antifungal) in water	*4*	-	-	-	*25*
		1	-	-	-	*20*
		0.5	-	-	-	*18*
	Benomyl (standard antifungal) in DMF	*4*	-	-	-	*40*
		1	-	-	-	*36*
		0.5	-	-	-	*30*

Table 8:21 Antimicrobial activities of the 3-aminomethylpyridine-based ligand 18 and its complexes

No.	Chemotherapeutic agent	Concn. mg/ml	Gram-negative		Gram-positive	Fungus
			E. coli	*P. aeruginosa*	*S. aureus*	*A. niger*
			Average zone size	*Average zone size*	*Average zone size*	*Average zone size*
18	pvan3pico	*4*	*13*	*17*	*13*	*23*
		1	*13*	*15*	*13*	*15*
		0.5	*13*	*13*	*13*	*14*
18A	$Co(pvan3pico)_2Cl_2$	*4*	*14*	*14*	*14*	*14*
		1	*13*	*13*	*13*	*14*
		0.5	*13*	*13*	*13*	*14*
18B	$Co(pvan3pico)_2.½H_2O$	*4*	*13*	*14*	*13*	*18*
		1	*13*	*13*	*13*	*15*
		0.5	*13*	*13*	*13*	*14*
18C	$Co(pvan3pico)_2.½H_2O$	*4*	*15*	*13*	*15*	*18*
		1	*13*	*13*	*14*	*14*
		0.5	*13*	*13*	*13*	*14*
	DMF (control)	*4*	*14*	*14*	*14*	*14*
		1	*13*	*13*	*13*	*14*
		0.5	*13*	*13*	*13*	*13*
	Ampicillin (standard antibacterial)	*4*	*30*	*30*	*32*	-
		1	*27*	*27*	*25*	-
		0.5	*21*	*20*	*22*	-
	Benomyl (standard antifungal) in water	*4*	-	-	-	*25*
		1	-	-	-	*20*
		0.5	-	-	-	*18*
	Benomyl (standard antifungal) in DMF	*4*	-	-	-	*40*
		1	-	-	-	*36*
		0.5	-	-	-	*30*

Table 8:22 Antimicrobial activities of the 3-aminomethylpyridine-based ligand 19 and its complexes

No.	Chemotherapeutic agent	Concn. mg/ml	Gram-negative		Gram-positive	Fungus
			E. coli	*P. aeruginosa*	*S. aureus*	*A. niger*
			Average zone size	*Average zone size*	*Average zone size*	*Average zone size*
19	ovan3pico	*4*	*13*	*14*	*13*	*20*
		1	*13*	*13*	*13*	*17*
		0.5	*13*	*13*	*13*	*15*
19A	$Co(ovan3pico)_2Cl_2.1½H_2O$	*4*	*13*	*14*	*13*	*24*
		1	*13*	*13*	*13*	*21*
		0.5	*13*	*13*	*13*	*17*
19B	$Co(ovan3pico)_2.H_2O$	*4*	*13*	*14*	*13*	*19*
		1	*13*	*13*	*13*	*18*
		0.5	*13*	*13*	*13*	*18*
19C	$Co(ovan3pico)_2.H_2O$	*4*	*14*	*14*	*13*	*23*
		1	*13*	*13*	*13*	*20*
		0.5	*13*	*13*	*13*	*14*
	DMF (control)	*4*	*14*	*14*	*14*	*14*
		1	*13*	*13*	*13*	*14*
		0.5	*13*	*13*	*13*	*13*
	Ampicillin (standard antibacterial)	*4*	*30*	*30*	*32*	-
		1	*27*	*27*	*25*	-
		0.5	*21*	*20*	*22*	-
	Benomyl (standard antifungal) in water	*4*	-	-	-	*25*
		1	-	-	-	*20*
		0.5	-	-	-	*18*
	Benomyl (standard antifungal) in DMF	*4*	-	-	-	*40*
		1	-	-	-	*36*
		0.5	-	-	-	*30*

Table 8:23 Antimicrobial activities of the complexes of the 2-aminomethylpyridine-based ligand 21

No.	Chemotherapeutic agent	Concn. mg/ml	Gram-negative *E. coli* *Average zone size*	Gram-negative *P. aeruginosa* *Average zone size*	Gram-positive *S. aureus* *Average zone size*	Fungus *A. niger* *Average zone size*
21	sal2pico	*4*	*13*	*13*	*13*	*14*
		1	*13*	*13*	*13*	*14*
		0.5	*13*	*13*	*13*	*13*
21A	$Co(sal2pico)_2$	*4*	*13*	*13*	*13*	*13*
		1	*13*	*13*	*13*	*13*
		0.5	*13*	*13*	*13*	*13*
21B	$Co(sal2pico)_2.4H_2O$	*4*	*13*	*13*	*13*	*13*
		1	*13*	*13*	*13*	*13*
		0.5	*13*	*13*	*13*	*13*
21C	$Co(sal2pico)_2.4H_2O$	*4*	*13*	*13*	*13*	*13*
		1	*13*	*13*	*13*	*13*
		0.5	*13*	*13*	*13*	*13*
	DMF (control)	*4*	*14*	*14*	*14*	*14*
		1	*13*	*13*	*13*	*14*
		0.5	*13*	*13*	*13*	*13*
	Ampicillin (standard antibacterial)	*4*	*30*	*30*	*32*	-
		1	*27*	*27*	*25*	-
		0.5	*21*	*20*	*22*	-
	Benomyl (standard antifungal) in water	*4*	-	-	-	*25*
		1	-	-	-	*20*
		0.5	-	-	-	*18*
	Benomyl (standard antifungal) in DMF	*4*	-	-	-	*40*
		1	-	-	-	*36*
		0.5	-	-	-	*30*

Table 8:24 Antimicrobial activities of the 2-aminomethylpyridine-based ligand 22 and its complexes

No.	Chemotherapeutic agent	Concn. mg/ml	Gram-negative *E. coli* Average zone size	Gram-negative *P. aeruginosa* Average zone size	Gram-positive *S. aureus* Average zone size	Fungus *A. niger* Average zone size
22	pvan2pico	*4*	*17*	*15*	*15*	*15*
		1	*14*	*14*	*13*	*14*
		0.5	*13*	*13*	*13*	14
22A	$Co(pvan2pico)_2Cl_2.2H_2O$	*4*	*13*	*13*	*13*	*13*
		1	*13*	*13*	*13*	*13*
		0.5	*13*	*13*	*13*	*13*
22B	$Co(pvan2pico)_2.4H_2O$	*4*	*13*	*13*	*13*	*13*
		1	*13*	*13*	*13*	*13*
		0.5	*13*	*13*	*13*	*13*
22C	$Co(pvan2pico)_2.4½H_2O$	*4*	*13*	*13*	*13*	*13*
		1	*13*	*13*	*13*	*13*
		0.5	*13*	*13*	*13*	*13*
	DMF (control)	*4*	*14*	*14*	*14*	*14*
		1	*13*	*13*	*13*	*14*
		0.5	*13*	*13*	*13*	*13*
	Ampicillin (standard antibacterial)	*4*	*30*	*30*	*32*	-
		1	*27*	*27*	*25*	-
		0.5	*21*	*20*	*22*	-
	Benomyl (standard antifungal) in water	*4*	-	-	-	*25*
		1	-	-	-	*20*
		0.5	-	-	-	*18*
	Benomyl (standard antifungal) in DMF	*4*	-	-	-	*40*
		1	-	-	-	*36*
		0.5	-	-	-	*30*

Table 8:25 Antimicrobial activities of the complexes of the 2-aminomethylpyridine-based ligand 23

No.	Chemotherapeutic agent	Concn. mg/ ml	Gram-negative		Gram-positive	Fungus
			E. coli	*P. aeruginosa*	*S. aureus*	*A. niger*
			Average zone size	*Average zone size*	*Average zone size*	*Average zone size*
23	ovan2pico	*4*	*13*	*14*	*13*	*15*
		1	*13*	*13*	*13*	*14*
		0.5	*13*	*13*	*13*	*14*
23A	$Co(ovan2pico)_2Cl_2.3H_2O$	*4*	*13*	*13*	*13*	*13*
		1	*13*	*13*	*13*	*13*
		0.5	*13*	*13*	*13*	*13*
23B	$Co(ovan2pico)_2.2½H_2O$	*4*	*13*	*13*	*13*	*13*
		1	*13*	*13*	*13*	*13*
		0.5	*13*	*13*	*13*	*13*
23C	$Co(ovan2pico)_2.3½H_2O$	*4*	*13*	*13*	*13*	*13*
		1	*13*	*13*	*13*	*13*
		0.5	*13*	*13*	*13*	*13*
	DMF (control)	*4*	*14*	*14*	*14*	*14*
		1	*13*	*13*	*13*	*14*
		0.5	*13*	*13*	*13*	*13*
	Ampicillin (standard antibacterial)	*4*	*30*	*30*	*32*	-
		1	*27*	*27*	*25*	-
		0.5	*21*	*20*	*22*	-
	Benomyl (standard antifungal) in water	*4*	-	-	-	*25*
		1	-	-	-	*20*
		0.5	-	-	-	*18*
	Benomyl (standard antifungal) in DMF	*4*	-	-	-	*40*
		1	-	-	-	*36*
		0.5	-	-	-	*30*

Table 8:26 Antimicrobial activities of the complexes of the 2-aminomethylpyridine-based ligand 24

No.	Chemotherapeutic agent	Concn. mg/ml	Gram-negative *E. coli* *Average zone size*	Gram-negative *P. aeruginosa* *Average zone size*	Gram-positive *S. aureus* *Average zone size*	Fungus *A. niger* *Average zone size*
24	van2pico	*4*	*15*	*13*	*13*	*18*
		1	*14*	*13*	*13*	*18*
		0.5	*13*	*13*	*13*	*17*
24A	$Co(van2pico)_2Cl_2.H_2O$	*4*	*13*	*13*	*13*	*13*
		1	*13*	*13*	*13*	*13*
		0.5	*13*	*13*	*13*	*13*
24B	$Co(van2pico)_2.4H_2O$	*4*	*13*	*13*	*13*	*13*
		1	*13*	*13*	*13*	*13*
		0.5	*13*	*13*	*13*	*13*
	DMF (control)	*4*	*14*	*14*	*14*	*14*
		1	*13*	*13*	*13*	*14*
		0.5	*13*	*13*	*13*	*13*
	Ampicillin (standard antibacterial)	*4*	*30*	*30*	*32*	-
		1	*27*	*27*	*25*	-
		0.5	*21*	*20*	*22*	-
	Benomyl (standard antifungal) in water	*4*	-	-	-	*25*
		1	-	-	-	*20*
		0.5	-	-	-	*18*
	Benomyl (standard antifungal) in DMF	*4*	-	-	-	*40*
		1	-	-	-	*36*
		0.5	-	-	-	*30*

Table 8:27 Antimicrobial activities of the aniline-based ligands against *S. aureus* in DMF and methanol

No.	Chemotherapeutic agent	Average zone size in DMF	Average zone size in methanol	Difference
1	saani	*21*	*18*	+3
2	pvaani	*22*	*24*	-2
3	ovaani	*30*	*33*	-3
4	vaani	*22*	*24*	-2
	DMF or methanol (control)	*15*	*17*	-2
	Ampicillin (standard antibacterial)	*40*	*38*	+2

Table 8:28 Antimicrobial activities of the aniline-based ligand 1 and its complexes against *S.aureus* in DMF and methanol

No.	Chemotherapeutic agent	Average zone size in DMF	Average zone size in methanol	Difference
1	saani	*21*	*18*	+3
1A	$Co(saani)_3.Cl_2 1½H_2O$	*25*	*29*	-4
1B	$Co(saani)_2.½H_2O$	*31*	*26*	+5
1C	$Co(saani)_2$	*30*	*30*	0
	DMF or methanol (control)	*15*	*17*	-2
	Ampicillin (standard antibacterial)	*40*	*38*	+2

Table 8:29 Antimicrobial activities of the aniline-based ligand 2 and its complexes against *S. aureus* in DMF and methanol

No.	Chemotherapeutic agent	Average zone size in DMF	Average zone size in methanol	Difference
2	pvaani	*22*	*24*	-2
2A	$Co(pvaani)_2Cl_2$	*29*	*32*	-3
2B	$Co(pvaani)_2$	*30*	*30*	0
2C	$Co(pvaani)_2.½H_2O$	*26*	*31*	-5
	DMF or methanol (control)	*15*	*17*	-2
	Ampicillin (standard antibacterial)	*40*	*38*	+2

Table 8:30 Antimicrobial activities of the aniline-based ligand 3 and its complexes against *S.aureus* in DMF and methanol

No.	Chemotherapeutic agent	Average zone size in DMF	Average zone size in methanol	Difference
3	ovaani	*30*	*33*	-3
3A	$Co(ovaani)_2Cl_2½H_2O$	*29*	*30*	-1
3B	$Co(ovaani)_2.2H_2O$	*26*	*28*	-2
3C	$Co(ovaani)_2.½H_2O$	*30*	*28*	+2
	DMF or methanol (control)	*15*	*17*	-2
	Ampicillin (standard antibacterial)	*40*	*38*	+2

Table 8:31 Antimicrobial activities of the aniline-based ligand 4 and its complex against *S. aureus* in DMF and methanol

No.	Chemotherapeutic agent	Average zone size in DMF	Average zone size in methanol	Difference
4	vaani	*22*	*24*	-2
4A	$Co(vaani)Cl_4.3H_2O$	*32*	*30*	+2
	DMF or methanol (control)	*15*	*17*	-2
	Ampicillin (standard antibacterial)	*40*	*38*	+2

Table 8:32 Antimicrobial activities of the 1-aminonaphthalene-based ligands against *S. aureus* in DMF and methanol

No.	Chemotherapeutic agent	Average zone size in DMF	Average zone size in methanol	Difference
6	pvan1amnap	*26*	*32*	-8
7	ovan1amnap	*24*	*34*	-10
	DMF or methanol (control)	*15*	*17*	-2
	Ampicillin (standard antibacterial)	*40*	*38*	+2

Table 8:33 Antimicrobial activities of the 1-aminonaphthalene-based ligand 7 and its complex against *S.aureus* a in DMF and methanol

No.	Chemotherapeutic agent	Average zone size in DMF	Average zone size in methanol	Difference
7	ovan1amnap	*24*	*34*	-10
7A	$Co(ovan1amnap)_2.3H_2O$	*31*	*36*	-5
	DMF or methanol (control)	*15*	*17*	-2
	Ampicillin (standard antibacterial)	*40*	*38*	+2

Table 8:34 Antimicrobial activities of aminonaphthalene-ligand 7 and its complex against *S.aureus* in DMF and methanol

No.	Chemotherapeutic agent	Average zone size in DMF	Average zone size in methanol	Difference
9A	$Co(sal4amp)_2Cl_2$	*26*	*25*	+1
9B	$Co(sal4amp)_2$	*26*	*27*	-1
9C	$Co(sal4amp)_2.2H_2O$	*25*	*31*	-6
11B	$Co(ovan4amp)_2.5H_2O$	*25*	*29*	-4
	DMF or methanol (control)	*15*	*17*	-2
	Ampicillin (standard antibacterial)	*40*	*38*	+2

Table 8:35 Antimicrobial activities of 3-aminopyridine-based ligands against *S.aureus* in DMF and methanol

No.	Chemotherapeutic agent	Average zone size in DMF	Average zone size in methanol	Difference
13	sal3amp	*22*	*27*	-5
14	pvan3amp	*28*	*33*	-5
15	ovan3amp	*26*	*33*	-7
16	van3amp	*21*	*30*	-9
	DMF or methanol (control)	*15*	*17*	-2
	Ampicillin (standard antibacterial)	*40*	*38*	+2

8.2 Brine shrimp lethality assay results

Table 8:36 Brine shrimp lethality activities of the aniline-based ligands

No.	Compound	Concentration (ppm)	No. of brine shrimp	No. affected	% kill	LD_{50}	S.E	pseudoR^2
1	saani	400	34	34	100	2.72	0.04	0.993
		200	31	31	100			
		100	32	32	100			
		50	16	16	100			
		25	41	36	88			
		12.5	30	8	27			
		6.25	17	1	6			
		3.13	18	0	0			
2	pvaani	400	40	40	100	3.29	0.04	0.997
		200	24	24	100			
		100	31	31	100			
		50	26	25	96			
		25	26	10	38			
		12.5	19	1	5			
		6.25	18	0	0			
		3.13	20	0	0			
3	ovaani	400	46	46	100	3.17	0.04	0.985
		200	38	38	100			
		100	28	28	100			
		50	17	16	94			
		25	24	15	63			
		12.5	18	0	0			
		6.25	20	0	0			
		3.13	18	0	0			
4	vaani	400	49	49	100	2.40	0.07	0.998
		200	40	40	100			
		100	25	25	100			
		50	23	23	100			
		25	26	26	100			
		12.5	72	31	89			
		6.25	0	0	0			
		3.13	0	0	0			

Table 8:37 Brine shrimp lethality activities of the aniline-based ligand 1 and its complexes

No.	Compound	Concentration (ppm)	No. of brine shrimp	No. affected	% kill	LD_{50}	S.E	pseudoR^2
1	saani	400	34	34	100	2.72	0.04	0.993
		200	31	31	100			
		100	32	32	100			
		50	16	16	100			
		25	41	36	88			
		12.5	30	8	27			
		6.25	17	1	6			
		3.13	18	0	0			
1A	$Co(saani)_2.Cl_2$	400	29	29	100	3.66	0.04	0.999
		200	40	40	100			
		100	35	35	100			
		50	45	40	80			
		25	13	1	8			
		12.5	18	0	0			
		6.25	15	0	0			
		3.13	18	0	0			
1B	$Co(saani)_2.½H_2O$	400	35	35	100	2.57	0.05	0.933
		200	25	25	100			
		100	30	30	100			
		50	21	21	100			
		25	44	34	77			
		12.5	18	12	67			
		6.25	17	0	0			
		3.13	19	0	0			
1C	$Co(saani)_2$	400	30	30	100	3.00	0.06	0.931
		200	34	34	100			
		100	28	28	100			
		50	29	27	93			
		25	27	16	43			
		12.5	26	6	23			
		6.25	25	3	12			
		3.13	28	3	10			

Table 8:38 Brine shrimp lethality activities of the aniline-based ligand 2 and its complexes

No.	Compound	Concentration (ppm)	No. of brine shrimp	No. affected	% kill (p)	LD_{50}	S.E	pseudoR^2
	pvaani	400	40	40	100	3.29	0.04	0.997
		200	24	24	100			
		100	31	31	100			
		50	26	25	96			
		25	26	10	38			
		12.5	19	1	5			
		6.25	18	0	0			
		3.13	20	0	0			
2A	$Co(pvaani)_2Cl_2$	400	46	46	100	3.82	0.03	0.997
		200	27	27	100			
		100	24	24	100			
		50	23	14	61			
		25	26	1	4			
		12.5	20	0	0			
		6.25	24	0	0			
		3.13	27	0	0			
2B	$Co(pvaani)_2$	400	23	21	91	4.73	0.07	0.973
		200	32	22	69			
		100	25	10	40			
		50	35	10	29			
		25	30	2	7			
		12.5	23	0	0			
		6.25	30	0	0			
		3.13	19	0	0			
2C	$Co(pvaani)_2.½H_2O$	400	24	22	92	4.75	0.07	0.976
		200	29	19	66			
		100	24	10	42			
		50	28	7	25			
		25	23	2	9			
		12.5	24	0	0			
		6.25	21	0	0			
		3.13	25	0	0			

Table 8:39 Brine shrimp lethality activities of the aniline-based ligand 3 and its complexes

No.	Compound	Concentration (ppm)	No. of brine shrimp	No. affected	% kill	LD_{50}	S.E	pseudoR^2
3	ovaani	400	46	46	100	3.17	0.04	0.985
		200	38	38	100			
		100	28	28	100			
		50	17	16	94			
		25	24	15	63			
		12.5	18	0	0			
		6.25	20	0	0			
		3.13	18	0	0			
3A	$Co(ovaani)_2Cl_2.½H_2O$	400	26	22	85	5.05	0.06	0.964
		200	18	10	55			
		100	24	10	42			
		50	22	2	9			
		25	25	0	0			
		12.5	20	0	0			
		6.25	20	0	0			
		3.13	24	0	0			
3B	$Co(ovaani)_2.2H_2O$	400	38	38	100	3.89	0.05	0.978
		200	18	17	94			
		100	26	9	35			
		50	19	0	0			
		25	21	0	0			
		12.5	16	0	0			
		6.25	18	0	0			
		3.13	18	0	0			
3C	$Co(ovaani)_2.½H_2O$	400	35	35	100	3.92	0.02	0.900
		200	36	32	88			
		100	25	21	85			
		50	35	26	75			
		25	35	0	0			
		12.5	32	0	0			
		6.25	25	0	0			
		3.13	18	0	0			

Table 8:40 Brine shrimp lethality activities of the aniline-based ligand 4 and its complex

No.	Compound	Concentration (ppm)	No. of brine shrimp	No. affected	% kill	LD_{50}	S.E.	pseudoR^2
4	vaani	400	49	49	100	2.40	0.06	0.998
		200	40	40	100			
		100	25	25	100			
		50	23	23	100			
		25	26	26	100			
		12.5	72	31	89			
		6.25	0	0	0			
		3.13	0	0	0			
4A	$Co(vaani)Cl_2$	400	38	38	100	3.45	0.04	0.990
		200	36	36	100			
		100	16	16	100			
		50	38	36	95			
		25	26	5	19			
		12.5	30	0	0			
		6.25	23	0	0			
		3.13	19	0	0			

Table 8:41 Brine shrimp lethality activities of the 1-aminonaphthalene-based ligands

No.	Compound	Concentration (ppm)	No. of brine shrimp	No. affected	% kill	LD_{50}	S.E.	pseudoR^2
6	pvan1amnap	400	19	19	100	4.34	0.043	0.977
		200	11	11	100			
		100	10	7	70			
		50	11	2	18			
7	ovan1amnap	400	13	10	77	3.78	0.31	0.964
		200	11	8	73			
		100	11	7	64			
		50	10	5	50			

Table 8:42 Brine shrimp lethality activities of the 1-aminonaphthalene-based ligand 6 and its complexes

No.	Compound	Concentration (ppm)	No. of brine shrimp	No. affected	% kill	LD_{50}	S.E.	pseudoR^2
6	pvan1amnap	400	19	19	100	4.34	0.04	0.978
		200	11	11	100			
		100	10	7	70			
		50	11	2	18			
6A	$Co(pvan1amnap)_2.Cl_2.½H_2O$	400	17	16	94	5.22	0.04	0.994
		200	10	6	60			
		100	16	1	7			
		50	12	0	0			
6C	$Co(pvan1amnap)_2.2H_2O$	400	11	11	100	4.47	0.05	0.977
		200	11	10	91			
		100	13	7	54			
		50	14	3	21			

Table 8:43 Brine shrimp lethality activities of the 1-aminonaphthalene-based ligand 7 and its complex

No.	Compound	Concentration (ppm)	No. of brine shrimp	No. affected	% kill	LD_{50}	S.E.	pseudoR^2
7	ovan1amnap	400	13	10	77	3.78	0.31	0.964
		200	11	8	73			
		100	11	7	64			
		50	10	5	50			
7A	$Co(ovan1amnap)_2.3H_2O$	400	12	12	100	4.11	0.06	0.97
		200	14	13	93			
		100	11	9	82			
		50	11	4	36			
		200	13	8	62			
		100	10	3	30			
		50	11	0	0			

Table 8:44 Brine shrimp lethality activities of the 4-aminopyridine-based ligands

No.	Compound	Concentration (ppm)	No. of brine shrimp	No. affected	% kill	LD_{50}	S.E.	pseudoR^2
9	sal4amp	400	24	24	100	4.97	0.04	0.958
		200	18	14	78			
		100	16	2	13			
		50	16	1	6			
10	pvan4amp(2½ H_20)	400	10	10	100	5.49	0.12	0.879
		200	16	6	38			
		100	10	2	20			
		50	11	0	0			
11	ovan4amp(H_2O)	400	12	12	100	5.32	0.05	0.776
		200	12	3	25			
		100	15	2	13			
		50	13	1	8			

Table 8:45 Brine shrimp lethality activities of the 4-aminopyridine-based ligand 9 and its complexes

No.	Compound	Concentration (ppm)	No. of brine shrimp	No. affected	% kill	LD_{50}	S.E.	pseudoR^2
9	sal4amp	400	24	24	100	4.97	0.04	0.958
		200	18	14	78			
		100	16	2	13			
		50	16	1	6			
9A	$Co(sal4amp)_2Cl_2$	400	18	18	100	4.513	0.12	0.999
		200	14	14	100			
		100	26	22	85			
		50	27	0	0			
9B	$Co(sal4amp)_2$	400	13	13	100	4.54	0.10	0.910
		200	12	12	100			
		100	12	9	75			
		50	11	0	0			
9C	$Co(sal4amp)_2.2H_2O$	400	25	25	100	4.92	0.05	0.949
		200	16	12	75			
		100	10	2	20			
		50	11	1	9			

Table 8:46 Brine shrimp lethality activities of the 4-aminopyridine-based ligand 10 and its complexes

No.	Compound	Concentration (ppm)	No. of brine shrimp	No. affected	% kill	LD_{50}	S.E.	pseudoR^2
10	pvan4amp(2½ H_2O)	400	10	10	100	5.49	0.12	0.879
		200	16	6	38			
		100	10	2	20			
		50	11	0	0			
10A	$Co(pvan4amp)_2Cl_2.2H_2O$	400	13	12	92	5.24	0.05	0.973
		200	10	5	50			
		100	11	2	18			
		50	10	0	0			
10B	$Co(pvan4amp)_2.6H_2O$	400	18	18	100	4.63	0.062	0.999
		200	14	14	100			
		100	18	7	38			
		50	15	0	0			
10C	$Co(pvan4amp)_2.7H_2O$	400	14	14	100	4.66	0.04	0.921
		200	14	14	100			
		100	13	4	31			
		50	10	0	0			

Table 8:47 Brine shrimp lethality activities of the 4-aminopyridine-based ligand 11 and its complexes

No.	Compound	Concentration (ppm)	No. of brine shrimp	No. affected	% kill	LD_{50}	S.E.	pseudoR^2
11	ovan4amp(H_2O)	400	12	12	100	5.32	0.05	0.776
		200	12	3	25			
		100	15	2	13			
		50	13	1	8			
11A	$Co(ovan4amp)_2Cl_2.3H_2O$	400	12	8	67	5.62	0.05	0.907
		200	16	6	38			
		100	12	0	0			
		50	11	0	0			
11B	$Co(ovan4amp)_2.5H_2O$	400	17	13	77	5.34	0.05	0.832
		200	13	9	67			
		100	12	0	0			
		50	10	0	0			
11C	$Co(ovan4amp)_2.3H_2O$	400	20	18	90	5.36	0.06	0.906
		200	12	4	33			
		100	13	2	15			
		50	13	1	8			

Table 8:48 Brine shrimp lethality activities of the 4-aminopyridine-based ligand 12 and its complexes

No.	Compound	Concentration (ppm)	No. of brine shrimp	No. affected	% kill	LD_{50}	S.E.	pseudoR^2
12A	$Co_2(van4amp)_3Cl_2.5H_2O$	400	16	12	75	5.59	0.06	0.949
		200	15	4	27			
		100	14	2	14			
		50	14	0	0			
12B	$Co(van4amp)_2.2½H_2O$	400	16	4	25	6.74	0.27	0.852
		200	14	2	14			
		100	13	1	8			
		50	13	0	0			
12C	$Co(van4amp)_2.3H_2O$	400	15	3	20	7.00	0.36	0.804
		200	14	2	14			
		100	14	1	7			
		50	14	0	0			

Table 8:49 Brine shrimp lethality activities of the 3-aminopyridine-based ligands

No.	Compound	Concentration (ppm)	No. of brine shrimp	No. affected	% kill	LD_{50}	S.E.	pseudoR^2
13	sal3amp	400	10	9	90	4.58	0.08	0.999
		200	12	9	75			
		100	12	6	50			
		50	11	3	27			
14	pvan3amp	400	10	10	100	4.30	0.06	0.980
		200	11	10	91			
		100	11	8	73			
		50	12	3	25			
15	ovan3amp	400	15	15	100	4.49	0.04	0.930
		200	14	13	93			
		100	12	9	75			
		50	10	0	0			
16	van3amp	400	25	25	100	4.75	0.04	0.962
		200	13	12	92			
		100	11	3	27			
		50	11	1	9			

Table 8:50 Brine shrimp lethality activities of the 3-aminopyridine-based ligand 13 and its complexes

No.	Compound	Concentration (ppm)	No. of brine shrimp	No. affected	% kill	LD_{50}	S.E.	pseudoR^2
13	sal3amp	400	10	9	90	4.58	0.08	0.999
		200	12	9	75			
		100	12	6	50			
		50	11	3	27			
13A	$Co(sal3amp)_2Cl_2$	400	10	10	100	4.89	0.06	0.859
		200	10	6	60			
		100	10	3	30			
		50	11	2	18			
13B	$Co(sal3amp)_2.½H_2O$	400	12	5	42	6.18	0.19	0.959
		200	12	4	33			
		100	14	2	14			
		50	14	1	7			
13C	$Co(sal3amp)_2.½H_2O$	400	12	5	42	6.17	0.20	0.936
		200	14	5	36			
		100	12	2	17			
		50	12	1	8			

Table 8:51 Brine shrimp lethality activities of the 3-aminopyridine-based ligand 14 and its complexes

No.	Compound	Concentration (ppm)	No. of brine shrimp	No. affected	% kill	LD_{50}	S.E.	pseudoR^2
14	pvan3amp	400	10	10	100	4.30	0.06	0.980
		200	11	10	91			
		100	11	8	73			
		50	12	3	25			
14A	$Co(pvan3amp)_2Cl.H_2O$	400	14	12	86	4.25	0.11	0.900
		200	14	11	79			
		100	14	10	71			
		50	15	4	33			
14B	$Co(pvan3amp)_2.½H_2O$	400	14	9	64	5.47	0.12	0.991
		200	14	6	43			
		100	13	4	31			
		50	12	2	17			
14C	$Co(pvan3amp)_2.3H_2O$	400	16	11	69	5.21	0.12	0.988
		200	18	9	50			
		100	17	6	35			
		50	16	4	25			

Table 8:52 Brine shrimp lethality activities of the 3-aminopyridine-based ligand 15 and its complexes

No.	Compound	Concentration (ppm)	No. of brine shrimp	No. affected	% kill	LD_{50}	S.E.	pseudoR^2
15	ovan3amp	400	15	15	100	4.49	0.04	0.930
		200	14	13	93			
		100	12	9	75			
		50	10	0	0			
15A	Co(ovan3amp)Cl.H_2O.	400	13	11	85	4.46	0.14	0.906
		200	13	8	61			
		100	19	10	52			
		50	17	7	41			
15B	Co(ovan3amp)$_2$.½H_2O	400	13	12	92	3.96	0.17	0.889
		200	14	10	71			
		100	12	8	67			
		50	12	6	50			
15C	Co(ovan3amp)$_2$.½H_2O	400	11	8	72	5.62	0.08	0.913
		200	12	3	25			
		100	12	2	17			
		50	12	1	8			

Table 8:53 Brine shrimp lethality activities of the 3-aminopyridine-based ligand 16 and its complexes

No.	Compound	Concentration (ppm)	No. of brine shrimp	No. affected	% kill	LD_{50}	S.E.	pseudoR^2
16	van3amp	400	25	25	100	4.75	0.04	0.962
		200	13	12	92			
		100	11	3	27			
		50	11	1	9			
16B	Co(van3amp).2H_2O	400	15	12	80	4.66	0.09	0.866
		200	12	9	74			
		100	20	12	60			
		50	12	2	17			
16C	Co(van3amp).2H_2O	400	10	8	80	4.63	0.10	0.969
		200	10	7	70			
		100	13	7	54			
		50	11	3	27			

Table 8:54 Brine shrimp lethality activities of the 3-aminomethylpyridine-based ligands

No.	Compound	Concentration (ppm)	Number of brine shrimp	Number affected	% kill	LD_{50}	S.E.	pseudoR^2
17	sal3pico	400	12	12	100	4.85	0.05	0.966
		200	12	10	83			
		100	13	3	23			
		50	13	1	8			
18	pvan3pico	400	11	11	100	5.38	0.12	0.999
		200	12	2	17			
		100	12	1	0			
		50	11	0	0			
20	van3pico	400	15	4	27	6.34	0.13	0.952
		200	13	1	8			
		100	11	0	0			
		50	12	0	0			

Table 8:55 Brine shrimp lethality activities of the 3-aminomethylpyridine-based ligand 17 and its complexes

No.	Compound	Concentration (ppm)	No. of brine shrimp	No. affected	% kill	LD_{50}	S.E.	pseudoR^2
17	sal3pico	400	12	12	100	4.85	0.05	0.966
		200	12	10	83			
		100	13	3	23			
		50	13	1	8			
17A	$Co(sal3pico)_2Cl_2.½H_2O$	400	12	5	42	6.15	0.12	0.945
		200	12	2	17			
		100	12	1	8			
		50	11	0	0			
17B	$Co(sal3pico)_2.H_2O$	400	11	5	46	6.07	0.10	0.932
		200	12	2	17			
		100	12	1	8			
		50	11	0	0			
17C	$Co(sal3pico)_2.1½H_2O$	400	11	5	46	6.03	0.06	0.984
		200	11	1	9			
		100	10	0	0			
		50	10	0	0			

Table 8:56 Brine shrimp lethality activities of the 3-aminomethylpyridine-based ligand 18 and its complexes

No.	Compound	Concentration (ppm)	No. of brine shrimp	No. affected	% kill	LD_{50}	S.E.	pseudoR^2
18	pvan3pico	400	11	11	100	5.38	0.12	0.999
		200	12	2	17			
		100	12	1	0			
		50	11	0	0			
18A	$Co(pvan3pico)_2Cl_2$	400	13	2	15	6.11	0.31	0.941
		200	11	0	0			
		100	12	0	0			
		50	10	0	0			
18B	$Co(pvan3pico)_2.½H_2O$	400	12	2	16	6.10	0.29	0.941
		200	12	0	0			
		100	10	0	0			
		50	11	0	0			
18C	$Co(pvan3pico)_2.½H_2O$	400	13	2	15	6.78	0.28	0.963
		200	12	1	8			
		100	12	0	0			
		50	11	0	0			

Table 8:57 Brine shrimp lethality activities of the 3-aminomethylpyridine-based ligand 18 and its complexes

No.	Compound	Concentration (ppm)	No. of brine shrimp	No. affected	% kill	LD_{50}	S.E.	pseudoR^2
19A	$Co(ovan3pico)_2Cl_2.1½H_2O$	400	11	2	18	6.09	0.25	0.999
		200	11	0	0			
		100	12	0	0			
		50	10	0	0			
19B	$Co(ovan3pico)_2.H_2O$	400	13	3	23	6.45	0.16	0.923
		200	13	1	8			
		100	12	0	0			
		50	10	0	0			
19C	$Co(ovan3pico)_2.H_2O$	400	14	4	29	7.31	0.06	0.960
		200	13	3	23			
		100	12	2	17			
		50	11	1	9			

Table 8:58 Brine shrimp lethality activities of the 2-aminomethylpyridine-based ligands

No.	Compound	Concentration (ppm)	No. of brine shrimp	No. affected	% kill	LD_{50}	S.E.	pseudoR^2
17	sal2pico	400	16	14	88	5.49	0.06	0.879
		200	18	4	22			
		100	18	2	11			
		50	17	1	6			
18	pvan2pico	400	19	2	15	6.10	0.29	0.999
		200	17	0	0			
		100	20	0	0			
		50	15	0	0			
19	ovan2pico	400	25	4	15	6.10	0.29	0.999
		200	18	0	0			
		100	15	0	0			
		50	16	0	0			

Table 8:59 Brine shrimp activity of the inactive tested Schiff base complexes

No.	Compound	Concentration (ppm)	No. of brine shrimp	No. affected	% kill	LD_{50}	S.E.	pseudoR^2
21A	$Co(sal2pico)_2$	400	16	0	0	na	na	na
		200	19	0	0			
		100	13	0	0			
		50	18	0	0			

* similar results were found for 21B, 21C, 22A, 22B, 22C, 23A, 23B, 23C, 24A, 24B.

Table 8:60 Brine shrimp activities of aniline, 1-aminonaphthalene, 3-picoline and 2-picoline

No.	Compound	Concentration (ppm)	No. of brine shrimp	No. affected	% kill	LD_{50}	S.E.	pseudoR^2
1	Aniline	400	28	28	100	1.01	0.16	0.999
		200	50	50	100			
		100	15	15	100			
		50	52	52	100			
		25	44	44	100			
		12.5	36	36	100			
		6.25	16	16	100			
		3.13	51	43	84			
2	1-amnap	400	46	46	100	2.52	0.01	0.999
		200	52	52	100			
		100	32	32	100			
		50	27	27	100			
		25	22	22	100			
		12.5	16	8	50			
3	3-ampy	400	54	54	100	3.65	0.15	0.892
		200	24	22	92			
		100	31	24	77			
		50	31	21	64			
4	3-picoline	400	35	30	86	4.39	0.11	0.893
		200	32	22	69			
		100	54	36	67			
		50	32	10	31			
4	2-picoline	400	31	24	77	5.65	0.05	0.937
		200	36	6	16			
		100	29	3	10			
		50	18	0	0			

Table 8:61 Brine shrimp activities of salicylaldehyde, pvanillin, ovanillin and vanillin

No.	Compound	Concentration (ppm)	No. of brine shrimp	No. affected	% kill	LD_{50}	S.E.	pseudoR^2
1	salicylaldehyde	400	44	44	100	4.77	0.05	0.853
		200	33	30	91			
		100	36	7	17			
		50	33	7	18			
2	*p*vanillin	400	50	50	100	4.88	0.04	0.960
		200	48	37	77			
		100	33	11	33			
		50	18	0	0			
3	*o*vanillin	400	36	36	100	4.63	0.07	0.999
		200	26	26	100			
		100	23	8	35			
		50	16	0	0			
4	vanillin	400	50	50	100	5.46	0.14	0.999
		200	23	1	04			
		100	14	0	0			
		50	18	0	0			

9 DISCUSSION (BIOLOGICAL STUDY)

9.1 Antimicrobial activity

Some of the ligands and their cobalt(II) complexes were tested for their *in vitro* growth inhibitory activity against the pathogenic bacteria, namely *Escherichia coli, Staphylococcus aureus, Pseudomonas aeruginosa* and the fungus, *Aspergillus niger* using the disk diffusion method. In one of the series of successful antibacterial assays carried out, DMF was used as solvent. In another successful test accomplished, some of the ligands and their corresponding complexes were dissolved in methanol and in DMF, to examine their effect on some of the aforementioned microorganisms.

The general trend observed was that the complexes were more active against the tested bacteria than their corresponding ligands but were less active than the standard antibacterial drug, ampicillin used. While this is generally true, there are cases in which the ligands are more active than their corresponding complexes. It is worthy mentioning that most of our ligands and their complexes are more active than the standard antifungal drug, benomyl used, particularly, when the antifungal drug was dissolved in water, the recommended solvent. However, the activity of the antifungal increases dramatically when dissolved in DMF.

The observed trends that the complexes are more active than their corresponding ligand is in agreement with known fact as well as most of the published work on antimicrobial activities of Schiff bases and their complexes. Some of the explanations put forward for this observation are highlighted below.

It is well known that chelation in compounds can be responsible for the antimicrobial activity.[1] The increase in toxicity may be considered in light of Tweedy's chelation theory.[2] It is believed that chelation considerably reduces the polarity of the metal ion because of partial sharing of its positive charge with donors and possible π-electron delocalization over the whole chelate ring. Such a chelation, Tweedy believed, could enhance the lipophillic character of the central metal atom, which subsequently favors its permeation through the lipid layers of cell membrane. The variation in the effectiveness of different compounds against different organisms depends either on the impermeability of cells of the microbes or on differences in ribosome of microbial cells.[3]

For the data listed in Tables 8:1 – 8:31, undiluted DMF was used as a control under the same condition used for each of the ligands and their cobalt(II) complexes tested. The diameters of zones of inhibition were measured and the results obtained were uncorrected.

The results of the antibacterial as well as the antifungal activities of the Schiff bases and their isolated cobalt(II) complexes are listed in Tables 8:1 – 8:22. The effect of each of the Schiff base on the Gram-negative and Gram-positive as well as the fungus is compared. Thereafter the effects of complexes on the microorganism are also compared. The data listed represent values of average of three replicates from the test against bacteria and fungus investigated.

9.1.1 Group 1: The antibacterial activities of the aniline-based ligands

The results of aniline-based Schiff bases are listed in Table 8:1. The activity of ligand 3 is more than those of 1, 2, and 4. The increased activity of ligand 3, more than those of ligand 1, 2 and 4 is ascribed to the presence of the methoxy group in the 3-position of the phenyl ring.

All the Schiff bases in this group have more activity on Gram-negative bacteria than the Gram-positive bacteria. Their effect is more on the Gram-negative *Pseudomonas aeruginosa* and may be due to differences in the morphology of these organisms. Ibrahim and Al-Deeb[4] reported positive bactericidal properties for Schiff bases possessing a hydroxyl group on the aniline. In this work, the hydroxyl group is on the phenyl ring of the asymmetric carbon. Tumer et al.[5] reported that having the hydroxyl as a substituent increases the activity of compounds. They found out that ligands having two free hydroxyl groups are more active than those with one hydroxy. This work revealed that having a methoxy group in addition to the free hydroxyl causes more activity. The aniline-based ligands showed moderate activity to standard antibacterial drug (ampicillin) used, more activity than the standard antifungal drug when the antifungal drug is dissolved in water but less when dissolved in DMF

9.1.1.1 Group 1: The antimicrobial activities of the complexes of the aniline-based ligands

Tables 8:2 – 8:5 show the list of antimicrobial results of the Schiff bases and complexes isolated from the aniline-based ligands. The complexes 1A, 1B and 1C (Table 8:2) showed more activity than ligand 1 (saani). 1B and 1C are slightly more active than 1A against the Gram-positive

bacterium and the fungus. The geometry of a complex may have contributive effect on the activity. The observed activities of the complexes are in accordance with Tweedy's chelation theory.[2] The effect of the ligands as well as those of the complexes on the fungus tested is far greater than those of the bacteria. This effect is attributable to the difference in morphology of the tested organisms.[6]

The antimicrobial results presented in Table 8:3 revealed that the pvaani complexes 2A, 2B and 2C have more activity on bacteria than the ligand. However, the ligand (pvaani) showed more activity against *Aspergillus niger* than the complexes. Complex 2B and C appears to be only moderately more active than 2A. But this series of complexes shows general broad antibacterial activity.

The results listed in Table 8:4 showed that for the complexes with ovaani (ligand 3), coordination reduces activity. The ligand was very active against the Gram-negative bacteria and the fungus tested but showed less activity against *S. aureus*. The activities of the complexes against Gram-positive bacteria test are higher than the ligand. Indeed, the tetrahedral complex (3B and 3C) is more active against the Gram-positive bacteria than is the ligand

The result of ligand 4 (vaani) and its only complex is listed in Table 8:5. The complex is more active than the ligand for all except the Gram-positive bacteria. This implies that chelation increased the toxicity of the ligand. The increase toxicity of the complex relative to the ligand on the fungus is substantial. Gram-negative bacteria are more affected than the Gram-positive *S. aureus*.

The results obtained here showed that the aniline-based ligands and their complexes are moderately active when compared with the standard antibacterial ampicillin as well as standard antifungal drugs used.

9.1.2 Group 2: The antimicrobial activities of the 1-aminonaphthalene-based ligands

The results of the antimicrobial activity of the 1-aminonaphthalene–based Schiff base are listed in Table 8:6. Only two of the four synthesized Schiff bases for this group were successfully synthesised as at the time of carrying out the biological studies. From the results, it was observed that like the aniline series, that the Schiff base with 3-methoxy substituent showed

more activity than its 4-methoxy analogue. When compared with their aniline based counterpart (ligand 2 and 3) they showed more activity against bacteria but less against fungus.

The activity is attributable to extra fused ring[7] and because the bulky group, 1-aminonaphthalene is not on the asymmetric carbon. Sakiyan et al. observed that having a bulky group on the asymmetric carbon reduces antimicrobial activity.[8] They also observed that the antifungal activity was much greater that the antibacterial activity.[8] This is contrary to the results obtained here. The difference in results is attributable to the position of the 1-aminonaphthalene in the Schiff bases studied in the two laboratories.

The activity of ligand 7 (ovan1amnap) is highly comparable to both antifungal and antibacterial drugs.

9.1.2.1 Group 2: The antimicrobial activities of the complexes of the 1-aminonaphthalene-based ligands

The complexes 5C, 6A, 6C, 8A and 8C were not successfully synthesised and purified as at the time of the biological study, hence there are no antimicrobial data for them. The result of the complex isolated from ligand 7 is listed in Tables 8:7. The ligand showed more activity against *Aspergillus niger* and *Pseudomonas aeruginosa* than the complex synthesized from it. On the other hand, *E. coli* and the Gram-positive *S. aureus* are more susceptible to the complex toxicity than do the free ligand. The complex 7A has higher activity against all the bacteria than it aniline-based analogue. The free Schiff bases were more effective than the complexes for both antifungal activities, of equivalent activity for the Gram negative bacteria, but the complexes were more effective than the free ligand against Gram positive *S. aureus*.[5]

9.1.3 Group 3: The antimicrobial activities of the 4-aminopyridine-based ligands

The results of the antimicrobial assays of 4-aminopyridines ligands are presented in Table 8:8. Van4amp, (i.e. ligand 12) was not successfully synthesised as at the time of the biological assay, hence no data for analysis is presented.

The ligands in this series show less activity against the bacteria although slightly toxic to P*seudomonas aeruginosa*, but showed stronger activities against *Aspergillus niger*. When compared to the aniline series, the 4-aminopyridines show little difference in activity for the salicylaldimine and *para*-vanaldimine, but shows a significant decrease for the activity of the *ortho*-vanaldimine. This makes it clear that replacing aniline with 4-aminopyridine reduces toxicity against bacteria, hence making the ligands obtained from 4-aminopyridines less effective chemotherapeutic agents for bacteria. However, their action against the fungus tested may still qualify them as potential antifungal agents. As earlier stated, they show more activity than the standard antifungal used, particularly when the antifungal is dissolved in water but less when the antifungal is dissolved in DMF.

9.1.3.1 Group 3: The antimicrobial activities of the complexes of the 4-aminopyridine-based ligands

The results of the antimicrobial activities of 4-aminopyridine-based complexes are presented in Tables 8:9 – 8:12. The results showed that the 4-aminopyridine-based complexes are more toxic when compared with their parent ligands against all the bacterial tested under identical conditions. The complexes obtained from the *p*- and o- methoxy substituted ligands (*p*-van4amp and *o*-van4amp) are highly toxic more than their corresponding parent ligands. The increase in the antifungal activity of metal chelates may be due to the effect of the metal ion on normal cell process.

The group presented very interesting activity trends. The result of the 4-aminopyridine ligands showed reduction in activity against the tested bacteria. The coordination to cobalt resulted in increased toxicity except for the salicylaldimine ligand. This is in agreement with the Tweedy chelation theory.[2] When compared with the aniline-based ligands, the 4-aminopyridine-based complexes are more toxic to *Aspergillus niger* than their aniline-based complexes. These activities qualify them as potential antifungal agents.

The complexes of van4amp are toxic to all the bacteria and the fungus, but not as toxic as the other complexes in this group. The reduced activity relative to other complexes in the group is probably due to the positions of the methoxy and the hydroxyl in the complexes. However, it is interesting to note that this group showed noticeable activities against Gram-positive bacteria.

The results presented here for the series of ligands and their complexes are contrary to the observation of Jarrahpour et al.[9] who found no microbial activity for the pyridine-based Schiff bases. However, the antimicrobial activities of the Schiff bases synthesised from 2-furancarboxaldehyde and 2-aminobenzoic acid by Omar et al.[10] agreed with the results presented in this work. They attributed the remarkable activity of the Schiff base ligands to the presence of the pyridyl-N and the hydroxyl groups.

9.1.4 Group 4: The antimicrobial activities of the 3-aminopyridine-based ligands

The antimicrobial activities of 3-aminopyridine–based ligands are listed in Tables 8:13. These ligands are slightly more toxic against most of the microorganisms than the 4-aminopyridine analogues and of similar toxicity to their aniline analogues. Their increased toxicity against Gram-negative *Pseudomonas aeruginosa* as well as the fungus *Aspergillus niger* was clearly observed. Within this group, ovan3amp and sal3amp (ligand 15 and ligand 13) are the most toxic. Based on these results obtained, one may conclude that the presence of hydroxyl group in the 2-position is important for the biological activity. The presence of methoxy group in *m*-position added to the activity, hence the reason for the high activity of *m*-methoxy substituted compounds across the board.

9.1.4.1 Group 4: The antimicrobial activities of the complexes of the 3-aminopyridine-based ligands

The antimicrobial activities of the 3-aminopyridine complexes are listed in Tables 8:14 - 8:17. The activities in this group varied from one complex to another. Consequently, each of the sub-group will be discussed briefly. It was observed in some instances that lower concentration gave slightly higher inhibition zone sizes than the higher concentration. This behaviour observed for the three ligand sets which can allow for chelation (13, 14, and 15) may indicate that at lower concentrations the complexes are undergoing dissociation, releasing more of the free ligand.

From Table 8:14, it was observed that there was general increase in the activities of most of the ligand 13 complexes relative to the ligand against most of the bacteria tested but the antifungal activity was reduced. This implies that chelation increases their activities against most of the bacteria tested but reduced their toxicity against *Aspergillus niger*.

The results of the antimicrobial assays of the 4-methoxy containing ligand-based complexes are listed in Table 8:15. The complex, 14A showed more broad range activity than any of the other complexes investigated, with the exception of the complex with ovan1aminonaphthalene. While chelation increases the toxicity of complex 14A, it resulted in the decrease of activities of complexes 14B and 14C respectively. The complexes 14B and 14C were also active against *E. coli* and the Gram-positive *S. aureus*, but less toxic to the Gram-negative *Pseudomonas aeruginosa* and *Aspergillus niger*.

For the compounds listed in Table 8:16, it was observed that the ligand was more toxic against most of the microorganism tested than all the complexes. At 4 ppm, the free ligand ovan3amp showed some degree of specificity to *Pseudomonas aeruginosa*. This activity is reduced on complexation.

The results of the antimicrobial activities of ligand 16, van3amp and it complex, 16C are presented in Table 8:17. The biological study of complex 16A was not done because the complex was only successfully synthesised after the completion of the antimicrobial assay. Chelation increases the toxicity of this complex against Gram-negative *E. coli*, but reduced or has no noticeable effect on their toxicity against *Pseudomonas aeruginosa* and *Staphylococcus aureus*. The effects of the complexes on *Aspergillus niger* is good, but activity not as high as the toxicity of the ligand. The decrease in activity can be ascribed to the position of the hydroxyl group.

With the exception of 14A, this group like their 4-aminopyridine analogues showed the lower toxicity to all the microorganisms tested when compared to their aniline analogues. The 4-aminopyridine analogues also showed more toxicity than this group, particularly with *Aspergillus niger*.

9.1.5 Group 5 and 6: The antimicrobial activities of the 3- and 2-aminomethylpyridine-based ligands

The results of the antimicrobial activities of 3- and 2-aminomethylpyridine-based Schiff bases are listed in Tables 8:18 and 8:19 respectively. The results showed that the ligands from these two groups are poorly active. The reason for their poor activities may be ascribed to the insertion

of the methylene group between their C=N and the pyridine ring. Their reduced activity is ascribed to the absence of conjugation between the pyridine ring and the phenyl ring.

9.1.5.1 Group 5: The antimicrobial activities of the complexes of the 3-aminomethylpyridine-based ligands

The results of the isolated complexes of 3-aminomethylpyridine tested for the antimicrobial assays are listed in Tables 8:20, 8:21 and 8:22 respectively. Complexes 20A and 20B antimicrobial activities were not studied because their synthesis and purification were not completed at the time of biological study.

Complexation does not increase the antibacterial activity of the tested 3-aminomethylpyridine-based complexes; however there is slight improvement on the antifungicidal ability.

9.1.5.2 Group 6: The antimicrobial activities of the complexes of the 2-aminomethylpyridine-based ligands

The result of the antimicrobial activities of 2-aminomethylpyridine-based complexes studied is listed in Tables 8:23-826. The complexes are poorly active. This poor activity can be attributed to the absence of conjugation due to the insertion of methylene between the pyridine and phenyl rings. In addition to the protocol of dissolving the complexes in DMF, the complexes obtained from 2-aminomethylpyridine are soluble in water. Hence they were also dissolved in water and tested against the microorganisms. The results in both solvents are identical. Unlike the 3-aminomethylpyridine analogues, there was no improvement on the antifungicidal ability of the 2-aminomethylpyridine.

9.2 Initial study of antimicrobial activity against *S. aureus*

In addition to the above work, in an initial study, two sets of twenty-five compounds were weighed and dissolved in methanol and DMF respectively at 4 mg/ml. They were tested in triplicate against 10^6 cfu *S. aureus* and the results of mean are tabulated in Tables 8:27 – 8:35. The result obtained here showed larger inhibition zones than those presented in Tables 8:1–8:26 against the same organism. This shows some of the problems faced when dealing with microorganisms. It is very difficult to get the same set of conditions to work for the same microorganism. The results that can be obtained from antimicrobial assays depend on factors such as the age and strain of the microorganism, quantity of microorganism, temperature,

solvent, medium of growth, etc. Consequently, obtaining reproducible results are always very difficult or almost impossible. Nevertheless, the trends in Tables 8:27 – 8:35 followed those earlier discussed.

The data confirmed that dissolving the tested compounds in methanol generally resulted in greater inhibition zones for both the ligands and complexes than when dissolved in DMF, particularly with ovan1amnap (ligand 7). Although the patterns of activities are complex, it was still possible to fashion out clear trends for most of the tested compounds.

From the data listed in Tables 8:27 – 8:35, it was observed that the complexes show higher activity against *S. aureus* relative to the control (DMF and methanol), the metal salts, and the ligands in most cases. The presence of a heterocyclic ring on the imine decreases activity. The presence of naphthalene moiety in the cobalt complexes gives rise to the greatest bactericidal properties. Though there is sufficient increase in the antibacterial activity of the complexes as well as the ligands, they could not fully reach the effectiveness of the standard drug, ampicillin.

9.3 Brine shrimp lethality bioassay

The results of the brine shrimp lethality test are presented in Tables 8:36 – 8:57. The results clearly demonstrate that most of the ligands and their isolated cobalt(II) complexes have significant activity against brine shrimp nauplii.

9.3.1 Group 1: Brine shrimp activities for the aniline-based ligands

The brine shrimp lethality assays for the aniline-based Schiff bases are listed in Table 8:36. The four compounds are highly toxic to nauplii. The result differs slightly from the antimicrobial assay result. This difference is ascribed to the differences in morphology of the brine shrimp from the tested bacteria and fungus. Surprisingly in light of it being the least effective microbicide, ligand 4 showed the highest toxicity against brine shrimp. This is also in agreement with the biological activity of benzalanilines studied by Vladimirtsev et al.[11] They studied the phytotoxic activity of some Schiff bases, and found that salicylalaniline derivatives were the most active, while 3-methoxy-4-hydroxybenzalanile (ligand 4) showed the highest stimulating activity.

9.3.1.1 Group 1: Brine shrimp activities for the complexes of the aniline-based ligands

The brine shrimp activities for the aniline–based complexes are listed in Tables 8:37-8:40. Recall, the lower the LD50, the more toxic is the compound and vice versa. Ligand 1 (saani) is more toxic than two of it complexes but less active than complex 1B. Ligand 2 (pvaani) is more toxic to brine shrimp than all it three complexes. Complex 2A showed more toxicity than complex 2B and 2C.

Schiff base 3 (ovaani) also showed more toxicity against brine shrimps than complex 3A, B and C. In contrast to the behaviour of the complexes obtained from pvaani, the ovaani complexes 3B and 3C are more active than 3A. Complex 4A similarly showed less lethality against the tested brine shrimps than its free ligand. This implies that chelation with cobalt resulted in decrease in toxicity. The brine shrimp assay results for these sets of ligands are different to the results of their antimicrobial assay. The result is summarized below.

vaani > saani > ovaani > pvaani	(Brine shrimp assay)
ovaani > pvaani ≈ vaani > saani	(Gram-negative)
ovaani > vaani > pvaani > saani	(Gram-positive)
ovaani > pvaani ≈ vaani ≈ saani	(Fungicidal)

While the complexes are less toxic than the ligand in the brine shrimp lethality tests, they were found to be highly toxic than their corresponding ligand in the antimicrobial assay.

The differences observed from the results obtained from the two methods can be attributed to the difference in morphology of brine shrimp, bacteria and the fungus tested. The activity of the aniline–based is not unprecedented. Aniline showed greater toxicity against shrimp than all the compounds and the starting material. This implies that forming Schiff bases and complexes from aniline reduces its toxicity. The brine shrimp activity of aniline and other amines used is shown in Table 8:60.

9.3.2 Group 2: Brine shrimp activities for the 1-aminonaphthalene-based ligands

The brine lethality assay data for the 1-aminonaphthalene-based ligands successfully synthesised and purified as at the time of this assay is listed in Table 8:41. Their toxicity is less than those of aniline-based ligands. Replacement of aniline with 1-aminonaphthalene reduces toxicity unlike in antimicrobial studies in which there was substantial increase in activities. As a result of the reduced activity, the concentrations were run between 400 -50 ppm.

Nevertheless, the reduced activity of the aminonaphthalene-based ligands against brine shrimp is similar to their actions against *Aspergillus niger*. Like the aniline-based ligands, the 3-methoxy substituted ligand 7 showed more toxicity towards the shrimps than their 4-methoxy substituted analogue. Their activity is summarized below.

ovan1amnap > pvan1amnap	(Brine shrimp assay)
ovan1amnap > pvan1amnap	(Gram-negative)
ovan1amnap ≈ pvan1amnap	(Gram-positive)
ovan1amnap > pvan1amnap	(Fungicidal)

9.3.2.1 Group 2: Brine shrimp activities for the complexes of the 1-aminonaphthalene-based ligands

The activities of the 1-aminonaphthalene-based complexes are listed in Table 8:42 and 8:43. In contrast to the aniline-based system, the activities of the 1-aminonaphthalene based ligands are similar to their microbial activity. As observed in their studies against bacteria, chelation reduces their toxicity. The activities of the isolated complexes showed no correlation with the aniline-based complexes. For instance, while complex 6A is less active than 6C, 2A is more active than 2B and 2C.

9.3.3 Group 3: Brine shrimp activities for the 4-aminopyridine-based ligands

The activities of the 4-aminopyridine-based ligands are listed in Table 8:44. The replacement of aniline with 4-aminopyridine resulted in a marked reduction in toxicity against brine shrimp. Their activities against brine shrimp are akin to their lethality against bacteria and the fungus tested. Their activities in the biological methods used are summarized below.

sal4amp > ovan4amp > pvan4amp (Brine shrimp)
sal4amp ≈ ovan4amp ≈ pvan4amp (Gram-negative)
sal4amp ≈ ovan4amp ≈ pvan4amp (Gram-positive)
sal4amp > ovan4amp > pvan4amp (Fungicidal)

9.3.3.1 Group 3: Brine shrimp activities for the complexes of the 4-aminopyridine-based ligands

The activities of the complexes of the 4-aminopyridine-based complexes are listed in Table 8:45-8:48. The complexes of ligand 9 (sal4amp) are more toxic against brine shrimp than the ligand. Similar trend was also observed for the complexes of ligand 10 (pvan4amp). There were no apparent differences in the activities of complexes 9A, 9B and 9C, while complexes 10B and 10C showed more toxicity towards brine shrimp than complex 10A and the ligand.

For ovan4amp (ligand 11), there is little difference in activity between the free ligand and the complexes with the exception of 11A, which is less active. Recall, the antimicrobial results for these complexes are different from their effects on brine shrimps, in that complexation significantly enhanced activity of all but the complexes of sal4amp (ligand 9).

Ligand 12 had not been purified enough for use at the time this assay was concluded; consequently, the data is not available for analysis. When the van4amp complexes are compared with others in this series, the results showed the decrease in activities. The varied behaviour of this series of complexes must be due to the varied structure of the complexes (for example 12A) as well as to the changing of the electronic properties of the substituents in the complexes relative to others.

9.3.4 Group 4: Brine shrimp activities for the 3-aminopyridine-based ligands

The activities of the 3-aminopyridine-based ligands against brine shrimps are listed in Table 8:49. The 3-aminopyridine ligands showed greater activity against brine shrimps than their 4-aminopyridine-based analogues. However, their toxicological effect on brine shrimps is less relatively to the aniline-based ligands. The observed activities are different to their effects on bacteria and *Aspergillus niger*. The summary of their biological activities is listed below.

pvan3amp > ovan3amp > sal3amp > van3amp	(Brine shrimp)
ovan3amp > pvan3amp > sal3amp > van3amp	(Gram-negative)
sal3amp > ovan3amp ≈ pvan3amp ≈ van3amp	(Gram-positive)
ovan4amp > sal3amp > pvan4amp > van3amp	(Fungicidal)

9.3.4.1 Group 4: Brine shrimp activities for the complexes of the 3-aminopyridine-based ligands

The activities of the complexes of the 3-aminopyridine-based complexes are listed in Tables 8:50-8:53. Ligand 13 (sal3amp) distinctly showed higher toxicity against brine shrimps than all its complexes. However, the complex 13A is more active than the 13B and 13C.

Complex 14A showed more activity than the other two complexes and slightly more than the ligand (pvan4amp). For both sal3amp and pvan3amp (ligands 13 and 14 respectively) the series "A" complexes are far more active than the "B" and "C" series. The results signified that chelation reduced their activity drastically.

Some of the complexes of ligand 15 and 16 are more toxic than the corresponding Schiff base, ovan3amp, and van3amp, respectively. This implies that forming the complexes reduces polarity, and hence improves toxicity. The activity observed for the "A" series of complexes are similar to their activity against the fungus tested. The "B" and "C" series differs slightly.

9.3.5 Group 5: Brine shrimp activities for the 3-aminomethylpyridine-based ligands

The activity of the 3-aminomethylpyridine-based ligands is listed in Table 8:54. The activities of the 3-aminomethylpyridine-based Schiff bases are less toxic than the 3-aminopyridine-based analogue. The reduced activity is ascribed to the insertion of methylene between the C=N and the pyridine ring. The order of behaviour of the ligands is again different to their antimicrobial activity. The summary of the biological assays for this series of ligands is listed below.

sal3pico > pvan3pico > van3pico	(Brine shrimp)
pvan3pico > van3pico > ovan3pico > sal3pico	(Gram-negative)
pvan3pico > van3pico > ovan3pico > sal3pico	(Gram-positive)
pvan3pico > ovan3pico > sal3pico > van3pico	(Fungicidal)

9.3.5.1 Group 5: Brine shrimp activities for the complexes of the 3-aminomethylpyridine-based ligands

The activities of all the complexes of the 3-aminomethylpyridine-based complexes are listed in Table 8:55-8:57. All the isolated complexes have lower activity than their corresponding ligands. Their low toxicity against brine shrimp is attributable to their low solubilities in both aqueous and organic media.

9.3.6 Group 6: Brine shrimp activities for the 2-aminomethylpyridine-based ligand

The activity of the 2-aminomethylpyridine ligands against brine shrimps is listed in Table 8:58. Three of the four ligands in this series were tested. The activities of the 2-aminomethylpyridine-based ligands are less toxic than the 3-aminomethylpyridine-based analogue. The reduced activity is also ascribed to the insertion of methylene between the C=N and the pyridine ring. The order of behaviour of the ligands is also different to their antimicrobial activity. The summary of the biological assays is listed below.

sal2pico > pvan2pico ≈ ovan2pico	(Brine shrimp)
pvan2pico > van2pico > ovan2pico ≈ sal2pico	(Gram-negative)
pvan2pico > van2pico > ovan2pico ≈ sal2pico	(Gram-positive)
van2pico > pvan2pico ≈ ovan2pico >sal2pico	(Fungicidal)

9.3.6.1 Group 6: Brine shrimp activities for the 2-aminomethylpyridine-based complexes

Table 8:59 represent all brine shrimps inactive compounds. Surprisingly, all the isolated complexes of 2-aminomethylpyridine-based ligands are not active against brine shrimps. These sets of compounds are soluble in water. This solubility in water does not help their activities against brine shrimps.

9.4 References

1. S. Albert, *Selective Toxicity*; Methuen and Co. Ltd., 1960.
2. B. G. Tweedy, Phytopath.; 1964, 55, 910.
3. G. Venkatachalam, R. Ramesh, Spectrochim. Acta A; 2005, **61**, 2081-87.
4. M. N. Ibrahim, H.K. Al-Deeb, E.-J. Chem.; 2006, **13**, 257-61.
5. M. Tumer, C. Celik, H. Koksal, S. Serin, Trans. Met. Chem.; 1999, **24**, 525-32.
6. T. J. Franklin, G. A. Snow, *Biochemistry of antimicrobial action*, 2nd ed. Chapman and Hall, London, 1975.
7. R. Fioravanti, A. Panico, P. Mazzone, M. R. Pinizzotto, A. Garozzo, P. M. Furneri, Eur. J. Med. Chem, 1994, **29**, 781-85.
8. I. Sakiyan, E. Logoglu, S. Arslan, N. Sari, N. Sakiyan, BioMet.; 2004, **17**, 115-20.
9. A. A. Jarrahpour, M. Motamedifar, H. Mousavipour, N. Hadi, M. Zarei, Molbank; 2004, M364, CAN 142:134263.
10. M. M. Omar, G. G. Mohamed, A. M. M. Hindt, J. Therm. Anal.; 2006, **86**, 315-25.
11. I. F. Vladimirtsev, Y. V. Karabonov, V. Yu, S. S. Khripko, I. V. Boldyrev, Fiziologicheski; 1972, **4**, 136-8, (CAN 79:39226).

10 GENERAL SUMMARY AND FUTURE WORK

A lot of investigations on the synthesis, characterization and biological activity of Schiff bases and their corresponding metal complexes have been done recently. These investigations have revealed that these compounds have activity against bacteria, fungi, viruses, brine shrimps and cancers.[1]

The screening of the synthesized Schiff bases and their isolated Co(II) complexes against the three pathogenic bacteria, namely *Escherichia coli, Staphylococcus aureus, Pseudomonas aeruginosa* and a fungus, *Aspergillus niger* revealed that some of these compounds exhibit strong activities against all these organisms, and sometimes given almost equal activity as the standard antibacterial drug, ampicillin or give larger inhibition zones than the standard antifungal drug, benomyl as shown in the Tables listed in chapter 8.

As a result of the antimicrobial effects of these compounds, some of them have good chemotherapeutic potential for use as antimicrobial agents against the tested pathogenic organism. For instance, the ligand obtained from the condensation of *ortho*-vanillin with 1-aminonaphthalene (ovan1amnap, ligand 7) is the most promising ligand. Others ligands with remarkable activity include ovaani (ligand 3), ovan3amp (ligand 15) and pvan3amp (ligand 14). They show remarkable activity against Gram-negative *P. aeruginosa and E. coli*, Gram-positive *S. aureus*, as well as the fungus tested, *Aspergillus niger*. The complex of ligand 7, and some of the complexes of aniline-based ligands, the 4- and 3-aminopyridine-based ligands also showed noticeable toxicity against the bacteria tested. The activity of the some of the ligands and their complexes against Gram-negative bacteria tested as well as their lethality to brine shrimps can be used to predict their anticancer activity based on the following published works.

It has been established that Gram-negative bacteria are considered a quantitative microbiological method testing beneficial and important drugs in both clinical and experimental tumor chemotherapy.[2, 3] Platinum complexes were observed to inhibit[4,5] cell division in Gram-negative *E. coli* and cause the development of long filaments. This discovery led to the synthesis of the first known inorganic anticancer drug (Cisplatin) and hence the reason for continuous research in bioinorganic research with the hope of discovering more chemotherapy agents. Based on the highlighted published works, ligand 7 (ovan1amnap) and its complex (7A) are the most promising compounds. Aniline-based ligands and their complexes as well as some of the ligands and the complexes of the 4- and the 3-aminopyridine-based Schiff bases are also promising.

McLaughlin et al.[6] reported that brine shrimp lethality is superior to or as equally predictive as solid tumour cytotoxicities. Carballo et al.[7] work confirmed the consistency in the correlation previously established between cytotoxicity and brine shrimp lethality in plant extracts. Solis et al.[8] also confirmed that brine shrimp assay was predictive of cytotoxicity for the compounds they tested, except for compounds known to require activation. Using the information from these published works and others, the aniline-based ligands and their complexes are promising anticancer candidates for testing. The 4- and 3-aminopyridine-based ligands and their complexes are most likely also suitable candidates for anticancer testing.

While the aniline-based ligands and their complexes showed high toxicity against the shrimps, the cobalt complexes of the 2-aminomethylpyridine show no activity against the brine shrimps. Although they show no activity on brine shrimp and low toxicity to the bacteria and fungus tested, it is recommend that further bioassays be carried out on them as they may be acting as a prodrug. While brine shrimp lethality test have been used to predict cytotoxicity, the method has not been able to detect compounds acting as prodrugs,[6] i.e. drugs requiring activation by hepatic metabolism.

In accounting for the variable selective activity of the bacteria, fungi and the brine shrimp towards the various groups of the Schiff bases synthesised, and their corresponding cobalt(II) complexes, one evident distinction lies in their general structure. Their ability to withstand considerable changes in osmolarity determines the extent of attack.[9] For instance, while Gram-negative bacteria have low osmolarity because they do not concentrate nutrients and metabolites, Gram-positive have low molecular weight in their cytoplasm, and consequently, have a high internal osmolarity.[9] This may account for the differences in their responses to the attacks of the Schiff bases, the complexes, the DMF as well as the standard antimicrobial agents used.

The differente responses of the tested organisms to the attacks of the tested compounds lie in the absence or the presence of murein. Murein[9] gives strength and shape to the cell and enables it to withstand a high internal osmotic pressure. The size of murein is about 12 nm in Gram-positive bacteria, 2 nm in Gram-negative bacteria hence the reason for the differences.[9]

Unlike the bacteria, the walls of fungi do not contain murein;[9] hence the antibody that helps bacteria to fight attack is inactive against these microorganisms. In fungi cell, the rigid structural

feature is poly-N-acetylglucosamine known as chitin. For the bacteria, antibiotics are known to have primary action on murein biosynthesis while antifungal drugs inhibit the synthesis of chitin.[9] The ligands and the complexes that have shown remarkable activity may also have affected the biosynthesis of murein and chitin in the tested microorganisms.

The Schiff bases and complexes that have shown remarkable activity against the bacteria and fungus tested, hence could qualify to be administered safely for the treatments of infections caused by any of these particular strains of bacteria or the fungus.

The structure-activity relationship studies revealed that the aniline-based ligands and complexes appeared to be more active against all the tested microorganisms than the other groups studied. The structural activity relationship revealed that antimicrobial and cytotoxicity decreased as the aniline is replaced by the aminopyridines. There was further decrease in activities as the amine substitution changes from aniline to the aminomethylpyridine.

The antimicrobial activity results showed that Schiff bases and complexes containing 3-methoxy and 2-OH groups are somewhat better than those of the compounds from the other aldehydes. The outcome of this study also demonstrate that substitution in the aldehyde moiety is desirable especially for OH in the 2-position in contrast to the OH in the 4-position for the antimicrobial assay. This observation concurs with the conclusion of Hodnett and Dunn,[10] who studied the structural-antitumor activity correlation of some Schiff bases. In contrast, the brine shrimp lethality assay revealed that the Schiff base with OH in 4-position showed more toxicity to the shrimps than the rest of the Schiff bases and their complexes.

The study has given room for further studies. Areas that has been identified as future work includes:
Synthesis of complexes with a 1:1 metal-to-ligand ratio and a comparison of their activity against the complexes with a 2:1 metal-to-ligand ratio. According to the work of Zhu et al.[11] the monochelates exhibit higher inhibition effects against the bacteria and the fungus studied than the bis-chelates.

The antimicrobial activity of some complexes has been observed to increase when mixed ligands are used to synthesised the complexes.[12] Hence, synthesizing complexes of neutral N, N

bidentate ligands such as 2,2-bipyridine or 1,10 phenanthroline might increase the biological activities of these complexes.

The isolated Schiff bases and their cobalt(II) complexes have been screened against pathogenic bacteria and fungus. However, the presence of o-hydroxy group has been known to be essential for antiviral activity. Consequently, it is recommended that the Schiff bases and their complexes are screen for further biological activities in order to know more about their activities.

Using the right reaction conditions, it is possible to synthesize the N-oxide from the aminopyridines and the aminomethylpyridines. The possibility that the N-oxides might help to control the growth of oxygen-deficient cancer cells should be pursued.

And finally, the present NMR study suggests that the 4-aminopyridine salicylaldimines may offer an opportunity to examine, by NMR spectroscopy, the tautomer equilibria in a variety of solvents.

10.1 References

1. Y. Huang, H. Shen, S. Long, Syth. React. Inorg. Met-Org. Chem.; 2002, **32**, 1611-24.
2. G. G. Mohamed, M.M. Omar, A.M. Hindy, Turk J. Chem.; 2006, **30**, 361-82
3. G. G. Mohamed, M.M. Omar, A.M. Hindy, Spectrochim. Acta A.; 2005, **62**, 1140-50.
4. B. Rosenberg, L. Van Camp, T. Krigas, Nature, 1965, **206**, 698 -9.
5. B. Rosenberg, L. Van Camp, E. B. Grimley, A. J. Thomson, J. Bio. Chem.; 1967, **242**, 1347-52.
6. J. E. Anderson, C. M. Goetz, J. L. McLaughlin, Phytochem. Analys.; 1991, **2**, 107-111.
7. J. L. Carballo, Z. L. Hernandez-Inda, P. Perez, M. D. Gravalos, Bio. Med. Cent. Biotech.; 2002, **2**, 17-21.
8. P. N. Solis, C. W. Wright, M. M. Anderson, M. P. Gupta, J. D. Phillipson, Plant Med.; 1993, **59**, 250-52.
9. T. J. Franklin, G. A. Snow, *Biochemistry of antimicrobial action*, 2nd ed. Chapman and Hall, London, 1975.
10. E. M. Hodnett, W. J. Dunn, III, J. Med. Chem.; 1970, **13**, 768-70.